Static Elastic Properties of Composite Materials Containing Microspheres

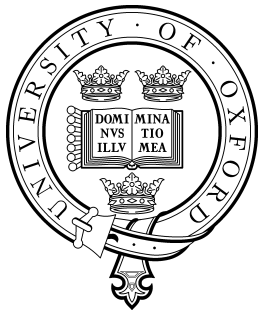

Gareth Wyn Jones

Jesus College

University of Oxford

A thesis submitted for the degree of

Doctor of Philosophy

Michaelmas 2007

Static Elastic Properties of Composite Materials Containing Microspheres

Gareth Wyn Jones

Jesus College
University of Oxford

A thesis submitted for the degree of Doctor of Philosophy

Michaelmas 2007

Abstract

This thesis aims to model the uniaxial deformation of a class of materials consisting of microscopic spherical shells embedded in a rubber matrix. These shells are assumed to buckle as the stress on the material increases.

To motivate the analysis we consider the paradigm problem of the debonding of a distribution of cylindrical inclusions in an elastic material undergoing antiplane shear, with bonded and debonded inclusions playing the role of unbuckled and buckled shells respectively.

We begin the modelling of the microsphere-containing material by considering the buckling of an isolated embedded shell inclusion with a uniaxial stress field at infinity, using Koiter's theory of shallow shells. The resulting energy functional is solved as an eigenvalue problem by the Rayleigh–Ritz method. Subsequently, we analyse the buckling criterion asymptotically in the limit as the thickness ratio tends to zero by analogy with the WKB analysis of a beam on a variable-stiffness substrate.

To model the shell after buckling we consider the simplified case of an embedded shell with a crack around its equator. The system is solved by expressing the displacements in the shell and matrix as series of Love stress functions, with the resulting infinite system of equations solved numerically with the aid of a convergence acceleration method.

Finally we consider a composite material consisting of a homogenised dilute distribution of buckled and unbuckled shells, with the proportion of each type of shell dependent on the stress applied to the material, according to an asymptotic formula relating the size of the inclusions and the critical buckling stress that was obtained previously.

Acknowledgements

In the first place I would like to thank my supervisor Jon Chapman for his patience and for all the assistance he has given to me over these past three and a half years. In addition I am grateful to my Technology Translator David Allwright who has acted as a second supervisor in providing many ingenious mathematical arguments during the course of my time here.

This work is inspired by a problem proposed by John Smith at Dstl, and thanks are due to them for their assistance and financial support. Similarly I thank EPSRC for funding the project, and Jesus College for providing a roof over my head and many enjoyable experiences.

I would also like to thank everyone at OCIAM for many stimulating discussions, crosswords and bridge games, and especially the past and present tenants of DH9, DH10 and DH11 for diversionary discussions at work and elsewhere.

Finally I thank my family for all their kindness and support.

Contents

List of Figures

Chapter 1

Introduction

1.1 Industrial motivation

For over sixty years, anechoic tiles [16, 100] have been used as coatings for submarines and other underwater structures. These tiles can take many forms, but their main function is to match with the acoustic impedance of water so that their reflection coefficient is minimised [58].

One material that is often used for this purpose is vulcanised rubber. This material is used due to its viscoelastic property that *shear* elastic waves are attenuated quickly on passing through it. However, incident waves on the material generate mainly *compressive* waves in the material. To take advantage of the material's attenuation property, small *microspheres* are introduced into the material before setting. These microspheres are hollow shells of around 20 µm in radius and are depicted in Figure 1.1. The spheres have the property that a compressive wave impinging on an

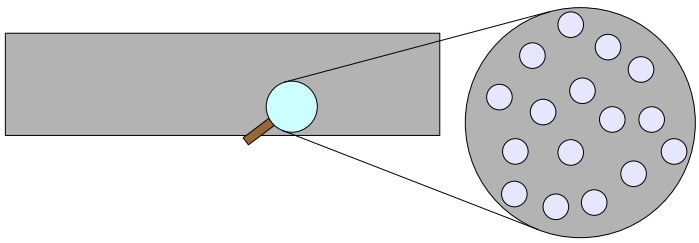

Figure 1.1: Depiction of microspheres in the composite material.

embedded sphere causes the energy of the wave to be partly converted into *shear wave* energy (this is known as *mode conversion*), which is then attenuated by the matrix material. By this mechanism, the energy of the incident acoustic wave is dissipated throughout the material.

However, the motivation for the work in this thesis is not the actual attenuative mechanism. Instead we consider how the coatings may be damaged by static loads

such as water pressure. To analyse the static properties of the material, an experiment is set up (see Figure 1.2) whereby the material is placed in a tank of water under a rigid block, and subjected to increasing pressure to simulate the uniaxial compression that the material would experience in reality. The displacement of the rigid block is measured for both increasing and decreasing water pressure.

A representation of the results is shown in Figure 1.3. There are four main features of the graph, which are labelled 1–4. Initially, as the material is first loaded, the graph is linear up to some critical pressure, at which point the stiffness lessens considerably. The resulting 'kink' in the graph need not be as pronounced as shown, but the sharpness is dependent on the distribution of the sizes of the microspheres. Secondly, if the material is loaded up to a point A and then unloaded, the deformation takes place along curve AB, displaying a marked *stress-softening* or hysteresis effect. This phenomenon is related to the *Mullins effect* seen in filled rubbers (see Section 1.2). The third feature of the graph is a (semi-)permanent set once the material is fully unloaded from A. (This set only occurs if the material has been deformed past the critical pressure, or 'kink'.) If further loading occurs, it will happen along the curve BA. If the material is deformed past the point A, it will follow the original loading curve, with unloading occuring along a new softened curve, with greater displacements than curve AB. The fourth effect is that if a material has been unloaded to the point B, the permanent set disappears fairly rapidly. However, the material's behaviour under compression does not return to the curve O1A for a period of 24 hours. This is also a phenomenon associated with the Mullins effect.

Given that anechoic tiles have an obvious military application, research on their properties is hard to find in publicly available journals. Parnell [79] and Allwright, Jones and Parnell [1] considered the scattering of sound from a single microsphere, modelled as a void for simplicity. The material surrounding the void was assumed to be under hydrostatic stress at infinity, inducing a strain field in the immediate vicinity of the void. This strained material scatters an incident acoustic wave, and the strength of this scattered field was determined. Meanwhile the static problem has been analysed by Fok [31] and Fok and Allwright [32]. These two references consider the hydrostatic compression at infinity of an embedded microsphere. Chapter 3 of this thesis includes this problem as a special case.

1.2 Rubber elasticity and the Mullins effect

Vulcanised rubber is an elastic material which satisfies a nonlinear stress–strain relation. This is characterised by the *strain energy function* of the material. The most

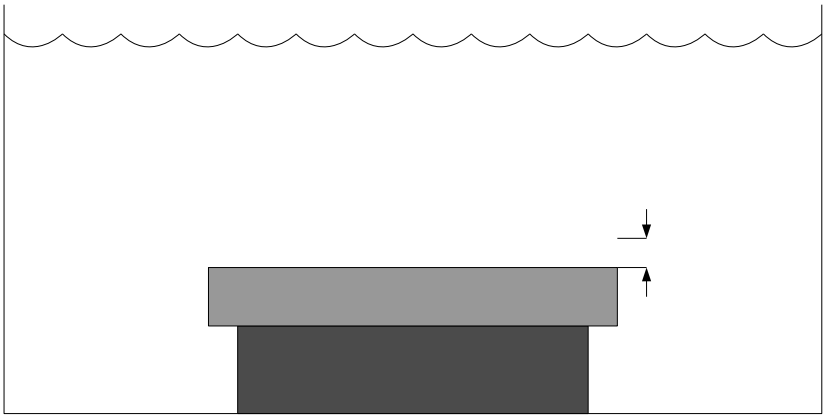

Figure 1.2: An experiment to determine the properties of the material.

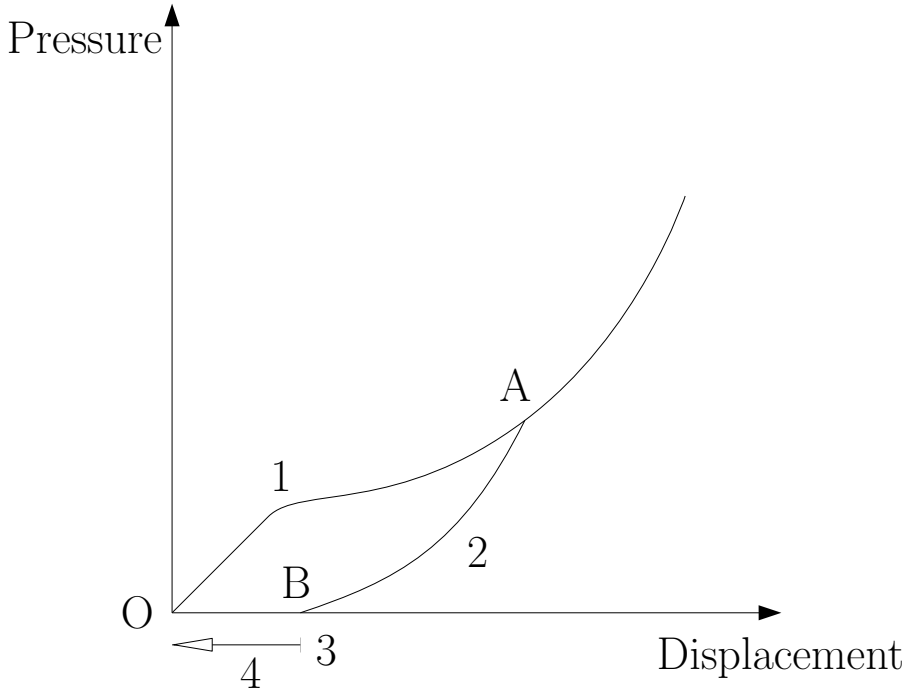

Figure 1.3: Behaviour of the composite material.

common strain energy functions used for rubber are the *Neo-Hookean* and *Mooney–Rivlin* material models. However, these have been supplanted in recent times by more sophisticated models such as the *Ogden* material model [44]. All these models treat the material as incompressible, due to the fact that the compressibility of rubber is very small [93].

We will now consider the models which have been proposed for the explanation of the Mullins effect, which may give an insight into properties 2–4 of Figure 1.3. The main similarity between carbon black-filled rubber, for which the Mullins effect was first described, and anechoic tiles is that both materials are formed from vulcanised rubber filled with microscopic particles. However in black-filled rubbers the inclusions are small particles of carbon, which can be treated as rigid in comparison to the rubber. The similarities are close enough that we can transfer some of the knowledge of the Mullins effect to the case of anechoic tiles.

The Mullins effect in filled rubbers is usually demonstrated by a uniaxial tension test. The results of a typical test are shown in Figure 1.4. The material in its virgin

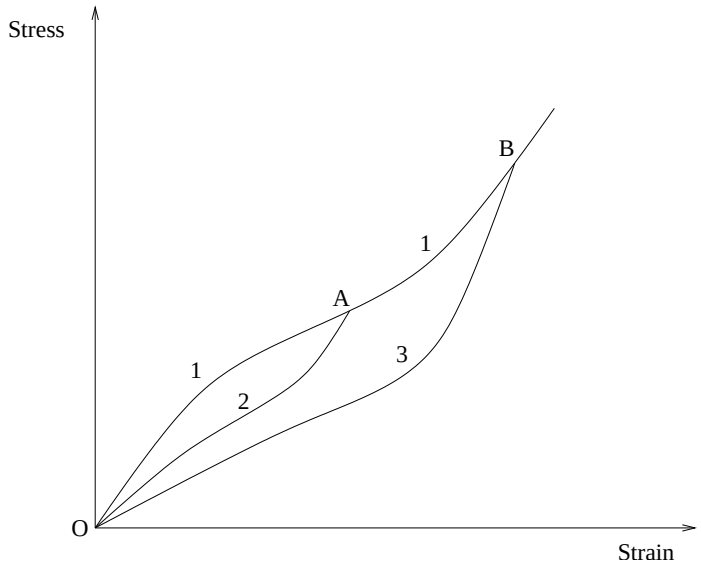

Figure 1.4: Schematic diagram of the Mullins effect.

form, that is, having not been previously deformed, follows curve 1 along OAB. If the material is stretched along this curve from O to A and retracted, we find that the retraction follows curve 2 from A to O. All further deformations from O to A and back then follow curve 2. If the material is now stretched from O to B, it follows curve 2 to A and then curve 1 from A to B. On retraction, it follows curve 3, and all further deformations from O to B follow this curve.

The Mullins effect has also been noticed in simple shear tests and uniaxial compression tests, but to a lesser extent than for uniaxial extension. Although a permanent

set and hysteresis are also observed in all tests, only the idealised behaviour given above is usually considered when modelling the effect.

An additional property of filled rubbers is that the stiffness is regained after a period of time. At room temperature the recovery is slow, but at 100°C up to 50% of the stiffness is recovered after an hour [43]. This effect is known as *healing*.

1.2.1 Experimental evidence

Although the Mullins effect was noted as far back as 1903 [11], and was studied by Holt [43] for example, the first major experimental study was made by Mullins [71, 72, 73]. He performed tensile stress–strain experiments on unfilled and filled rubber vulcanisates, and found that filled vulcanisates were considerably softer on the second stretching. Unfilled rubbers were only slightly affected by previous stretching. It was also found that the stress–strain properties of the previously stretched material were anisotropic, and that the stiffness returned to the structure after some time, but only at significantly higher temperatures than room temperature. Mullins attributed these effects to a breakdown in the structure of the carbon black particles as the material was stretched.

Blanchard and Parkinson [10] disagreed. By measuring the resistivity of the rubber as it was being stretched under uniaxial tension, they noticed no significant change in the structure of the carbon filler particles. Their explanation for the Mullins effect was the breakage of bonds between the rubber and the carbon particles, and they derived an empirical relation based on the molecular theory of rubber.

Later, Harwood *et al.* [40, 41] performed more experiments, and found that in fact unfilled rubbers do exhibit a similar stress-softening effect to filled rubbers in uniaxial tension tests, if strains of up to 5 are considered. They concluded that the most likely cause of the Mullins effect was a change in the orientation or entanglement of the polymer chains in the rubber.

More recently Dorfmann and Ogden [28] presented experimental results that showed that, at least for strains of up to around 1.5, the Mullins effect is hardly seen in rubber with low concentrations of carbon black, so that for relatively low strains the effect can be primarily attributed to the presence of inclusions.

1.2.2 Molecular-based theories

Bueche [14, 15] agreed that the cause of the Mullins effect was primarily due to the breaking of bonds between the rubber and the particles. He proposed a molecular model which considered the probability that a polymer chain attached to two carbon black particles would come loose when the particles are displaced.

Govindjee and Simo [34, 36, 35] reviewed the explanations for the Mullins effect, and also favoured this explanation. Expanding upon Bueche's work, they modelled the rubber by taking a statistically representative sample volume of rubber, calculating its strain energy function using an averaging theory, and relating it to the average strain history of the material using ideas from statistical mechanics. An averaged strain energy function is obtained, together with slightly modified stress–strain equations which are dependent on the volume fraction of particles in the rubber.

1.2.3 Empirical theories

Due to the necessity of modelling large deformations of rubber with nonlinear elasticity, an alternative approach to modelling the Mullins effect has been to devise *empirical* notions of 'damage' to the material. Mullins and Tobin [74] constructed a model which attempted to explain the effect in terms of 'hard' and 'soft' phases of the rubber. They assumed that most of the rubber would be in the hard phase to begin with, but after deformation a larger proportion of the rubber will be in the soft phase. The words 'hard' and 'soft' here do not necessarily refer to the filler and the rubber respectively.

Later, Johnson and Beatty [49, 48, 50] developed a theory to explain the Mullins effect for any nonlinear elastic material, parametrising the damage done to the material by the *maximum previous strain*. Beatty and Krishnaswamy [5, 53, 4, 54] gave this theory an overhaul. They adapted the model of Mullins and Tobin of the existence of hard and soft phases in the rubber, with the volume fraction of the soft phase increasing if the strain is increased past its maximum previous strain. However, there is no need to interpret the rubber as having hard and soft phases. We can consider the volume fraction of soft phase as an abstract *damage parameter* which varies between 0 in the undamaged (virgin) state, and 1 (totally damaged). Here damage is defined as loading past the maximum previous strain. The results work with any strain energy function, but a specific dependence on the maximum previous strain (softening function) is chosen for analytical simplicity and to fit experimental data.

More recently, Ogden and co-workers [77, 28] developed a theory similar to that of Beatty and Krishnaswamy in that it is based around the strain energy function of the material, with a damage parameter modelling the amount of damage being done to the material; however, in this theory the damage is modelled in a much more abstract way. The strain energy function of the material is modified so that it depends on a damage parameter labelled η, making the material 'pseudo-elastic'. In this theory, η is constant *if damage is being done to the material* — a counterintuitive idea, but useful since the loading curve for an undamaged material can thus be modelled by a known strain energy function. The parameter η should therefore be treated purely

as a mathematical construct, with no physical basis. Like Beatty and Krishnaswamy, Ogden and Roxburgh introduce a 'damage function' which expresses how the strain energy function depends on η when η varies. The validity of the model is checked by fitting the material constants of the strain energy function and constants in the damage function to data from Mullins and Tobin's original experiments, but the model chosen has no physical justification for its form.

There have been many other theories that attempt to describe the Mullins effect. Miehe [68] and later Laraba-Abbes *et al.* [56] employed a model which considered a strain energy function $(1-d)W$ where W is a given strain energy function and d is a damage parameter. A different course was taken by Marckmann *et al.* [66], who used a 'network alteration theory', adapting a rubber model based on considerations of how chains of molecules deform. DeSimone *et al.* [27] created a model which simplified the behaviour in Figure 1.4 to a piecewise linear relation, and invoked a damage parameter model similar to Beatty and Krishnaswamy to explain stress-softening in that case. Lin and Schomburg [59] attempted to create a full phenomenological model for rubber, incorporating viscoelasticity and plasticity as well as the Mullins effect, but without considering any microscopic effects. All these theories are essentially *empirical* relations, that mainly seek to predict the stress–strain curve in Figure 1.4 by fitting experimental data to a curve rather than appeal to the rubber molecules' bonds breaking.

1.3 Application to anechoic tiles

The strains that the microsphere-filled material will experience are much less than 5, so by the results of Dorfmann and Ogden [28], we can confidently assume that the main mechanism by which the material loses stiffness is the slippage or rupture of bonds between the matrix and the inclusions (which will be referred to henceforth as 'debonding'). The reason for this is that the softening effect is barely seen at these strains in unfilled rubbers. If we assume that the 'kink' in Figure 1.3 is due to the buckling of the microspheres, we conclude that the debonding occurs *after* buckling, in light of the observation that no stress-softening occurs if the loading never reaches the kink.

The conjectured reasons for the behaviour of the material in Figure 1.3 are therefore that the material behaves naturally for small strains, until a critical stress causes most of the shells to buckle (increasingly large strains will eventually cause all shells to buckle). This buckling will cause slippage or rupture in the bonds between the inclusions and the matrix, and the degree to which this occurs becomes greater as the stress is increased. The degree of debonding is referred to as the *damage* done to the

material. No damage is conjectured to occur on unloading, so that each unloading curve (such as A–B in Figure 1.3) represents the stress–strain relation for a given damage parameter and will thus be the same on loading since reloading the material up to the maximum previous strain would not cause the damage to increase greatly. The permanent set is assumed to be due to shells remaining buckled on full unloading, and the healing effect seen after 24 hours is presumably due to the reformation of bonds between the inclusions and the matrix, as for carbon black-filled rubbers.

Analytically solving the problem of a debonding nonlinearly elastic matrix from a buckling shell is a near-impossible task, so it will not be considered here. On the other hand, by making the simplification to *linear* elasticity, the buckling problem itself can be tackled analytically, giving an explanation of the first effect in Figure 1.3. Modelling the debonding, though, would still be too difficult, which means that we will only consider the inclusions as having two states: unbuckled and buckled, both with full attachment to the matrix. Ideally there would be a continuum of states of the inclusion, from pristine (unbuckled) to a very damaged state (buckled and with a large region of debonding from the matrix). However with only two states of the inclusion we can consider the damage parameter to be given by the proportion of shells which have buckled. Nevertheless, it is hoped that the results can begin to explain the loading curve for the material.

1.4 Thesis outline

Before considering the buckling problem, in Chapter 2 we analyse the paradigm problem of infinitely long cylindrical fibres in antiplane strain. We will first consider how one inclusion debonds from the matrix under this mode of deformation, before considering the homogenised problem of many inclusions embedded in the matrix. Two homogenisation approaches are analysed, namely the multiple scales homogenisation which assumes a grid distribution of inclusions, and the point inclusion method, which assumes that the fibres are infinitely far apart.

In Chapter 3 we analyse the problem of a spherical shell embedded in a linearly elastic matrix. We apply a stress field at infinity and find the critical stress at which the inclusion buckles. The background theory for this chapter is in Appendix A, which is presented in terms of general curvilinear coordinates, before specialising to spherical polar coordinates. In Chapter 4 we analyse the limit as the shell thickness ratio tends to zero. This will give us an approximate *analytic* expression for the critical stress and buckling pattern, as opposed to the numerical results of Chapter 3.

Chapter 5 analyses a model for the behaviour of the shell *after* buckling has occured. We do not consider the full post-buckling behaviour of the shell. Rather, we assume that the shell is assumed to lose its stiffness around its equator, resulting effectively in a *split* shell. The final solution is found numerically. In Chapter 6 we take the leading-order solutions at infinity of the pre-buckled and post-buckled shells, and use these results to find the behaviour of a homogenised material formed from a distribution of these microsphere inclusions, via a method similar to the point inclusion method of Chapter 2. We finally draw our conclusions in Chapter 7.

Throughout the thesis we will assume that the shell and the matrix are linearly elastic materials, with dimensions and physical properties as given in Table 1.1. The matrix shear modulus is not given because all stresses will be given in terms of this quantity.

Physical quantity	Value
Shell mid-surface radius $\widehat{R}$	$20\,\mu\text{m}$
Shell thickness h	$0.02\,\widehat{R}$
Matrix shear modulus G_m	—
Matrix Poisson ratio ν_m	0.45
Shell shear modulus G_s	$100\,G_\text{m}$
Shell Poisson ratio ν_s	0.35

Table 1.1: Typical values of physical constants.

1.5 Statement of originality

In Chapter 2, originality is claimed for Section 2.3 insofar as it discusses the particular configuration shown in Figure 2.2 and the calculation of stress intensity factors. The initial theory of the section is entirely due to Tamate and Yamada [91]. For the multiple scales analysis of Section 2.4.1, the results are not original but originality is claimed for the method by which they were derived (the results have not been derived by the multiple scales homogenisation method previously). Section 2.4.2 and onwards is original work.

In Chapter 3, originality is claimed for the results of Section 3.3 and the entirety of the remainder of the chapter. Chapter 4 is original from Section 4.3.2 onwards, as is the entirety of Chapter 5 except where noted. In Chapter 6 up to Section 6.3.2, the mechanism of finding the effective elastic tensor by averaging the polarisation is not original, however the analysis of splitting the solution into inner and outer solutions and the averaging analysis is original. The work of Section 6.3.2 onwards is all original. The appendices are not original, apart from Section C.1 and Appendix D.

Chapter 2

A Paradigm Problem

In this chapter we will be studying a paradigm problem which will introduce the homogenisation process to be used in Chapter 6. The model studied here is the debonding of a fibre embedded in an elastic medium (both linearly elastic), undergoing antiplane shear parallel to the fibres. The main similarity between the antiplane shear of embedded fibres and the buckling of embedded shells is that in both cases an individual inclusion undergoes a transition between a 'virgin' and a 'damaged' state. In the antiplane case these states correspond to being respectively bonded and debonded to the matrix, while in the case of an embedded shell we consider unbuckled and buckled states. In this chapter we show that if we know the far-field behaviour of a single inclusion in a matrix which has a stress field applied at infinity, in both the virgin and damaged states, together with a criterion for the transition from the first state to the second, we can consider a continuous distribution of inclusions with varying properties, and analyse how the damaging of individual inclusions affects the large-scale properties of the composite material. These methods will be applied to a distribution of embedded shells in Chapter 6.

We first solve the problem of one fully attached fibre, before considering its debonding from the matrix, using complex variable theory. Following this we consider two methods of homogenisation for the problem — by multiple scales (assuming the fibres are arranged in a grid), and by the point inclusion method (assuming the fibres are far apart). We compare the two methods and conclude that the simpler point inclusion method is accurate enough for our needs. Finally this method is applied to the problem of a distribution of debonding fibres.

2.1 Governing equations

In elasticity theory, antiplane deformations are characterised by having only one non-zero component of displacement, which we will assume is in the z-direction. This

displacement is assumed not to depend on z. In other words, in Cartesian coordinates,

$$u = 0 , \tag{2.1}$$

$$v = 0 , \tag{2.2}$$

$$w = f(x, y) . \tag{2.3}$$

This gives us only two non-zero components of strain,

$$e_{xz} = \frac{1}{2}\frac{\partial f}{\partial x} , \tag{2.4}$$

$$e_{yz} = \frac{1}{2}\frac{\partial f}{\partial y} , \tag{2.5}$$

and hence only two non-zero components of stress,

$$\tau_{xz} = G\frac{\partial f}{\partial x} , \tag{2.6}$$

$$\tau_{yz} = G\frac{\partial f}{\partial y} , \tag{2.7}$$

where G is the shear modulus of the material, assumed to depend on x and y only. Substituting these into the steady equilibrium equation with no body forces,

$$\frac{\partial \tau_{ij}}{\partial x_j} = 0 , \tag{2.8}$$

gives us the equation to be solved for f,

$$\nabla \cdot (G \nabla f) = 0 , \tag{2.9}$$

in two dimensions.[1] The dilatation $\nabla \cdot \boldsymbol{u}$ is zero, showing that all antiplane deformations are automatically volume-preserving.

2.2 The matrix–fibre problem

In this section we will consider the problem of a single, infinitely long circular cylindrical fibre embedded in an elastic matrix, undergoing a shearing stress field at infinity, as depicted in Figure 2.1. For simplicity we assume that $\tau_{xz}|_\infty$ is zero and $\tau_{yz}|_\infty = \tau_0$. The matrix is assumed to have constant shear modulus G_m, and in the fibre the shear modulus is G_f, also constant. We define two displacements f_m and f_f for the displacements in the matrix and fibre respectively.

[1] Had we been considering a Mooney–Rivlin or Neo-Hookean material in nonlinear elasticity (see Section 1.2), we would have the same equation to solve (see [46]), although the stress field would have non-zero components other than those given above.

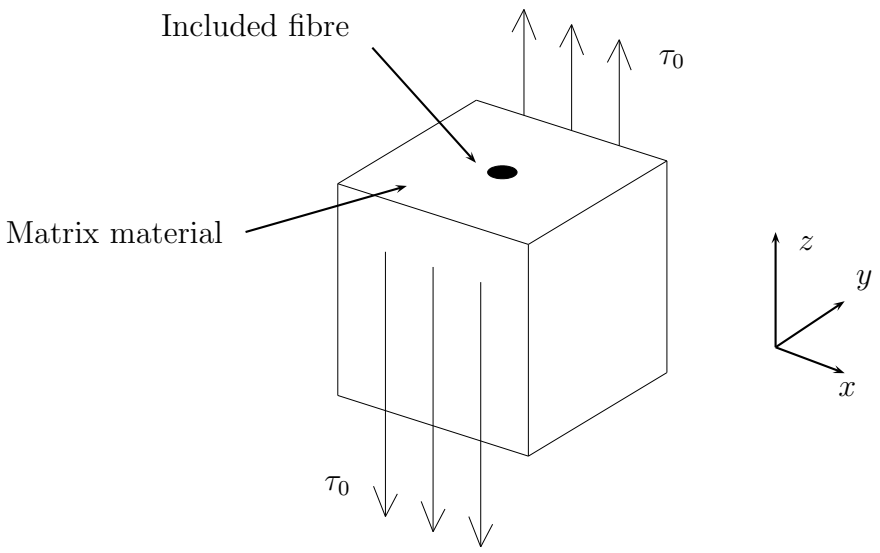

Figure 2.1: A depiction of the stress field acting on the included fibre.

The radius of the fibre is assumed to be a, and the displacement and tractions are to be matched at $x^2 + y^2 = a^2$. From the previous section the problem thus becomes

$$\frac{\partial^2 f_\mathrm{f}}{\partial x^2} + \frac{\partial^2 f_\mathrm{f}}{\partial y^2} = 0 \qquad \text{in } x^2 + y^2 < a^2, \tag{2.10}$$

$$\frac{\partial^2 f_\mathrm{m}}{\partial x^2} + \frac{\partial^2 f_\mathrm{m}}{\partial y^2} = 0 \qquad \text{in } x^2 + y^2 > a^2, \tag{2.11}$$

$$f_\mathrm{m} - f_\mathrm{f} = 0 \qquad \text{at } x^2 + y^2 = a^2, \tag{2.12}$$

$$G_\mathrm{m}\frac{\partial f_\mathrm{m}}{\partial r} - G_\mathrm{f}\frac{\partial f_\mathrm{f}}{\partial r} = 0 \qquad \text{at } x^2 + y^2 = a^2, \tag{2.13}$$

$$G_\mathrm{m}\frac{\partial f_\mathrm{m}}{\partial y} \to \tau_0 \qquad \text{as } x^2 + y^2 \to \infty, \tag{2.14}$$

$$G_\mathrm{m}\frac{\partial f_\mathrm{m}}{\partial x} \to 0 \qquad \text{as } x^2 + y^2 \to \infty. \tag{2.15}$$

This problem is best solved by changing to cylindrical polar coordinates,

$$r = \sqrt{x^2 + y^2}\,, \tag{2.16}$$

$$\theta = \tan^{-1}\left(\frac{y}{x}\right)\,. \tag{2.17}$$

The system to be solved becomes

$$\frac{1}{r}\frac{\partial}{\partial r}\left(r\frac{\partial f_\mathrm{f}}{\partial r}\right) + \frac{1}{r^2}\frac{\partial^2 f_\mathrm{f}}{\partial \theta^2} = 0 \qquad \text{in } r < a, \tag{2.18}$$

$$\frac{1}{r}\frac{\partial}{\partial r}\left(r\frac{\partial f_\mathrm{m}}{\partial r}\right) + \frac{1}{r^2}\frac{\partial^2 f_\mathrm{m}}{\partial \theta^2} = 0 \qquad \text{in } r > a, \tag{2.19}$$

$$f_\mathrm{m} - f_\mathrm{f} = 0 \qquad \text{at } r = a, \tag{2.20}$$

$$G_\mathrm{m}\frac{\partial f_\mathrm{m}}{\partial r} - G_\mathrm{f}\frac{\partial f_\mathrm{f}}{\partial r} = 0 \qquad \text{at } r = a, \tag{2.21}$$

$$f_\mathrm{m} \sim \frac{\tau_0}{G_\mathrm{m}} r\sin\theta \qquad \text{as } r \to \infty\,. \tag{2.22}$$

We assume that the displacements are of the form

$$f_{\mathrm{m}} = F_{\mathrm{m}}(r)\sin\theta\ , \tag{2.23}$$

$$f_{\mathrm{f}} = F_{\mathrm{f}}(r)\sin\theta\ , \tag{2.24}$$

due to the condition at infinity. Substituting these into equations (2.18)–(2.19) gives

$$F_{\mathrm{m}} = Ar + \frac{B}{r}\ , \tag{2.25}$$

$$F_{\mathrm{f}} = Cr + \frac{D}{r}\ , \tag{2.26}$$

where A, B, C and D are arbitrary constants. We immediately set $D = 0$ so that the displacement is finite in the fibre. We also set

$$A = \frac{\tau_0}{G_{\mathrm{m}}} \tag{2.27}$$

to match to the condition at infinity. Comparing the displacements at $r = a$ gives

$$C = \frac{\tau_0}{G_{\mathrm{m}}} + \frac{B}{a^2}\ , \tag{2.28}$$

and finally, matching the tractions gives

$$B = \frac{\tau_0 a^2}{G_{\mathrm{m}}}\left(\frac{G_{\mathrm{m}} - G_{\mathrm{f}}}{G_{\mathrm{m}} + G_{\mathrm{f}}}\right)\ . \tag{2.29}$$

Therefore, altogether we have

$$f_{\mathrm{m}} = \frac{\tau_0}{G_{\mathrm{m}}}\left[r + \frac{a^2}{r}\left(\frac{G_{\mathrm{m}} - G_{\mathrm{f}}}{G_{\mathrm{m}} + G_{\mathrm{f}}}\right)\right]\sin\theta\ , \tag{2.30}$$

$$f_{\mathrm{f}} = \frac{\tau_0}{G_{\mathrm{m}}}\left[r + r\left(\frac{G_{\mathrm{m}} - G_{\mathrm{f}}}{G_{\mathrm{m}} + G_{\mathrm{f}}}\right)\right]\sin\theta \tag{2.31}$$

$$= \frac{2\tau_0\sin\theta}{G_{\mathrm{m}} + G_{\mathrm{f}}}\ . \tag{2.32}$$

The two limiting cases $G_{\mathrm{f}} \to \infty$ and $G_{\mathrm{f}} \to 0$ are of interest to us. The first models the case where the fibre becomes infinitely stiff, or in other words, rigid. In the second limit, the fibre becomes infinitely soft, namely a void. This case also corresponds to the traction being zero on $r = a$, so it could equally well model the situation where the matrix has *fully debonded* from its inclusion, with no traction between the two.

In the two limits $G_{\mathrm{f}} \to \infty$ and $G_{\mathrm{f}} \to 0$, the matrix displacement becomes

$$f_{\mathrm{m}} = \frac{\tau_0}{G_{\mathrm{m}}}\left(r \mp \frac{a^2}{r}\right)\sin\theta \tag{2.33}$$

respectively.

We note that we could also consider the case where the shear at infinity was aligned differently, *i.e.*

$$G_{\mathrm{m}}\,\nabla f|_{|\boldsymbol{x}|\to\infty} \;=\; \tau_0\widehat{\boldsymbol{p}}\,, \tag{2.34}$$

where $\widehat{\boldsymbol{p}} = (\widehat{p}_1, \widehat{p}_2)$ is a unit vector. In that case the solution for the displacement becomes

$$f_{\mathrm{m}} \;=\; \frac{\tau_0}{G_{\mathrm{m}}}\left[r + \frac{a^2}{r}\left(\frac{G_{\mathrm{m}} - G_{\mathrm{f}}}{G_{\mathrm{m}} + G_{\mathrm{f}}}\right)\right](\widehat{p}_1\cos\theta + \widehat{p}_2\sin\theta)\,, \tag{2.35}$$

$$f_{\mathrm{f}} \;=\; \frac{\tau_0}{G_{\mathrm{m}}}\left[r + r\left(\frac{G_{\mathrm{m}} - G_{\mathrm{f}}}{G_{\mathrm{m}} + G_{\mathrm{f}}}\right)\right](\widehat{p}_1\cos\theta + \widehat{p}_2\sin\theta)\,. \tag{2.36}$$

2.3 Debonding

Having calculated the displacement field in the matrix for a fully-attached and a fully-detached inclusion, we now want to consider the case of a *partly*-attached inclusion, so that we can model the debonding process. We assume that the inclusion is bonded along b_1a_2 and b_2a_1 in Figure 2.2 and unbonded along a_1b_1 and a_2b_2 in the same figure. The reason for choosing this configuration is that we assume that the material will begin debonding at the region of greatest stress, namely at $\theta = \pm\pi/2$. Then, as the stress at infinity increases we suppose that the extent of the debonding will also increase, yielding a configuration as shown in Figure 2.2.

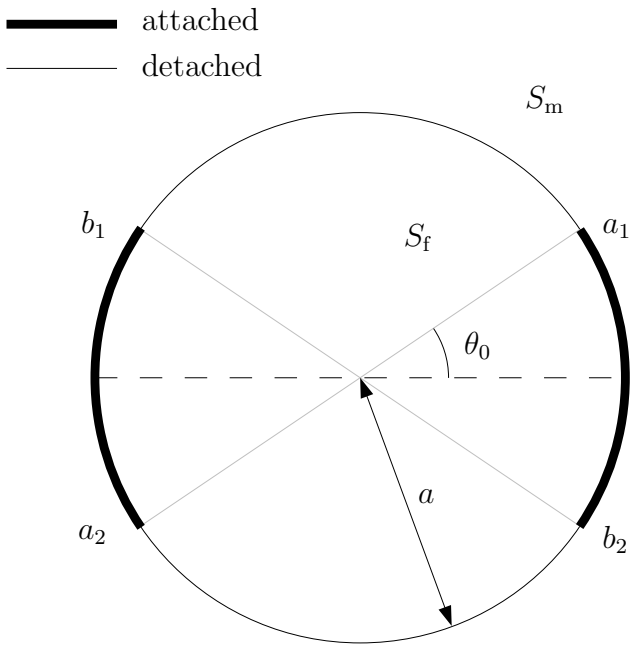

Figure 2.2: Configuration of the partly-attached fibre.

This problem has already been solved by Tamate and Yamada [91]. Although they didn't give an explicit solution for the displacement, they used complex function theory to find the stress fields around the crack tips, which enabled them to find the stress intensity factors. We will use their solution method to find these stress intensity factors so that we can predict the debonding of the fibre from the matrix.

We define two regions S_f and S_m which are separated by a circle of radius a, as shown in Figure 2.2. In S_f we have a linear elastic material with shear modulus G_f, and in S_m we have a material with modulus G_m. As before, at infinity a stress field $\tau_{yz} = \tau_0$ is applied, which can be rewritten as

$$\tau_{xz} - \mathrm{i}\tau_{yz} \;=\; -\mathrm{i}\tau_0 \tag{2.37}$$

in preparation for the use of complex variable theory. The arc a_1b_1 is referred to as L_1' and a_2b_2 is designated L_2'. Along these arcs the two materials are unattached. We denote

$$L' \;=\; L_1' \cup L_2' \tag{2.38}$$

to be the unbonded curve. Similarly, b_1a_2 is denoted L_1'' and b_2a_1 is denoted L_2''. We define

$$L'' \;=\; L_1'' \cup L_2'' \tag{2.39}$$

to be the bonded curve — the materials are attached along here. In our problem, the points a_i, b_i have complex values

$$a_1 \;=\; a\mathrm{e}^{\mathrm{i}\theta_0}\,, \tag{2.40}$$
$$b_1 \;=\; a\mathrm{e}^{\mathrm{i}(\pi-\theta_0)}\,, \tag{2.41}$$
$$a_2 \;=\; a\mathrm{e}^{\mathrm{i}(\pi+\theta_0)}\,, \tag{2.42}$$
$$b_2 \;=\; a\mathrm{e}^{\mathrm{i}(2\pi-\theta_0)}\,. \tag{2.43}$$

Now, the displacements in both regions are given by a solution of Laplace's equation. It is well known that in a simply-connected domain, any solution of Laplace's equation,

$$\frac{\partial^2 f}{\partial x^2} + \frac{\partial^2 f}{\partial y^2} \;=\; 0\,, \tag{2.44}$$

can be given by

$$f \;=\; \Re\big(\chi(\zeta)\big) \tag{2.45}$$
$$\;=\; \frac{1}{2}\big(\chi(\zeta) + \overline{\chi(\zeta)}\big) \tag{2.46}$$

where $\zeta = x + \mathrm{i}y$, $\Re$ denotes the real part, and $\chi(\zeta)$ is an analytic function. In this section an overbar represents the complex conjugate. For the annular region S_m, the solution is given by equation (2.46) added to a multiple of $\log(|\zeta|)$ [29]. Then if f_f is the z-displacement in S_f and f_m is the z-displacement in S_m, we can find the solutions

$$f_\mathrm{f} = \frac{1}{2}\big(\chi_\mathrm{f}(\zeta) + \overline{\chi_\mathrm{f}(\zeta)}\big)\,, \tag{2.47}$$

$$f_\mathrm{m} = \frac{1}{2}\big(\chi_\mathrm{m}(\zeta) + \overline{\chi_\mathrm{m}(\zeta)}\big) + \alpha\log(|\zeta|) \tag{2.48}$$

for as yet unknown analytic functions $\chi_\mathrm{f}(\zeta)$ and $\chi_\mathrm{m}(\zeta)$ and real constant α.

The stresses τ_{xz} and τ_{yz} in a linear material are given by equations (2.6)–(2.7). We find that this implies

$$\tau_{xz} - \mathrm{i}\tau_{yz} = \begin{cases} G_\mathrm{f}\chi_\mathrm{f}'(\zeta) & \text{in the fibre} \\ G_\mathrm{m}\chi_\mathrm{m}'(\zeta) + \dfrac{G_\mathrm{m}\alpha}{\zeta} & \text{in the matrix,} \end{cases} \tag{2.49}$$

on using equation (2.46). Hence, on using equation (2.37) we have our condition at infinity:

$$\chi_\mathrm{m}'(\zeta) \to -\frac{\mathrm{i}\tau_0}{G_\mathrm{m}} \qquad \text{as } |\zeta| \to \infty. \tag{2.50}$$

The stress components referred to cylindrical coordinates (r, θ, z) can be written as

$$\tau_{rz} - \mathrm{i}\tau_{\theta z} = \begin{cases} G_\mathrm{f}\chi_\mathrm{f}'(\zeta)\dfrac{\zeta}{|\zeta|} & \text{in the fibre} \\ G_\mathrm{m}\chi_\mathrm{m}'(\zeta)\dfrac{\zeta}{|\zeta|} + \dfrac{G_\mathrm{m}\alpha}{|\zeta|} & \text{in the matrix.} \end{cases} \tag{2.51}$$

The fibre is in a state of equilibrium, so that the integral of τ_{rz} in the fibre around the boundary of S_f is zero. From (2.51), integrating the matrix value of $\tau_{rz} - \mathrm{i}\tau_{\theta z}$ around the same contour gives $2\pi G_\mathrm{m}\alpha$. However, τ_{rz} is continuous across the contour, either through matching tractions on the bonded sections or by setting $\tau_{rz} = 0$ on either side of the detached sections. Thus we obtain $\alpha = 0$. Now, we demand that $\tau_{rz} = 0$ on L', so that on this curve

$$\sigma\chi_\mathrm{f}'^{+}(\sigma) + \bar{\sigma}\overline{\chi_\mathrm{f}'^{+}(\sigma)} = 0\,, \tag{2.52}$$

$$\sigma\chi_\mathrm{m}'^{-}(\sigma) + \bar{\sigma}\overline{\chi_\mathrm{m}'^{-}(\sigma)} = 0\,, \tag{2.53}$$

where $\sigma = a\mathrm{e}^{\mathrm{i}\theta}$ and superscript $+$ and $-$ refer to which side of L' the $\chi_i(\zeta)$ are defined on: '$+$' refers to the S_f side and '$-$' to the S_m side. Along the bonded edge L'', we demand continuity in τ_{rz} and in f (or $\partial f/\partial\theta$). These conditions tell us that we require

$$G_\mathrm{f}\left[\sigma\chi_\mathrm{f}'^{+}(\sigma) + \bar{\sigma}\overline{\chi_\mathrm{f}'^{+}(\sigma)}\right] = G_\mathrm{m}\left[\sigma\chi_\mathrm{m}'^{-}(\sigma) + \bar{\sigma}\overline{\chi_\mathrm{m}'^{-}(\sigma)}\right]\,, \tag{2.54}$$

$$\sigma\chi_\mathrm{f}'^{+}(\sigma) - \bar{\sigma}\overline{\chi_\mathrm{f}'^{+}(\sigma)} = \sigma\chi_\mathrm{m}'^{-}(\sigma) - \bar{\sigma}\overline{\chi_\mathrm{m}'^{-}(\sigma)} \tag{2.55}$$

along L''. The problem is therefore to find two analytic functions $\chi_{\rm f}(\zeta)$, $\chi_{\rm m}(\zeta)$ which satisfy the conditions (2.52), (2.53), (2.54) and (2.55) on the interface between $S_{\rm f}$ and $S_{\rm m}$, and (2.50) at infinity.

Tamate and Yamada solved the problem by analytically extending $\chi_{\rm f}(\zeta)$ and $\chi_{\rm m}(\zeta)$, which are currently only defined in $S_{\rm f}$ and $S_{\rm m}$ respectively, to the entire plane $S_{\rm f} \cup S_{\rm m}$ (with the possible exception of branch cuts). To this end, we define functions $\omega_1(\zeta)$ and $\omega_2(\zeta)$ by

$$\omega_1(\zeta) \;=\; \begin{cases} \zeta\chi_{\rm f}'(\zeta) & \text{in } S_{\rm f} \\ -\dfrac{a^2}{\zeta}\overline{\chi_{\rm f}'}\left(\dfrac{a^2}{\zeta}\right) & \text{in } S_{\rm m}, \end{cases} \tag{2.56}$$

$$\omega_2(\zeta) \;=\; \begin{cases} -\dfrac{a^2}{\zeta}\overline{\chi_{\rm m}'}\left(\dfrac{a^2}{\zeta}\right) & \text{in } S_{\rm f} \\ \zeta\chi_{\rm m}'(\zeta) & \text{in } S_{\rm m}, \end{cases} \tag{2.57}$$

so that for each $j = 1, 2$ we have

$$\overline{\omega_j}\left(\frac{a^2}{\zeta}\right) \;=\; -\omega_j(\zeta) \qquad \text{in } S_{\rm f} \cup S_{\rm m}. \tag{2.58}$$

This implies that on $\zeta = \sigma = a{\rm e}^{{\rm i}\theta}$,

$$\overline{\omega_j^{\pm}(\sigma)} \;=\; -\omega_j^{\mp}(\sigma)\,. \tag{2.59}$$

These functions (2.56) and (2.57) have been chosen so that the boundary conditions on L' imply that $\omega_1(\zeta)$ and $\omega_2(\zeta)$ are analytic on the whole complex plane, cut along L'' (the bonded curve). On using (2.59), the conditions along L'' become

$$\left[G_{\rm f}\omega_1^+(\sigma) + G_{\rm m}\omega_2^+(\sigma)\right] \;=\; \left[G_{\rm f}\omega_1^-(\sigma) + G_{\rm m}\omega_2^-(\sigma)\right]\,, \tag{2.60}$$

$$\left[\omega_1^+(\sigma) - \omega_2^+(\sigma)\right] \;=\; -\left[\omega_1^-(\sigma) - \omega_2^-(\sigma)\right]\,. \tag{2.61}$$

In addition, from the behaviour of $\chi_{\rm f}'(\zeta)$ and $\chi_{\rm m}'(\zeta)$ at infinity, we find that

$$\omega_1(\zeta) \;\sim\; a_0\zeta + O(\zeta^2) \qquad \text{as } \zeta \to 0\,, \tag{2.62}$$

$$\omega_1(\zeta) \;\sim\; -a_0\frac{a^2}{\zeta} + O(\zeta^{-2}) \qquad \text{as } \zeta \to \infty\,, \tag{2.63}$$

$$\omega_2(\zeta) \;\sim\; -\frac{{\rm i}\tau_0}{G_{\rm m}}\zeta + O(\zeta^{-1}) \qquad \text{as } \zeta \to \infty\,, \tag{2.64}$$

$$\omega_2(\zeta) \;\sim\; -\frac{{\rm i}\tau_0}{G_{\rm m}}\frac{a^2}{\zeta} + O(\zeta) \qquad \text{as } \zeta \to 0\,, \tag{2.65}$$

where a_0 is some constant. The problem has thus reduced to finding the two functions $\omega_1(\zeta)$ and $\omega_2(\zeta)$ which are analytic on the whole complex plane cut along L'', and

which satisfy equations (2.60) and (2.61) on L'' together with (2.62)–(2.65) at infinity and zero.

Now, consider the function

$$H(\zeta) \;=\; G_{\rm f}\omega_1 + G_{\rm m}\omega_2 + {\rm i}\tau_0\zeta + \frac{{\rm i}\tau_0 a^2}{\zeta}\;. \tag{2.66}$$

This is analytic on $\mathbb{C}$ by (2.60), and we have $H(\zeta) \to 0$ as $\zeta \to 0, \infty$ by (2.62)–(2.65). Thus H is bounded on $\mathbb{C}$ and analytic, so by Liouville's theorem, $H = \text{constant} = 0$. This gives us

$$G_{\rm f}\omega_1(\zeta) + G_{\rm m}\omega_2(\zeta) \;=\; -{\rm i}\tau_0\left(\zeta + \frac{a^2}{\zeta}\right)\;. \tag{2.67}$$

This leaves us with the problem of finding the function

$$\Phi(\zeta) = \omega_1(\zeta) - \omega_2(\zeta)\;, \tag{2.68}$$

which is analytic on $\mathbb{C} \setminus L''$, and which satisfies

$$\Phi^+(\sigma) \;=\; -\Phi^-(\sigma) \qquad \text{on } L'', \tag{2.69}$$

by equation (2.61). This is a homogeneous Hilbert problem for open contours; an explanation of the problem and a solution method can be found in Green and Zerna [37].

The solution here is given by

$$\Phi(\zeta) \;=\; X(\zeta)R(\zeta)\;, \tag{2.70}$$

where

$$X(\zeta) \;=\; (\zeta - a_1)^{-1/2}(\zeta - b_1)^{-1/2}(\zeta - a_2)^{-1/2}(\zeta - b_2)^{-1/2}\;, \tag{2.71}$$

$$R(\zeta) \;=\; c_{-1}\zeta^{-1} + c_0 + c_1\zeta + c_2\zeta^2 + c_3\zeta^3\;, \tag{2.72}$$

and we take the branch of $X(\zeta)$ which is single-valued on the plane cut along L'' and which has the form

$$X(\zeta) \;\sim\; \zeta^{-2} + A_1\zeta^{-3} + \cdots \tag{2.73}$$

at infinity. The solution is finally determined by calculating the five constants c_k.

Once $\Phi(\zeta)$ is found, the functions $\omega_1(\zeta)$, $\omega_2(\zeta)$ can be found from equations (2.67) and (2.68). Solving these gives us

$$\omega_1(\zeta) \;=\; \frac{G_{\rm m}}{G_{\rm m}+G_{\rm f}}\Phi(\zeta) - \frac{\rm i}{G_{\rm m}+G_{\rm f}}\tau_0\left(\zeta + \frac{a^2}{\zeta}\right)\;, \tag{2.74}$$

$$\omega_2(\zeta) \;=\; -\frac{G_{\rm f}}{G_{\rm m}+G_{\rm f}}\Phi(\zeta) - \frac{\rm i}{G_{\rm m}+G_{\rm f}}\tau_0\left(\zeta + \frac{a^2}{\zeta}\right)\;. \tag{2.75}$$

Hence, on using the limits of $\omega_2(\zeta)$ at infinity and zero in equations (2.64) and (2.65), and the expansion (which can be found)

$$X(\zeta) \sim -\frac{1}{a^2} + B_1\zeta + O(\zeta^2) \qquad \text{as } \zeta \to 0, \tag{2.76}$$

we find that

$$c_{-1} = -\frac{\mathrm{i}\tau_0 a^4}{G_\mathrm{m}}\,, \tag{2.77}$$

$$c_3 = \frac{\mathrm{i}\tau_0}{G_\mathrm{m}}\,. \tag{2.78}$$

By expanding $X(\zeta)$ at zero and infinity, it can be shown that A_1 and B_1 are both zero in the above expansions of $X(\zeta)$, and hence that c_0 and c_2 are also zero. We are left with the task of determining c_1. This comes from the condition that the difference in the displacement f at L_k'' is zero for each $k = 1, 2$, *i.e.* for each attached arc.

So we require

$$[f_1 - f_2]_{L''} = 0 \tag{2.79}$$

$$\Rightarrow \qquad \int_{L''} \left(\frac{\partial f_1}{\partial\theta} - \frac{\partial f_2}{\partial\theta}\right) \mathrm{d}\theta = 0 \tag{2.80}$$

$$\Rightarrow \qquad \int_{L''} \left[\omega_1^+(\sigma) + \omega_1^-(\sigma) - \omega_2^+(\sigma) - \omega_2^-(\sigma)\right] \mathrm{d}\theta = 0 \tag{2.81}$$

$$\Rightarrow \qquad \int_{L''} (\Phi^+ + \Phi^-)\,\mathrm{d}\theta = 0 \tag{2.82}$$

$$\Rightarrow \qquad \int_{L''} \Phi^-\,\mathrm{d}\theta = 0 \tag{2.83}$$

$$\Rightarrow \qquad \int_{L''} X^-(\sigma)R(\sigma)\,\mathrm{d}\theta = 0\,. \tag{2.84}$$

Some algebraic manipulation (taking care of course with the branch cuts) shows that (recalling $\sigma = a\mathrm{e}^{\mathrm{i}\theta}$)

$$X^-(a\mathrm{e}^{\mathrm{i}\theta}) = |X^-(a\mathrm{e}^{\mathrm{i}\theta})|\mathrm{e}^{\mathrm{i}\Theta}\,, \tag{2.85}$$

where

$$|X^-(a\mathrm{e}^{\mathrm{i}\theta})| = \frac{1}{\sqrt{2}a^2\sqrt{\cos 2\theta - \cos 2\theta_0}} \tag{2.86}$$

$$\begin{aligned}\Theta = -\frac{1}{2}\Bigg[&\tan^{-1}\left(\frac{\sin\theta - \sin\theta_0}{\cos\theta - \cos\theta_0}\right) + \tan^{-1}\left(\frac{\sin\theta - \sin\theta_0}{\cos\theta + \cos\theta_0}\right) \\ &+ \tan^{-1}\left(\frac{\sin\theta + \sin\theta_0}{\cos\theta + \cos\theta_0}\right) + \tan^{-1}\left(\frac{\sin\theta + \sin\theta_0}{\cos\theta - \cos\theta_0}\right)\Bigg]\,.\end{aligned} \tag{2.87}$$

We choose the branch of the inverse trigonometric functions such that

$$\tan^{-1} x + \cot^{-1} x = \frac{\pi}{2}\,. \tag{2.88}$$

We also choose

$$\tan^{-1}(\tan x) \;=\; x - n\pi \;, \tag{2.89}$$

where $n \in \mathbb{N}$ is chosen so that $-\pi/2 < x - n\pi < \pi/2$, and

$$\cot^{-1}(\cot x) \;=\; x - n\pi \;, \tag{2.90}$$

where $n \in \mathbb{N}$ is chosen so that $0 < x - n\pi < \pi$. Then, using trigonometric identities we find that Θ simplifies to give

$$\mathrm{e}^{\mathrm{i}\Theta} \;=\; \mathrm{e}^{-\mathrm{i}\theta} \qquad \text{for } -\theta_0 < \theta < \theta_0 \;, \tag{2.91}$$

$$\mathrm{e}^{\mathrm{i}\Theta} \;=\; -\mathrm{e}^{-\mathrm{i}\theta} \qquad \text{for } \pi - \theta_0 < \theta < \pi + \theta_0 \;. \tag{2.92}$$

We will substitute these values into equation (2.84) to find c_1. We will calculate the integral around L_2'', which is the arc from $\theta = -\theta_0$ to $\theta = \theta_0$ — choosing the other arc gives the same result. We obtain

$$\int_{-\theta_0}^{\theta_0} \frac{\left(\frac{c_{-1}}{a}\mathrm{e}^{-\mathrm{i}\theta} + ac_1\mathrm{e}^{\mathrm{i}\theta} + a^3c_3\mathrm{e}^{3\mathrm{i}\theta}\right)}{\sqrt{2}a^2\sqrt{\cos 2\theta - \cos 2\theta_0}} \cdot \mathrm{e}^{-\mathrm{i}\theta}\,\mathrm{d}\theta \;=\; 0 \;. \tag{2.93}$$

Using the results (2.77), (2.78) for c_{-1} and c_3, we find that this simplifies to

$$-\frac{\sqrt{2}\tau_0 a}{G_\mathrm{m}} \int_{-\theta_0}^{\theta_0} \frac{\sin 2\theta}{\sqrt{\cos 2\theta - \cos 2\theta_0}}\,\mathrm{d}\theta + \frac{c_1}{\sqrt{2}a} \int_{-\theta_0}^{\theta_0} \frac{\mathrm{d}\theta}{\sqrt{\cos 2\theta - \cos 2\theta_0}} \;=\; 0 \;. \tag{2.94}$$

The integrands are respectively odd and even, so the first integral is zero while the second is nonzero. This tells us that $c_1 = 0$. Therefore

$$R(\zeta) \;=\; \frac{\mathrm{i}\tau_0 a^3}{G_\mathrm{m}} \left(\frac{\zeta^3}{a^3} - \frac{a}{\zeta}\right) \;. \tag{2.95}$$

2.3.1 Calculation of stress intensity factors

We will now attempt to find the stress intensity factor of the τ_{rz} component of stress at the crack tip $\zeta = a\mathrm{e}^{\mathrm{i}\theta_0}$. By symmetry it should be the same at the other crack tips. We will consider the stress along the arc a_1b_2 in Figure 2.2, assuming that the stress has a square-root-singularity in the arc-length parameter $a\psi$, ψ being the angle measured anticlockwise from a_1.

By the previous section, the stress τ_{rz} at $\zeta = \sigma$ in the matrix is given by

$$\tau_{rz}\big|_{\zeta=\sigma} \;=\; \Re\left[\frac{G_\mathrm{m}\sigma}{a}\chi_\mathrm{m}'(\sigma)\right] \tag{2.96}$$

$$\;=\; \Re\left[\frac{G_\mathrm{m}}{a}\omega_2^-(\sigma)\right] \tag{2.97}$$

$$\;=\; -\frac{G_\mathrm{m}}{a}\Re\left[\frac{G_\mathrm{f}\Phi^-(\sigma)}{G_\mathrm{m}+G_\mathrm{f}} + \frac{\mathrm{i}\tau_0}{G_\mathrm{m}+G_\mathrm{f}}\left(\sigma + \frac{a^2}{\sigma}\right)\right] \;. \tag{2.98}$$

We will be looking near the crack tips, where the square root singularity from the $\Phi(\zeta)$ term dominates. Therefore, near here,

$$\tau_{rz}|_{\zeta=\sigma} \sim -\frac{G_{\rm m}G_{\rm f}}{a(G_{\rm m}+G_{\rm f})}\Re\left(\Phi^-(\sigma)\right) \tag{2.99}$$

$$= \frac{G_{\rm f}\tau_0 a^2}{G_{\rm m}+G_{\rm f}}\Re\left(\mathrm{i}X^-(\sigma)\left(\frac{a}{\sigma}-\frac{\sigma^3}{a^3}\right)\right) . \tag{2.100}$$

As stated previously, we wish to find τ_{rz} at $\zeta = a\exp(\mathrm{i}(\theta_0-\psi))$, which is

$$\tau_{rz}|_{\zeta=a\exp(\mathrm{i}(\theta_0-\psi))} \sim \frac{G_{\rm f}\tau_0 a^2}{G_{\rm m}+G_{\rm f}}\Re\left[\mathrm{i}X^-(a\mathrm{e}^{\mathrm{i}(\theta_0-\psi)})(\mathrm{e}^{\mathrm{i}(\psi-\theta_0)}-\mathrm{e}^{3\mathrm{i}(\theta_0-\psi)})\right] , \tag{2.101}$$

or, by equations (2.85)–(2.87),

$$\tau_{rz}|_{\zeta=a\mathrm{e}^{\mathrm{i}(\theta_0-\psi)}} \sim \frac{G_{\rm f}\tau_0}{(G_{\rm m}+G_{\rm f})\sqrt{2}\sqrt{\cos 2(\theta_0-\psi)-\cos 2\theta_0}} \times\Re\left[\mathrm{i}\mathrm{e}^{\mathrm{i}(\psi-\theta_0)}\left(\mathrm{e}^{\mathrm{i}(\psi-\theta_0)}-\mathrm{e}^{3\mathrm{i}(\theta_0-\psi)}\right)\right] \tag{2.102}$$

$$= \frac{\sqrt{2}G_{\rm f}\tau_0\sin 2(\theta_0-\psi)}{(G_{\rm m}+G_{\rm f})\sqrt{\cos 2(\theta_0-\psi)-\cos 2\theta_0}} . \tag{2.103}$$

Now, we assume that

$$\tau_{rz}|_{\zeta=a\mathrm{e}^{\mathrm{i}(\theta_0-\psi)}} = \frac{K_{rz}}{\sqrt{a\psi}}+\cdots \tag{2.104}$$

for small $a\psi$, where K_{rz} is the stress intensity factor. We find that

$$K_{rz} = \lim_{\psi\to 0}\sqrt{a\psi}\;\tau_{rz}|_{\zeta=a\mathrm{e}^{\mathrm{i}(\theta_0-\psi)}} \tag{2.105}$$

$$= \lim_{\psi\to 0}\left[\frac{\sqrt{2a\psi}G_{\rm f}\tau_0\sin 2(\theta_0-\psi)}{(G_{\rm m}+G_{\rm f})\sqrt{\cos 2(\theta_0-\psi)-\cos 2\theta_0}}\right] \tag{2.106}$$

$$= \frac{G_{\rm f}\tau_0\sqrt{a\sin 2\theta_0}}{G_{\rm m}+G_{\rm f}} . \tag{2.107}$$

In order to model the debonding of the material from the inclusion, we will model the interface as a crack where the material has debonded, and a *potential* crack where it has not. We apply the Griffith criterion for crack opening, which states that the crack will extend if the energy released in doing so is greater than the additional surface energy of the crack.[2] This is equivalent to saying that the crack opens if the stress intensity factor increases past a critical parameter $K_{\rm crit}$ [87]. This leads to a condition on τ_0 for crack growth,

$$K_{rz} \geqslant K_{\rm crit} \tag{2.108}$$

$$\Rightarrow \quad \tau_0 \geqslant \frac{(G_{\rm f}+G_{\rm m})K_{\rm crit}}{G_{\rm f}\sqrt{a\sin 2\theta_0}} . \tag{2.109}$$

[2] A more physically realistic model of crack growth is the Barenblatt model, which assumes that near the crack tip there exists a region where cohesive forces ameliorate the singularity in the stress component. However, Willis [97] showed that the Barenblatt and Griffith models only differ for *dynamic* crack propagation, as opposed to static (or quasistatic) deformations, as we consider here.

However, if we assume that $\theta_0 = \pi/2$ at the start of the process, then we would require an infinite stress at infinity to begin debonding. To resolve this problem we assume that *there already exists* a small crack, so that we start not from $\theta_0 = \pi/2$ but from $\theta_0 = \pi/2 - \varepsilon$, where $\varepsilon \ll 1$. This is a reasonable assumption because it is unlikely that the bonding of an inclusion is ever perfect. The one simplification that we make is that the initially debonded patches are at the poles, at the region of greatest strain.

Now, we find that if there exists a crack with $\theta_0 = \pi/2 - \varepsilon$, then as soon as τ_0 satisfies (2.109), the crack will extend a little. But this implies that θ_0 decreases, so the right-hand side of (2.109) decreases. Therefore the extended crack also satisfies (2.109) at this value of τ_0, decreasing θ_0 even more. We find that θ_0 continues decreasing until $\theta = \varepsilon$. Therefore, as soon as a critical stress τ_{crit} is reached, the crack goes from $\theta_0 = \pi/2 - \varepsilon$ to $\theta_0 = \varepsilon$ instantaneously, with any further increase of stress decreasing θ_0 still further (but never actually reaching 0). In practical terms, we consider the transition being from a fully bonded inclusion to full decohesion, as soon as $\tau_0 \geqslant \tau_{\text{crit}}$. The critical stress is given by

$$\tau_{\text{crit}} = \frac{G_{\text{f}} + G_{\text{m}}}{G_{\text{f}}} \frac{K_{\text{crit}}}{\sqrt{a \sin 2(\frac{\pi}{2} - \varepsilon)}} \tag{2.110}$$

$$= \frac{G_{\text{f}} + G_{\text{m}}}{G_{\text{f}}} \frac{\widetilde{K}_{\text{crit}}}{\sqrt{a}} \,, \tag{2.111}$$

where

$$\widetilde{K}_{\text{crit}} = \frac{K_{\text{crit}}}{\sqrt{\sin 2\varepsilon}} \tag{2.112}$$

is a modified stress intensity factor.

2.4 Homogenisation

The second part of this chapter involves the consideration of a distribution of inclusions. The theory of finding the effective material constants of a medium based on its microscale is known as homogenisation. We will consider two different homogenisation methods. Firstly we will analyse multiple-scales homogenisation, where inclusions can be as close as is necessary to each other, but need to be arranged in a grid. Secondly we will look at a method which is easier to apply and is not restricted to a grid structure, but which assumes that the inclusions are placed far from each other. Finally we will compare the two methods to see whether we could be justified in using the second, simpler method rather than the more complicated multiple scales approach.

The model (2.9) is mathematically identical to a number of other physical phenomena, many of which are listed by Batchelor [3]. This has resulted in an active field of research in the homogenisation of material properties relating to these phenomena. The constants which take the place of G in (2.9) are known as transport properties in the other models, which include:

- Conduction of heat or electrical current, for which the transport property is the thermal or electrical conductivity κ or σ;
- Steady flow in a porous medium, for which the transport property is the Darcy parameter k/μ; here k is the permeability while μ is the fluid's viscosity;
- The electric field in an insulating material, for which the transport property is the dielectric constant ε.

2.4.1 Multiple-scales homogenisation

Multiple scale analysis can be used when there are at least two length scales involved in the problem. In our case, we have the long scale (the dimensions of the material itself) and the short scale or microscale (the dimensions of the inclusions). We assume that the properties of the material are doubly periodic in the small scale. The methodology used in the solution of such problems is well-established; see for example [7, 84, 2]. What follows is an overview of the method, specifically for the case where the microscale is a square lattice of small side ε, that $\boldsymbol{x} = (x_1, x_2)$, and that we want to solve the equation

$$\frac{\partial}{\partial x_i}\left(a\left(\boldsymbol{x}, \frac{\boldsymbol{x}}{\varepsilon}\right)\frac{\partial f}{\partial x_i}\right) \;=\; q(\boldsymbol{x}) \tag{2.113}$$

(where the summation convention applies over $i = 1, 2$). There are specified boundary conditions around the boundary of the body (which could be of Dirichlet, Neumann or mixed type, but this has no effect on the homogenisation process), and $a(\boldsymbol{x}, \boldsymbol{x}/\varepsilon)$ is assumed to be periodic in both components of $\boldsymbol{x}/\varepsilon$ with period 1. In addition we suppose that $a > 0$.

We introduce a new coordinate

$$\boldsymbol{X} = \frac{\boldsymbol{x}}{\varepsilon} \tag{2.114}$$

which is the local, or 'fast' coordinate with components $\boldsymbol{X} = (X_1, X_2)$. We now treat $\boldsymbol{x}$ and $\boldsymbol{X}$ as independent variables, so that

$$\frac{\partial}{\partial x_k} \quad \text{becomes} \quad \frac{\partial}{\partial x_k} + \frac{1}{\varepsilon}\frac{\partial}{\partial X_k}\,, \tag{2.115}$$

which means that equation (2.113) becomes

$$\begin{aligned}\frac{1}{\varepsilon^2}\nabla_X\cdot\Big(a(\boldsymbol{x},\boldsymbol{X})\nabla_X f\Big)\\ +\frac{1}{\varepsilon}\Big[\nabla_X\cdot\Big(a(\boldsymbol{x},\boldsymbol{X})\nabla_x f\Big)+\nabla_x\cdot\Big(a(\boldsymbol{x},\boldsymbol{X})\nabla_X f\Big)\Big]\\ +\nabla_x\cdot\Big(a(\boldsymbol{x},\boldsymbol{X})\nabla_x f\Big) &= q(\boldsymbol{x})\,, \end{aligned}\qquad (2.116)$$

where $\nabla_x = \partial/\partial x_i$ and $\nabla_X = \partial/\partial X_i$. We expand f in an asymptotic expansion

$$f(\boldsymbol{x},\boldsymbol{X}) \;\sim\; f_0(\boldsymbol{x},\boldsymbol{X})+\varepsilon f_1(\boldsymbol{x},\boldsymbol{X})+\varepsilon^2 f_2(\boldsymbol{x},\boldsymbol{X})+\cdots\,, \qquad (2.117)$$

with each term 1-periodic in $\boldsymbol{X}$, and equate all the coefficients of successive powers of ε in equation (2.116) to zero. At $O(\varepsilon^{-2})$,

$$\nabla_X\cdot\Big(a(\boldsymbol{x},\boldsymbol{X})\nabla_X f_0\Big) \;=\; 0\,, \qquad (2.118)$$

with f_0 1-periodic in $\boldsymbol{X}$. However, the only 1-periodic solutions g to the equation

$$\frac{\partial}{\partial X_j}\left(b_{ij}(\boldsymbol{x},\boldsymbol{X})\frac{\partial g}{\partial X_i}\right) \;=\; 0 \qquad (2.119)$$

are those which are constant in $\boldsymbol{X}$ (provided that the matrix (b_{ij}) is positive definite, which is the case here since $a>0$). Hence we have $f_0 = f_0(\boldsymbol{x})$.

In light of this, the $O(\varepsilon^{-1})$ equation becomes

$$\nabla_X\cdot\Big(a(\boldsymbol{x},\boldsymbol{X})\nabla_X f_1\Big) \;=\; -\nabla_X a\cdot\nabla_x f_0\,. \qquad (2.120)$$

Now, according to the Fredholm alternative solvability condition, this (inhomogeneous self-adjoint) equation has no periodic solutions f_1 unless the integral over the domain of $\boldsymbol{X}$ (the unit cell) of the right-hand side of the equation multiplied by the solution of the homogeneous equation equals zero. By equation (2.119), solutions of the homogeneous equation are constant in $\boldsymbol{X}$, so

$$\int_{\substack{\text{unit}\\ \text{cell}}} \nabla_X a\cdot\nabla_x f_0\,\mathrm{d}X_1\,\mathrm{d}X_2 \;=\; 0\,, \qquad (2.121)$$

where we take any unit cell of the lattice. However, if $p(\boldsymbol{X})$ is any function periodic on the unit cell, it can easily be verified that

$$\int_0^1\int_0^1 \frac{\partial p}{\partial X_i}\,\mathrm{d}X_1\,\mathrm{d}X_2 \;=\; 0\,. \qquad (2.122)$$

Therefore, condition (2.121) is satisfied identically. To solve equation (2.120) we assume that $f_1(\boldsymbol{x},\boldsymbol{X})$ has the form

$$f_1(\boldsymbol{x},\boldsymbol{X}) \;=\; \chi_j(\boldsymbol{x},\boldsymbol{X})\frac{\partial f_0}{\partial x_j}+\widehat{f}_1(\boldsymbol{x}) \qquad (2.123)$$

(the summation convention applies here), where $\widehat{f}_1(\boldsymbol{x})$ is an arbitrary function which has no effect on our solution. Then, from equation (2.120),

$$\left[\frac{\partial}{\partial X_i}\left(a(\boldsymbol{x},\boldsymbol{X})\frac{\partial\chi_j}{\partial X_i}\right)+\frac{\partial a}{\partial X_j}\right]\frac{\partial f_0}{\partial x_j} \;=\; 0\,. \tag{2.124}$$

This is true for arbitrary $\partial f_0/\partial x_j$ only if

$$\frac{\partial}{\partial X_i}\left(a(\boldsymbol{x},\boldsymbol{X})\frac{\partial\chi_j}{\partial X_i}\right)+\frac{\partial a}{\partial X_j} \;=\; 0 \tag{2.125}$$

for $j=1,2$.

We have now reached the essential stage of the homogenisation procedure, namely the *cell problem*. This requires finding 1-periodic functions $\chi_j(\boldsymbol{x},\boldsymbol{X})$ that satisfy equation (2.125). Note that any solution of this will be unique up to the addition of an arbitrary function of $\boldsymbol{x}$: consideration of $\Delta\chi_j=\chi_j-\widetilde{\chi}_j$ for two solutions $\chi_j,\widetilde{\chi}_j$ gives us

$$\frac{\partial}{\partial X_i}\left(a(\boldsymbol{x},\boldsymbol{X})\frac{\partial}{\partial X_i}\Delta\chi_j\right) \;=\; 0\,, \tag{2.126}$$

whose solution is an arbitrary function of $\boldsymbol{x}$ as in equation (2.119). This is why $\widehat{f}_1(\boldsymbol{x})$ is arbitrary in equation (2.123).

Once we know the functions $\chi_j(\boldsymbol{x},\boldsymbol{X})$, we can proceed to the $O(1)$ equation,

$$\begin{aligned}\nabla_X\cdot\Big(a(\boldsymbol{x},\boldsymbol{X})\nabla_X f_2\Big) \;=\; & q(\boldsymbol{x})-\nabla_X\cdot\Big(a(\boldsymbol{x},\boldsymbol{X})\nabla_x f_1\Big)-\nabla_x\cdot\Big(a(\boldsymbol{x},\boldsymbol{X})\nabla_X f_1\Big)\\ & -\nabla_x\cdot\Big(a(\boldsymbol{x},\boldsymbol{X})\nabla_x f_0\Big)\,.\end{aligned} \tag{2.127}$$

By the Fredholm alternative we demand that the integral of the right hand side over the unit cell in $\boldsymbol{X}$ is zero, for the same reason as our previous calculation at $O(\varepsilon^{-1})$. Apart from $q(\boldsymbol{x})$, which remains after integration, the first term is:

$$\mathscr{I}_1 \;=\; -\int_0^1\int_0^1\frac{\partial}{\partial X_i}\left(a\frac{\partial f_1}{\partial x_i}\right)\mathrm{d}X_1\,\mathrm{d}X_2\,. \tag{2.128}$$

However, this is zero because of (2.122).

Integrating the second term on the right hand side of equation (2.127) gives

$$\mathscr{I}_2 \;=\; -\int_0^1\int_0^1\frac{\partial}{\partial x_i}\left(a\frac{\partial f_1}{\partial X_i}\right)\mathrm{d}X_1\,\mathrm{d}X_2 \tag{2.129}$$

$$\;=\; -\int_0^1\int_0^1\frac{\partial}{\partial x_i}\left(a\frac{\partial\chi_j}{\partial X_i}\frac{\partial f_0}{\partial x_j}\right)\mathrm{d}X_1\,\mathrm{d}X_2\,, \tag{2.130}$$

and for the third term we have

$$\mathscr{I}_3 \;=\; -\int_0^1\int_0^1\frac{\partial}{\partial x_i}\left(a\frac{\partial f_0}{\partial x_i}\right)\mathrm{d}X_1\,\mathrm{d}X_2\,. \tag{2.131}$$

We need $\mathscr{I}_1 + \mathscr{I}_2 + \mathscr{I}_3 + q(\boldsymbol{x}) = 0$, or

$$\int_0^1 \int_0^1 \frac{\partial}{\partial x_i} \left[a(\boldsymbol{x}, \boldsymbol{X}) \left(\delta_{ij} + \frac{\partial \chi_j}{\partial X_i} \right) \frac{\partial f_0}{\partial x_j} \right] \mathrm{d}X_1 \, \mathrm{d}X_2 \;=\; q(\boldsymbol{x}) \; . \tag{2.132}$$

This finally leads to the homogenised equation,

$$\frac{\partial}{\partial x_i} \left(\widehat{a}_{ij}(\boldsymbol{x}) \frac{\partial f_0}{\partial x_j} \right) \;=\; q(\boldsymbol{x}) \; , \tag{2.133}$$

where

$$\widehat{a}_{ij}(\boldsymbol{x}) \;=\; \int_0^1 \int_0^1 a(\boldsymbol{x}, \boldsymbol{X}) \left(\delta_{ij} + \frac{\partial \chi_j}{\partial X_i} \right) \mathrm{d}X_1 \, \mathrm{d}X_2 \tag{2.134}$$

are the homogenised coefficients. The matrix $(\widehat{a}_{ij})$ can be shown to be positive definite (see, for example, [21]).

2.4.1.1 A specific example

Due to the difficulty in determining the cell functions χ_j, there are few situations for which analytical solutions exist. As an example, consider the case where a is a function of X_2 only. One solution for the cell functions (and hence *the* solution, given that χ_j are unique up to an arbitrary function of $\boldsymbol{x}$) is that $\chi_1 = 0$, and that χ_2 satisfies

$$\frac{\partial \chi_2}{\partial X_1} \;=\; 0 \; , \tag{2.135}$$

$$\frac{\partial \chi_2}{\partial X_2} \;=\; \frac{1}{a(X_2) \displaystyle\int_0^1 \frac{\mathrm{d}X_2}{a(X_2)}} - 1 \; . \tag{2.136}$$

Then the homogenised coefficients become

$$\widehat{a}_{11} \;=\; \int_0^1 a(X_2) \, \mathrm{d}X_2 \; , \tag{2.137}$$

$$\widehat{a}_{12} \;=\; 0 \; , \tag{2.138}$$

$$\widehat{a}_{21} \;=\; 0 \; , \tag{2.139}$$

$$\widehat{a}_{22} \;=\; \frac{1}{\displaystyle\int_0^1 \frac{\mathrm{d}X_2}{a(X_2)}} \; , \tag{2.140}$$

one coefficient being the arithmetic average and the other being the harmonic average. In the analogous electrical conductivity problem, this is just the fact that wires connected in series have a resistivity which is the arithmetic average of the individual wires', whereas for wires connected in parallel the overall resistivity is the harmonic average.

2.4.1.2 Application to antiplane strain

We will now consider the antiplane shear at infinity of a material which consists of a periodic array of inclusions of radius $\varepsilon\gamma/2$, $0 < \gamma < 1$, whose centres are separated by a distance ε. The inclusions are assumed to have shear modulus G_{f}, and the matrix has a modulus of G_{m}. The system satisfies the equation

$$\frac{\partial}{\partial x_i}\left(a(\boldsymbol{x}/\varepsilon)\frac{\partial f}{\partial x_i}\right) \;=\; 0 \tag{2.141}$$

with stress conditions at infinity, irrelevant to the homogenisation procedure (although this is where the homogenised coefficients influence the solution). The quantity a takes the value G_{f} in the inclusion and G_{m} in the matrix.

This problem has already been considered by Cioranescu *et al.* [22] in the context of torsion of non-homogeneous elastic cylinders. The problem that will be presented has been solved before, in the context of electrical conductance, by Rayleigh [89], with improvements by Runge [82]. These solutions were recapped by Perrins *et al.* [81, 80], while Nicorovici and McPhedran [76] considered the equivalent problem for elliptic inclusions. However, none of these papers considered the problem from a multiple scales homogenisation viewpoint, as presented earlier in this section. Instead they simply assumed that the medium was infinitely large and periodic with an applied constant field at infinity. The advantage of the multiple-scales approach that we will study is that we can consider a material whose properties vary on a much larger scale than the inclusion's dimensions. In contrast the papers cited above only considered a strictly periodic medium. Nevertheless, they will serve to verify our workings.

The cell problem can be solved using complex variable methods and Rayleigh's multipole method [89] to ensure periodicity. In the notation of the previous section, we have $q(\boldsymbol{x}) = 0$, and $a(\boldsymbol{x}, \boldsymbol{X}) = a(\boldsymbol{X})$, given by

$$a(\boldsymbol{X}) \;=\; \begin{cases} G_{\mathrm{f}} & \text{if } \boldsymbol{X} \in P_{\mathrm{f}} \\ G_{\mathrm{m}} & \text{if } \boldsymbol{X} \in P_{\mathrm{m}}\,. \end{cases} \tag{2.142}$$

Of course, there is no reason why G_{f} and G_{m} are not able to be functions of $\boldsymbol{x}$, but for simplicity we will assume that they are constants. We define

$$P_{\mathrm{f}} \;=\; \left\{\boldsymbol{X} \in \left[-\frac{1}{2},\frac{1}{2}\right]^2 \;:\; |\boldsymbol{X}| \leqslant \frac{\gamma}{2}\right\}\,, \tag{2.143}$$

$$P_{\mathrm{m}} \;=\; \left[-\frac{1}{2},\frac{1}{2}\right]^2 \setminus P_{\mathrm{f}}\,, \tag{2.144}$$

as depicted in Figure 2.3. Thus the unit cell is now centred on the point $(0, 0)$ rather than $(1/2, 1/2)$ as in the theory of Section 2.4.1. This makes no practical difference but simplifies the mathematical derivation of the effective modulus.

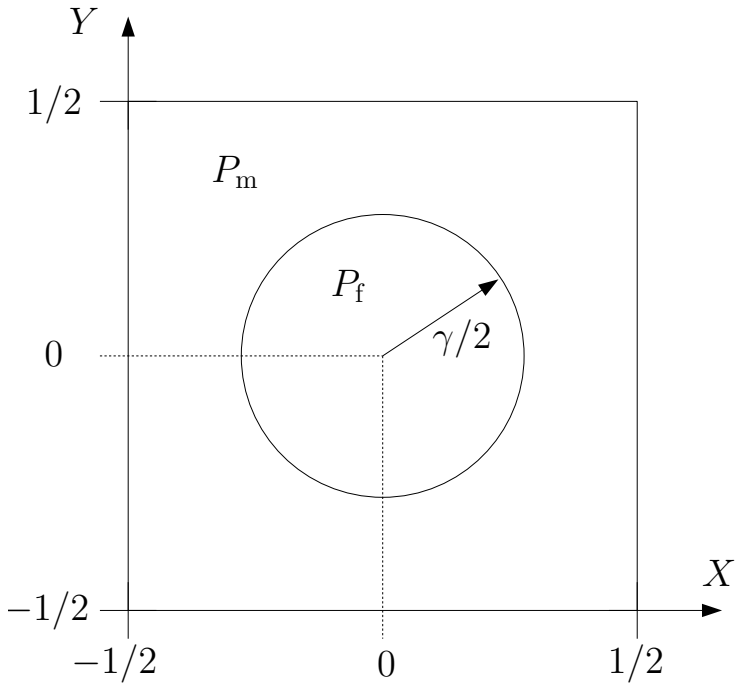

Figure 2.3: The unit cell.

The discontinuity of $a(\boldsymbol{X})$ creates difficulties in the homogenisation procedure which can be overcome by prescribing physically consistent conditions on the boundary between the inclusions and the matrix. In addition to the obvious continuity of displacement, we impose continuity of traction. In other words,

- f is continuous across $|\boldsymbol{X}| = \gamma/2$,
- $a\partial f/\partial n$ is continuous across $|\boldsymbol{X}| = \gamma/2$, where $\boldsymbol{n}$ is the unit normal vector to P_{f}.

Now we simply follow the method outlined earlier in this section. At leading order, we obtain

$$f_0 = f_0(\boldsymbol{x}) \tag{2.145}$$

from equation (2.118). At the next order, as in equation (2.125), we have a cell problem to solve,

$$\frac{\partial^2 \chi_j}{\partial X_i \, \partial X_i} \;=\; 0 \,, \tag{2.146}$$

in P_{f} and P_{m} separately. Three conditions apply to the two functions

$$\chi_j^{(\mathrm{f})} \;=\; \chi_j|_{P_{\mathrm{f}}} \,, \tag{2.147}$$

$$\chi_j^{(\mathrm{m})} \;=\; \chi_j|_{P_{\mathrm{m}}} \,, \tag{2.148}$$

namely periodicity, and continuity of displacement and traction. We need to express the traction condition in terms of χ_j. We could achieve this by expanding the traction $a\boldsymbol{n}\cdot\nabla f$ in powers of ε by using (2.115) and (2.117), but the result is the same as would be obtained by intergrating the equation (2.125) over the unit cell, namely that

$$\left[an_j + a\frac{\partial\chi_j}{\partial n}\right]^{(\mathrm{f})}_{(\mathrm{m})} = 0\,, \tag{2.149}$$

where $[\cdot]^{(\mathrm{f})}_{(\mathrm{m})}$ denotes the difference between the value in P_f and P_m across their boundary.

The cell problem thus reduces to solving the following:

$$\nabla^2\chi_j^{(\mathrm{f})} = 0 \qquad \text{in } P_\mathrm{f}\,, \tag{2.150}$$

$$\nabla^2\chi_j^{(\mathrm{m})} = 0 \qquad \text{in } P_\mathrm{m}\,, \tag{2.151}$$

$$\chi_j^{(\mathrm{m})} \text{ periodic} \qquad \text{on the unit cell}\,, \tag{2.152}$$

$$[\chi_j]^{(\mathrm{f})}_{(\mathrm{m})} = 0 \qquad \text{along } |\boldsymbol{X}| = \gamma/2\,, \tag{2.153}$$

$$\left[an_j + a\frac{\partial\chi_j}{\partial n}\right]^{(\mathrm{f})}_{(\mathrm{m})} = 0 \qquad \text{along } |\boldsymbol{X}| = \gamma/2\,. \tag{2.154}$$

2.4.1.3 Solution of the cell problem

The system is best solved by changing to complex variables,

$$Z = X_1 + \mathrm{i}X_2\,. \tag{2.155}$$

Then the solution of (2.150), as shown in Section 2.3, is given by

$$\chi_j^{(\mathrm{f})} = \frac{1}{2}\left[\phi_j^{(\mathrm{f})}(Z) + \overline{\phi_j^{(\mathrm{f})}(Z)}\right]\,, \tag{2.156}$$

which is the real part of the analytic function $\phi_j^{(\mathrm{f})}(Z)$. This we expand as a power series:

$$\phi_j^{(\mathrm{f})} = \sum_{n=0}^{\infty} a_n^j Z^n\,. \tag{2.157}$$

Similarly, the solution to equation (2.151) is

$$\chi_j^{(\mathrm{m})} = \frac{1}{2}\left[\phi_j^{(\mathrm{m})}(Z) + \overline{\phi_j^{(\mathrm{m})}(Z)}\right]\,, \tag{2.158}$$

$$\text{where} \qquad \phi_j^{(\mathrm{m})} = b_0^j + \sum_{n=1}^{\infty}(b_n^j Z^n + c_n^j Z^{-n})\,. \tag{2.159}$$

The function $\phi_j^{(\mathrm{m})}(Z)$ is expanded as a Laurent series rather than a power series because it is defined on an annulus containing P_m. There is no logarithmic term in

this quantity for the same reason as that explained in Section 2.3 on page 17. Now, since any periodic function remains periodic after the addition of a constant, we may set $a_0^j = 0$ without loss of generality, by subtracting from the whole solution its value at the origin.

To ensure that (2.152) is satisfied, we turn to Rayleigh's multipole method [89]. Any function that is holomorphic on the punctured plane $0 < |Z - (k + \mathrm{i}l)| < \infty$ can be written as

$$\mathscr{F}_{(k,l)} \;=\; \beta_0 + \sum_{n=1}^{\infty} \Big[\beta_n \big(Z - (k+\mathrm{i}l)\big)^n + \gamma_n \big(Z - (k+\mathrm{i}l)\big)^{-n} \Big] \;. \qquad (2.160)$$

Using this, we can construct a doubly-periodic function $\widetilde{\mathscr{F}}$, holomorphic except at the cell centres, by summing over all integer pairs (k, l):

$$\widetilde{\mathscr{F}} \;=\; \sum_{k=-\infty}^{\infty} \sum_{l=-\infty}^{\infty} \mathscr{F}_{(k,l)} \;, \qquad (2.161)$$

assuming that β_n, γ_n are chosen so that $\widetilde{\mathscr{F}}$ converges (in particular we must set $\beta_0 = 0$). By setting $\phi_j^{(\mathrm{m})} = \widetilde{\mathscr{F}}$, we hope to satisfy the periodicity constraint by forming a relation between the coefficients b_n^j and c_n^j. Thus

$$\sum_{n=1}^{\infty} \Bigg\{ \sum_{k=-\infty}^{\infty} \sum_{l=-\infty}^{\infty} \Big[\beta_n \big(Z - (k+\mathrm{i}l)\big)^n + \gamma_n \big(Z - (k+\mathrm{i}l)\big)^{-n} \Big] - b_n^j Z^n - c_n^j Z^{-n} \Bigg\} - b_0^j \;=\; 0 \;. \qquad (2.162)$$

Now,

$$\eta \;:=\; \sum_{n=1}^{\infty} \sum_{k=-\infty}^{\infty} \sum_{l=-\infty}^{\infty} \beta_n \big(Z - (k+\mathrm{i}l)\big)^n \qquad (2.163)$$

is a function which is analytic on $\mathbb{C}$ and periodic. Since it has no poles it is bounded on $\mathbb{C}$, and hence (by Liouville's theorem) it is constant. Then

$$\sum_{n=1}^{\infty} \Bigg\{ \sum_{k=-\infty}^{\infty} \sum_{l=-\infty}^{\infty} \gamma_n \big(Z - (k+\mathrm{i}l)\big)^{-n} - b_n^j Z^n - c_n^j Z^{-n} \Bigg\} - (b_0^j - \eta) \;=\; 0 \;. \qquad (2.164)$$

By the linear independence of the remaining terms in the double sum we see that we must have $\gamma_n = c_n^j$. Then, on defining

$$\Lambda \;=\; \big\{ (k,l) \in \mathbb{Z}^2 \;:\; (k,l) \neq (0,0) \big\} \;, \qquad (2.165)$$

we obtain

$$\sum_{n=1}^{\infty} \Bigg\{ \sum_{(k,l)\in\Lambda} c_n^j \big(Z - (k+\mathrm{i}l)\big)^{-n} - b_n^j Z^n \Bigg\} - (b_0^j - \eta) \;=\; 0 \;. \qquad (2.166)$$

Now, note that

$$\big(Z-(k+\mathrm{i}l)\big)^{-n} \;=\; \sum_{m=0}^{\infty}\binom{n+m-1}{m}(-1)^n(k+\mathrm{i}l)^{-(n+m)}Z^m\;, \qquad (2.167)$$

so that

$$\sum_{n=1}^{\infty}\left\{\sum_{(k,l)\in\Lambda}c_n^j\sum_{m=0}^{\infty}\binom{n+m-1}{m}(-1)^n(k+\mathrm{i}l)^{-(n+m)}Z^m-b_n^jZ^n\right\} -(b_0^j-\eta) \;=\; 0\;. \qquad (2.168)$$

We define

$$S_n \;=\; \sum_{(k,l)\in\Lambda}(k+\mathrm{i}l)^{-n}\;. \qquad (2.169)$$

These are known as *Coulombic lattice sums* and have been computed by Huang [47]. In our geometry, for $n\geqslant 3$ we have $S_n=0$ unless n is a multiple of 4. The lattice sums are absolutely convergent, apart from the special case S_2 which we will discuss later [89].

Our relation now becomes

$$\sum_{n=1}^{\infty}c_n^j\sum_{m=0}^{\infty}\left[\binom{n+m-1}{m}(-1)^nS_{n+m}Z^m\right] \;=\; (b_0^j-\eta)+\sum_{n=1}^{\infty}b_n^jZ^n\;. \qquad (2.170)$$

Equating term-by-term, we get

$$\sum_{n=1}^{\infty}c_n^j(-1)^n\binom{n+k-1}{k}S_{n+k} \;=\; b_k^j \qquad (2.171)$$

for $k=1,2,3,\ldots$; and $b_0^j=\eta$, namely that b_0^j is an undetermined constant.

In order to satisfy equation (2.153), we simply substitute $Z=\frac{1}{2}\gamma\mathrm{e}^{\mathrm{i}\theta}$ into the expressions for $\chi_j^{(\mathrm{f})}$ and $\chi_j^{(\mathrm{m})}$ and equate powers of $\mathrm{e}^{\mathrm{i}\theta}$ in each expression. We obtain

$$\sum_{n=1}^{\infty}\left[a_n^j\frac{\gamma^n}{2^n}\mathrm{e}^{\mathrm{i}n\theta}+\overline{a_n^j}\frac{\gamma^n}{2^n}\mathrm{e}^{-\mathrm{i}n\theta}\right] \;=\; \Re b_0^j+\sum_{n=1}^{\infty}\left[b_n^j\frac{\gamma^n}{2^n}\mathrm{e}^{\mathrm{i}n\theta}+\overline{b_n^j}\frac{\gamma^n}{2^n}\mathrm{e}^{-\mathrm{i}n\theta}+c_n^j\frac{\gamma^{-n}}{2^{-n}}\mathrm{e}^{-\mathrm{i}n\theta}+\overline{c_n^j}\frac{\gamma^{-n}}{2^{-n}}\mathrm{e}^{\mathrm{i}n\theta}\right]\;, \qquad (2.172)$$

giving us $\Re b_0^j=0$ (we may also set $\Im b_0^j=0$ since this value is never used) and a condition for each n and j,

$$\overline{c_n^j} \;=\; \left(\frac{\gamma}{2}\right)^{2n}(a_n^j-b_n^j)\;. \qquad (2.173)$$

We can treat the traction condition (2.154) in a similar way. In complex coordinates it reduces to

$$\left[a(Z+\bar{Z})+2a\left(Z\frac{\partial\chi_1}{\partial Z}+\bar{Z}\frac{\partial\chi_1}{\partial\bar{Z}}\right)\right]_{(\mathrm{m})}^{(\mathrm{f})} = 0 \qquad (j=1)\,, \quad (2.174)$$

$$\left[-a\mathrm{i}(Z-\bar{Z})+2a\left(Z\frac{\partial\chi_2}{\partial Z}+\bar{Z}\frac{\partial\chi_2}{\partial\bar{Z}}\right)\right]_{(\mathrm{m})}^{(\mathrm{f})} = 0 \qquad (j=2)\,. \quad (2.175)$$

Following the same process of equating powers of $\mathrm{e}^{\mathrm{i}\theta}$ gives us the final relation

$$\overline{c_n^j} = \left(\frac{\gamma}{2}\right)^{2n}\left[(b_n^j+I_n^j)-\alpha(a_n^j+I_n^j)\right]\,, \quad (2.176)$$

where

$$I_n^j = \begin{cases} +1 & n=1,\ j=1 \\ -\mathrm{i} & n=1,\ j=2 \\ 0 & n>1\,, \end{cases} \quad (2.177)$$

and

$$\alpha = \frac{G_{\mathrm{f}}}{G_{\mathrm{m}}}\,. \quad (2.178)$$

The functions χ_j are therefore determined by the values of the constants a_n^j, b_n^j and c_n^j, which are given by the simultaneous solution of equations (2.171), (2.173) and (2.176). By writing

$$a_n^j = \left(\frac{2}{1-\alpha}\right)\overline{d_n^j}-I_n^j\,, \quad (2.179)$$

$$b_n^j = \left(\frac{1+\alpha}{1-\alpha}\right)\overline{d_n^j}-I_n^j\,, \quad (2.180)$$

$$c_n^j = \left(\frac{\gamma}{2}\right)^{2n} d_n^j\,, \quad (2.181)$$

we can turn this system into one set of equations,

$$\left(\frac{1+\alpha}{1-\alpha}\right)\overline{d_n^j}-I_n^j = \sum_{m=1}^{\infty}(-1)^m\left(\frac{\gamma}{2}\right)^{2m} d_m^j\binom{m+n-1}{n}S_{m+n}\,. \quad (2.182)$$

Now let $d_n^j=\phi_n^j+\mathrm{i}\psi_n^j$. Consider first the case $j=1$. As I_n^1 is real, we find (assuming that the system is nonsingular) that $\psi_n^1=0$ for each n, on taking real and imaginary parts. Similarly, for $j=2$, we find that $\phi_n^2=0$ for each n, as I_n^2 is purely imaginary. Thus we write

$$\phi_n = \phi_n^1\,, \quad (2.183)$$

$$\psi_n = \psi_n^2\,, \quad (2.184)$$

and we have the solution to the cell problem,

$$\chi_1^{(\mathrm{f})} = -X_1 + \Re\left[\sum_{n=1}^{\infty}\left(\frac{2}{1-\alpha}\right)\phi_n Z^n\right] , \tag{2.185}$$

$$\chi_1^{(\mathrm{m})} = -X_1 + \Re\left[\sum_{n=1}^{\infty}\left\{\left(\frac{1+\alpha}{1-\alpha}\right)\phi_n Z^n + \left(\frac{\gamma}{2}\right)^{2n}\phi_n Z^{-n}\right\}\right] , \tag{2.186}$$

$$\chi_2^{(\mathrm{f})} = -X_2 + \Re\left[\sum_{n=1}^{\infty}\left(\frac{-2\mathrm{i}}{1-\alpha}\right)\psi_n Z^n\right] , \tag{2.187}$$

$$\chi_2^{(\mathrm{m})} = -X_2 + \Re\left[\sum_{n=1}^{\infty}\left\{-\mathrm{i}\left(\frac{1+\alpha}{1-\alpha}\right)\psi_n Z^n + \mathrm{i}\left(\frac{\gamma}{2}\right)^{2n}\psi_n Z^{-n}\right\}\right] , \tag{2.188}$$

where the constants ϕ_n and ψ_n are given by

$$\left(\frac{1+\alpha}{1-\alpha}\right)\phi_n - \delta_{1n} = \sum_{m=1}^{\infty}(-1)^m\left(\frac{\gamma}{2}\right)^{2m}\phi_m\binom{m+n-1}{n}S_{m+n} , \tag{2.189}$$

$$-\left(\frac{1+\alpha}{1-\alpha}\right)\psi_n + \delta_{1n} = \sum_{m=1}^{\infty}(-1)^m\left(\frac{\gamma}{2}\right)^{2m}\psi_m\binom{m+n-1}{n}S_{m+n} . \tag{2.190}$$

Here δ_{1n} is the Kronecker delta. For periodicity to hold we must take $S_2 = \pi$ in equation (2.189), and $S_2 = -\pi$ in equation (2.190). Rayleigh [89] chose $S_2 = \pi$ on the basis that his composite material was infinitely longer in one of the principal directions than the other. In our case this is not an option, given that the dimensions of the macro-scale body have no effect on the homogenisation process. However, we show in Section C.1 of Appendix C that if S_2 doesn't take the values above, the functions χ_j would not be periodic. Additionally, it can be verified that

$$\psi_n = (-1)^{(n-1)/2}\phi_n , \tag{2.191}$$

using the behaviour of the lattice sums S_k. Thus ϕ_n, ψ_n are zero unless n is odd.

Having (theoretically) determined the functions χ_j by a numerical method for the coefficients ϕ_n, ψ_n, we can substitute them into equation (2.134) and integrate to find the constant homogenised coefficients $\widehat{a}_{ij}$.

2.4.1.4 Homogenised coefficients

From equation (2.134), we see that the homogenised coefficients of the problem become

$$\widehat{a}_{ij} = G_{\mathrm{f}}\int_{P_{\mathrm{f}}}\left(\delta_{ij} + \frac{\partial\chi_j^{(\mathrm{f})}}{\partial X_i}\right)\mathrm{d}^2\boldsymbol{X} + G_{\mathrm{m}}\int_{P_{\mathrm{m}}}\left(\delta_{ij} + \frac{\partial\chi_j^{(\mathrm{m})}}{\partial X_i}\right)\mathrm{d}^2\boldsymbol{X} . \tag{2.192}$$

Consider first the integral over P_{m}, which we denote by

$$\mathscr{I}_{ij} = G_{\mathrm{m}}\int_{P_{\mathrm{m}}}\left(\delta_{ij} + \frac{\partial\chi_j}{\partial X_i}\right)\mathrm{d}^2\boldsymbol{X} , \tag{2.193}$$

where

$$\chi_j \;=\; -X_j + K_j + L_j \;, \tag{2.194}$$

and the functions K_j and L_j are given by

$$K_1 \;=\; \Re\left[\sum_{n=1}^{\infty}\left(\frac{1+\alpha}{1-\alpha}\right)\phi_n Z^n\right] \;, \tag{2.195}$$

$$K_2 \;=\; \Re\left[\sum_{n=1}^{\infty}\left(\frac{1+\alpha}{1-\alpha}\right)(-\mathrm{i}\psi_n Z^n)\right] \;, \tag{2.196}$$

$$L_1 \;=\; \Re\left[\sum_{n=1}^{\infty}\left(\frac{\gamma}{2}\right)^{2n}\phi_n Z^{-n}\right] \;, \tag{2.197}$$

$$L_2 \;=\; \Re\left[\sum_{n=1}^{\infty}\mathrm{i}\left(\frac{\gamma}{2}\right)^{2n}\psi_n Z^{-n}\right] \;. \tag{2.198}$$

Thus

$$\mathscr{I}_{ij} \;=\; G_{\mathrm{m}}\int_{P_{\mathrm{m}}}\left(\frac{\partial K_j}{\partial X_i}+\frac{\partial L_j}{\partial X_i}\right)\mathrm{d}^2\boldsymbol{X} \;. \tag{2.199}$$

Rewriting the functions K_j and L_j in terms of Z and $\bar{Z}$, we get

$$K_1 \;=\; \frac{1}{2}\left(\frac{1+\alpha}{1-\alpha}\right)\sum_{n=1}^{\infty}\phi_n(Z^n+\bar{Z}^n) \;, \tag{2.200}$$

$$K_2 \;=\; \frac{1}{2}\left(\frac{1+\alpha}{1-\alpha}\right)\sum_{n=1}^{\infty}\mathrm{i}\psi_n(-Z^n+\bar{Z}^n) \;, \tag{2.201}$$

$$L_1 \;=\; \frac{1}{2}\sum_{n=1}^{\infty}\left(\frac{\gamma}{2}\right)^{2n}\phi_n(Z^{-n}+\bar{Z}^{-n}) \;, \tag{2.202}$$

$$L_2 \;=\; \frac{1}{2}\sum_{n=1}^{\infty}\mathrm{i}\left(\frac{\gamma}{2}\right)^{2n}\psi_n(Z^{-n}-\bar{Z}^{-n}) \;. \tag{2.203}$$

Using the relations

$$\frac{\partial}{\partial X_1} \;=\; \frac{\partial}{\partial Z}+\frac{\partial}{\partial \bar{Z}} \;, \tag{2.204}$$

$$\frac{\partial}{\partial X_2} \;=\; \mathrm{i}\left(\frac{\partial}{\partial Z}-\frac{\partial}{\partial \bar{Z}}\right) \;, \tag{2.205}$$

and substituting $Z = r\mathrm{e}^{\mathrm{i}\theta}$, we obtain

$$\frac{\partial K_1}{\partial X_1} \;=\; \frac{1}{2}\left(\frac{1+\alpha}{1-\alpha}\right)\sum_{n=1}^{\infty}n\phi_n(Z^{n-1}+\bar{Z}^{n-1}) \tag{2.206}$$

$$\;=\; \frac{1}{2}\left(\frac{1+\alpha}{1-\alpha}\right)\sum_{n=1}^{\infty}n\phi_n r^{n-1}(\mathrm{e}^{\mathrm{i}(n-1)\theta}+\mathrm{e}^{-\mathrm{i}(n-1)\theta}) \tag{2.207}$$

$$\;=\; \left(\frac{1+\alpha}{1-\alpha}\right)\sum_{n=1}^{\infty}nr^{n-1}\phi_n\cos(n-1)\theta \;. \tag{2.208}$$

Similarly,

$$\frac{\partial K_2}{\partial X_1} = \left(\frac{1+\alpha}{1-\alpha}\right)\sum_{n=1}^{\infty} nr^{n-1}\psi_n \sin(n-1)\theta \,, \tag{2.209}$$

$$\frac{\partial K_1}{\partial X_2} = -\left(\frac{1+\alpha}{1-\alpha}\right)\sum_{n=1}^{\infty} nr^{n-1}\phi_n \sin(n-1)\theta \,, \tag{2.210}$$

$$\frac{\partial K_2}{\partial X_2} = \left(\frac{1+\alpha}{1-\alpha}\right)\sum_{n=1}^{\infty} nr^{n-1}\psi_n \cos(n-1)\theta \,, \tag{2.211}$$

$$\frac{\partial L_1}{\partial X_1} = -\sum_{n=1}^{\infty} nr^{-(n+1)}\left(\frac{\gamma}{2}\right)^{2n}\phi_n \cos(n+1)\theta \,, \tag{2.212}$$

$$\frac{\partial L_2}{\partial X_1} = -\sum_{n=1}^{\infty} nr^{-(n+1)}\left(\frac{\gamma}{2}\right)^{2n}\psi_n \sin(n+1)\theta \,, \tag{2.213}$$

$$\frac{\partial L_1}{\partial X_2} = -\sum_{n=1}^{\infty} nr^{-(n+1)}\left(\frac{\gamma}{2}\right)^{2n}\phi_n \sin(n+1)\theta \,, \tag{2.214}$$

$$\frac{\partial L_2}{\partial X_2} = \sum_{n=1}^{\infty} nr^{-(n+1)}\left(\frac{\gamma}{2}\right)^{2n}\psi_n \cos(n+1)\theta \,. \tag{2.215}$$

We will now attempt to integrate these over P_{m}. By dividing the region of integration into four parts, as in Figure 2.4, we can write

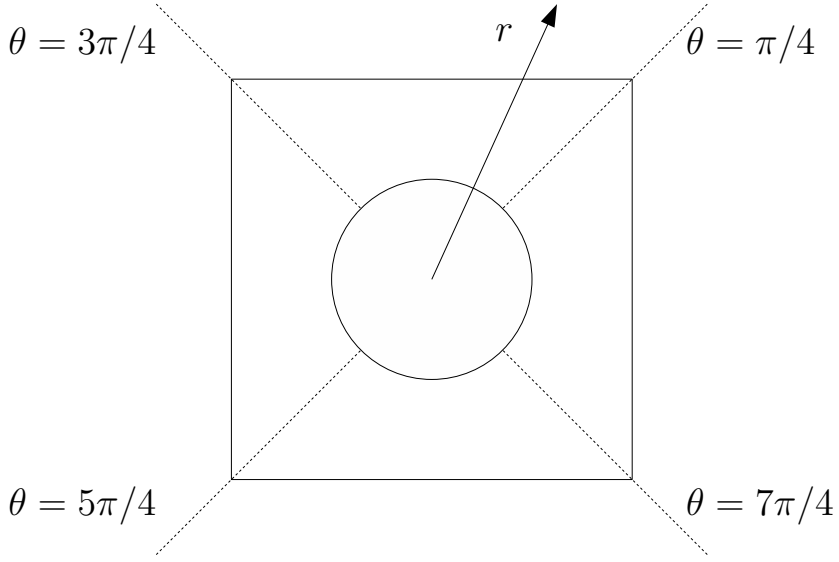

Figure 2.4: Regions of integration for P_m.

$$\begin{aligned}\iint_{P_{\mathrm{m}}} F\,\mathrm{d}^2\boldsymbol{X} &= \int_{-\pi/4}^{\pi/4}\int_{\gamma/2}^{(1/2)/(\cos\theta)} F\,r\,\mathrm{d}r\,\mathrm{d}\theta + \int_{\pi/4}^{3\pi/4}\int_{\gamma/2}^{(1/2)/(\cos(\theta-\pi/2))} F\,r\,\mathrm{d}r\,\mathrm{d}\theta \\ &\quad + \int_{3\pi/4}^{5\pi/4}\int_{\gamma/2}^{(1/2)/(\cos(\theta-\pi))} Fr\,\mathrm{d}r\,\mathrm{d}\theta + \int_{5\pi/4}^{7\pi/4}\int_{\gamma/2}^{(1/2)/(\cos(\theta-3\pi/2))} Fr\,\mathrm{d}r\,\mathrm{d}\theta\end{aligned} \tag{2.216}$$

$$= \int_{-\pi/4}^{\pi/4}\int_{\gamma/2}^{(1/2)/\cos\chi} \Big[F|_{\theta=\chi} + F|_{\theta=\chi+\pi/2} + F|_{\theta=\chi+\pi} + F|_{\theta=\chi+3\pi/2} \Big] r\,\mathrm{d}r\,\mathrm{d}\chi\,. \tag{2.217}$$

We will now begin to calculate the components. For the $\widehat{a}_{11}$ component, the integral becomes

$$\mathscr{I}_{11} = G_{\mathrm{m}} \int_{P_{\mathrm{m}}} \left(\frac{\partial K_1}{\partial X_1} + \frac{\partial L_1}{\partial X_1} \right) \mathrm{d}^2\boldsymbol{X} \tag{2.218}$$

$$\begin{aligned} = G_{\mathrm{m}} \int_{-\pi/4}^{\pi/4}\int_{\gamma/2}^{1/(2\cos\chi)} \sum_{n=1}^{\infty} \Big[& nr^{n-1}\phi_n \left(\frac{1+\alpha}{1-\alpha} \right) \big[\cos(n-1)\chi \\ & + \cos(n-1)(\chi+\pi/2) + \cos(n-1)(\chi+\pi) + \cos(n-1)(\chi+3\pi/2) \big] \\ & - nr^{-(n+1)} \left(\frac{\gamma}{2} \right)^{2n} \phi_n \big[\cos(n+1)\chi + \cos(n+1)(\chi+\pi/2) \\ & + \cos(n+1)(\chi+\pi) + \cos(n+1)(\chi+3\pi/2) \big] \Big] r\mathrm{d}r\,\mathrm{d}\chi\,. \end{aligned} \tag{2.219}$$

However,

$$\cos(n-1)(\chi+\pi) = (-1)^{n-1}\cos(n-1)\chi\,, \tag{2.220}$$

$$\cos(n-1)(\chi+3\pi/2) = (-1)^{n-1}\cos(n-1)(\chi+\pi/2)\,. \tag{2.221}$$

Thus equation (2.219) can be simplified, to give

$$\begin{aligned} \mathscr{I}_{11} = 2G_{\mathrm{m}} \sum_{\substack{n=1 \\ n\ \mathrm{odd}}}^{\infty} \int_{-\pi/4}^{\pi/4}\int_{\gamma/2}^{1/(2\cos\chi)} \Big[& nr^{n}\phi_n \left(\frac{1+\alpha}{1-\alpha} \right) \big[\cos(n-1)\chi \\ & + \cos(n-1)(\chi+\pi/2) \big] \\ & - nr^{-n} \left(\frac{\gamma}{2} \right)^{2n} \phi_n \big[\cos(n+1)\chi + \cos(n+1)(\chi+\pi/2) \big] \Big] \mathrm{d}r\,\mathrm{d}\chi. \end{aligned} \tag{2.222}$$

By the properties of the cosines, the first two terms survive only if $n-1$ is an integer multiple of 4. Similarly, the second two terms survive only if $n+1$ is an integer multiple of 4. We write $n-1 = 4(j-1)$ for the first two terms, and $n+1 = 4j$ for the other two terms, where in each case $j = 1, 2, \ldots$. The integral simplifies to:

$$\begin{aligned} \mathscr{I}_{11} = 4G_{\mathrm{m}} \sum_{j=1}^{\infty} \int_{-\pi/4}^{\pi/4} \Bigg[& (4j-3)\phi_{4j-3} \left(\frac{1+\alpha}{1-\alpha} \right) \cos 4(j-1)\chi \\ & \times \left[\frac{1}{(2\cos\chi)^{4j-2}(4j-2)} - \frac{(\gamma/2)^{4j-2}}{4j-2} \right] \\ & - (4j-1)\phi_{4j-1} \left(\frac{\gamma}{2} \right)^{8j-2} \cos 4j\chi \\ & \times \left[\frac{(2\cos\chi)^{4j-2}}{2-4j} - \left(\frac{\gamma}{2} \right)^{2-4j} \frac{1}{2-4j} \right] \Bigg] \mathrm{d}\chi\,. \end{aligned} \tag{2.223}$$

On expanding the terms in the integrand, we will have four terms contributing to the integral. In the second term, we are integrating $\cos 4(j-1)\chi$ over $[-\pi/4, \pi/4]$ so only the $j = 1$ term will survive. For the same reason, the fourth term will disappear. On integrating the one surviving term of the second term, we get

$$\begin{aligned} (\text{2nd term}) &= 4G_{\rm m} \cdot 1 \cdot \phi_1 \left(\frac{1+\alpha}{1-\alpha}\right) \left(\frac{\pi}{4} + \frac{\pi}{4}\right) \cdot \left(-\frac{(\gamma/2)^2}{2}\right) && (2.224) \\ &= -\frac{G_{\rm m}\pi\phi_1\gamma^2}{4} \left(\frac{1+\alpha}{1-\alpha}\right) . && (2.225) \end{aligned}$$

Define

$$\Phi = \frac{\pi\phi_1\gamma^2}{4} \left(\frac{1+\alpha}{1-\alpha}\right) , \qquad (2.226)$$

so that the second term becomes $-G_{\rm m}\Phi$. The remaining terms can be written as $G_{\rm m}\Sigma$, where

$$\begin{aligned} \Sigma = \sum_{j=1}^{\infty} \Bigg\{ & \frac{4(4j-3)}{4j-2} \phi_{4j-3} \left(\frac{1+\alpha}{1-\alpha}\right) \int_{-\pi/4}^{\pi/4} \frac{\cos 4(j-1)\chi}{(2\cos\chi)^{4j-2}} \, {\rm d}\chi \\ & + \frac{4(4j-1)}{2^{4j}(4j-2)} \gamma^{8j-2} \phi_{4j-1} \int_{-\pi/4}^{\pi/4} (\cos\chi)^{4j-2} \cos 4j\chi \, {\rm d}\chi \Bigg\} . \qquad (2.227) \end{aligned}$$

However,

$$\int \cos kx \cos^{k-2} x \, {\rm d}x = \left[\frac{\sin(k-1)x \cos^{k-1} x}{k-1}\right] , \qquad (2.228)$$

so the expression above for Σ becomes

$$\Sigma = \sum_{j=1}^{\infty} \frac{(-1)^{j-1}}{2^{2(j-1)}(2j-1)} \left[\left(\frac{1+\alpha}{1-\alpha}\right) \phi_{4j-3} + \frac{\gamma^{8j-2}}{2^{4j}} \phi_{4j-1}\right] . \qquad (2.229)$$

Then

$$\mathscr{I}_{11} = G_{\rm m}(\Sigma - \Phi) . \qquad (2.230)$$

On considering $\mathscr{I}_{12}$ and $\mathscr{I}_{21}$, we find that the cosine terms are replaced by sines (except in the upper limit of the integral). This makes the integrands of the coefficients odd functions of χ, so that these integrals disappear. Finally, on considering $\mathscr{I}_{22}$, we get

$$\mathscr{I}_{22} = G_{\rm m}(\Sigma_{22} - \Phi_{22}) , \qquad (2.231)$$

where the two quantities Σ_{22} and Φ_{22} are the same as Σ and Φ but with ϕ_n replaced by ψ_n, and the second term in Σ subtracted rather than added. However, by the

relationship between ϕ_n and ψ_n in equation (2.191), we get $\Sigma_{22} = \Sigma$ and $\Phi_{22} = \Phi$, so that

$$\mathscr{I}_{ij} \;=\; G_{\rm m}(\Sigma - \Phi)\delta_{ij} \; . \tag{2.232}$$

We will now consider the contribution to $\widehat{a}_{ij}$ by the integral over $P_{\rm f}$,

$$\mathscr{J}_{ij} \;=\; G_{\rm f} \int_{P_{\rm f}} \left(\delta_{ij} + \frac{\partial \chi_j^{(\rm f)}}{\partial X_i} \right) {\rm d}^2 \boldsymbol{X} \; . \tag{2.233}$$

If we set

$$C_1 \;=\; \Re \left[\sum_{n=1}^{\infty} \phi_n Z^n \right] \; , \tag{2.234}$$

$$C_2 \;=\; \Re \left[\sum_{n=1}^{\infty} -{\rm i}\psi_n Z^n \right] \; , \tag{2.235}$$

we find that the integral is given by

$$\mathscr{J}_{ij} \;=\; \left(\frac{2G_{\rm f}}{1-\alpha} \right) \int_{P_{\rm f}} \frac{\partial C_j}{\partial X_i} \, {\rm d}^2 \boldsymbol{X} \; . \tag{2.236}$$

Now, we find that

$$\frac{\partial C_1}{\partial X_1} \;=\; \frac{1}{2} \sum_{n=1}^{\infty} n\phi_n (Z^{n-1} + \bar{Z}^{n-1}) \tag{2.237}$$

$$\;=\; \sum_{n=1}^{\infty} n\phi_n r^{n-1} \cos(n-1)\theta \; ; \tag{2.238}$$

similarly

$$\frac{\partial C_1}{\partial X_2} \;=\; -\sum_{n=1}^{\infty} n\phi_n r^{n-1} \sin(n-1)\theta \; , \tag{2.239}$$

$$\frac{\partial C_2}{\partial X_1} \;=\; \sum_{n=1}^{\infty} n\psi_n r^{n-1} \sin(n-1)\theta \; , \tag{2.240}$$

$$\frac{\partial C_2}{\partial X_2} \;=\; \sum_{n=1}^{\infty} n\psi_n r^{n-1} \cos(n-1)\theta \; . \tag{2.241}$$

On integrating these over the region $P_{\rm f}$, all terms disappear except for the $n = 1$ term in $\cos(n-1)\theta$. Hence

$$\iint_{P_{\rm f}} \frac{\partial C_1}{\partial X_1} \, {\rm d}^2 \boldsymbol{X} \;=\; \int_0^{2\pi} \int_0^{\gamma/2} \phi_1 r \, {\rm d}r \, {\rm d}\theta \tag{2.242}$$

$$\;=\; 2\pi\phi_1 \frac{(\gamma/2)^2}{2} \tag{2.243}$$

$$\;=\; \frac{\pi\gamma^2\phi_1}{4} \; . \tag{2.244}$$

Similarly,

$$\iint_{P_{\rm f}} \frac{\partial C_2}{\partial X_2}\,{\rm d}^2\boldsymbol{X} \;=\; \frac{\pi\gamma^2\psi_1}{4} \;=\; \frac{\pi\gamma^2\phi_1}{4}\,. \tag{2.245}$$

Hence

$$\mathscr{J}_{ij} \;=\; \left(\frac{2G_{\rm f}}{1-\alpha}\right)\frac{\pi\gamma^2\phi_1}{4}\delta_{ij} \tag{2.246}$$

$$\;=\; \frac{\pi G_{\rm m}\alpha\gamma^2\phi_1}{2(1-\alpha)}\delta_{ij} \tag{2.247}$$

$$\;=\; 2G_{\rm m}\frac{\alpha}{1+\alpha}\Phi\delta_{ij} \tag{2.248}$$

by equation (2.226). So, overall,

$$\widehat{a}_{ij} \;=\; \mathscr{I}_{ij} + \mathscr{J}_{ij} \tag{2.249}$$

$$\;=\; G_{\rm m}\left(\Sigma - \Phi + \frac{2\alpha}{1+\alpha}\Phi\right)\delta_{ij} \tag{2.250}$$

$$\;=\; G_{\rm m}\left[\Sigma - \left(\frac{1-\alpha}{1+\alpha}\right)\Phi\right]\delta_{ij}\,. \tag{2.251}$$

On collecting all the previous results, and defining

$$\Psi \;=\; \left(\frac{1-\alpha}{1+\alpha}\right)\Phi\,, \tag{2.252}$$

the homogenised tensor $\widehat{a}_{ij}$ is given by

$$\widehat{a}_{ij} \;=\; \widehat{G}\delta_{ij}\,, \tag{2.253}$$

where the homogenised shear modulus is

$$\widehat{G} \;=\; G_{\rm m}(\Sigma - \Psi)\,, \tag{2.254}$$

where

$$\Psi \;=\; \frac{\pi\gamma^2\phi_1}{4}\,, \tag{2.255}$$

$$\Sigma \;=\; \sum_{j=1}^{\infty}\frac{(-1)^{j-1}}{2^{2(j-1)}(2j-1)}\left[\left(\frac{1+\alpha}{1-\alpha}\right)\phi_{4j-3} + \frac{\gamma^{8j-2}}{2^{4j}}\phi_{4j-1}\right]\,, \tag{2.256}$$

and ϕ_n satisfies

$$\left(\frac{1+\alpha}{1-\alpha}\right)\phi_n - \delta_{1n} \;=\; \sum_{m=1}^{\infty}(-1)^m\left(\frac{\gamma}{2}\right)^{2m}\phi_m\binom{m+n-1}{n}S_{m+n} \tag{2.257}$$

with $S_2 = \pi$.

However, the definition (2.256) of Σ can be simplified greatly, with a little analysis. On substituting for $\left(\frac{1+\alpha}{1-\alpha}\right)\phi_{4j-3}$ from equation (2.257), we obtain

$$\begin{aligned}\Sigma &= \sum_{j=1}^{\infty}\frac{(-1)^{j-1}}{2^{2j-2}(2j-1)}\left\{\left[\delta_{1,4j-3}+\sum_{m=1}^{\infty}(-1)^m\left(\frac{\gamma}{2}\right)^{2m}\phi_m\binom{m+4j-4}{4j-3}S_{m+4j-3}\right]\right. \\ &\qquad \left.+\frac{\gamma^{8j-2}}{2^{4j}}\phi_{4j-1}\right\} \qquad (2.258)\\ &= 1+\sum_{j=1}^{\infty}\frac{(-1)^{j-1}}{2^{2j-2}(2j-1)}\left\{\frac{\gamma^{8j-2}}{2^{4j}}\phi_{4j-1}\right. \\ &\qquad \left.+\sum_{m=1}^{\infty}(-1)^m\left(\frac{\gamma}{2}\right)^{2m}\phi_m\binom{m+4j-4}{4j-3}S_{m+4j-3}\right\}. \qquad (2.259)\end{aligned}$$

Now, S_m is zero unless either $m=4l$ for some integer $l\geqslant 1$, or $m=2$. The second of these cases is found on taking $m=j=1$ in the inner sum, which yields $-\pi\gamma^2\phi_1/4$. Therefore

$$\Sigma = 1-\frac{\pi\gamma^2\phi_1}{4}+\widetilde{\Sigma}\,, \qquad (2.260)$$

where

$$\begin{aligned}\widetilde{\Sigma} &= \sum_{j=1}^{\infty}\frac{(-1)^{j-1}}{2^{2j-2}(2j-1)}\left\{\frac{\gamma^{8j-2}}{2^{4j}}\phi_{4j-1}\right. \\ &\qquad \left.-\sum_{i=1}^{\infty}\left(\frac{\gamma}{2}\right)^{8i-2}\phi_{4i-1}\binom{4i+4j-5}{4j-3}S_{4i+4j-4}\right\}. \qquad (2.261)\end{aligned}$$

We can write this quantity as

$$\widetilde{\Sigma} = \sum_{j=1}^{\infty}\sum_{i=1}^{\infty}\frac{(-1)^{j-1}}{2^{2j-2}(2j-1)}\left\{\frac{\delta_{ij}}{2^{4j}}-\frac{1}{2^{8i-2}}\binom{4i+4j-5}{4j-3}S_{4i+4j-4}\right\}\gamma^{8i-2}\phi_{4i-1}\,, \qquad (2.262)$$

or, on swapping the order of summation,

$$\widetilde{\Sigma} = \sum_{i=1}^{\infty}\Gamma_i\gamma^{8i-2}\phi_{4i-1}\,, \qquad (2.263)$$

where

$$\Gamma_i = \sum_{j=1}^{\infty}\frac{(-1)^{j-1}}{2^{2j-2}(2j-1)}\left\{\frac{\delta_{ij}}{2^{4i}}-\frac{1}{2^{8i-2}}\binom{4i+4j-5}{4j-3}S_{4i+4j-4}\right\}. \qquad (2.264)$$

Simplifying,

$$\Gamma_i = \frac{(-1)^{i-1}}{2^{6i-2}(2i-1)} - \sum_{j=1}^{\infty} \frac{(-1)^{j-1}}{2^{8i+2j-4}(2j-1)} \binom{4i+4j-5}{4j-3} S_{4i+4j-4} \tag{2.265}$$

$$= \frac{(-1)^{i-1}}{2^{6i-2}(2i-1)} \left\{ 1 - \sum_{j=1}^{\infty} \frac{(-1)^{i+j}}{2^{2i+2j-2}} \left(\frac{2i-1}{2j-1} \right) \binom{4i+4j-5}{4j-3} S_{4i+4j-4} \right\} \tag{2.266}$$

$$= \frac{(-1)^{i-1}}{2^{6i-2}(2i-1)} \left\{ 1 - \sum_{j=1}^{\infty} \frac{(-1)^{i+j}}{2^{2i+2j-2}} \binom{4i+4j-5}{4j-2} S_{4i+4j-4} \right\} . \tag{2.267}$$

However, it can be shown (see Section C.2 of Appendix C) that

$$\sum_{j=1}^{\infty} \frac{(-1)^{i+j}}{2^{2i+2j-2}} \binom{4i+4j-5}{4j-2} S_{4i+4j-4} = 1 , \tag{2.268}$$

so that Γ_i and hence $\widetilde{\Sigma}$ are zero. Thus

$$\Sigma = 1 - \frac{\pi\gamma^2\phi_1}{4} \tag{2.269}$$

$$= 1 - \Psi , \tag{2.270}$$

and the homogenised shear modulus from equation (2.254) becomes

$$\widehat{G} = G_{\mathrm{m}} (1 - 2\Psi) \tag{2.271}$$

$$= G_{\mathrm{m}} \left(1 - \frac{\pi\gamma^2\phi_1}{2} \right) , \tag{2.272}$$

where ϕ_1 is found by solving the system (2.257). This agrees exactly with the solution found by Perrins *et al.* [81].

2.4.1.5 The small inclusion limit

We will now take the equations (2.272) and (2.257) and find the asymptotic behaviour as $\gamma \to 0$. This is in order to compare this behaviour to the corresponding result from the point inclusion method, which we will study shortly. We can simplify the notation by introducing a *compliance parameter*

$$s = \frac{1-\alpha}{1+\alpha} = \frac{G_{\mathrm{m}} - G_{\mathrm{f}}}{G_{\mathrm{m}} + G_{\mathrm{f}}} , \tag{2.273}$$

so that voids can be considered as inclusions with compliance parameter 1, rigid inclusions have $s = -1$, and inclusions with compliance parameter $s \lesseqgtr 0$ are respectively stiffer or more compliant than the surrounding matrix.

First, we notice that the whole problem only depends on γ through powers of γ^2. We thus make an asymptotic expansion

$$\phi_n \sim \phi_n^{(0)} + \gamma^2\phi_n^{(2)} + \gamma^4\phi_n^{(4)} + O(\gamma^6) , \tag{2.274}$$

which we now substitute into equation (2.257). To leading order,

$$\phi_n^{(0)} = s\delta_{1n} \,. \tag{2.275}$$

At the next order,

$$\frac{1}{s}\gamma^2\phi_n^{(2)} = -\frac{\gamma^2}{4}\phi_1^{(0)}\binom{n}{n}S_{n+1} \tag{2.276}$$

$$\Rightarrow \quad \phi_n^{(2)} = -s^2\frac{S_{n+1}}{4} \,. \tag{2.277}$$

Continuing the process, we obtain

$$\phi_n^{(4)} = s^3\frac{S_2 S_{n+1}}{16} \,, \tag{2.278}$$

$$\phi_n^{(6)} = -s^4\frac{S_2^2 S_{n+1}}{64} \,. \tag{2.279}$$

Thus the coefficients become

$$\phi_n \sim s\delta_{1n} - \frac{\gamma^2 s^2 S_{n+1}}{4} + \frac{\gamma^4 s^3 S_2 S_{n+1}}{16} - \frac{\gamma^6 s^4 S_2^2 S_{n+1}}{64} + O(\gamma^8) \,. \tag{2.280}$$

In particular,

$$\phi_1 \sim s - \frac{\pi s^2\gamma^2}{4} + \frac{\pi^2 s^3\gamma^4}{16} - \frac{\pi^3 s^4\gamma^6}{64} + O(\gamma^8) \,. \tag{2.281}$$

Thus, from equation (2.272),

$$\widehat{G} \sim G_{\mathrm{m}}\left[1 - \frac{\pi s\gamma^2}{2} + \frac{\pi^2 s^2\gamma^4}{8} - \frac{\pi^3 s^3\gamma^6}{32} + O(\gamma^8)\right] \,. \tag{2.282}$$

2.4.2 The point inclusion method

This method is derived from a different viewpoint from the multiple scales approach. Put simply, we consider the problem of one inclusion, and find the leading order behaviour at infinity. This inner solution will match to the outer solution, which will satisfy an equation in $\mathbb{R}^2$ with a particular singularity at the origin. We then consider a distribution of singularities which will correspond to a homogenised material. This method is an *approximation*, which is *a priori* valid for dilute distributions of inclusions. The exposition in this section is rather elementary in character; a more thorough analysis is performed in Chapter 6.

Before exploring the method, we first need to consider the lengthscales of the problem. Suppose that the characteristic length of an inclusion is a, and that the characteristic separation distance between inclusions is β. Then the method is valid only if $a/\beta \ll 1$. In order to apply this method to our problem, we return to the results of Section 2.2, where we considered the inner displacement of the problem: the

antiplane shear at infinity of an elastic matrix containing one elastic (fibre) inclusion. Given a condition at infinity of

$$\nabla f_{\text{inner}}|_{|\boldsymbol{x}|\to\infty} \;=\; \frac{\tau_0}{G_{\text{m}}}\widehat{\boldsymbol{p}}\,, \tag{2.283}$$

we found the resulting inner displacement in the matrix in equation (2.35):

$$f_{\text{inner}} \;=\; \frac{\tau_0}{G_{\text{m}}}\left[r+\frac{a^2 s}{r}\right](\widehat{p}_1\cos\theta+\widehat{p}_2\sin\theta)\,, \tag{2.284}$$

on using the compliance parameter s defined in equation (2.273). The *outer* solution represents the inclusion as a point at the origin, so that

$$\nabla^2 f_{\text{outer}} \;=\; 0 \qquad \text{for } \boldsymbol{X}\neq\boldsymbol{0}\,, \tag{2.285}$$

where $\boldsymbol{X}=(a/\beta)\boldsymbol{x}$ is the position vector for the outer problem. We have a matching condition between the outer and inner solutions:

$$\lim_{\boldsymbol{X}\to\boldsymbol{0}} f_{\text{outer}} \;=\; \lim_{\boldsymbol{x}\to\infty} f_{\text{inner}}\,. \tag{2.286}$$

This is a rather simplistic formulation; in reality the matching would take place in an intermediate domain between $\boldsymbol{x}$ and $\boldsymbol{X}$. Equivalently, one may use a matching procedure such as van Dyke's rule. This is performed in Section 6.2.1, and we find that in fact

$$\lim_{\boldsymbol{x}\to\infty} f_{\text{inner}} \;=\; \lim_{\boldsymbol{X}\to\boldsymbol{0}} f^{(\text{reg})}_{\text{outer}}\,, \tag{2.287}$$

where $f^{(\text{reg})}_{\text{outer}}$ is the *regular* part of f_{outer}, *i.e.* a solution without singularities, which may be found by solving (2.285) for *all* $\boldsymbol{X}$.

Equation (2.285) and its boundary condition (2.287) can be replaced by a generalised equation $\nabla^2 f_{\text{outer}}=H$, where H is some distribution. To find H, consider the equation which defines the Green's function Γ for Laplace's equation in $\mathbb{R}^2$,

$$\nabla^2\Gamma \;=\; \delta(X)\delta(Y)\,. \tag{2.288}$$

Formally, we can take the directional derivative $\boldsymbol{b}\cdot\nabla$ of both sides, where $\boldsymbol{b}=(b_1,b_2)$ is some vector. Then

$$\nabla^2(\boldsymbol{b}\cdot\nabla\Gamma) \;=\; \boldsymbol{b}\cdot\nabla\big(\delta(X)\delta(Y)\big)\,. \tag{2.289}$$

However, we know that the solution to equation (2.288) is given by

$$\Gamma \;=\; \frac{1}{2\pi}\log R\,, \tag{2.290}$$

where $R = \sqrt{X^2 + Y^2}$. Hence

$$\boldsymbol{b} \cdot \nabla\Gamma \;=\; \frac{1}{2\pi R}(b_1 \cos\theta + b_2 \sin\theta) \; . \tag{2.291}$$

If we let $f_{\text{outer}} = \boldsymbol{b} \cdot \nabla\Gamma$, then we need to satisfy the matching condition (2.287). Comparing the term in $1/r$, we find that[3]

$$\begin{aligned}
\boldsymbol{b} &= \frac{2\pi s a^2 \tau_0}{G_{\text{m}}} \widehat{\boldsymbol{p}} && (2.292)\\
&= 2\pi s a^2 \left(\lim_{\boldsymbol{x} \to \infty} \nabla f_{\text{inner}} \right) \qquad \text{by (2.283)} && (2.293)\\
&= 2\pi s a^2 \left(\lim_{\boldsymbol{X} \to \boldsymbol{0}} \nabla f_{\text{outer}}^{(\text{reg})} \right) \qquad \text{by the matching condition.} && (2.294)
\end{aligned}$$

Now, from equation (2.289), the equation that f_{outer} satisfies is

$$\begin{aligned}
\nabla^2 f_{\text{outer}} &= \boldsymbol{b} \cdot \nabla\big(\delta(X)\delta(Y)\big) && (2.295)\\
&= 2\pi s a^2 \left(\lim_{\boldsymbol{X} \to \boldsymbol{0}} \nabla f_{\text{outer}}^{(\text{reg})} \right) \cdot \nabla\big(\delta(X)\delta(Y)\big) && (2.296)\\
&= 2\pi s a^2 \nabla f_{\text{outer}}^{(\text{reg})} \cdot \nabla\big(\delta(X)\delta(Y)\big) \; , && (2.297)
\end{aligned}$$

since $\delta(X)\delta(Y)$ is zero if $(X, Y) \neq \boldsymbol{0}$.

2.4.2.1 Homogenisation of point inclusions

On taking equation (2.297) as the inner asymptotic solution near one inclusion in a distribution of many, we find that the corresponding outer solution satisfies

$$\nabla^2 f_{\text{outer}} \;=\; 2\pi a^2 s \nabla f_{\text{outer}}^{(\text{reg})} \cdot \nabla \left(\sum_p \delta(\boldsymbol{X} - \boldsymbol{X}_p) \right) \; , \tag{2.298}$$

where the inclusions are placed at $\boldsymbol{X}_p$, for $p = 1, 2, \ldots, P$. On homogenising this result, allowing the separation between the inclusions to tend to zero, this equation becomes

$$\nabla^2 f \;=\; 2\pi a^2 s \nabla f \cdot \nabla\omega \; , \tag{2.299}$$

where $\omega(\boldsymbol{X})$ is the number density of inclusions, or the number of inclusions per unit area. This homogenisation process, which effectively removes the difference between the total and regular parts of f_{outer}, will be studied in greater depth in Chapter 6.

We now compare this result to the case of a homogenised material with an effective shear modulus $\widehat{G}(\boldsymbol{X})$. In this case the displacement satisfies

$$\begin{aligned}
\nabla \cdot (\widehat{G} \nabla f) &= 0 && (2.300)\\
\Rightarrow \qquad \nabla\widehat{G} \cdot \nabla f + \widehat{G} \nabla^2 f &= 0 && (2.301)\\
\Rightarrow \qquad \nabla^2 f &= -\frac{1}{\widehat{G}} \nabla\widehat{G} \cdot \nabla f && (2.302)\\
&= -\nabla(\log \widehat{G}) \cdot \nabla f \; . && (2.303)
\end{aligned}$$

[3]The linear term in f_{inner} will be matched by the regular part of the outer solution, $f_{\text{outer}}^{(\text{reg})}$.

This is compared with equation (2.299), to show that we must have

$$\nabla f \cdot \nabla \left[\log \widehat{G} + 2\pi a^2 s\omega \right] \;=\; 0 \,. \tag{2.304}$$

For arbitrary deformations, we must therefore have

$$\log \widehat{G} \;=\; -2\pi a^2 s\omega + \text{constant} \tag{2.305}$$

$$\Rightarrow \qquad \widehat{G} \;=\; A \exp\left(-2\pi a^2 s\omega\right) \,. \tag{2.306}$$

However, if ω were zero, the effective modulus would simply be the modulus of the matrix, G_{m}. Hence

$$\widehat{G} \;=\; G_{\mathrm{m}} \exp\left(-2\pi a^2 s\omega\right) \,. \tag{2.307}$$

Many other homogenisation theories consider the *area fraction* of an inclusion instead of the density, so for completeness we will now state result (2.307) in terms of the area fraction. If ω, the density of inclusions, is equal to the number of inclusions per unit area, and each inclusion has area πa^2, then the area fraction of inclusions is given by

$$\rho \;=\; \pi a^2 \omega \,. \tag{2.308}$$

Then the effective shear modulus of a material with inclusions of uniform size will be given by

$$\widehat{G} \;=\; G_{\mathrm{m}} \mathrm{e}^{-2s\rho} \tag{2.309}$$

in terms of the area fraction of inclusions, ρ, and the compliance parameter, s.

2.4.3 Comparison

Now we wish to compare the result of the effective shear modulus $\widehat{G}^{\mathrm{PI}}$ found by the point inclusion method of Section 2.4.2 to the effective shear modulus $\widehat{G}^{\mathrm{MS}}$ found by the multiple-scales method of Section 2.4.1. This involves first applying the point inclusion method to a square lattice of inclusions. We can then compare this result to the asymptotic result of Section 2.4.1.5, which considered the limit of small inclusion size (compared to the separation distance of inclusion centres).

So, we consider equation (2.307). We need to assume that ω refers to a square lattice of inclusions, with one inclusion per square of area ε^2. Thus $\omega = 1/\varepsilon^2$, and the radius of the inclusions is $a = \varepsilon\gamma/2$. Hence

$$\widehat{G}^{\mathrm{PI}} \;=\; G_{\mathrm{m}} \exp\left(-\frac{\pi s \gamma^2}{2}\right) \tag{2.310}$$

$$\sim\; G_{\mathrm{m}} \left[1 - \frac{\pi s\gamma^2}{2} + \frac{\pi^2 s^2 \gamma^4}{8} - \frac{\pi^3 s^3 \gamma^6}{48} + O(\gamma^8)\right] \qquad \text{as } \gamma \to 0 \,. \tag{2.311}$$

Comparing this approximation to that obtained from the multiple-scales expansion (2.282), which gave us

$$\widehat{G}^{\mathrm{MS}} \sim G_{\mathrm{m}}\left[1-\frac{\pi s\gamma^2}{2}+\frac{\pi^2 s^2\gamma^4}{8}-\frac{\pi^3 s^3\gamma^6}{32}+O(\gamma^8)\right] \qquad \text{as } \gamma\to 0\ , \quad (2.312)$$

we find that the two approximations agree[4] up to $O(\gamma^4)$.

Therefore, the point inclusion approach gives a very good approximation to the multiple scales method even when $\gamma \approx 0.5$, the case where the separation of the inclusions is of the order of their diameters. This is a very good result for a theory which assumes that the inclusions are infinitely far apart.

2.4.4 Extension of the point inclusion approach

Our final task in this chapter is to determine how the material's stiffness would vary if some inclusions are bonded while others are debonded. We begin by considering a distribution of differently-sized inclusions, before generalising this result to a dispersion of inclusions whose size and stiffness vary according to a given statistical distribution. Debonding is taken into account by only considering rigid inclusions and voids (which model the debonded rigid inclusions), with the proportion of debonded inclusions dependent on the distribution of the sizes of the inclusions and the applied stress on the composite material.

2.4.4.1 Distributions of dissimilar particles

A simple method of considering a uniform distribution of inclusions with different radius or material parameters is to consider the relative densities ω. As an example, suppose that we had inclusions of two different radii, a_1 and a_2. If these occur in the composite material in proportions ϕ_1 and ϕ_2 respectively ($\phi_1+\phi_2=1$) then the densities of the two types of inclusion will be $\phi_1\omega$ and $\phi_2\omega$. Substituting this information into equation (2.299) gives

$$\nabla^2 f = 2\pi s\nabla f\cdot\nabla\left(a_1^2\phi_1\omega+a_2^2\phi_2\omega\right)\ , \quad (2.313)$$

so that the effective modulus becomes

$$\widehat{G} = G_{\mathrm{m}}\exp\left(-2\pi s\left(a_1^2\phi_1\omega+a_2^2\phi_2\omega\right)\right)\ . \quad (2.314)$$

Using this simple example we can consider a composite containing n types of inclusion, with radii a_i and compliance parameter s_i (for $i=1,\ldots,n$). If the proportion

[4]This order of agreement is also seen for fibres which are arranged isometrically in the composite material; the effective modulus in this case is given by Perrins *et al.* [80].

of the inclusions which are of type i is ϕ_i, with

$$\sum_{i=1}^{n} \phi_i \;=\; 1 \;, \tag{2.315}$$

then the effective modulus of the material is

$$\widehat{G} \;=\; G_{\mathrm{m}} \exp\left(-2\pi\omega \sum_{i=1}^{n} s_i a_i^2 \phi_i \right) \;. \tag{2.316}$$

The above result can be generalised further, to the case where the inclusions are distributed according to a multivariate statistical distribution. We will assume that the inclusion radius a and the compliance parameter s are distributed randomly with the probability density function $F(a, s)$. For comparison, the probability density function giving rise to the effective modulus in equation (2.316) is

$$F(a, s) \;=\; \sum_{i=1}^{n} \phi_i \delta(a - a_i)\delta(s - s_i) \;, \tag{2.317}$$

where $\delta(\cdot)$ is Dirac's delta function. Modifying equation (2.299) to take this distribution into account gives us

$$\nabla^2 f \;=\; 2\pi \nabla f \cdot \nabla \left[\omega \iint_S s a^2 F(a, s) \,\mathrm{d}a \,\mathrm{d}s \right] \;, \tag{2.318}$$

where

$$S \;=\; \{(a, s) \;:\; 0 \leqslant a < \infty, -1 \leqslant s \leqslant 1\} \tag{2.319}$$

is the parameter range of a and s. Performing the homogenisation for this general distribution of inclusions gives

$$\widehat{G} \;=\; G_{\mathrm{m}} \exp\left(-2\pi Q \omega\right) \;, \tag{2.320}$$

where

$$Q \;=\; \iint_S s a^2 F(a, s) \,\mathrm{d}a \,\mathrm{d}s \;. \tag{2.321}$$

2.4.4.2 Debonding

A specific application of the previous section is to consider the varying stiffness of a composite material as the inclusions are debonding. Recall from Section 2.3.1 that we could consider the debonding process as a sudden jump from being fully bonded to being fully detached. Crucially, this occured at a critical value of τ_0, the stress at infinity. Equation (2.111) gave this as

$$\tau_{\mathrm{crit}} \;=\; \frac{\lambda(G_{\mathrm{f}} + G_{\mathrm{m}})}{G_{\mathrm{f}}\sqrt{a}} \;, \tag{2.322}$$

where λ is the modified stress intensity factor. Analysis in Chapter 6 will show that the critical stress at a point in the homogenised material will also equal this value. Incorporating the shear moduli into λ, we obtain

$$\tau_{\text{crit}} \;=\; \frac{\lambda}{\sqrt{a}}\,. \tag{2.323}$$

Now, our probability density function $F(a,s)$ needs to capture the fact that, for a given stress at infinity τ, the inclusions are bonded (or $s=-1$) if $a < a_{\text{crit}}$, and debonded (or $s=1$) for $a > a_{\text{crit}}$, where a_{crit} is found from equation (2.323),

$$a_{\text{crit}}(\tau) \;=\; \frac{\lambda^2}{\tau^2}\,. \tag{2.324}$$

So, if we assume that the radii of the inclusions vary according to the probability density function $\widetilde{F}(a)$, then we can write

$$F(a,s) \;=\; G(a,s)\widetilde{F}(a)\,, \tag{2.325}$$

where $G(a,s)$ captures the variation in stiffness. But if the inclusions are either attached or detached, according to whether $a \lessgtr a_{\text{crit}}$, then

$$G(a,s) \;=\; \begin{cases} \delta(s+1) & a < a_{\text{crit}} \\ \delta(s-1) & a > a_{\text{crit}}\,. \end{cases} \tag{2.326}$$

Thus the quantity Q from equation (2.321), now dependent on the stress at infinity, becomes

$$\begin{aligned} Q(\tau) \;&=\; -\int_0^{\lambda^2/\tau^2} a^2\widetilde{F}(a)\,\mathrm{d}a + \int_{\lambda^2/\tau^2}^{\infty} a^2\widetilde{F}(a)\,\mathrm{d}a & (2.327)\\ &=\; \int_0^{\infty} a^2\widetilde{F}(a)\,\mathrm{d}a - 2\int_0^{\lambda^2/\tau^2} a^2\widetilde{F}(a)\,\mathrm{d}a & (2.328)\\ &=\; \mathrm{E}(X^2) - 2\int_0^{\lambda^2/\tau^2} a^2\widetilde{F}(a)\,\mathrm{d}a\,. & (2.329) \end{aligned}$$

Here $\mathrm{E}(X^2)$ is the expected value of X^2, where the random variable X is distributed according to the probability density function $\widetilde{F}(a)$. The quantity $Q(\tau)$ is then substituted into the expression for the effective modulus in equation (2.320).

Finally in this chapter we will model an experiment whereby a material containing a distribution of fibres experiences an ever-increasing loading. This loading is assumed to be such that a constant stress field is induced in the (homogenised) material. The fibres are initially bonded to the matrix but may undergo debonding. We consider how the debonding process might occur with two different distributions of rigid inclusions. The two distributions we discuss are:

1. All inclusions being of the same size, or

$$\widetilde{F}(a) \;=\; \delta(a-a_0)\;, \tag{2.330}$$

2. A normal distribution of inclusions, with mean a_0 and variance σ^2, with

$$\widetilde{F}(a) \;=\; \frac{1}{\sqrt{2\pi\sigma^2}}\exp\left(-\frac{(a-a_0)^2}{2\sigma^2}\right)\;. \tag{2.331}$$

In both cases we will find $Q(\tau)$ which will give us an effective shear modulus that depends on the applied stress in the material. However, we will want to interpret this in terms of a force–displacement graph. The simplest way of achieving this is to consider an infinite body with shear modulus $\widehat{G}$, applying a stress $\tau_{yz}|_\infty = \tau$. Then at any point in the body the displacement will be proportional to $\tau/\widehat{G}$. We thus choose a representative displacement, for plotting graphs, as

$$\text{displacement} \;=\; \frac{\tau}{\widehat{G}(\tau)}\;. \tag{2.332}$$

We will first consider the case where all inclusions are the same size. The quantity $Q(\tau)$ is given as

$$Q(\tau) \;=\; \begin{cases} -a_0^2 & \text{if } \dfrac{\lambda^2}{\tau^2} > a_0 \\[2ex] a_0^2 & \text{if } \dfrac{\lambda^2}{\tau^2} < a_0\;, \end{cases} \tag{2.333}$$

so that the effective shear modulus, as a function of the loading stress τ, becomes

$$\widehat{G}(\tau) \;=\; \begin{cases} G_{\rm m}\exp\left(2\pi a_0^2\omega\right) & \text{if } \tau < \dfrac{\lambda}{\sqrt{a_0}} \\[2ex] G_{\rm m}\exp\left(-2\pi a_0^2\omega\right) & \text{if } \tau > \dfrac{\lambda}{\sqrt{a_0}}\;. \end{cases} \tag{2.334}$$

We can find the effective shear modulus in the same way for the normal distribution of inclusions, (2.331). On finding the quantity $Q(\tau)$ from equation (2.329) (we do not write down the exact expression here as the form is irrelevant), we substitute it into the definition of the effective shear modulus, to find

$$\widehat{G}(\tau) \;=\; G_{\rm m}\exp\left(-2\pi Q(\tau)\omega\right)\;. \tag{2.335}$$

These effective moduli are substituted into the definition of a typical displacement, (2.332), and stress–displacement graphs drawn. In plotting these, we choose the inclusions to have the property that the spacing between the inclusions is the same order as their diameter. Assuming a square grid, as in Section 2.4.3, this implies that $\omega = 1$ and $a_0 = 1/4$ in the system of units for which the length of the unit cell is

1 (here a_0 refers to the size of the inclusions in the first case, or the *mean* size of inclusions in the second case). We arbitrarily choose $\lambda = 1$ (implying that the critical stress τ_{crit} equals 2 for inclusions of size 1/4), and equally arbitrarily set the standard deviation σ equal to a_0 for the normal distribution. We set $G_{\text{m}} = 1$ without loss of generality because it can be absorbed into the constant of proportionality which links the stress to displacement.

The results can be seen in Figures 2.5 and 2.6. The first graph shows that as soon as the stress reaches the value of 2, all the inclusions debond simultaneously (as indicated above). The second graph, on the other hand, shows a *gradual* softening of the material as the larger inclusions debond, followed by the smaller inclusions until the curve asymptotes to the curve in the first graph once the proportion of debonded inclusions approaches 1. If the standard deviation σ were smaller, the second graph would become closer to the first, since the probability density function (2.331) tends to the function (2.330) in the sense of distributions as $\sigma \to 0$.

These graphs, it is to be stressed, show the initial loading curve: while the material would follow these curves on loading, on unloading they would follow a different curve (in fact, a straight line towards the origin), given that there is no re-bonding of the matrix to the inclusions. We say that the materials are undergoing damage, because they are softening as the stress is increased.

The similarity of the second graph to Figure 1.3 is striking. This gives us reason to believe that the mechanism that we have postulated for the effect seen in the anechoic tiles is reasonably correct.

2.5 Conclusion

In this chapter we have analysed the antiplane shear of a distribution of embedded fibres, as a simple analogy to the distribution of spherical shells which will be studied in the remaining chapters. We have found the effective shear modulus for a distribution of fibres, using the point-inclusion approach, which was subsequently generalised to the case of a dispersion of fibres with varying properties. Using this generalised expression we were able to consider two states of the fibre, namely attached and detached, distributed throughout the medium. Whether the fibres were bonded or debonded depended on the stress in the material (or, more accurately, the *maximum previous stress*), which can be linked to the stress far from the inclusion when considering the fibres as being isolated (the inner problem). The transition between the two states is given (for a given size of inclusion) by the results of Section 2.3.

One possible improvement to the debonding model is to relax the assumption that the initial debonded patches occur at the regions of greatest stress. This may cause

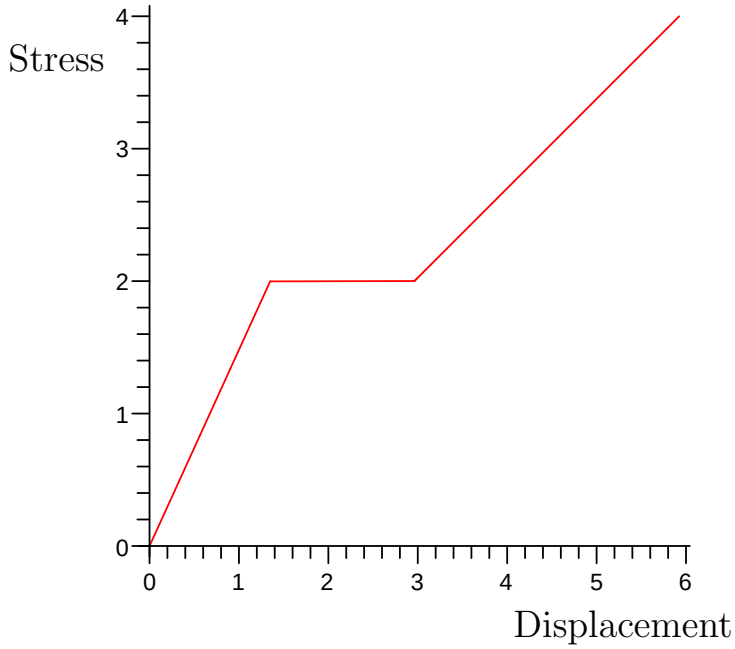

Figure 2.5: Stress–displacement graph for a composite material containing identical inclusions undergoing damage.

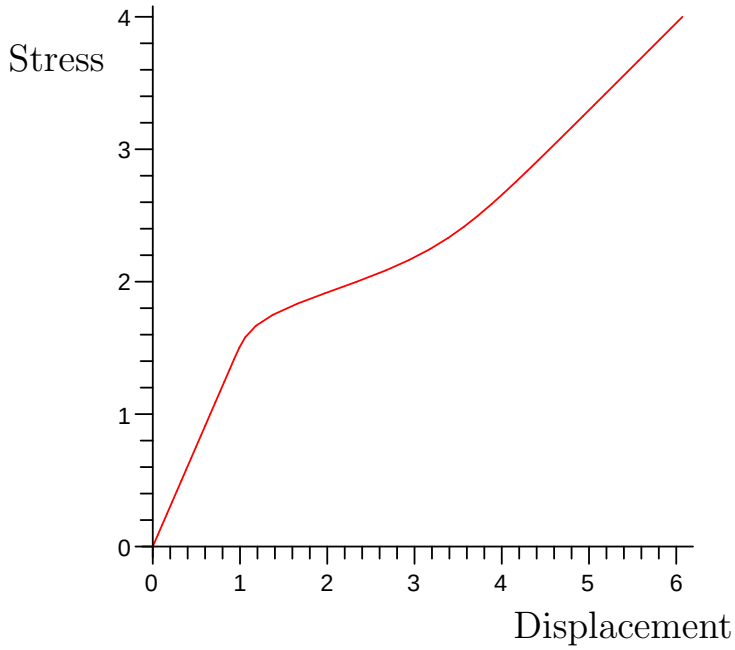

Figure 2.6: Stress–displacement graph for a composite material containing a normal distribution of inclusions undergoing damage.

some inclusions to debond at a higher applied stress, thus giving a more gradual variation in the proportion of debonded fibres as the applied stress increases.

In Chapter 6, we will apply this process to the study of the buckling of a distribution of embedded shells. The debonding of the fibres corresponds to the buckling of the shells, so that we have two states of an inclusion: unbuckled and buckled. These states will be found in Chapters 3 and 5 respectively, while an analytic expression for the critical stress at which buckling occurs is found in Chapter 4. Finally, in Chapter 6 we will analyse the method of Section 2.4.2 in more depth in order to apply it to the three-dimensional case. A distribution of buckling shells will be considered, following the method of Section 2.4.4.

Chapter 3

Buckling of an Embedded Sphere

In this chapter we intend to analyse the deformation and subsequent buckling of a spherical shell embedded in an elastic matrix with an applied stress field at infinity. In order to find the buckling criterion we will need to investigate the change in stability of the pre-buckled state from stable to unstable. To this end we first review the Trefftz criterion which will give us the condition required for the change in stability. Following this we will find the pre-buckled state, by a method of Love [64]. This will feed into the expression for the change in potential energy required by the Trefftz criterion, which will also require expanding the virtual displacement of the shell in terms of Legendre functions, assuming an axisymmetric buckling pattern. The point at which change in stability occurs is finally calculated by the Rayleigh–Ritz method.

3.1 Physical description of the problem

We consider a spherical shell, depicted in Figure 3.1, with internal radius R_0 and external radius R_1 embedded in an isotropic linearly elastic matrix. By setting

$$R_0 = \widehat{R} - \frac{h}{2}\,, \tag{3.1}$$

$$R_1 = \widehat{R} + \frac{h}{2}\,, \tag{3.2}$$

we can alternatively say that the shell has a spherical mid-surface of radius $\widehat{R}$ and a constant thickness h. The matrix is characterised by its shear modulus G_{m} and Poisson ratio ν_{m}, and likewise the shell is characterised by G_{s} and ν_{s}. The shell is hollow, with a hydrostatic pressure applied on the inner surface.

We assume that the shell is tightly bonded to the matrix, so that the displacement and traction at $R = R_1$ are continuous. Finally, we impose that the state of stress in the shell is a superposition of two states of stress: the response to a uniaxial stress $\tau_{zz}|_{\infty} = -q_z$ at infinity, and the (purely radial) response to the applied stresses $\tau_{RR}|_{\infty} = -q_R$ and $\tau_{RR}|_{R_0} = -q_{\mathrm{in}}$.

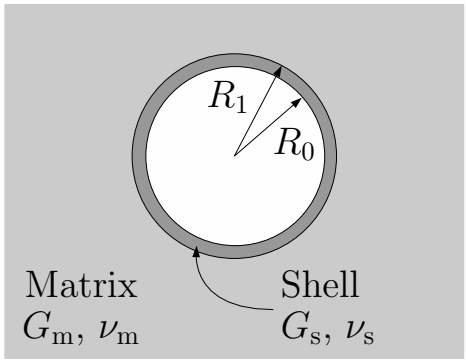

Figure 3.1: Configuration of the physical problem.

3.2 Conditions for change in stability

We will now review the conditions for the change in stability of a mechanical system. Suppose that a mechanical system is in a state I. To investigate the stability of this state, we superimpose a *virtual* displacement, to create a second state II. The state of the system is characterised by its potential energy.

Denoting the potential energy of the system by W, we define the change in potential energy as

$$\Delta W \;=\; W_\mathrm{II} - W_\mathrm{I}\,, \tag{3.3}$$

where the subscripts refer to the state of the system. Suppose that the virtual displacement is given by $\boldsymbol{v}$. We can split ΔW into terms which are linear in $\boldsymbol{v}$, quadratic terms, and terms of higher order:

$$\Delta W \;=\; \Delta W_1 + \Delta W_2 + \cdots\,. \tag{3.4}$$

The equilibrium state of the system can be found by setting $\Delta W_1 = 0$ for all variations $\boldsymbol{v}$ and using the calculus of variations to find the Euler equations for the system. Then [12] the equilibrium state is stable if $\Delta W_2 > 0$ for all variations $\boldsymbol{v}$. The *critical load* for a continuous system is the lowest load for which ΔW_2 is nonpositive for at least one possible variation. At this load the equilibrium changes from stable to unstable. The *Trefftz criterion* for stability states that the transition from stability to instability, in terms of the loading parameter of state I, is found at a stationary value of ΔW_2 (with respect to $\boldsymbol{v}$).

We now consider how this theory applies to the shell embedded in a matrix. First, we state that the virtual displacement $\boldsymbol{v}$ will refer to the virtual shell displacement; the virtual displacement in the matrix will be found as a linear function of $\boldsymbol{v}$, as the matrix obeys linear elasticity. The total potential energy of the system will be given

by the sum of the potential energy in the shell and the potential energy in the matrix. We will first consider the shell.

Denoting quantities pertaining to state I by a superscript (I), we suppose as before that the displacement in the shell in state I is given by $\boldsymbol{v}^{(\mathrm{I})} + \boldsymbol{v}$, where $\boldsymbol{v}$ is the virtual displacement. Using the expression (A.168) for the potential energy density in the shell, the change in potential energy density, denoted ΔV, is given by

$$\begin{aligned}\Delta V &= \frac{h}{2}E^{\alpha\beta\lambda\mu}\left(\gamma^{(\mathrm{I})}_{\alpha\beta}+\gamma_{\alpha\beta}\right)\left(\gamma^{(\mathrm{I})}_{\lambda\mu}+\gamma_{\lambda\mu}\right)+\frac{h^3}{24}E^{\alpha\beta\lambda\mu}\left(\rho^{(\mathrm{I})}_{\alpha\beta}+\rho_{\alpha\beta}\right)\left(\rho^{(\mathrm{I})}_{\lambda\mu}+\rho_{\lambda\mu}\right)\\ &\qquad -\frac{h}{2}E^{\alpha\beta\lambda\mu}\gamma^{(\mathrm{I})}_{\alpha\beta}\gamma^{(\mathrm{I})}_{\lambda\mu}-\frac{h^3}{24}E^{\alpha\beta\lambda\mu}\rho^{(\mathrm{I})}_{\alpha\beta}\rho^{(\mathrm{I})}_{\lambda\mu} \qquad (3.5)\\ &= \frac{h}{2}E^{\alpha\beta\lambda\mu}\left(\gamma^{(\mathrm{I})}_{\alpha\beta}\gamma_{\lambda\mu}+\gamma_{\alpha\beta}\gamma^{(\mathrm{I})}_{\lambda\mu}+\gamma_{\alpha\beta}\gamma_{\lambda\mu}\right)\\ &\qquad +\frac{h^3}{24}E^{\alpha\beta\lambda\mu}\left(\rho^{(\mathrm{I})}_{\alpha\beta}\rho_{\lambda\mu}+\rho_{\alpha\beta}\rho^{(\mathrm{I})}_{\lambda\mu}+\rho_{\alpha\beta}\rho_{\lambda\mu}\right)\ , \qquad (3.6)\end{aligned}$$

where $\gamma_{\alpha\beta}$ is the middle-surface strain tensor of the shell and $\rho_{\alpha\beta}$ is the tensor of changes of curvature. The quantity $E^{\alpha\beta\lambda\mu}$ is the elasticity tensor for shells, defined in (A.167).

We will determine the pre-buckled state I using the hypothesis of *linear* elasticity, so that terms which are of quadratic order or higher in the strain tensor are negligible. Thus we replace the middle-surface strain tensor for state I, defined $\gamma^{(\mathrm{I})}_{\alpha\beta}$, by its linearised counterpart $\theta^{(\mathrm{I})}_{\alpha\beta}$, as defined in equation (A.160). Then we have

$$\begin{aligned}\Delta V &= \frac{h}{2}E^{\alpha\beta\lambda\mu}\left(\theta^{(\mathrm{I})}_{\alpha\beta}\gamma_{\lambda\mu}+\gamma_{\alpha\beta}\theta^{(\mathrm{I})}_{\lambda\mu}+\gamma_{\alpha\beta}\gamma_{\lambda\mu}\right)\\ &\qquad +\frac{h^3}{24}E^{\alpha\beta\lambda\mu}\left(\rho^{(\mathrm{I})}_{\alpha\beta}\rho_{\lambda\mu}+\rho_{\alpha\beta}\rho^{(\mathrm{I})}_{\lambda\mu}+\rho_{\alpha\beta}\rho_{\lambda\mu}\right)\ . \qquad (3.7)\end{aligned}$$

We then assume that the middle-surface strain tensor and the tensor of changes of curvature are related to the stress resultants and stress couples of the shell in state I by equations (A.165)–(A.166). These equations hold within the fundamental approximation of shell theory, *i.e.* that the thickness of the shell is small compared with its radius of curvature, so that

$$\begin{aligned}{}^{(\mathrm{I})}n^{\alpha\beta} &= hE^{\alpha\beta\lambda\mu}\theta^{(\mathrm{I})}_{\lambda\mu}\left[1+O(h/\widehat{R})\right]\ , \qquad (3.8)\\ {}^{(\mathrm{I})}m^{\alpha\beta} &= \frac{h^3}{12}E^{\alpha\beta\lambda\mu}\rho^{(\mathrm{I})}_{\lambda\mu}\left[1+O(h/\widehat{R})\right]\ . \qquad (3.9)\end{aligned}$$

Thus we can write

$$\Delta V = {}^{(\mathrm{I})}n^{\alpha\beta}\gamma_{\alpha\beta}+{}^{(\mathrm{I})}m^{\alpha\beta}\rho_{\alpha\beta}+\frac{h}{2}E^{\alpha\beta\lambda\mu}\gamma_{\alpha\beta}\gamma_{\lambda\mu}+\frac{h^3}{24}E^{\alpha\beta\lambda\mu}\rho_{\alpha\beta}\rho_{\lambda\mu} \qquad (3.10)$$

where ${}^{(\mathrm{I})}n^{\alpha\beta}$, ${}^{(\mathrm{I})}m^{\alpha\beta}$ are the stress resultants and stress couples of the pre-buckled state.

We now assume that the virtual displacement satisfies the *nonlinear shallow shell theory* of Section A.4.2, where $\gamma_{\alpha\beta}$ and $\rho_{\alpha\beta}$ are given by equations (A.158)–(A.159). We can thus take ΔV and split it into linear terms, quadratic terms, and terms of higher order. The linear terms are

$$\Delta V_1 = {}^{(\mathrm{I})}n^{\alpha\beta}\theta_{\alpha\beta} + {}^{(\mathrm{I})}m^{\alpha\beta}\rho_{\alpha\beta} \tag{3.11}$$

and the quadratic terms are

$$\Delta V_2 = \frac{1}{2}{}^{(\mathrm{I})}n^{\alpha\beta}w_{,\alpha}w_{,\beta} + \frac{h}{2}E^{\alpha\beta\lambda\mu}\theta_{\alpha\beta}\theta_{\lambda\mu} + \frac{h^3}{24}E^{\alpha\beta\lambda\mu}\rho_{\alpha\beta}\rho_{\lambda\mu} \tag{3.12}$$

where $\theta_{\alpha\beta}$, the linearised middle-surface strain tensor, is given by (A.160), and w is the normal displacement of the shell. The reason for choosing the nonlinear theory for the virtual displacement is now apparent, since if we had not included the nonlinear term $\frac{1}{2}w_{,\alpha}w_{,\beta}$ in $\gamma_{\alpha\beta}$, then ΔV_2 would be independent of the pre-buckled state I.

Then the change in potential energy of the shell become

$$\begin{aligned}\Delta W_{\mathrm{s}} = {} & \iint_{\substack{\text{mid-shell}\\ \text{surface}}} \left({}^{(\mathrm{I})}n^{\alpha\beta}\theta_{\alpha\beta} + {}^{(\mathrm{I})}m^{\alpha\beta}\rho_{\alpha\beta}\right) \mathrm{d}S \\ & + \iint_{\substack{\text{mid-shell}\\ \text{surface}}} \left(\frac{1}{2}{}^{(\mathrm{I})}n^{\alpha\beta}w_{,\alpha}w_{,\beta} + \frac{h}{2}E^{\alpha\beta\lambda\mu}\theta_{\alpha\beta}\theta_{\lambda\mu} + \frac{h^3}{24}E^{\alpha\beta\lambda\mu}\rho_{\alpha\beta}\rho_{\lambda\mu}\right) \mathrm{d}S \\ & + \text{higher order terms.}\end{aligned} \tag{3.13}$$

We now consider the matrix. There will be a virtual displacement $\boldsymbol{u}$ which arises due to the virtual displacement $\boldsymbol{v}$ of the shell, and in addition we need to consider the pre-buckling matrix displacement $\boldsymbol{u}^{(\mathrm{I})}$, giving a total displacement of $\boldsymbol{u}^{(\mathrm{I})} + \boldsymbol{u}$. From equation (A.49), we can see that the change in potential energy density between states I and II is

$$\Delta V = \frac{1}{2}A^{ijkl}\left(e^{(\mathrm{I})}_{ij}e^{(\mathrm{I})}_{kl} + e^{(\mathrm{I})}_{ij}e_{kl} + e_{ij}e^{(\mathrm{I})}_{kl} + e_{ij}e_{kl}\right) - \frac{1}{2}A^{ijkl}e^{(\mathrm{I})}_{ij}e^{(\mathrm{I})}_{kl} \tag{3.14}$$

$$= \frac{1}{2}A^{ijkl}\left(e^{(\mathrm{I})}_{ij}e_{kl} + e_{ij}e^{(\mathrm{I})}_{kl} + e_{ij}e_{kl}\right) , \tag{3.15}$$

where $e^{(\mathrm{I})}_{ij}$, e_{ij} are strain tensors formed from $\boldsymbol{u}^{(\mathrm{I})}$, $\boldsymbol{u}$ respectively. The first two terms in the expression above are linear in the virtual displacement $\boldsymbol{u}$ (and hence linear in $\boldsymbol{v}$). The linear and quadratic terms in the change of potential energy of the matrix thus become

$$\begin{aligned}\Delta W_{\mathrm{m}} = {} & \iiint_{R>R_1} \frac{1}{2}A^{ijkl}\left(e^{(\mathrm{I})}_{ij}e_{kl} + e_{ij}e^{(\mathrm{I})}_{kl}\right) \mathrm{d}V \\ & + \iiint_{R>R_1} \frac{1}{2}A^{ijkl}e_{ij}e_{kl}\,\mathrm{d}V \ .\end{aligned} \tag{3.16}$$

Finally, we note that if a hydrostatic pressure q_{in} is applied to the inner surface of the shell, the potential energy of this loading will be given by

$$\Delta W_{\text{in}} \;=\; -\iint_{R=R_0} q_{\text{in}} w \,\mathrm{d}S \;, \tag{3.17}$$

which is linear in the virtual displacement.

Therefore, the total change in potential energy is given by the sum of equations (3.13), (3.16) and (3.17), or

$$\Delta W \;=\; \Delta W_{\text{s}} + \Delta W_{\text{m}} + \Delta W_{\text{in}} \;. \tag{3.18}$$

However this is written as the sum of terms which are linear and quadratic in the virtual displacement, as in equation (3.4). We find that

$$\begin{aligned} \Delta W_1 \;=\; & \iint_{\substack{\text{mid-shell}\\ \text{surface}}} \left({}^{(\text{I})}n^{\alpha\beta}\theta_{\alpha\beta} + {}^{(\text{I})}m^{\alpha\beta}\rho_{\alpha\beta} \right) \mathrm{d}S \\ & + \iiint_{R>R_1} \frac{1}{2} A^{ijkl} \left(e^{(\text{I})}_{ij} e_{kl} + e_{ij} e^{(\text{I})}_{kl} \right) \mathrm{d}V - \iint_{R=R_0} q_{\text{in}} w \,\mathrm{d}S \;, \end{aligned} \tag{3.19}$$

and

$$\Delta W_2 \;=\; \mathscr{I}_1 + \mathscr{I}_2 + \mathscr{I}_3 \;, \tag{3.20}$$

where

$$\mathscr{I}_1 \;=\; \iint_{\substack{\text{mid-shell}\\ \text{surface}}} \frac{1}{2} {}^{(\text{I})}n^{\alpha\beta} w_{,\alpha} w_{,\beta} \,\mathrm{d}S \;, \tag{3.21}$$

$$\mathscr{I}_2 \;=\; \iint_{\substack{\text{mid-shell}\\ \text{surface}}} \left(\frac{h}{2} E^{\alpha\beta\lambda\mu} \theta_{\alpha\beta} \theta_{\lambda\mu} + \frac{h^3}{24} E^{\alpha\beta\lambda\mu} \rho_{\alpha\beta} \rho_{\lambda\mu} \right) \mathrm{d}S \;, \tag{3.22}$$

$$\mathscr{I}_3 \;=\; \iiint_{R>R_1} \frac{1}{2} A^{ijkl} e_{ij} e_{kl} \,\mathrm{d}V \;. \tag{3.23}$$

It will become convenient to consider these three contributions to the energy integral separately.

Now, as stated previously, in order to obtain the pre-buckled state I, we solve the variational problem $\Delta W_1 = 0$ for each possible virtual displacement $\boldsymbol{v}$. However, a different method is to obtain the pre-buckled state by another means, and *assume* that ΔW_1 is zero, or at least small in the limit of shell theory. Then the critical buckling stress is found at a stationary point of ΔW_2.

3.2.1 The Rayleigh–Ritz method

Before determining the deformation in the prebuckled state, we consider the problem of finding the critical load by finding the stationary point of equation (3.20), by the

Trefftz criterion. We limit our consideration to axisymmetric buckling patterns, so that we can write

$$\boldsymbol{v} \;=\; v_R \boldsymbol{e}_R + v_\theta \boldsymbol{e}_\theta \;, \tag{3.24}$$

where v_R, v_θ are functions of R and θ only. By equations (A.199) and (A.200), we have

$$v_1 \;=\; \widehat{R} v_\theta \;, \tag{3.25}$$

$$w \;=\; v_R \;. \tag{3.26}$$

To find the stationary value of (3.20), we will use the Rayleigh–Ritz approach [55] which involves writing the virtual displacement as an infinite series,

$$v_R \;=\; \sum_{n=0}^{\infty} \mathscr{U}_n P_n^{(0)}(\mu) \;, \tag{3.27}$$

$$v_\theta \;=\; \sum_{n=1}^{\infty} \mathscr{V}_n P_n^{(1)}(\mu) \;, \tag{3.28}$$

or equivalently

$$w \;=\; \sum_{n=0}^{\infty} \mathscr{U}_n P_n^{(0)}(\mu) \;, \tag{3.29}$$

$$v_1 \;=\; \sum_{n=1}^{\infty} \widehat{R} \mathscr{V}_n P_n^{(1)}(\mu) \;. \tag{3.30}$$

In these expressions, $P_n^{(0)}(\mu)$ is a Legendre polynomial, $P_n^{(1)}(\mu)$ is an associated Legendre function as defined in (B.4), $\mu = \cos\theta$ and $\mathscr{U}_n$, $\mathscr{V}_n$ are constant coefficients. These coefficients are then found by solving

$$\frac{\partial}{\partial \mathscr{U}_n} \Delta W_2 \;=\; 0 \;, \tag{3.31}$$

$$\frac{\partial}{\partial \mathscr{V}_n} \Delta W_2 \;=\; 0 \;. \tag{3.32}$$

We will get an infinite system of linear equations whose determinant must be set to zero for a nonzero buckling deformation. The critical value for the applied stress at infinity will be found from this condition.

Finally we note that since the buckling deformations are axisymmetric, we have $w_{,2} = 0$ and so the only term of the stress resultant tensor ${}^{(\mathrm{I})}n^{\alpha\beta}$ that contributes to the integral (3.21) is ${}^{(\mathrm{I})}n^{11}$. Thus only the component $\tau_{\theta\theta}$ of stress in the shell will be used in the determination of the critical buckling parameter.

3.3 Pre-buckled state of stress

As stated in Section 3.1, the state of stress in the pre-buckled shell will be found by considering two states of stress and superposing the results. The first state of stress is a uniaxial compression at infinity, and the second is a purely radial deformation. The deformed state will be found by the full theory of linear elasticity, and the information required for the buckling problem (namely the stress resultant ${}^{(\mathrm{I})}n^{11}$) will be extracted from this state.

For the first case we assume that the only applied stress is a component

$$\tau_{zz}|_{\infty} \;=\; -q_z \;. \tag{3.33}$$

This implies that the deformation of the system will be axisymmetric, for which the displacement component u_ϕ is zero and all quantities are independent of the coordinate ϕ. The state of stress in the shell before buckling will be solved by a method of Love [64], which was used by Goodier [33] to solve the problem of a spherical elastic inclusion embedded in a dissimilar elastic matrix. This work was repeated by Liu and Nauman [63] and Bilgen and Insana [8]. Mazzullo [67] has built on previous work on the case of a multi-layered inclusion, which is solved numerically due to the large system of equations that results from the analysis.

The method solves the problem by combining two types of harmonic function to construct a solution. A harmonic function, by definition, satisfies Laplace's equation,

$$\nabla^2\Phi \;=\; 0 \;. \tag{3.34}$$

In spherical polar coordinates with axisymmetry,

$$\frac{1}{R^2}\frac{\partial}{\partial R}\left(R^2\frac{\partial\Phi}{\partial R}\right) + \frac{1}{R^2\sin\theta}\frac{\partial}{\partial\theta}\left(\sin\theta\frac{\partial\Phi}{\partial\theta}\right) \;=\; 0 \;. \tag{3.35}$$

By separating solutions, one can show that

$$\Phi \;=\; R^n P_n^{(0)}(\mu) \tag{3.36}$$

is a solution for all integers n, where

$$\mu \;=\; \cos\theta \tag{3.37}$$

and $P_n^{(0)}(\mu)$ is a Legendre polynomial (see Appendix B). The solution (3.36) is known as an axisymmetric harmonic of order n. By equation (B.2) we have

$$\Phi_n \;=\; \begin{cases} R^n P_n^{(0)}(\mu) & \text{if } n \geqslant 0 \\ R^n P_{-n-1}^{(0)}(\mu) & \text{if } n < 0 \;. \end{cases} \tag{3.38}$$

The two types of spherical harmonic function used for the solution are denoted $\phi^{(n)}$ and $\omega^{(n)}$ where n is the order of the harmonic. When limited to axisymmetric deformations, the displacements and dilatation in terms of the first solution are

$$u_R = \frac{\partial \phi^{(n)}}{\partial R} , \tag{3.39}$$

$$u_\theta = \frac{1}{R}\frac{\partial \phi^{(n)}}{\partial \theta} = -\frac{\sqrt{1-\mu^2}}{R}\frac{\partial \phi^{(n)}}{\partial \mu} , \tag{3.40}$$

$$\Delta = 0 . \tag{3.41}$$

For the second solution,

$$u_R = R^2\frac{\partial \omega^{(n)}}{\partial R} + \alpha_n R\omega^{(n)} , \tag{3.42}$$

$$u_\theta = R\frac{\partial \omega^{(n)}}{\partial \theta} = -R\sqrt{1-\mu^2}\frac{\partial \omega^{(n)}}{\partial \mu} , \tag{3.43}$$

$$\Delta = \big(2n + (3+n)\alpha_n\big)\omega^{(n)} , \tag{3.44}$$

where
$$\alpha_n = \frac{-2\big(3n+1-2(2n+1)\nu\big)}{n+5-4\nu} . \tag{3.45}$$

The two stress components which are required for matching are, from equations (A.126) and (A.128),

$$\tau_{RR} = 2G\left(\frac{\partial u_R}{\partial R} + \frac{\nu}{1-2\nu}\Delta\right) , \tag{3.46}$$

$$\tau_{R\theta} = G\left(\frac{1}{R}\frac{\partial u_R}{\partial \theta} + R\frac{\partial}{\partial R}\left(\frac{u_\theta}{R}\right)\right) \tag{3.47}$$

$$= G\left(-\frac{\sqrt{1-\mu^2}}{R}\frac{\partial u_R}{\partial \mu} + R\frac{\partial}{\partial R}\left(\frac{u_\theta}{R}\right)\right) , \tag{3.48}$$

on using (A.46) to write λ in terms of ν and G.

In the matrix, we choose the three harmonic functions

$$\phi^{(-1)} = \frac{A}{R}P_0^{(0)}(\mu) , \tag{3.49}$$

$$\phi^{(-3)} = \frac{B}{R^3}P_2^{(0)}(\mu) , \tag{3.50}$$

$$\omega^{(-3)} = \frac{C}{R^3}P_2^{(0)}(\mu) , \tag{3.51}$$

(where A, B and C are undetermined constants) together with a homogeneous field $\boldsymbol{u}^\infty$ which is the displacement given by a constant stress field with only one component, $\tau_{zz} = -q_z$.

First we will find the displacements and stresses due to the three harmonic functions. We find that the displacements become, on using equations (3.39), (3.40),

(3.42) and (3.43),

$$u_R = -\frac{A}{R^2}P_0^{(0)}(\mu) + \left(-\frac{3B}{R^4} - \frac{3C}{R^2} + \frac{C\alpha_{-3}^{(\mathrm{m})}}{R^2}\right)P_2^{(0)}(\mu)\ , \tag{3.52}$$

$$u_\theta = \frac{B}{R^4}P_2^{(1)}(\mu) + \frac{C}{R^2}P_2^{(1)}(\mu)\ , \tag{3.53}$$

applying (B.4). The stress components are

$$\tau_{RR} = 2G_{\mathrm{m}}\left[\frac{2A}{R^3}P_0^{(0)}(\mu) + \left(\frac{12B}{R^5} + \frac{6C}{R^3} - \frac{2C\alpha_{-3}^{(\mathrm{m})}}{R^3} - \frac{6C\nu_{\mathrm{m}}}{(1-2\nu_{\mathrm{m}})R^3}\right)P_2^{(0)}(\mu)\right] \tag{3.54}$$

$$\tau_{R\theta} = G_{\mathrm{m}}\left[-\frac{8B}{R^5} - \frac{6C}{R^3} + \frac{C\alpha_{-3}^{(\mathrm{m})}}{R^3}\right]P_2^{(1)}(\mu)\ , \tag{3.55}$$

using (3.46) and (3.48). Here the superscript (m) on the α_n constants refer to the fact that the matrix elastic constants are those that are used in the evaluation of α_n.

Next the solution $\boldsymbol{u}^\infty$ is found by solving the six equations contained in the stress–strain relation of equation (A.43) in Cartesian coordinates,

$$\tau_{ij} = \lambda e_{kk}\delta_{ij} + 2Ge_{ij}\ , \tag{3.56}$$

where the only nonzero left-hand side is $\tau_{zz} = -q_z$. We soon find that

$$e_{xx} = e_{yy} = \frac{\nu_{\mathrm{m}}q_z}{E_{\mathrm{m}}}\ , \tag{3.57}$$

$$e_{zz} = -\frac{q_z}{E_{\mathrm{m}}}\ , \tag{3.58}$$

$$e_{ij} = 0 \qquad \text{if } i \neq j\ , \tag{3.59}$$

where E_{m} is the Young's modulus in the matrix. Eventually we obtain

$$\boldsymbol{u}^\infty = \frac{q_z R}{6G_{\mathrm{m}}}\left(\frac{2\nu_{\mathrm{m}}-1}{\nu_{\mathrm{m}}+1}P_0^{(0)}(\mu) - 2P_2^{(0)}(\mu)\right)\boldsymbol{e}_R - \frac{q_z R}{6G_{\mathrm{m}}}P_2^{(1)}(\mu)\boldsymbol{e}_\theta\ , \tag{3.60}$$

on integrating equations (3.57)–(3.58), changing to spherical polar coordinates and using $\mu = \cos\theta$. The corresponding stress components for this solution are

$$\tau_{RR} = -\frac{q_z}{3}P_0^{(0)}(\mu) - \frac{2q_z}{3}P_2^{(0)}(\mu)\ , \tag{3.61}$$

$$\tau_{R\theta} = -\frac{q_z}{3}P_2^{(1)}(\mu)\ , \tag{3.62}$$

on writing $\tau_{zz} = -q_z$ in spherical polar coordinates.

The displacement in the matrix is written as the sum of equations (3.52), (3.53) and (3.60), or

$$u_R = -\frac{A}{R^2}P_0^{(0)}(\mu) + \left(-\frac{3B}{R^4} - \frac{3C}{R^2} + \frac{C\alpha_{-3}^{(\mathrm{m})}}{R^2}\right)P_2^{(0)}(\mu) + \frac{q_z R}{6G_{\mathrm{m}}}\left(\frac{2\nu_{\mathrm{m}}-1}{\nu_{\mathrm{m}}+1}P_0^{(0)}(\mu) - 2P_2^{(0)}(\mu)\right)\ , \tag{3.63}$$

$$u_\theta = \frac{B}{R^4}P_2^{(1)}(\mu) + \frac{C}{R^2}P_2^{(1)}(\mu) - \frac{q_z R}{6G_{\mathrm{m}}}P_2^{(1)}(\mu)\ . \tag{3.64}$$

Similarly the relevant stress components in the matrix are given by the sum of equations (3.54) and (3.61), and (3.55) and (3.62), or

$$\tau_{RR} = 2G_{\rm m}\left[\frac{2A}{R^3}P_0^{(0)}(\mu)+\left(\frac{12B}{R^5}+\frac{6C}{R^3}-\frac{2C\alpha_{-3}^{(\rm m)}}{R^3}-\frac{6C\nu_{\rm m}}{(1-2\nu_{\rm m})R^3}\right)P_2^{(0)}(\mu)\right] - \frac{q_z}{3}P_0^{(0)}(\mu)-\frac{2q_z}{3}P_2^{(0)}(\mu)\ , \tag{3.65}$$

$$\tau_{R\theta} = G_{\rm m}\left[-\frac{8B}{R^5}-\frac{6C}{R^3}+\frac{C\alpha_{-3}^{(\rm m)}}{R^3}\right]P_2^{(1)}(\mu)-\frac{q_z}{3}P_2^{(1)}(\mu)\ . \tag{3.66}$$

In the shell, we use the potential functions

$$\phi^{(-1)} = \frac{D}{R}P_0^{(0)}(\mu)\ , \tag{3.67}$$

$$\phi^{(-3)} = \frac{E}{R^3}P_2^{(0)}(\mu)\ , \tag{3.68}$$

$$\omega^{(-3)} = \frac{F}{R^3}P_2^{(0)}(\mu)\ , \tag{3.69}$$

$$\phi^{(2)} = GR^2P_2^{(0)}(\mu)\ , \tag{3.70}$$

$$\omega^{(2)} = HR^2P_2^{(0)}(\mu)\ , \tag{3.71}$$

$$\omega^{(0)} = IP_0^{(0)}(\mu)\ , \tag{3.72}$$

where D to I are undetermined constants. After similar analysis to the matrix, we find that the displacement and stress components in the shell become

$$u_R = \left(-\frac{D}{R^2}+\alpha_0^{(\rm s)}RI\right)P_0^{(0)}(\mu) + \left(-\frac{3E}{R^4}+2GR-\frac{3F}{R^2}+\frac{\alpha_{-3}^{(\rm s)}F}{R^2}+2HR^3+\alpha_2^{(\rm s)}R^3H\right)P_2^{(0)}(\mu)\ , \tag{3.73}$$

$$u_\theta = \left(\frac{E}{R^4}+\frac{F}{R^2}+GR+HR^3\right)P_2^{(1)}(\mu)\ , \tag{3.74}$$

$$\tau_{RR} = 2G_{\rm s}\left(\frac{2D}{R^3}+\alpha_0^{(\rm s)}I+\frac{3\alpha_0^{(\rm s)}I\nu_{\rm s}}{1-2\nu_{\rm s}}\right)P_0^{(0)}(\mu) + 2G_{\rm s}\left\{\frac{12E}{R^5}+2G+(6-2\alpha_{-3}^{(\rm s)})\frac{F}{R^3}+3(2+\alpha_2^{(\rm s)})R^2H + \frac{\nu_{\rm s}}{1-2\nu_{\rm s}}\left(-\frac{6F}{R^3}+(4+5\alpha_2^{(\rm s)})HR^2\right)\right\}P_2^{(0)}(\mu)\ , \tag{3.75}$$

$$\tau_{R\theta} = G_{\rm s}\left(\frac{-8E}{R^5}+2G-\frac{6F}{R^3}+\frac{\alpha_{-3}^{(\rm s)}F}{R^3}+4HR^2+\alpha_2^{(\rm s)}R^2H\right)P_2^{(1)}(\mu)\ , \tag{3.76}$$

where the (s) superscript denotes that shell elastic constants should be used.

The nine constants A to I are found by equating the displacement components u_R and u_θ and the stress components τ_{RR} and $\tau_{R\theta}$ at $R = R_1$, and letting τ_{RR} and

$\tau_{R\theta}$ be zero at $R = R_0$. The matching takes place by equating coefficients of $P_0^{(0)}(\mu)$, $P_2^{(0)}(\mu)$ and $P_2^{(1)}(\mu)$. The resulting linear system to be solved is

$$\frac{1}{R_1^2}A - \frac{1}{R_1^2}D + \alpha_0^{(\mathrm{s})}R_1 I = \frac{q_z R_1(2\nu_\mathrm{m}-1)}{6G_\mathrm{m}(1+\nu_\mathrm{m})}\,, \tag{3.77}$$

$$-\frac{3}{R_1^4}B + \left(\frac{\alpha_{-3}^{(\mathrm{m})}-3}{R_1^2}\right)C + \frac{3}{R_1^4}E + \left(\frac{3-\alpha_{-3}^{(\mathrm{s})}}{R_1^2}\right)F - 2R_1 G - (2+\alpha_2^{(\mathrm{s})})R_1^3 H = \frac{q_z R_1}{3G_\mathrm{m}}\,, \tag{3.78}$$

$$\frac{1}{R_1^4}B + \frac{1}{R_1^2}C - \frac{1}{R_1^4}E - \frac{1}{R_1^2}F - R_1 G - R_1^3 H = \frac{q_z R_1}{6G_\mathrm{m}}\,, \tag{3.79}$$

$$\frac{2}{R_0^3}D + \frac{1+\nu_\mathrm{s}}{1-2\nu_\mathrm{s}}\alpha_0^{(\mathrm{s})} I = 0\,, \tag{3.80}$$

$$\frac{12}{R_0^5}E + \left(\frac{6-2\alpha_{-3}^{(\mathrm{s})}}{R_0^3} - \frac{6\nu_\mathrm{s}}{R_0^3(1-2\nu_\mathrm{s})}\right)F + 2G + \left[3R_0^2(2+\alpha_2^{(\mathrm{s})}) + \frac{\nu_\mathrm{s}(4+5\alpha_2^{(\mathrm{s})})}{1-2\nu_\mathrm{s}}R_0^2\right]H = 0\,, \tag{3.81}$$

$$-\frac{8}{R_0^5}E + \frac{\alpha_{-3}^{(\mathrm{s})}-6}{R_0^3}F + 2G + (4+\alpha_2^{(\mathrm{s})})R_0^2 H = 0\,, \tag{3.82}$$

$$-\frac{2G_\mathrm{m}}{G_\mathrm{s}R_1^3}A + \frac{2}{R_1^3}D + \frac{1+\nu_\mathrm{s}}{1-2\nu_\mathrm{s}}\alpha_0^{(\mathrm{s})} I = -\frac{q_z}{6G_\mathrm{s}}\,, \tag{3.83}$$

$$\frac{12G_\mathrm{m}}{R_1^5 G_\mathrm{s}}B + \left(\frac{6-2\alpha_{-3}^{(\mathrm{m})}}{R_1^3} - \frac{6\nu_\mathrm{m}}{(1-2\nu_\mathrm{m})R_1^3}\right)\frac{G_\mathrm{m}}{G_\mathrm{s}}C - \frac{12}{R_1^5}E - \left(\frac{6-2\alpha_{-3}^{(\mathrm{s})}}{R_1^3} - \frac{6\nu_\mathrm{s}}{(1-2\nu_\mathrm{s})R_1^3}\right)F - 2G - \left(3(2+\alpha_2^{(\mathrm{s})})R_1^2 + \frac{(4+5\alpha_2^{(\mathrm{s})})\nu_\mathrm{s}R_1^2}{1-2\nu_\mathrm{s}}\right)H = \frac{q_z}{3G_\mathrm{s}}\,, \tag{3.84}$$

$$-\frac{8G_\mathrm{m}}{R_1^5 G_\mathrm{s}}B + \frac{G_\mathrm{m}}{G_\mathrm{s}}\left(\frac{\alpha_{-3}^{(\mathrm{m})}-6}{R_1^3}\right)C + \frac{8}{R_1^5}E + \left(\frac{6-\alpha_{-3}^{(\mathrm{s})}}{R_1^3}\right)F - 2G - (4R_1^2 + \alpha_2^{(\mathrm{s})}R_1^2)H = \frac{q_z}{3G_\mathrm{s}}\,. \tag{3.85}$$

The analytical solution to the above system can be found using a symbolic computation package such as Maple.

We now consider the case where the state of stress is purely radial, with

$$\tau_{RR}|_\infty = -q_R \tag{3.86}$$

$$\text{and} \quad \tau_{RR}|_{R_0} = -q_\mathrm{in}\,. \tag{3.87}$$

Then, the pre-buckling displacement will also be purely radial, with

$$\boldsymbol{u} = \left(A_{\rm s}R + \frac{B_{\rm s}}{R^2}\right)\boldsymbol{e}_R \,, \tag{3.88}$$

$$\boldsymbol{u} = \left(A_{\rm m}R + \frac{B_{\rm m}}{R^2}\right)\boldsymbol{e}_R \tag{3.89}$$

in the shell and the matrix respectively [64]. We find that the corresponding radial stress component becomes

$$\tau_{RR} = (3\lambda + 2G)A - \frac{4GB}{R^3} \,, \tag{3.90}$$

where A, B, λ and G have different values in the shell and the matrix, denoted by a suffix 'm' or 's'.

Using conditions (3.86) and (3.87), and matching τ_{RR} and $\boldsymbol{u}$ at $R = R_1$, we find that

$$A_{\rm m} = -\frac{q_R}{3\lambda_{\rm m} + 2G_{\rm m}} \,, \tag{3.91}$$

$$B_{\rm s} = \frac{(3\lambda_{\rm s} + 2G_{\rm s})R_0^3}{4G_{\rm s}}A_{\rm s} + \frac{R_0^3 q_{\rm in}}{4G_{\rm s}} \,, \tag{3.92}$$

$$B_{\rm m} = \frac{R_1^3}{4G_{\rm m}}\left[(3\lambda_{\rm s} + 2G_{\rm s})A_{\rm s}\left(\frac{R_0^3}{R_1^3} - 1\right) + \left(\frac{R_0^3 q_{\rm in}}{R_1^3} - q_R\right)\right] \,, \tag{3.93}$$

$$A_{\rm s} = \frac{\dfrac{q_{\rm in}R_0^3}{4R_1^3}\left(\dfrac{1}{G_{\rm m}} - \dfrac{1}{G_{\rm s}}\right) - q_R\left(\dfrac{1}{3\lambda_{\rm m} + 2G_{\rm m}} + \dfrac{1}{4G_{\rm m}}\right)}{\left\{1 + \dfrac{(3\lambda_{\rm s} + 2G_{\rm s})}{4}\left[\dfrac{R_0^3}{G_{\rm s}R_1^3} + \dfrac{1}{G_{\rm m}}\left(1 - \dfrac{R_0^3}{R_1^3}\right)\right]\right\}} \,. \tag{3.94}$$

3.3.1 Finding the stress resultant

From equations (A.95), (A.115), (A.107) and (A.108), the stress component $\tau_{\theta\theta}$ in the shell is

$$\tau_{\theta\theta} = 2G_{\rm s}\left(\frac{1}{R}\frac{\partial u_\theta}{\partial\theta} + \frac{u_R}{R} + \frac{\nu_{\rm s}}{1 - 2\nu_{\rm s}}\Delta\right) \tag{3.95}$$

$$= 2G_{\rm s}\left(-\frac{\sqrt{1-\mu^2}}{R}\frac{\partial u_\theta}{\partial\mu} + \frac{u_R}{R} + \frac{\nu_{\rm s}}{1 - 2\nu_{\rm s}}\Delta\right) \,. \tag{3.96}$$

First we will find $\tau_{\theta\theta}$ for both modes of deformation described earlier. From the first calculation, where the only applied stress was $\tau_{zz} = -q_z$ at infinity, we find that

$$\begin{aligned}\tau_{\theta\theta} = {} & 2G_{\rm s}\left(-\frac{D}{R^3} + \alpha_0^{(\rm s)}I + \frac{E}{R^5} + \frac{F}{R^3} + G + HR^2 + \frac{3\nu_{\rm s}\alpha_0^{(\rm s)}I}{1 - 2\nu_{\rm s}}\right)P_0^{(0)}(\mu) \\ & + 2G_{\rm s}\left[-\frac{7E}{R^5} - 2G + \frac{(-7 + \alpha_{-3}^{(\rm s)})F}{R^3} + (-2 + \alpha_2^{(\rm s)})R^2H \right. \\ & \left. + \frac{\nu_{\rm s}}{1 - 2\nu_{\rm s}}\left(-\frac{6F}{R^3} + (4 + 5\alpha_2^{(\rm s)})HR^2\right)\right]P_2^{(0)}(\mu) \,. \end{aligned} \tag{3.97}$$

For the second type of deformation, which was purely radial, we find that

$$\tau_{\theta\theta} = (3\lambda_\mathrm{s} + 2G_\mathrm{s})A_\mathrm{s} + \frac{2G_\mathrm{s}B_\mathrm{s}}{R^3} \tag{3.98}$$

$$= (3\lambda_\mathrm{s} + 2G_\mathrm{s})A_\mathrm{s}\left(1 + \frac{R_0^3}{2R^3}\right) + \frac{q_\mathrm{in}R_0^3}{2R^3}\ . \tag{3.99}$$

Hence overall,

$$\begin{aligned}\tau_{\theta\theta} = \Bigg[&2G_\mathrm{s}\left(-\frac{D}{R^3} + \alpha_0^{(\mathrm{s})}I + \frac{E}{R^5} + \frac{F}{R^3} + G + HR^2 + \frac{3\nu_\mathrm{s}\alpha_0^{(\mathrm{s})}I}{1-2\nu_\mathrm{s}}\right)\\ &+ (3\lambda_\mathrm{s} + 2G_\mathrm{s})A_\mathrm{s}\left(1 + \frac{R_0^3}{2R^3}\right) + \frac{q_\mathrm{in}R_0^3}{2R^3}\Bigg]P_0^{(0)}(\mu)\\ &+2G_\mathrm{s}\Bigg[-\frac{7E}{R^5} - 2G + \frac{(-7+\alpha_{-3}^{(\mathrm{s})})F}{R^3} + (-2+\alpha_2^{(\mathrm{s})})R^2H\\ &+\frac{\nu_\mathrm{s}}{1-2\nu_\mathrm{s}}\left(-\frac{6F}{R^3} + (4+5\alpha_2^{(\mathrm{s})})HR^2\right)\Bigg]P_2^{(0)}(\mu)\ .\end{aligned} \tag{3.100}$$

Next we will find the stress resultant n^{11} from this value of $\tau_{\theta\theta}$. From equation (A.163),

$$n^{11} = \int_{-h/2}^{h/2}\sigma^{11}\,\mathrm{d}\theta_3\ , \tag{3.101}$$

where θ_3, defined in (A.129), is the coordinate which is directed normal to the shell. However, $\theta_3 \in [-h/2, h/2]$ and $h/\widehat{R} \ll 1$, so let

$$\theta_3 = h\xi\ , \tag{3.102}$$

then

$$n^{11} = h\int_{-1/2}^{1/2}\sigma^{11}\,\mathrm{d}\xi\ . \tag{3.103}$$

We will further assume that

$$n^{11} \sim h\int_{-1/2}^{1/2}\left(\lim_{h/\widehat{R}\to 0}\sigma^{11}\right)\mathrm{d}\xi\ , \tag{3.104}$$

because we will only require the first term of n^{11} (regarded as an asymptotic expansion in $h/\widehat{R}$) for the shell buckling problem; any terms of higher order are neglected. But from equation (A.162),

$$\sigma^{11} = (1 - 2\theta_3 H + \theta_3^2 K)(1 - \theta_3 b_1^1)\tau^{11} \tag{3.105}$$

$$= \left(1 + \frac{\theta_3}{\widehat{R}}\right)^3\tau^{11}\ . \tag{3.106}$$

Here τ^{11} is the stress component referred to base vectors $\boldsymbol{g}_i$, where the coordinates are the shell coordinates (A.170)–(A.172). Therefore

$$\begin{aligned}
\tau^{11} &= \frac{1}{R^2}\tau_{\theta\theta} && (3.107)\\
\Rightarrow \qquad \sigma^{11} &= \left(1+\frac{\theta_3}{\widehat{R}}\right)^3 \frac{\tau_{\theta\theta}}{R^2} && (3.108)\\
&= \left(1+\frac{h\xi}{\widehat{R}}\right)^3 \frac{\tau_{\theta\theta}}{(\widehat{R}+h\xi)^2} && (3.109)\\
&= \frac{1}{\widehat{R}^2}\left(1+\frac{h\xi}{\widehat{R}}\right)\tau_{\theta\theta}\ . && (3.110)
\end{aligned}$$

Therefore

$$\lim_{h/\widehat{R}\to 0} \sigma^{11} = \frac{1}{\widehat{R}^2} \lim_{h/\widehat{R}\to 0} \tau_{\theta\theta}\ . \qquad (3.111)$$

But

$$\begin{aligned}
\lim_{h/\widehat{R}\to 0} \tau_{\theta\theta} = \Bigg[& 2G_{\rm s}\left(-\frac{\bar{D}}{\widehat{R}^3}+\frac{\bar{E}}{\widehat{R}^5}+\frac{\bar{F}}{\widehat{R}^3}+\bar{G}+\bar{H}\widehat{R}^2+\frac{(1+\nu_{\rm s})\alpha_0^{(\rm s)}\bar{I}}{1-2\nu_{\rm s}}\right)\\
& +\frac{3}{2}(3\lambda_{\rm s}+2G_{\rm s})\bar{A}_{\rm s}+\frac{q_{\rm in}}{2}\Bigg] P_0^{(0)}(\mu)\\
& +2G_{\rm s}\Bigg[-\frac{7\bar{E}}{\widehat{R}^5}-2\bar{G}+\frac{(-7+\alpha_{-3}^{(\rm s)})\bar{F}}{\widehat{R}^3}+(-2+\alpha_2^{(\rm s)})\widehat{R}^2\bar{H}\\
& +\frac{\nu_{\rm s}}{1-2\nu_{\rm s}}\left(-\frac{6\bar{F}}{\widehat{R}^3}+(4+5\alpha_2^{(\rm s)})\bar{H}\widehat{R}^2\right)\Bigg] P_2^{(0)}(\mu)\ , \qquad (3.112)
\end{aligned}$$

where $\bar{D}$ to $\bar{I}$ and $\bar{A}_{\rm s}$ are the values as $h/\widehat{R}\to 0$, given by

$$\begin{aligned}
\bar{D} &= \frac{q_z\widehat{R}^3}{12G_{\rm m}}\frac{(1+\nu_{\rm s})(1-\nu_{\rm m})}{(1-\nu_{\rm s})(1+\nu_{\rm m})}\ , && (3.113)\\
\bar{E} &= -\frac{q_z\widehat{R}^5}{2G_{\rm m}}\frac{(1-\nu_{\rm m})}{(1-\nu_{\rm s})(7-5\nu_{\rm m})}\ , && (3.114)\\
\bar{F} &= -\frac{5q_z\widehat{R}^3}{6G_{\rm m}}\frac{(1-\nu_{\rm m})(1-2\nu_{\rm s})}{(1-\nu_{\rm s})(7-5\nu_{\rm m})}\ , && (3.115)\\
\bar{G} &= -\frac{q_z}{6G_{\rm m}}\frac{(1-\nu_{\rm m})(7-5\nu_{\rm s})}{(1-\nu_{\rm s})(7-5\nu_{\rm m})}\ , && (3.116)\\
\bar{H} &= 0\ , && (3.117)\\
\bar{I} &= \frac{q_z}{12G_{\rm m}}\frac{(1-\nu_{\rm m})(5-4\nu_{\rm s})}{(1-\nu_{\rm s})(1+\nu_{\rm m})}\ , && (3.118)\\
(3\lambda_{\rm s}+2G_{\rm s})\bar{A}_{\rm s} &= \frac{1+\nu_{\rm s}}{3(1-\nu_{\rm s})}\left[q_{\rm in}\left(\frac{G_{\rm s}}{G_{\rm m}}-1\right)-3q_R\frac{G_{\rm s}}{G_{\rm m}}\frac{(1-\nu_{\rm m})}{(1+\nu_{\rm m})}\right]\ . && (3.119)
\end{aligned}$$

Substituting these into

$$n^{11} = \frac{h}{\widehat{R}^2}\int_{-1/2}^{1/2}\left(\lim_{h/\widehat{R}\to 0}\tau_{\theta\theta}\right)\,{\rm d}\xi\ , \qquad (3.120)$$

we find (as $\lim_{h/\widehat{R}\to 0}\tau_{\theta\theta}$ is constant),

$$n^{11} = \frac{h}{\widehat{R}^2}\lim_{h/\widehat{R}\to 0}\tau_{\theta\theta} \tag{3.121}$$

$$= p_0 P_0^{(0)}(\mu) + p_2 P_2^{(0)}(\mu)\ , \tag{3.122}$$

where

$$p_0 = \frac{q_z h G_\mathrm{s}}{2\widehat{R}^2 G_\mathrm{m}}\frac{(1-\nu_\mathrm{m})(-5\nu_\mathrm{m}+15\nu_\mathrm{m}\nu_\mathrm{s}-17+3\nu_\mathrm{s})}{(1-\nu_\mathrm{s})(7-5\nu_\mathrm{m})(1+\nu_\mathrm{m})} + \frac{h(1+\nu_\mathrm{s})}{2\widehat{R}^2(1-\nu_\mathrm{s})}\left[q_\mathrm{in}\left(\frac{G_\mathrm{s}}{G_\mathrm{m}}-1\right) - 3q_R\frac{G_\mathrm{s}}{G_\mathrm{m}}\frac{(1-\nu_\mathrm{m})}{(1+\nu_\mathrm{m})}\right] + \frac{q_\mathrm{in}h}{2\widehat{R}^2}\ , \tag{3.123}$$

$$p_2 = \frac{10 q_z h G_\mathrm{s}(1-\nu_\mathrm{m})}{\widehat{R}^2 G_\mathrm{m}(1-\nu_\mathrm{s})(7-5\nu_\mathrm{m})}\ . \tag{3.124}$$

3.3.2 Interpretation

Given the stress resultant calculated in the previous section, we now wish to find which regions of the shell are in compression and tension. We have

$$n^{11} = p_0 + \frac{p_2}{2}(3\cos^2\theta - 1) \tag{3.125}$$

$$= p_0 + \frac{p_2}{4} + \frac{3p_2}{4}\cos 2\theta\ . \tag{3.126}$$

Now, if we are looking for the transition point between tension and compression, we have $n^{11}=0$ at that point, or

$$\cos 2\theta = -\frac{4}{3p_2}\left(p_0 + \frac{p_2}{4}\right)\ , \tag{3.127}$$

giving

$$\theta = \left\{\frac{1}{2}\cos^{-1}\left[-\frac{4}{3p_2}\left(p_0+\frac{p_2}{4}\right)\right], \pi - \frac{1}{2}\cos^{-1}\left[-\frac{4}{3p_2}\left(p_0+\frac{p_2}{4}\right)\right]\right\}\ , \tag{3.128}$$

assuming that

$$\left|\frac{4}{3p_2}\left(p_0+\frac{p_2}{4}\right)\right| < 1\ . \tag{3.129}$$

Now, in the case that $q_z > 0$ (compression at infinity), we have that $n^{11} < 0$ in between the values in equation (3.128), assuming condition (3.129) still holds. (If $q_z < 0$, $n^{11} > 0$ in between the two values.)

Note in particular that if $q_R = q_\mathrm{in} = 0$, the values in equation (3.128) depend only on the Poisson ratios ν_m and ν_s. For example, taking the values for ν_s and ν_m from Table 1.1 and setting $q_R = q_\mathrm{in} = 0$, we have

$$-\frac{4}{3p_2}\left(p_0+\frac{p_2}{4}\right) = 0.395\ , \tag{3.130}$$

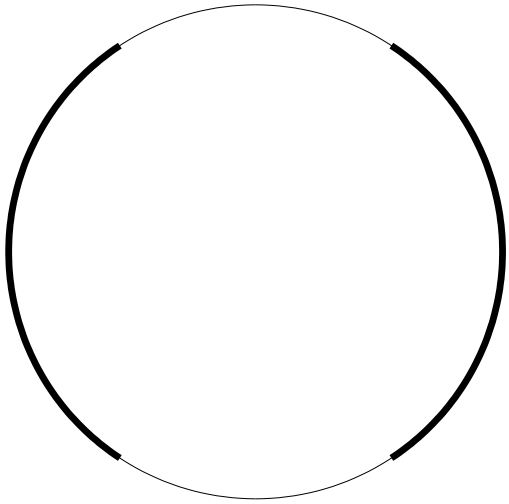

Figure 3.2: Areas of the spherical shell in compression (thick) and tension (thin).

telling us that we are in compression for

$$\theta \in (0.582, 2.559) \,, \tag{3.131}$$

independently of the shear moduli of the materials and the magnitude of the applied stress at infinity. The region of compression is shown as the thick curve in Figure 3.2 (the thin curve representing areas in tension).

3.4 The functional in terms of the Legendre coefficients

We will now return to the expression for the change in potential energy derived at the end of Section 3.2. Recall that we had considered the linear terms ΔW_1 and the quadratic terms ΔW_2. We stated that the equation $\Delta W_1 = 0$ would give the equilibrium (pre-buckling) state. However, we have calculated this state already by the full equations of linear elasticity, and we thus *assume* that $\Delta W_1 = 0$. Indeed, it can be shown that by substituting the full linear solution obtained earlier into ΔW_1, we have that

$$\Delta W_1 \;\; = \;\; O(h^2/\widehat{R}^2) \,, \tag{3.132}$$

which is small compared to the individual terms in the integral.

Now consider the quadratic terms, given by equation (3.20). First we will consider $\mathscr{I}_1$. Given that w is independent of the coordinate ϕ, from equation (3.21) we have

that

$$\mathscr{I}_1 \;=\; \iint_{\rm shell} \frac{{}^{\rm (I)}n^{11}}{2}\left(\frac{{\rm d}w}{{\rm d}\theta}\right)^2 {\rm d}S\;, \tag{3.133}$$

where we take as read that 'shell' means the mid-shell surface. The stress resultant will be given by equation (3.122), but for simplicity we will consider two cases only: firstly $q_z = q_\infty$, $q_R = 0$ and $q_{\rm in} = 0$; and secondly $q_z = 0$, $q_R = q_\infty$ and $q_{\rm in} = 0$. Thus

$${}^{\rm (I)}n^{11} \;=\; q_\infty\left(p_0 P_0^{(0)}(\mu) + p_2 P_2^{(0)}(\mu)\right)\;, \tag{3.134}$$

where for the first case we redefine

$$p_0 \;=\; \frac{hG_{\rm s}}{2\widehat{R}^2 G_{\rm m}}\frac{(1-\nu_{\rm m})(-5\nu_{\rm m}+15\nu_{\rm m}\nu_{\rm s}-17+3\nu_{\rm s})}{(1-\nu_{\rm s})(7-5\nu_{\rm m})(1+\nu_{\rm m})}\;, \tag{3.135}$$

$$p_2 \;=\; \frac{10hG_{\rm s}(1-\nu_{\rm m})}{\widehat{R}^2 G_{\rm m}(1-\nu_{\rm s})(7-5\nu_{\rm m})}\;, \tag{3.136}$$

and for the second case

$$p_0 \;=\; -\frac{3hG_{\rm s}(1+\nu_{\rm s})(1-\nu_{\rm m})}{2\widehat{R}^2 G_{\rm m}(1+\nu_{\rm m})(1-\nu_{\rm s})}\;, \tag{3.137}$$

$$p_2 \;=\; 0\;. \tag{3.138}$$

Now, if $F(\theta)$ is independent of ϕ, then

$$\iint_{\rm shell} F(\theta)\,{\rm d}S \;=\; \int_0^{2\pi}\int_0^{\pi} F(\theta)\widehat{R}^2\sin\theta\,{\rm d}\theta{\rm d}\phi \tag{3.139}$$

$$\;=\; 2\pi\widehat{R}^2\int_0^{\pi} F(\theta)\sin\theta\,{\rm d}\theta \tag{3.140}$$

$$\;=\; 2\pi\widehat{R}^2\int_{-1}^{1} F(\mu)\,{\rm d}\mu\;. \tag{3.141}$$

Then, from equation (3.134) we have that

$${}^{\rm (I)}n^{11} \;=\; q_\infty\left(p_0-\frac{p_2}{2}\right)+q_\infty\frac{3p_2}{2}\mu^2\;, \tag{3.142}$$

which we can substitute together with equation (3.29) and the result (3.141) into the expression for $\mathscr{I}_1$ to get

$$\mathscr{I}_1 \;=\; \pi q_\infty\left(p_0-\frac{p_2}{2}\right)\widehat{R}^2\sum_{n,m=1}^{\infty}\int_{-1}^{1}\mathscr{U}_n P_n^{(1)}(\mu)\mathscr{U}_m P_m^{(1)}(\mu)\,{\rm d}\mu$$
$$+\frac{3\pi q_\infty p_2\widehat{R}^2}{2}\sum_{n,m=1}^{\infty}\int_{-1}^{1}\mu^2\mathscr{U}_n P_n^{(1)}(\mu)\mathscr{U}_m P_m^{(1)}(\mu)\,{\rm d}\mu \tag{3.143}$$

$$\;=\; 2\pi q_\infty\left(p_0-\frac{p_2}{2}\right)\widehat{R}^2\sum_{n=1}^{\infty}\frac{n(n+1)}{2n+1}\mathscr{U}_n^2$$
$$+\frac{3\pi q_\infty p_2\widehat{R}^2}{2}\sum_{n,m=1}^{\infty}\mathscr{U}_n\mathscr{U}_m\int_{-1}^{1}\mu P_n^{(1)}(\mu)\cdot\mu P_m^{(1)}(\mu)\,{\rm d}\mu\;, \tag{3.144}$$

using the orthogonality condition (B.12).

Using relation (B.7) we find that the second term above is equal to

$$\frac{3\pi q_\infty p_2 \widehat{R}^2}{2} \sum_{n,m=1}^{\infty} \frac{\mathscr{U}_n}{2n+1} \frac{\mathscr{U}_m}{2m+1} \int_{-1}^{1} \left(nP_{n+1}^{(1)}(\mu) + (n+1)P_{n-1}^{(1)}(\mu) \right) \times \left(mP_{m+1}^{(1)}(\mu) + (m+1)P_{m-1}^{(1)}(\mu) \right) \mathrm{d}\mu \qquad (3.145)$$

which, on using the orthogonality condition, becomes

$$\frac{3\pi q_\infty p_2 \widehat{R}^2}{2} \sum_{n=1}^{\infty} \left\{ \left[\frac{2n^2(n+1)(n+2)}{(2n+1)^2(2n+3)} + \frac{2(n-1)n(n+1)^2}{(2n-1)(2n+1)^2} \right] \mathscr{U}_n^2 + \frac{4n(n+1)(n+2)(n+3)}{(2n+1)(2n+3)(2n+5)} \mathscr{U}_n \mathscr{U}_{n+2} \right\} . \qquad (3.146)$$

Therefore we finally obtain

$$\begin{aligned} \mathscr{I}_1 &= \pi q_\infty \widehat{R}^2 \sum_{n=1}^{\infty} \left[\left\{ (2p_0 - p_2) \frac{n(n+1)}{2n+1} \right. \right. \\ &\quad \left. + 3p_2 \left[\frac{n^2(n+1)(n+2)}{(2n+1)^2(2n+3)} + \frac{(n-1)n(n+1)^2}{(2n-1)(2n+1)^2} \right] \right\} \mathscr{U}_n^2 \\ &\quad \left. + \frac{6p_2 n(n+1)(n+2)(n+3)}{(2n+1)(2n+3)(2n+5)} \mathscr{U}_n \mathscr{U}_{n+2} \right] . \qquad (3.147) \end{aligned}$$

Now we will consider $\mathscr{I}_2$ from equation (3.22). Recall from equation (3.30) that

$$v_1 = \widehat{R} \sum_{n=1}^{\infty} \mathscr{V}_n P_n^{(1)}(\mu) . \qquad (3.148)$$

Koiter [52] employed the van der Neut substitution,

$$v_\alpha = \psi_{,\alpha} + \varepsilon_{\alpha\lambda} a^{\lambda\mu} \chi_{,\mu} , \qquad (3.149)$$

where $\varepsilon_{\alpha\lambda}$ is the surface alternating tensor and ψ, χ are functions to be determined. Under our assumption of axisymmetry, this simplifies to

$$v_\alpha = \psi_{,\alpha} , \qquad (3.150)$$

where

$$\psi = \sum_{n=0}^{\infty} \left(\widehat{R} \mathscr{V}_n \right) P_n^{(0)}(\mu) , \qquad (3.151)$$

$\mathscr{V}_0$ being arbitrary (we will set it to zero without loss of generality). Then the linearised strain tensor $\theta_{\alpha\beta}$ of equation (A.160) becomes

$$\theta_{\alpha\beta} = \frac{1}{2}(v_\alpha|_\beta + v_\beta|_\alpha) - \frac{w}{\widehat{R}} a_{\alpha\beta} \qquad (3.152)$$

$$= \psi|_{\alpha\beta} - \frac{w}{\widehat{R}} a_{\alpha\beta} , \qquad (3.153)$$

since in shallow buckling the order of covariant differentiation is irrelevant [52]. Hence the integrand in $\mathscr{I}_2$ becomes

$$\frac{h}{2}E^{\alpha\beta\lambda\mu}\frac{w^2}{\widehat{R}^2}a_{\alpha\beta}a_{\lambda\mu} - hE^{\alpha\beta\lambda\mu}\psi|_{\alpha\beta}\frac{w}{\widehat{R}}a_{\lambda\mu} + \frac{h}{2}E^{\alpha\beta\lambda\mu}\psi|_{\alpha\beta}\psi|_{\lambda\mu} + \frac{h^3}{24}E^{\alpha\beta\lambda\mu}w|_{\alpha\beta}w|_{\lambda\mu} \ , \tag{3.154}$$

using equation (A.159) to determine $\rho_{\alpha\beta}$. From equation (A.167), we find that the first term becomes

$$\frac{2hG_{\mathrm{s}}(1+\nu_{\mathrm{s}})}{1-\nu_{\mathrm{s}}}\frac{w^2}{\widehat{R}^2} \ , \tag{3.155}$$

and the second term becomes

$$-\frac{2hG_{\mathrm{s}}(1+\nu_{\mathrm{s}})}{\widehat{R}(1-\nu_{\mathrm{s}})}w\nabla^2\psi \ , \tag{3.156}$$

using the fact that

$$a^{\alpha\beta}\psi|_{\alpha\beta} \ = \ \nabla^2\psi \tag{3.157}$$

is the surface Laplacian on the shell. The integrals of the other two terms are both of the form

$$\iint_{\mathrm{shell}} E^{\alpha\beta\lambda\mu}\omega|_{\alpha\beta}\omega|_{\lambda\mu}\,\mathrm{d}S \ . \tag{3.158}$$

Given that $E^{\alpha\beta\lambda\mu}$ is composed entirely of $a^{\alpha\beta}$ terms, we have $E^{\alpha\beta\lambda\mu}|_{\rho} = 0$ since $a^{\alpha\beta}|_{\rho} = a_{\alpha\beta}|_{\rho} = 0$ from equation (A.152). Hence the integral (3.158) becomes

$$\iint_{\mathrm{shell}} \Big[\big(E^{\alpha\beta\lambda\mu}\omega|_{\alpha\beta}\omega|_{\lambda}\big)\big|_{\mu} - E^{\alpha\beta\lambda\mu}\omega|_{\alpha\beta\mu}\omega|_{\lambda} \Big]\,\mathrm{d}S \ , \tag{3.159}$$

where the first term disappears by the divergence theorem (as the shell is closed). Applying the same process we get

$$\iint_{\mathrm{shell}} E^{\alpha\beta\lambda\mu}\omega|_{\alpha\beta\lambda\mu}\omega\,\mathrm{d}S \ , \tag{3.160}$$

changing the order of covariant differentiation as we're dealing with shallow shells. We finally obtain

$$\frac{2G_{\mathrm{s}}}{1-\nu_{\mathrm{s}}}\iint_{\mathrm{shell}} \omega\nabla^4\omega\,\mathrm{d}S \ , \tag{3.161}$$

which becomes

$$\frac{2G_{\mathrm{s}}}{1-\nu_{\mathrm{s}}}\iint_{\mathrm{shell}} \big(\nabla^2\omega\big)^2\,\mathrm{d}S \tag{3.162}$$

on using Green's theorem.

Putting the above together gives us

$$\mathscr{I}_2 = \frac{hG_\mathrm{s}}{1-\nu_\mathrm{s}} \iint_{\mathrm{shell}} \left[\left(\nabla^2\psi - (1+\nu_\mathrm{s})\frac{w}{\widehat{R}} \right)^2 + (1-\nu_\mathrm{s}^2)\frac{w^2}{\widehat{R}^2} + \frac{h^2}{12}\left(\nabla^2 w\right)^2 \right] \mathrm{d}S \; . \tag{3.163}$$

Now, we have from equation (3.157) that

$$\nabla^2\psi = \frac{1}{\widehat{R}^2}\psi|_{11} + \frac{1}{\widehat{R}^2\sin^2\theta}\psi|_{22} \; . \tag{3.164}$$

In addition,

$$\psi_{,2} = 0 \tag{3.165}$$

and

$$\psi|_{\alpha\beta} = (\psi_{,\alpha})|_\beta \tag{3.166}$$

$$= \psi_{,\alpha\beta} - \bar{\Gamma}^\gamma_{\alpha\beta}\psi_{,\gamma} \tag{3.167}$$

from equation (A.149), so that

$$\nabla^2\psi = \frac{1}{\widehat{R}^2}(\psi_{,11} + \cot\theta\psi_{,1}) \tag{3.168}$$

and similarly

$$\nabla^2 w = \frac{1}{\widehat{R}^2}(w_{,11} + \cot\theta w_{,1}) \; . \tag{3.169}$$

From these, using equations (3.151), (3.29) and (B.1), we find that

$$\nabla^2\psi = -\sum_{n=0}^{\infty} \frac{n(n+1)\mathscr{V}_n}{\widehat{R}} P_n^{(0)}(\mu) \; , \tag{3.170}$$

$$\nabla^2 w = -\sum_{n=0}^{\infty} \frac{n(n+1)\mathscr{U}_n}{\widehat{R}^2} P_n^{(0)}(\mu) \; , \tag{3.171}$$

which, on substitution into equation (3.163) and using the orthogonality condition on Legendre functions, gives us that

$$\mathscr{I}_2 = \frac{4\pi hG_\mathrm{s}}{\widehat{R}^2(1-\nu_\mathrm{s})} \sum_{n=0}^{\infty} \frac{1}{2n+1} \left[\left(n(n+1)\mathscr{V}_n + (1+\nu_\mathrm{s})\mathscr{U}_n\right)^2 \widehat{R}^2 + (1-\nu_\mathrm{s}^2)\widehat{R}^2\mathscr{U}_n^2 + \frac{h^2n^2(n+1)^2\mathscr{U}_n^2}{12} \right] \; . \tag{3.172}$$

In order to calculate $\mathscr{I}_3$ from equation (3.23), we need to determine the displacement field $\boldsymbol{u}$ that is induced in the elastic matrix from the virtual deformation $\boldsymbol{v}$ of the shell. This is found by solving the elasticity equations for $\boldsymbol{u}$ with a displacement boundary condition

$$\boldsymbol{u}|_{R=R_1} \;=\; \boldsymbol{v}\;, \tag{3.173}$$

assuming that the displacement on the outer shell surface is approximately equal to the mid-surface displacement $\boldsymbol{v}$. We also state that the stress field vanishes as $R \to \infty$. This problem has been solved by Lur'e [65]. Firstly the boundary displacement is decomposed into a series of homogeneous vector spherical harmonics,

$$\boldsymbol{v} \;=\; \sum_{n=0}^{\infty} \boldsymbol{Y}_n(\theta,\phi)\;. \tag{3.174}$$

Then the vector

$$\boldsymbol{U}_{-n-1} = \left(\frac{R_1}{R}\right)^{n+1} \boldsymbol{Y}_n(\theta,\phi) \tag{3.175}$$

is formed, which gives us the final solution

$$\boldsymbol{u} \;=\; \sum_{n=0}^{\infty}\left[\boldsymbol{U}_{-n-1} - \frac{1}{2}(R_1^2-R^2)\frac{\nabla(\nabla\cdot\boldsymbol{U}_{-n-1})}{(3-4\nu_{\mathrm{m}})(n+1)+2(1-\nu_{\mathrm{m}})}\right]\;. \tag{3.176}$$

The first difficulty we find when trying to solve this problem is that the terms in the series in equations (3.27) and (3.28), taken together, are not homogeneous surface vector spherical harmonics. We need to write $\boldsymbol{v}$ as a series of the following:

$$\boldsymbol{Y}_n \;=\; \alpha_n P_n^{(1)}(\mu)(\cos\phi\,\boldsymbol{e}_x + \sin\phi\,\boldsymbol{e}_y) + \beta_n P_n^{(0)}(\mu)\boldsymbol{e}_z\;. \tag{3.177}$$

On using the relations in (A.102), we can transform to spherical coordinates:

$$\begin{aligned}\boldsymbol{Y}_n \;=\;& \left(\alpha_n\sqrt{1-\mu^2}P_n^{(1)}(\mu) + \beta_n\mu P_n^{(0)}(\mu)\right)\boldsymbol{e}_R \\ &+ \left(\alpha_n\mu P_n^{(1)}(\mu) - \beta_n\sqrt{1-\mu^2}P_n^{(0)}(\mu)\right)\boldsymbol{e}_\theta\;.\end{aligned} \tag{3.178}$$

From equations (B.8) and (B.10) we find that

$$\begin{aligned}\boldsymbol{Y}_n \;=\;& \left((n\alpha_n+\beta_n)\mu P_n^{(0)}(\mu) - n\alpha_n P_{n-1}^{(0)}(\mu)\right)\boldsymbol{e}_R \\ &+ \left(\alpha_n\mu P_n^{(1)}(\mu) - \beta_n\sqrt{1-\mu^2}P_n^{(0)}(\mu)\right)\boldsymbol{e}_\theta\;.\end{aligned} \tag{3.179}$$

Now, from equation (B.6),

$$\sqrt{1-\mu^2}P_n^{(0)}(\mu) \;=\; \frac{\sqrt{1-\mu^2}}{2n+1}\left(P_{n+1}^{(0)\,\prime}(\mu) - P_{n-1}^{(0)\,\prime}(\mu)\right) \tag{3.180}$$

$$\;=\; \frac{P_{n-1}^{(1)}(\mu) - P_{n+1}^{(1)}(\mu)}{2n+1}\;. \tag{3.181}$$

Using this together with equation (B.7), we find that

$$\begin{aligned}\boldsymbol{Y}_n &= \Big(n(\gamma_n-\alpha_n)P_{n-1}^{(0)}(\mu)+(n+1)\gamma_n P_{n+1}^{(0)}(\mu)\Big)\,\boldsymbol{e}_R \\ &\quad+\Big((\alpha_n-\gamma_n)P_{n-1}^{(1)}(\mu)+\gamma_n P_{n+1}^{(1)}(\mu)\Big)\,\boldsymbol{e}_\theta\ , \end{aligned}\tag{3.182}$$

where

$$\gamma_n = \frac{n\alpha_n+\beta_n}{2n+1}\ .\tag{3.183}$$

Thus

$$\begin{aligned}\boldsymbol{v} &= \sum_{n=0}^{\infty}\Big[n(\gamma_n-\alpha_n)P_{n-1}^{(0)}+(n+1)\gamma_n P_{n+1}^{(0)}\Big]\,\boldsymbol{e}_R \\ &\quad+\sum_{n=0}^{\infty}\Big[(\alpha_n-\gamma_n)P_{n-1}^{(1)}+\gamma_n P_{n+1}^{(1)}\Big]\,\boldsymbol{e}_\theta\ . \end{aligned}\tag{3.184}$$

On rearranging the indices of the terms in the sums, we obtain

$$\begin{aligned}\boldsymbol{u} &= \sum_{m=0}^{\infty}\left[(m+1)(\gamma_{m+1}-\alpha_{m+1})+m\gamma_{m-1}\right]P_m^{(0)}(\mu)\boldsymbol{e}_R \\ &\quad+\sum_{m=1}^{\infty}\left[\alpha_{m+1}-\gamma_{m+1}+\gamma_{m-1}\right]P_m^{(1)}(\mu)\boldsymbol{e}_\theta\ , \end{aligned}\tag{3.185}$$

which we can compare with equations (3.27) and (3.28) to get

$$\mathscr{U}_n = (n+1)(\gamma_{n+1}-\alpha_{n+1})+n\gamma_{n-1}\ ,\tag{3.186}$$

$$\mathscr{V}_n = \alpha_{n+1}-\gamma_{n+1}+\gamma_{n-1}\ ,\tag{3.187}$$

or

$$\gamma_n-\alpha_n = \frac{\mathscr{U}_{n-1}-(n-1)\mathscr{V}_{n-1}}{2n-1}\ ,\tag{3.188}$$

$$\gamma_n = \frac{\mathscr{U}_{n+1}+(n+2)\mathscr{V}_{n+1}}{2n+3}\ ,\tag{3.189}$$

which we can substitute into the relations that we find for α_n and γ_n.

Now, from equations (3.182) and (3.175) we find that

$$\begin{aligned}\boldsymbol{U}_{-n-1} &= \left(\frac{R_1}{R}\right)^{n+1}\Big\{\Big[n(\gamma_n-\alpha_n)P_{n-1}^{(0)}(\mu)+(n+1)\gamma_n P_{n+1}^{(0)}(\mu)\Big]\,\boldsymbol{e}_R \\ &\quad+\Big[(\alpha_n-\gamma_n)P_{n-1}^{(1)}(\mu)+\gamma_n P_{n+1}^{(1)}(\mu)\Big]\,\boldsymbol{e}_\theta\Big\}\ . \end{aligned}\tag{3.190}$$

On using various identities of Appendix B, we find that

$$\begin{aligned}\nabla\left(\nabla\cdot\boldsymbol{U}_{-n-1}\right) &= \frac{(n+2)}{R_1^2}\left(\frac{R_1}{R}\right)^{n+3}(2n+1)(n+1)\gamma_n P_{n+1}^{(0)}(\mu)\boldsymbol{e}_R \\ &\quad-\frac{1}{R_1^2}\left(\frac{R_1}{R}\right)^{n+3}(2n+1)(n+1)\gamma_n P_{n+1}^{(1)}(\mu)\boldsymbol{e}_\theta\ . \end{aligned}\tag{3.191}$$

Thus, from equation (3.176), we find that the radial component of the virtual displacement field in the matrix is given by

$$\begin{aligned}\boldsymbol{u}\cdot\boldsymbol{e}_R &= \sum_{n=0}^{\infty}\left\{\left[n(\gamma_n-\alpha_n)P_{n-1}^{(0)}(\mu)+(n+1)\gamma_n P_{n+1}^{(0)}(\mu)\right]\left(\frac{R_1}{R}\right)^{n+1}\right.\\ &\qquad\left.-\frac{n+2}{2}\left(1-\frac{R^2}{R_1^2}\right)\left(\frac{R_1}{R}\right)^{n+3}\frac{(2n+1)(n+1)\gamma_n P_{n+1}^{(0)}(\mu)}{(3-4\nu_{\mathrm{m}})(n+1)+2(1-\nu_{\mathrm{m}})}\right\} \qquad (3.192)\end{aligned}$$

and the tangential component becomes

$$\begin{aligned}\boldsymbol{u}\cdot\boldsymbol{e}_\theta &= \sum_{n=0}^{\infty}\left\{\left[(\alpha_n-\gamma_n)P_{n-1}^{(1)}(\mu)+\gamma_n P_{n+1}^{(1)}(\mu)\right]\left(\frac{R_1}{R}\right)^{n+1}\right.\\ &\qquad\left.+\frac{1}{2}\left(1-\frac{R^2}{R_1^2}\right)\left(\frac{R_1}{R}\right)^{n+3}\frac{(2n+1)(n+1)\gamma_n P_{n+1}^{(1)}(\mu)}{(3-4\nu_{\mathrm{m}})(n+1)+2(1-\nu_{\mathrm{m}})}\right\}\ . \qquad (3.193)\end{aligned}$$

Rearranging the indices and using equations (3.188) and (3.189) gives

$$\begin{aligned}\boldsymbol{u} &= \sum_{m=0}^{\infty}\left[A_m\left(\frac{R_1}{R}\right)^{m+2}+B_m\left(\frac{R_1}{R}\right)^{m}\right]P_m^{(0)}(\mu)\boldsymbol{e}_R\\ &\qquad+\sum_{m=1}^{\infty}\left[C_m\left(\frac{R_1}{R}\right)^{m+2}+D_m\left(\frac{R_1}{R}\right)^{m}\right]P_m^{(1)}(\mu)\boldsymbol{e}_\theta\ , \qquad (3.194)\end{aligned}$$

where

$$A_n+B_n = \mathscr{U}_n\ , \qquad (3.195)$$

$$C_n+D_n = \mathscr{V}_n\ , \qquad (3.196)$$

and

$$A_n = -(n+1)C_n\ , \qquad (3.197)$$

$$C_n = \frac{1}{2n+1}\left\{n\mathscr{V}_n-\mathscr{U}_n+\frac{n(2n-1)}{2}\left[\frac{\mathscr{U}_n+(n+1)\mathscr{V}_n}{(3-4\nu_{\mathrm{m}})n+2(1-\nu_{\mathrm{m}})}\right]\right\}\ . \qquad (3.198)$$

Now consider the integral $\mathscr{I}_3$, from equation (3.23). The stress tensor from equation (A.43) is given by

$$\tau^{ij} = A^{ijkl}e_{kl}\ , \qquad (3.199)$$

so that

$$\mathscr{I}_3 = \frac{1}{2}\iiint_{R>R_1}\tau^{ij}e_{ij}\,\mathrm{d}V\ , \qquad (3.200)$$

or

$$\mathscr{I}_3 = \frac{1}{2}\iiint_{R>R_1}\tau^{ij}u_i|_j\,\mathrm{d}V \qquad (3.201)$$

by the symmetry of the stress tensor and equation (A.39). Next, we modify the integrand to find

$$\mathscr{I}_3 \;=\; \frac{1}{2}\iiint_{R>R_1}\Big[(\tau^{ij}u_i)\big|_j - \tau^{ij}|_j u_i\Big]\,\mathrm{d}V\;, \tag{3.202}$$

where the second term disappears by the equilibrium equation (A.41) for the stress tensor in the absence of body forces. Then, by the divergence theorem we have

$$\mathscr{I}_3 \;=\; \frac{1}{2}\iint_{\partial V}\tau^{ij}n_j u_i\,\mathrm{d}S\;, \tag{3.203}$$

where ∂V is the internal boundary of the region, $R = R_1$, since both the stresses and displacements vanish at infinity. The normal vector points inwards, so that the only non-zero component is $n_1 = -1$. This gives

$$\mathscr{I}_3 \;=\; -\frac{1}{2}\iint_{\partial V}\left(\tau^{11}u_1 + \tau^{12}u_2\right)\,\mathrm{d}S\;. \tag{3.204}$$

Now, from equations (A.92) and (A.93), we find that

$$\tau^{11} \;=\; 2G_{\mathrm{m}}e_{11} + \frac{2G_{\mathrm{m}}\nu_{\mathrm{m}}}{1-2\nu_{\mathrm{m}}}\Delta\;, \tag{3.205}$$

$$\tau^{12} \;=\; \frac{2G_{\mathrm{m}}}{R^2}e_{12}\;, \tag{3.206}$$

where

$$\Delta \;=\; e_{11} + \frac{1}{R^2}e_{22} + \frac{1}{R^2\sin^2\theta}e_{33}\;. \tag{3.207}$$

In terms of u_R and u_θ, we find that the relevant strain components become

$$e_{11} \;=\; \frac{\partial u_R}{\partial R}\;, \tag{3.208}$$

$$e_{12} \;=\; \frac{1}{2}\left(\frac{\partial u_R}{\partial\theta} + R\frac{\partial u_\theta}{\partial R} - u_\theta\right)\;, \tag{3.209}$$

$$\Delta \;=\; \frac{\partial u_R}{\partial R} + \frac{2u_R}{R} + \frac{1}{R}\frac{\partial u_\theta}{\partial\theta} + \frac{\cot\theta}{R}u_\theta\;. \tag{3.210}$$

We substitute the values for u_R and u_θ from equation (3.194) into equations (3.208)–(3.210), and then we substitute these into equations (3.205)–(3.206). These will be substituted into (3.204), with the identities

$$u_1 \;=\; u_R\;, \tag{3.211}$$

$$u_2 \;=\; Ru_\theta \tag{3.212}$$

from (A.107) and (A.108). Eventually we get an integral involving squares of Legendre functions. We finally obtain, using equations (3.195)–(3.197),

$$\begin{aligned}\mathscr{I}_3 &= 4\pi G_{\rm m} R_1 \sum_{n=0}^{\infty} \left\{ \frac{\mathscr{U}_n}{2n+1} \left[n\mathscr{U}_n - 2(n+1)C_n \right.\right. \\ &\qquad \left. + \frac{\nu_{\rm m}}{1-2\nu_{\rm m}} \left((n-2)\mathscr{U}_n - 2(n+1)C_n + n(n+1)\mathscr{V}_n \right) \right] \\ &\qquad \left. + \frac{n(n+1)\mathscr{V}_n}{2(2n+1)} \left[(n+1)\mathscr{V}_n + 2C_n - \mathscr{U}_n \right] \right\} , \end{aligned} \tag{3.213}$$

where C_n is given by equation (3.198).

3.5 The eigenvalue problem

Now we use the results (3.147), (3.172) and (3.213), and apply conditions (3.31) and (3.32). From the second of these, we have

$$\frac{\partial}{\partial \mathscr{V}_n}(\mathscr{I}_1 + \mathscr{I}_2 + \mathscr{I}_3) = 0 . \tag{3.214}$$

Now,

$$\frac{\partial \mathscr{I}_1}{\partial \mathscr{V}_n} = 0 , \tag{3.215}$$

$$\frac{\partial \mathscr{I}_2}{\partial \mathscr{V}_n} = \frac{8\pi h G_{\rm s} n(n+1)\left(n(n+1)\mathscr{V}_n + (1+\nu_{\rm s})\mathscr{U}_n\right)}{(1-\nu_{\rm s})(2n+1)} , \tag{3.216}$$

$$\begin{aligned}\frac{\partial \mathscr{I}_3}{\partial \mathscr{V}_n} &= \frac{4\pi G_{\rm m} R_1}{2n+1} \left\{ \mathscr{U}_n \left[-2(n+1)E_n + \frac{\nu_{\rm m}}{1-2\nu_{\rm m}} \left(n(n+1) - 2(n+1)E_n \right) \right] \right. \\ &\qquad \left. + \frac{1}{2} n(n+1) \left[2(n+1)\mathscr{V}_n + 2C_n - \mathscr{U}_n + 2E_n \mathscr{V}_n \right] \right\} , \end{aligned} \tag{3.217}$$

where C_n is given by equation (3.198) and we write

$$E_n = \frac{\partial C_n}{\partial \mathscr{V}_n} = \frac{1}{2n+1} \left[n + \frac{n(n+1)(2n-1)}{2\big((3-4\nu_{\rm m})n + 2(1-\nu_{\rm m})\big)} \right] . \tag{3.218}$$

Substituting the above into equation (3.214) gives us

$$\mathscr{V}_n = \mu_n \mathscr{U}_n , \tag{3.219}$$

where

$$\begin{aligned}\mu_n &= -\left\{ \frac{2hn(n+1)G_{\rm s}}{R_1(1-\nu_{\rm s})G_{\rm m}} + (n+1) + 2E_n \right\}^{-1} \left\{ \frac{2h(1+\nu_{\rm s})G_{\rm s}}{R_1(1-\nu_{\rm s})G_{\rm m}} - \frac{2E_n(1-\nu_{\rm m})}{n(1-2\nu_{\rm m})} \right. \\ &\qquad \left. + \frac{1}{2n+1} \left(\frac{n(2n-1)}{2\big((3-4\nu_{\rm m})n + 2(1-\nu_{\rm m})\big)} - 1 \right) - \frac{1}{2} + \frac{\nu_{\rm m}}{1-2\nu_{\rm m}} \right\} \end{aligned} \tag{3.220}$$

with $\mu_0 = 0$. Substituting this back in to the expressions for $\mathscr{I}_1$ to $\mathscr{I}_3$ gives us ΔW_2 in the form

$$\Delta W_2 \;=\; \sum_{n=0}^{\infty} \left[(a_n q_\infty + b_n)\mathscr{U}_n^2 + c_n q_\infty \mathscr{U}_n \mathscr{U}_{n+2} \right] \;, \tag{3.221}$$

where the coefficients are given by

$$\begin{aligned} a_n &= \pi \widehat{R}^2 \left\{ (2p_0 - p_2)\frac{n(n+1)}{2n+1} \right. \\ &\qquad \left. + 3p_2 \left[\frac{n^2(n+1)(n+2)}{(2n+1)^2(2n+3)} + \frac{(n-1)n(n+1)^2}{(2n-1)(2n+1)^2} \right] \right\} \;, \end{aligned} \tag{3.222}$$

$$\begin{aligned} b_n &= \frac{4\pi h G_{\mathrm{s}}}{\widehat{R}^2(1-\nu_{\mathrm{s}})(2n+1)} \left[\left(n(n+1)\mu_n + 1 + \nu_{\mathrm{s}} \right)^2 \widehat{R}^2 \right. \\ &\qquad \left. + (1-\nu_{\mathrm{s}}^2)\widehat{R}^2 + h^2 n^2 (n+1)^2/12 \right] \\ &\quad + \frac{4\pi G_{\mathrm{m}} R_1}{2n+1} \left[n - 2(n+1)F_n + \frac{\nu_{\mathrm{m}}}{1-2\nu_{\mathrm{m}}} \left(n - 2 - 2(n+1)F_n + n(n+1)\mu_n \right) \right. \\ &\qquad \left. + \frac{n(n+1)\mu_n}{2} \left((n+1)\mu_n + 2F_n - 1 \right) \right] \;, \end{aligned} \tag{3.223}$$

$$c_n \;=\; \frac{6\pi \widehat{R}^2 p_2 n(n+1)(n+2)(n+3)}{(2n+1)(2n+3)(2n+5)} \;, \tag{3.224}$$

where

$$\begin{aligned} F_n \;=\; \frac{C_n}{\mathscr{U}_n} \;&=\; \frac{1}{2n+1} \left\{ n\mu_n - 1 \right. \\ &\qquad \left. + \frac{n(2n-1)}{2} \left[\frac{1 + (n+1)\mu_n}{(3-4\nu_{\mathrm{m}})n + 2(1-\nu_{\mathrm{m}})} \right] \right\} \;. \end{aligned} \tag{3.225}$$

Then from equation (3.31) we have

$$2(a_n q_\infty + b_n)\mathscr{U}_n + c_{n-2} q_\infty \mathscr{U}_{n-2} + c_n q_\infty \mathscr{U}_{n+2} \;=\; 0 \;, \tag{3.226}$$

where c_{-2} and c_{-1} are both zero. If we let

$$\lambda \;=\; \frac{1}{q_\infty} \;, \tag{3.227}$$

then we have the system

$$\left(-\frac{a_n}{b_n} - \lambda \right) \mathscr{U}_n - \frac{c_{n-2}}{2b_n} \mathscr{U}_{n-2} - \frac{c_n}{2b_n} \mathscr{U}_{n+2} \;=\; 0 \;. \tag{3.228}$$

We can now split up our consideration of the $\mathscr{U}_n$ coefficients into odd and even n:

$$\left(-\frac{a_{2n-1}}{b_{2n-1}} - \lambda \right) \mathscr{U}_n^{\mathrm{odd}} - \frac{c_{2n-3}}{2b_{2n-1}} \mathscr{U}_{n-1}^{\mathrm{odd}} - \frac{c_{2n-1}}{2b_{2n-1}} \mathscr{U}_{n+1}^{\mathrm{odd}} \;=\; 0 \tag{3.229}$$

$$\left(-\frac{a_{2n-2}}{b_{2n-2}} - \lambda \right) \mathscr{U}_n^{\mathrm{even}} - \frac{c_{2n-4}}{2b_{2n-2}} \mathscr{U}_{n-1}^{\mathrm{even}} - \frac{c_{2n-2}}{2b_{2n-2}} \mathscr{U}_{n+1}^{\mathrm{even}} \;=\; 0 \tag{3.230}$$

for $n = 1, 2, \ldots$, where

$$\mathscr{U}_n^{\text{odd}} = \mathscr{U}_{2n-1} \,, \tag{3.231}$$

$$\mathscr{U}_n^{\text{even}} = \mathscr{U}_{2n-2} \,. \tag{3.232}$$

The equations (3.229)–(3.230) comprise two eigenvalue problems for infinite tridiagonal matrices:

$$\left(\boldsymbol{A}^{\text{odd}} - \lambda \boldsymbol{I}\right) \boldsymbol{\mathscr{U}}^{\text{odd}} = \boldsymbol{0} \,, \tag{3.233}$$

$$\left(\boldsymbol{A}^{\text{even}} - \lambda \boldsymbol{I}\right) \boldsymbol{\mathscr{U}}^{\text{even}} = \boldsymbol{0} \,, \tag{3.234}$$

which can be solved numerically.

3.6 Results

Recall that we planned to consider two modes of deformation only, namely uniaxial compression at infinity, where the stress field at infinity had only the component $\tau_{zz} = -q_\infty$, and a hydrostatic compression at infinity, for which $\tau_{RR} = -q_\infty$. We will consider the uniaxial case first.

The infinite systems of the previous section are truncated and solved numerically, with parameter values from Table 1.1 and using equations (3.135) and (3.136) for p_0 and p_2. We set $G_{\text{m}} = 1$ since we can scale q_∞ with the true value of G_{m} without changing the problem mathematically. We will be searching for the lowest positive value of q_∞, in order to find the first point at which the equilibrium solution becomes unstable (considering a gradual quasisteady loading of the material). This corresponds to finding the *largest* possible eigenvalue λ. Considering even and odd buckling modes separately, the largest positive eigenvalue in both cases is $\lambda = 18.18$, giving a lowest critical compressive stress at infinity of $q_\infty = 0.0550$. The corresponding eigenvectors in each case give us the constants $\mathscr{U}_n$, and hence from equation (3.219) the constants $\mathscr{V}_n$. We substitute these values of the coefficients into equations (3.27) and (3.28) to determine the displacement components of the characteristic buckling pattern which would occur at the critical buckling stress. These buckling patterns are shown in Figures 3.3 and 3.4.

It may seem surprising that the spheres buckle around the equator. After all, by common experience if a spherical shell is placed between two flat plates and compressed, which is a superficially similar mode of deformation, the spheres tend to buckle at the poles. However, compressing spherical shells between flat plates induces a different pattern of stresses in the shell than embedding them in an elastic material. An embedded spherical shell, under uniaxial compression at infinity, is in

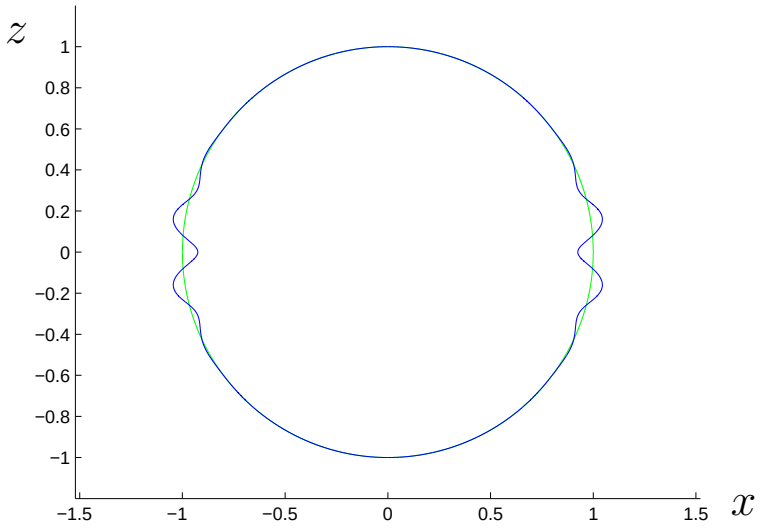

Figure 3.3: Even buckling pattern for the largest positive eigenvalue.

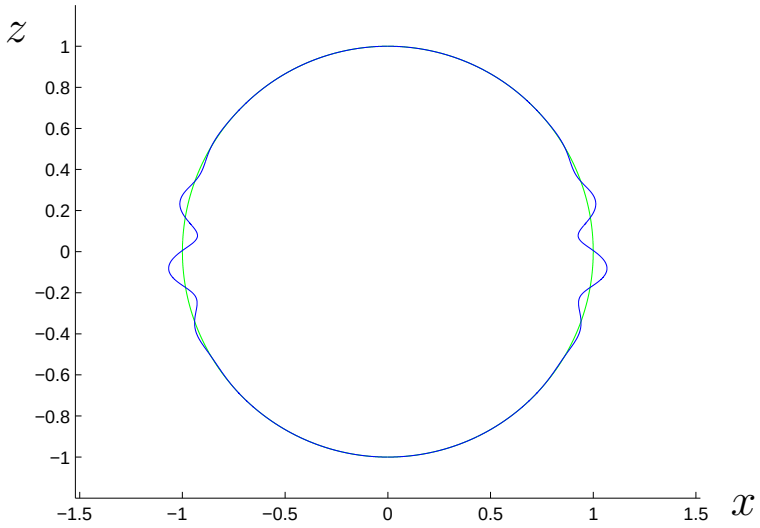

Figure 3.4: Odd buckling pattern for the largest positive eigenvalue.

compression (in the $\tau_{\theta\theta}$ component) around the equator while in tension around the poles (see Figure 3.2); this is why buckling occurs around the equator. Conversely, placing a shell between two flat plates and compressing it results in the region of highest compressive stress — and hence buckling — being around the poles.

Experimentalists should therefore be wary of modelling the buckling of embedded shells by sandwiching them between flat plates, for the reasons stated above. This approach does have its uses, however: if the shells are *not* bonded to the elastic matrix, and the matrix is much more compliant than the shell (as is the case here, from Table 1.1), then the shells will only be in contact with the matrix at the poles, mimicking the sandwiching approach. The likely true configuration of the spheres is *partial* bonding, which is outside the scope of this thesis, but would require us to solve a coupled delamination problem for the shells.

By solving the eigenvalue problem above, we are also able to find the largest negative eigenvalue. This corresponds to the lowest critical *tensile* stress at infinity for which the equilibrium configuration is unstable (restricting buckling patterns to axisymmetric deformations). In both odd and even cases we find the critical stress to be $-q_\infty = 0.1328$ for the material constants given previously. The corresponding buckling patterns are given in Figures 3.5 and 3.6.

These results are physically unrealistic for the simple reason that we only consider axisymmetric deformations. Had we considered buckling in the ϕ-direction, we would have taken account of the fact that the stress component $\tau_{\phi\phi}$ in the shell is in compression around the equator. Thus the most likely *lowest* critical stress for the case of tension at infinity would correspond to non-axisymmetric buckling around the equator.[1]

3.6.1 Hydrostatic stress at infinity

Finally, we will calculate the lowest critical stress in the case where a hydrostatic stress at infinity is used. We will use equations (3.137) and (3.138), and substitute them into the linear system (3.226). Now, $p_2 = 0$ so that $c_n = 0$ for all n. This means that (3.226) becomes

$$(a_n q_\infty + b_n)\mathscr{U}_n \;=\; 0\,. \tag{3.235}$$

[1] In the case of compression at infinity the component $\tau_{\phi\phi}$ is in compression around the poles. It is implausible that buckling in the ϕ-direction would occur here at a lower critical stress than the axisymmetric buckling mode.

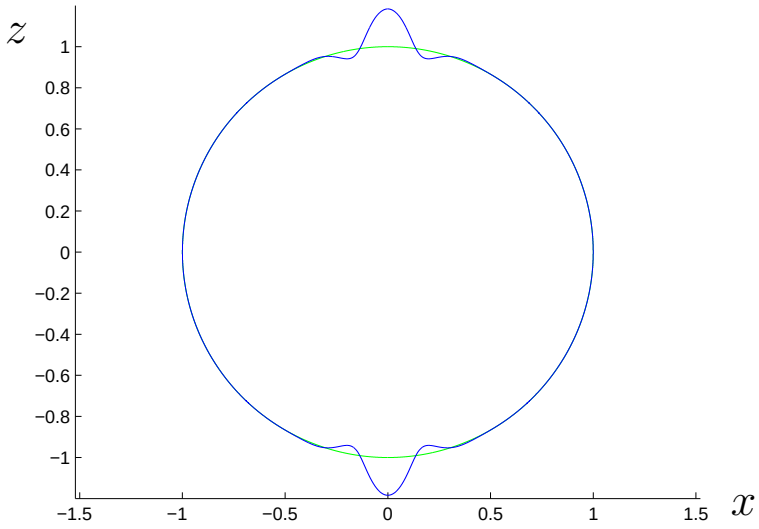

Figure 3.5: Even buckling pattern for the largest negative eigenvalue.

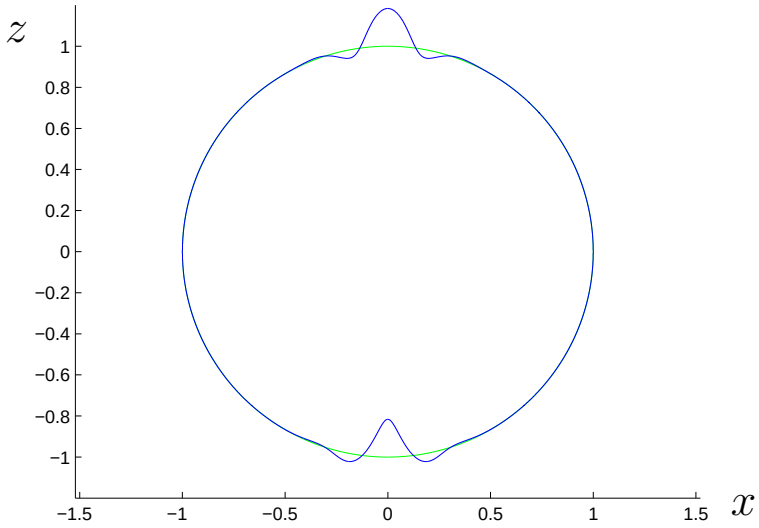

Figure 3.6: Odd buckling pattern for the largest negative eigenvalue.

Therefore each of the buckling modes are given from equations (3.27)–(3.28) by

$$v_R = \mathscr{U}_n P_n^{(0)}(\mu) \tag{3.236}$$

$$v_\theta = \mathscr{V}_n P_n^{(1)}(\mu) \tag{3.237}$$

$$= \mu_n \mathscr{U}_n P_n^{(1)}(\mu) \tag{3.238}$$

for each n, with corresponding critical stress

$$q_\infty = -\frac{b_n}{a_n} \,. \tag{3.239}$$

The constants b_n in this expression are unchanged from equation (3.223), and substituting the relevant value of p_0 gives

$$a_n = -\frac{3\pi h(1-\nu_\mathrm{m})(1+\nu_\mathrm{s})G_\mathrm{s}}{(1-\nu_\mathrm{s})(1+\nu_\mathrm{m})G_\mathrm{m}} \frac{n(n+1)}{(2n+1)} \,. \tag{3.240}$$

We require the lowest critical stress at infinity, which involves finding the minimum value of (3.239) over $n = 0, 1, 2, \ldots$. For the parameter values given previously, we find that the lowest critical stress is $q_\infty = 0.08072$, found when $n = 18$.

This result is to be compared with that of Fok and Allwright [32], who considered the buckling of an embedded shell with a hydrostatic stress field at infinity, but having introduced a simplifying assumption that the shell was inextensible, or that

$$\widehat{R}\nabla^2\psi + 2w = 0 \,. \tag{3.241}$$

This assumption gives $\mu_n = \frac{2}{n(n+1)}$, which is perhaps an oversimplification when compared to our result (3.220).

Fok and Allwright found that the critical stress at infinity satisfied

$$\begin{aligned} q_\infty = {} & \frac{4G_\mathrm{s}(1+\nu_\mathrm{s})(1+\nu_\mathrm{m})}{3(1-\nu_\mathrm{m})} \left[1 + \frac{G_\mathrm{m}(1-\nu_\mathrm{s})\widehat{R}}{G_\mathrm{s}(1+\nu_\mathrm{s})h}\right] \\ & \times \left\{ \frac{[n(n+1)-(1-\nu_\mathrm{s})]}{12(1-\nu_\mathrm{s}^2)} \frac{h^3}{\widehat{R}^3} + \frac{2h}{\widehat{R}(n-1)(n+2)(1+\nu_\mathrm{s})} \right. \\ & \left. + \frac{G_\mathrm{m}[(2n^3-n^2+3n+2)-\nu_\mathrm{m}(2n^3-3n^2+5n+2)]}{G_\mathrm{s}(1+\nu_\mathrm{s})(n-1)^2(n+2)[3n+2-2\nu_\mathrm{m}(2n+1)]} \right\} \end{aligned} \tag{3.242}$$

which, on minimising using our parameter values, gives the lowest critical stress as $q_\infty = 0.4215$ when $n = 18$. The value of q_∞ compares quite badly with our result, indicating that the simplifying inextensibility assumption of the authors is not valid in our parameter regime. Numerical experiments show that as $h/\widehat{R} \to 0$ the minimum q_∞ according to (3.242) becomes closer to the value given by our theory. Note nevertheless that the order $n = 18$ of the buckling pattern as calculated by Fok and Allwright agrees with the value arising from the theory of this chapter.

Chapter 4

Asymptotic Buckling Analysis

In Chapter 3 we succeeded in finding the critical stress at infinity sufficient to induce buckling in a shell embedded in a linearly elastic material. However, the results were found numerically rather than analytically. As a consequence, we cannot easily determine the dependence of the critical stress (and the resulting buckling pattern) on the material and geometric parameters of the problem. In this chapter we take the energy integrals of Chapter 3 for the case of a *uniaxial* stress field at infinity and consider the limit as the thickness ratio tends to zero. We obtain asymptotic forms for the critical stress and buckling patterns in this limit, and compare them to the numerical results found in Chapter 3.

4.1 Limiting cases

We begin by considering numerical experiments on the results of Chapter 3. The variation in the buckling pattern as $h/\widehat{R} \to 0$ is shown in Figure 4.1. In this figure we use $G_{\mathrm{s}}/G_{\mathrm{m}} = 100$ and values of the Poisson ratios from Table 1.1. We note that as $h/\widehat{R}$ decreases the wavelength of the buckling pattern decreases, while at the same time the extent of the buckled region also decreases. In this limit the critical stress tends to a constant. A similar pattern occurs in the case where we consider the quantity $G_{\mathrm{s}}/G_{\mathrm{m}} \to 0$, but not as rapidly, and the critical stress in this limit is unbounded. The behaviour of the buckling patterns in these limits ought to make the problem amenable to analysis, since problems resulting in highly oscillatory solutions can often be approximated using the WKB asymptotic method.

We stress here that the analysis of these limits is purely *mathematical* in nature. It may be the case that in one of the limits which we will study, one or more of our assumptions become invalid. Certainly the shallow shell assumption will remain valid because by definition it assumes that the buckling wavelength is much shorter than the radius of curvature of the unbuckled shell, which is confirmed by Figure 4.1. However, if the asymptotic value of the critical stress at infinity becomes very large,

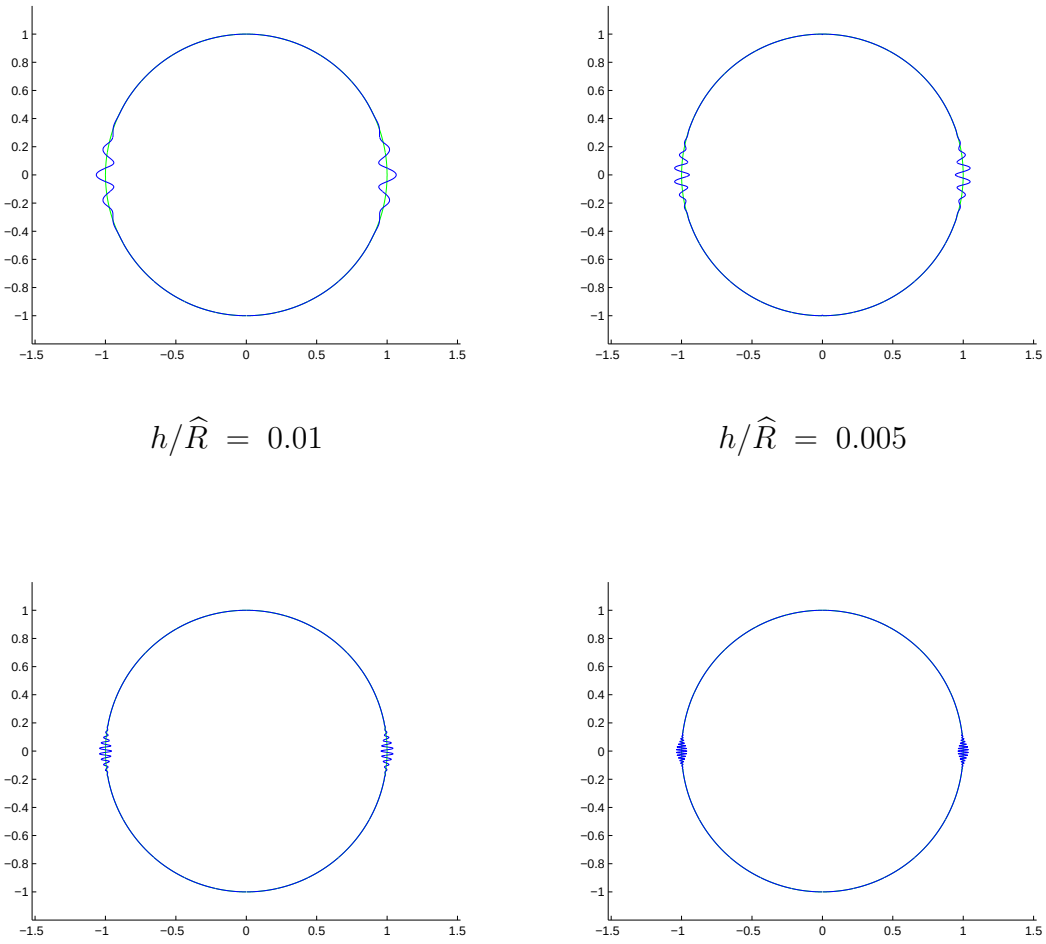

Figure 4.1: The buckling pattern as $h/\widehat{R} \to 0$.

as happens in the limit $G_{\rm s}/G_{\rm m} \to 0$, our assumption of linear elasticity for the matrix may be violated. Nevertheless, our aim is that the results of the asymptotic analysis should give a reasonably accurate analytic expression for both the buckling pattern and the critical stress at infinity in our parameter regime.

4.2 The Euler strut

In order to analyse the behaviour of the system in these limits, it would be preferable to start by considering a canonical problem, involving a structure that buckles to a localised buckling pattern as seen in Figure 4.1. One such problem is that of an Euler strut attached to a substrate of variable stiffness. This is a problem that has been

analysed by Coman [23]. The problem involves the deformation under buckling of a beam attached to a deformable substrate, as shown in Figure 4.2. The substrate will be assumed to be composed of linear springs, whose stiffness varies as a function of position.[1]

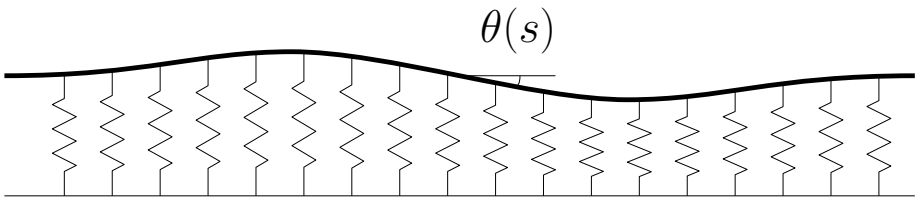

Figure 4.2: A diagram of a beam attached to an deformable substrate.

Consider the equations for the deformation of an elastic beam, as depicted in Figure 4.2,

$$EI\frac{\mathrm{d}^2\theta}{\mathrm{d}s^2} - F_x\sin\theta + F_y\cos\theta = 0\,, \tag{4.1}$$

$$\frac{\mathrm{d}F_x}{\mathrm{d}s} + f_x = 0\,, \tag{4.2}$$

$$\frac{\mathrm{d}F_y}{\mathrm{d}s} + f_y = 0\,, \tag{4.3}$$

where s is the arc-length along the beam, $\big(F_x(s), F_y(s)\big)$ are the (x,y)-components of the internal force along the beam, (f_x, f_y) are the components of the body force acting on the beam, $\theta(s)$ is the angle that the beam makes with the horizontal (x-) direction, and EI is the bending stiffness of the beam. The variable θ is related to x and y by

$$\frac{\mathrm{d}x}{\mathrm{d}s} = \cos\theta\,, \tag{4.4}$$

$$\frac{\mathrm{d}y}{\mathrm{d}s} = \sin\theta\,. \tag{4.5}$$

We suppose that the deflections are small, so that $\theta \approx 0$, and

$$\cos\theta \sim 1\,, \tag{4.6}$$

$$\sin\theta \sim \theta\,. \tag{4.7}$$

Then from equation (4.4) we have

$$\frac{\mathrm{d}x}{\mathrm{d}s} \sim 1 \qquad \Rightarrow \qquad x \sim s\,, \tag{4.8}$$

[1]We note that similar buckling patterns have been observed when the substrate is of constant but *nonlinear* stiffness [94], although the variable-stiffness case is analysed in this chapter as it seems particularly relevant to our sphere-buckling problem.

and from equation (4.5) we obtain

$$\frac{\mathrm{d}y}{\mathrm{d}s} \sim \theta \,. \tag{4.9}$$

To obtain the small-deflection equations, we therefore denote the centre-line of the beam by $y = w(x)$, replace s by x, and θ by $w'(x)$ (according to equation (4.9)). The main equation becomes

$$EI\frac{\mathrm{d}^3 w}{\mathrm{d}x^3} - F_x\frac{\mathrm{d}w}{\mathrm{d}x} + F_y = 0 \,, \tag{4.10}$$

where

$$\frac{\mathrm{d}F_x}{\mathrm{d}x} + f_x = 0 \,, \tag{4.11}$$

$$\frac{\mathrm{d}F_y}{\mathrm{d}x} + f_y = 0 \,. \tag{4.12}$$

We now consider the forces applied to our beam. We suppose that the only body forces applied are in the y-direction (due to the elastic foundation), denoted

$$f_y = -V(w(x), x) \,. \tag{4.13}$$

In reality, the elastic foundation would also apply a force f_x in the x-direction, but for simplicity this is neglected here. At either end of the beam we apply a compressive force P in the x-direction. Because there are no body forces in the x-direction, we have

$$\frac{\mathrm{d}F_x}{\mathrm{d}x} = 0 \,, \tag{4.14}$$

with $F_x = -P$ at either end of the beam, so that $F_x \equiv -P$. Now, from equation (4.10), we get

$$EI\frac{\mathrm{d}^3 w}{\mathrm{d}x^3} + P\frac{\mathrm{d}w}{\mathrm{d}x} + F_y = 0 \tag{4.15}$$

$$\Rightarrow \quad EI\frac{\mathrm{d}^4 w}{\mathrm{d}x^4} + P\frac{\mathrm{d}^2 w}{\mathrm{d}x^2} + \frac{\mathrm{d}F_y}{\mathrm{d}x} = 0 \tag{4.16}$$

$$\Rightarrow \quad EI\frac{\mathrm{d}^4 w}{\mathrm{d}x^4} + P\frac{\mathrm{d}^2 w}{\mathrm{d}x^2} + V(w(x), x) = 0 \,. \tag{4.17}$$

We now search for possible models for the elastic foundation. By far the simplest is the *Winkler foundation model*, which models the foundation as a continuum of linear springs of stiffness $k(x) > 0$ (varying in position along the beam), giving us

$$V = k(x)w(x) \,. \tag{4.18}$$

Of course, this is a very simplified model and doesn't take into account any interaction between springs. A more realistic model would use the equations of linear elasticity,

but this is quite difficult to express solely in terms of $w(x)$.[2] We will accordingly follow Coman and assume that the foundation is governed by the Winkler model with a variable stiffness coefficient $k(x)$.

The equation to be solved for the mid-beam displacement $w(x)$ is thus

$$EI\frac{\mathrm{d}^4 w}{\mathrm{d}x^4} + P\frac{\mathrm{d}^2 w}{\mathrm{d}x^2} + k(x)w \;=\; 0\,. \tag{4.19}$$

The beam is clamped at either end, so that

$$w(-L) \;=\; w(L) \;=\; w'(-L) \;=\; w'(L) \;=\; 0\,. \tag{4.20}$$

For localised buckling patterns of the kind seen in Figure 4.1, we require $k(x)$ to have a minimum at some point $x = x_0$ in the beam, so that $k(x_0) > 0$, $k'(x_0) = 0$ and $k''(x_0) > 0$.

4.2.1 Nondimensionalisation

We first nondimensionalise the equation. The scalings used are

$$x \;=\; L\widehat{x}\,, \qquad k(x) \;=\; K\widehat{k}(\widehat{x})\,, \qquad w(x) \;=\; W\widehat{w}(\widehat{x})\,, \tag{4.21}$$

giving

$$\frac{EI}{KL^4}\frac{\mathrm{d}^4 w}{\mathrm{d}x^4} + \frac{P}{KL^2}\frac{\mathrm{d}^2 w}{\mathrm{d}x^2} + k(x)w \;=\; 0\,, \tag{4.22}$$

where we have dropped the $\widehat{\ }$ notation for convenience. We suppose that the quantity multiplying the $w''''(x)$ term is small, so that we can define

$$\varepsilon^4 \;=\; \frac{EI}{KL^4}\,. \tag{4.23}$$

This parameter will be small if the foundation is stiffer than the beam, or if the beam is very long (compared to its thickness, characterised by I). These conditions are equivalent to the limiting cases in the sphere buckling problem discussed earlier, namely that the shear modulus ratio $G_\mathrm{s}/G_\mathrm{m}$ or the thickness ratio $h/\widehat{R}$ are small.

We then define the nondimensional loading parameter

$$\lambda \;=\; \frac{P}{2\sqrt{KEI}}\,, \tag{4.24}$$

[2] One attempt to bridge the gap between the Winkler model and the linear elastic model by introducing resistance to shearing is the *Pasternak model*, which has been derived in many different ways [99]. It takes the form

$$V \;=\; k(x)w(x) - \kappa(x)\frac{\mathrm{d}^2 w}{\mathrm{d}x^2}$$

where $\kappa(x)$ is a material parameter.

giving

$$\varepsilon^4 \frac{\mathrm{d}^4 w}{\mathrm{d}x^4} + 2\varepsilon^2 \lambda \frac{\mathrm{d}^2 w}{\mathrm{d}x^2} + k(x) w \;=\; 0\,. \tag{4.25}$$

For simplicity we will replace the end conditions (4.20) by

$$w(\pm\infty) \;=\; w'(\pm\infty) \;=\; 0\,. \tag{4.26}$$

We will limit our analysis to the case $\lambda > \lambda_{\mathrm{c}} = \sqrt{\min k(x)} = k(x_0)^{1/2}$. This is because there are no non-zero solutions to equation (4.25) and boundary conditions (4.26) when $\lambda \leqslant \lambda_{\mathrm{c}}$. To show this, take the differential equation and change coordinates $x = \varepsilon \widehat{x}$. Then (writing $\widehat{x}$ as x for simplicity),

$$w'''' + 2\lambda w'' + k(x) w \;=\; 0\,. \tag{4.27}$$

We then multiply this by w and integrate over $\mathbb{R}$. Integrating by parts, we obtain

$$\int_{\mathbb{R}} k w^2 \,\mathrm{d}x \;=\; -\int_{\mathbb{R}} \left(2\lambda w'' w + (w'')^2\right) \,\mathrm{d}x \tag{4.28}$$

$$\;=\; -\int_{\mathbb{R}} 2\lambda w'' w \,\mathrm{d}x - \|w''\|^2\,, \tag{4.29}$$

where $\|\cdot\|$ is the L_2 norm. Since the left hand side is positive, the first term on the right hand side must also be positive, so that

$$-\int_{\mathbb{R}} 2\lambda w'' w \,\mathrm{d}x \;\leqslant\; 2\lambda \|w''\| \cdot \|w\| \tag{4.30}$$

by the Cauchy–Schwartz inequality. Thus

$$\int_{\mathbb{R}} k(x) w^2 \,\mathrm{d}x \;\leqslant\; 2\lambda \|w''\| \cdot \|w\| - \|w''\|^2 \tag{4.31}$$

for all possible deformations w. Maximising the right hand side over $\|w''\|$, we find that

$$2\lambda \|w''\| \cdot \|w\| - \|w''\|^2 \;\leqslant\; \lambda^2 \|w\|^2\,. \tag{4.32}$$

Therefore

$$\int_{\mathbb{R}} k(x) w^2 \,\mathrm{d}x \;\leqslant\; \lambda^2 \|w\|^2 \tag{4.33}$$

$$\Rightarrow \int_{\mathbb{R}} \left(\lambda^2 - k(x)\right) w^2 \,\mathrm{d}x \;\geqslant\; 0\,. \tag{4.34}$$

Now, given that $k(x) > 0$ is not constant, if $\lambda^2 \leqslant \min k(x)$ we must have $w \equiv 0$ in order to satisfy (4.34). Hence, for nonzero solutions we must have

$$\lambda^2 \;>\; \min k(x)\,. \tag{4.35}$$

4.2.2 Coman's analysis

Coman's method [23] for solving the equation is rather *ad hoc* in character, and while we will be able to justify the assumptions he made in his analysis, we will summarise his results here first. The method relies on the WKB ansatz

$$w(x) \;=\; W(x)\exp\left(\frac{\mathrm{i}}{\varepsilon}S(x)\right)\;. \tag{4.36}$$

The equation is simplified by taking only the first two terms in the Taylor expansion of the function $S(x)$,

$$S(x) \;=\; S(x_0)+S'(x_0)(x-x_0)+\frac{1}{2}S''(x_0)(x-x_0)^2+O\big((x-x_0)^3\big)\;, \tag{4.37}$$

where x_0 is the minimum of $k(x)$, *i.e.* the weakest point of the material. We set

$$\eta_0 \;=\; S'(x_0)\;, \tag{4.38}$$
$$\sigma \;=\; S''(x_0)\;, \tag{4.39}$$

to be parameters which are to be found in the course of the analysis, and look at the region near $x=x_0$ by setting

$$\zeta \;=\; \varepsilon^{-1/2}(x-x_0) \tag{4.40}$$

to be an $O(1)$ position parameter. The ansatz substituted into the equation therefore becomes

$$w(x) \;=\; W(x)\exp\left(\mathrm{i}\varepsilon^{-1/2}\eta_0\zeta+\frac{\mathrm{i}\sigma}{2}\zeta^2\right)\;, \tag{4.41}$$

absorbing $S(x_0)$ into $W(x)$.

Now, the function $W(x)$ and the parameter λ are expanded in powers of $\varepsilon^{1/2}$ and ε respectively:

$$W(x) \;=\; W_0(x)+\varepsilon^{1/2}W_1(x)+\varepsilon W_2(x)+\cdots\;, \tag{4.42}$$
$$\lambda \;=\; \lambda_0+\varepsilon\lambda_1+\cdots\;. \tag{4.43}$$

Assuming that $k(x)$ has a minimum at x_0, asymptotic analysis of the equation (4.25) eventually yields

$$\eta_0 \;=\; k(x_0)^{1/4}\;, \tag{4.44}$$
$$\sigma \;=\; \mathrm{i}\Gamma_1\;, \tag{4.45}$$
$$\lambda_0 \;=\; k(x_0)^{1/2}\;, \tag{4.46}$$
$$\lambda_1 \;=\; 2\Gamma_1(1+2n)\;, \tag{4.47}$$
$$W_0(x) \;=\; H_n(\sqrt{\Gamma_1}\,\zeta)\;, \tag{4.48}$$

where $H_n(x)$ are Hermite polynomials, $n = 0, 1, 2, \ldots$, and

$$\Gamma_1 \;=\; \frac{\sqrt{k''(x_0)}}{2\sqrt{2}k(x_0)^{1/4}} \,. \tag{4.49}$$

This analysis works well for the beam equation above, yielding asymptotic forms of the buckling pattern and critical stress. However, the scalings used may only be particularly suited to the beam equation (4.25). Without a clear understanding of the underlying asymptotic behaviour of the solutions, we should not blindly apply the same process to the shell buckling problem. In the next section we will analyse the beam equation from a more fundamental point of view, to see if we can find a more general asymptotic approximation method which we can in turn apply to the shell problem.

4.3 WKB analysis

In this section we will examine equation (4.25) from a more systematic point of view, to understand the underlying structure of the equation. First, however, we will consider what turns out to be a related problem, namely that of the harmonic oscillator. We will analyse this equation by the WKB method, identifying Stokes and anti-Stokes lines, and using this information to solve the equation. This process will then be repeated for equation (4.25). Finally, we will show that a simplified method of solution can be applied to this equation if we are looking for the lowest eigenvalue. This method will then form the basis of our solution of the full spherical shell buckling problem.

The WKB method relies on the substitution of the ansatz

$$w \;=\; A(x)\mathrm{e}^{\mathrm{i}\phi(x)/\varepsilon} \tag{4.50}$$

into the equation under consideration. For future reference, we note that

$$\begin{aligned}
w &= A\mathrm{e}^{\mathrm{i}\phi/\varepsilon} \,, && (4.51)\\
w'' &= \left[-\frac{\phi'^2 A}{\varepsilon^2} + \frac{\mathrm{i}}{\varepsilon}(\phi'' A + 2\phi' A') + A''\right]\mathrm{e}^{\mathrm{i}\phi/\varepsilon} \,, && (4.52)\\
w'''' &= \left[\frac{\phi'^4 A}{\varepsilon^4} - \frac{\mathrm{i}}{\varepsilon^3}(6\phi''\phi'^2 A + 4\phi'^3 A')\right.\\
&\qquad -\frac{1}{\varepsilon^2}(3\phi''^2 A + 4\phi'''\phi' A + 12\phi''\phi' A' + 6\phi'^2 A'')\\
&\qquad \left.+\frac{\mathrm{i}}{\varepsilon}(\phi'''' A + 4\phi''' A' + 6\phi'' A'' + 4\phi' A''') + A''''\right]\mathrm{e}^{\mathrm{i}\phi/\varepsilon} \,. && (4.53)
\end{aligned}$$

4.3.1 The harmonic oscillator

It will transpire that the structure of equation (4.25) bears a close resemblance to the problem of the harmonic oscillator in quantum mechanics. This satisfies the equation

$$-w'' + x^2 w = \lambda w \,, \tag{4.54}$$

with $|w| \to 0$ as $|x| \to \infty$. Here λ represents the energy level. If we look for large λ, we set $\varepsilon = 1/\lambda$ and rescale x:

$$\varepsilon^2 w'' + (1 - x^2) w = 0 \,, \tag{4.55}$$

with $|w| \to 0$ as $|x| \to \infty$. We substitute the standard WKB ansatz (4.50) to find, at leading order

$$\left[-\phi'(x)^2 + (1 - x^2)\right] A_0(x) = 0 \,, \tag{4.56}$$

where A_0 is the leading order term in the asymptotic expansion of $A(x)$,

$$A(x) = A_0(x) + \varepsilon A_1(x) + \cdots \,. \tag{4.57}$$

Equation (4.56) is known as the *eikonal* equation. Solving for $\phi'(x)$, we find that

$$\phi' = \pm\sqrt{1 - x^2} \,, \tag{4.58}$$

where the $\pm$ denote the two branches of the multivalued function $(1 - x^2)^{1/2}$ in the complex plane, for which the branch cuts will be chosen to lie along the lines $x = -1 + \mathrm{i}p$, $x = 1 - \mathrm{i}p$ for $p \in (0, \infty)$. Clearly, the expression (4.58) may be integrated analytically, but we will assume otherwise in order to describe a method which may be applied to more complicated functions. At the next order in (4.55), we obtain

$$\mathrm{i}\left[\phi''(x) A_0(x) + 2\phi'(x) A_0'(x)\right] + \left[-\phi'(x)^2 + (1 - x^2)\right] A_1(x) = 0 \,, \tag{4.59}$$

whence we find

$$A_0 = (1 - x^2)^{-1/4} \,. \tag{4.60}$$

The two solutions to ϕ' that are given in equation (4.58) — denoted by ϕ_1' and ϕ_2' — describe two different WKB approximations w_1 and w_2 to the solution of the original equation (4.54), where

$$w_j(x) = A_0(x) \mathrm{e}^{\mathrm{i}\phi_j(x)/\varepsilon} \,. \tag{4.61}$$

It is the interaction between these two solutions that elucidates the properties of the full solution of (4.54). In order to examine these properties fully, we need to extend the two solutions found to the complex plane. Thus equation (4.58) now refers to two branches of the function in the complex plane, for $x \in \mathbb{C}$.

4.3.1.1 Stokes lines and anti-Stokes lines

Our next step in the analysis of the equation is to determine the Stokes lines and anti-Stokes lines associated with the asymptotic solutions $w_i(x)$. We will follow the theory from a general point of view, which assumes that we have n such solutions. Firstly, we determine the so-called *turning points* of ϕ. These are defined as the points x where $\phi_i'(x) = \phi_j'(x)$ for $i \neq j$. Given these turning points, we now turn to the definition of *Stokes lines*. Comparing two solutions $w_i(x)$ and $w_j(x)$, these are the lines (emanating from a turning point X) on which one of the solutions is maximally dominant over the other. This is equivalent to the condition that

$$\Re\left\{\int_X^x \left[\phi_i'(\zeta) - \phi_j'(\zeta)\right]\,\mathrm{d}\zeta\right\} \;=\; 0\,. \tag{4.62}$$

Conversely, *anti-Stokes lines* are lines (again, emanating from a turning point X) over which two solutions are equally dominant. This corresponds to the condition

$$\Im\left\{\int_X^x \left[\phi_i'(\zeta) - \phi_j'(\zeta)\right]\,\mathrm{d}\zeta\right\} \;=\; 0\,. \tag{4.63}$$

These definitions are unwieldy for the actual calculation of the lines. We will follow a procedure used by Yakubenko [98]. This paper contained a method for the calculation of anti-Stokes lines, which we extend to the calculation of Stokes lines.[3] The anti-Stokes line calculation begins by defining

$$F(x) \;=\; \int_X^x \left[\phi_i'(\zeta) - \phi_j'(\zeta)\right]\,\mathrm{d}\zeta\,, \tag{4.64}$$

so that the anti-Stokes lines are defined by

$$G(x) \;:=\; \Im F(x) \;=\; 0\,. \tag{4.65}$$

Now, if a path in $\mathbb{R}^2$ is defined by $G(x_1, x_2) = \text{constant}$, then a vector tangent to this path is given by

$$\left(-\frac{\partial G}{\partial x_2}, \frac{\partial G}{\partial x_1}\right)\,. \tag{4.66}$$

Thus if we set $\xi = \Re x$ and $\eta = \Im x$ then the vector

$$\left(-\frac{\partial G}{\partial \eta}, \frac{\partial G}{\partial \xi}\right) \tag{4.67}$$

[3] Yakubenko follows the convention that Stokes lines are defined by equation (4.63) and anti-Stokes lines by equation (4.62). This convention is mainly seen in the engineering and physics literature, while our definitions above are used predominantly in the mathematical literature.

is tangent to $G(x) = \text{constant}$ in the complex plane. Thus the curves $G(x) = \text{constant}$ are the integral curves of

$$\begin{aligned} \frac{\mathrm{d}\eta}{\mathrm{d}\xi} &= \frac{\partial G/\partial \xi}{-\partial G/\partial \eta} && (4.68)\\ &= \frac{\frac{\partial}{\partial \xi}(\Im F)}{-\frac{\partial}{\partial \eta}(\Im F)} && (4.69)\\ &= -\frac{\frac{\partial}{\partial \xi}(\Im F)}{\frac{\partial}{\partial \xi}(\Re F)} && (4.70)\\ &= -\frac{\Im(\partial F/\partial \xi)}{\Re(\partial F/\partial \xi)}\,, && (4.71) \end{aligned}$$

using the Cauchy-Riemann equations (assuming that F is analytic). Now, if

$$\begin{aligned} x &= \xi + \mathrm{i}\eta\,, && (4.72)\\ \bar{x} &= \xi - \mathrm{i}\eta\,, && (4.73) \end{aligned}$$

then

$$\begin{aligned} \frac{\partial F}{\partial \xi} &= \frac{\partial F}{\partial x}\frac{\partial x}{\partial \xi} + \frac{\partial F}{\partial \bar{x}}\frac{\partial \bar{x}}{\partial \xi} && (4.74)\\ &= \frac{\partial F}{\partial x}\,. && (4.75) \end{aligned}$$

Hence

$$\begin{aligned} \frac{\mathrm{d}\eta}{\mathrm{d}\xi} &= -\frac{\Im(\partial F/\partial x)}{\Re(\partial F/\partial x)} && (4.76)\\ &= -\frac{\Im\left[\phi_i'(x) - \phi_j'(x)\right]}{\Re\left[\phi_i'(x) - \phi_j'(x)\right]}\,. && (4.77) \end{aligned}$$

This relation can be solved numerically to give the solution to $G(x) = \text{constant}$. To pick out the anti-Stokes lines, which are given by $G(x) = 0$, we set the starting position to be the turning points (as the lines emanate from these).

If we follow the same process for the Stokes lines, defined by

$$H(x) := \Re F(x) = 0\,, \tag{4.78}$$

we find that the equivalent relation for calculation purposes becomes

$$\frac{\mathrm{d}\eta}{\mathrm{d}\xi} = \frac{\Re\left[\phi_i'(x) - \phi_j'(x)\right]}{\Im\left[\phi_i'(x) - \phi_j'(x)\right]}\,. \tag{4.79}$$

With regard to the asymptotic behaviour of a function, Stokes lines delimit areas in which the function has different asymptotic expansions. These regions will be referred to as 'Stokes regions'. For WKB approximations, the asymptotic solution w will be

formed from different combinations of the solutions w_i in each Stokes region. Taking any two solutions, recall that along anti-Stokes lines for those two solutions, neither solution is exponentially dominant over the other. Therefore, in regions delimited by anti-Stokes lines (and branch cuts), one solution is going to be exponentially dominant over the other. Consider the quotient

$$\frac{w_i}{w_j} = \frac{A_i(x)}{A_j(x)} \exp\left(\frac{\mathrm{i}}{\varepsilon}\int (\phi_i' - \phi_j')\ \mathrm{d}x\right) . \tag{4.80}$$

If this tends to infinity exponentially as $\varepsilon \to 0$, then w_i is exponentially dominant over w_j.

4.3.1.2 Analysis of the harmonic oscillator

Defining ϕ_1' and ϕ_2' to be the positive and negative roots of (4.58) respectively, we find that the turning points occur at $x = \pm 1$. The Stokes and anti-Stokes lines emanating from these turning points are shown in Figure 4.3, where the thick black lines are branch cuts.

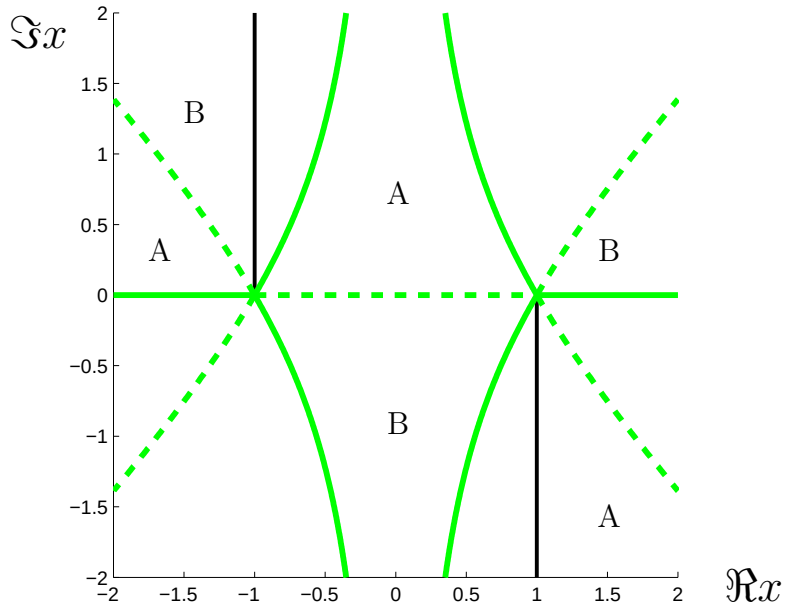

Figure 4.3: Stokes lines (unbroken) and anti-Stokes lines (broken) for the harmonic oscillator.

Now, in order to establish the relative dominance of the solutions w_1 and w_2, we note that $\phi_2 = -\phi_1$ throughout the complex plane. Applying condition (4.80) allows us to show that w_1 dominates as $\Re x \to -\infty$ while w_2 dominates as $\Re x \to +\infty$, where w_i is the solution given by (4.61). Using the fact that the dominance of the

two solutions switches on crossing an anti-Stokes line (or a branch cut), the complex plane in Figure 4.3 has been partitioned into regions labelled A and B, delimited by anti-Stokes lines and branch cuts. In regions A, w_1 is exponentially dominant over w_2 while in regions B w_2 dominates.

We are interested in the form of the solution along the real axis. Because the asymptotic solution for the problem has a different form in each Stokes region, we can consider three regions, where the solution will be formed of different combinations of the two solutions w_i. For the region $\Re x < -1$, we require the solution to decay as $\Re x \to -\infty$, so the solution is composed only of a constant multiple of the exponentially subdominant solution, *i.e.* $C_- w_2$. Similarly, for $\Re x > 1$, the required exponentially subdominant solution is $C_+ w_1$. In the remaining region, $\Re x \in (-1, 1)$, we have a certain linear combination of the two solutions, $C_1 w_1 + C_2 w_2$.

The common method of matching these solutions is to realise that each of the asymptotic solutions w_i is not valid in a region of the turning points, since A_0 is unbounded at these points. The original equation is expanded in the vicinity of the turning point to find an inner solution. (In the case of a simple turning point as we have at $x = \pm 1$, the inner solutions are Airy functions). The matching process gives us a *connection formula*, linking the coefficients of the outer solution on either side of the turning point.

The alternative method of solving the problem is to consider the solution along the real axis, but deformed around the turning points as shown in Figure 4.4. We

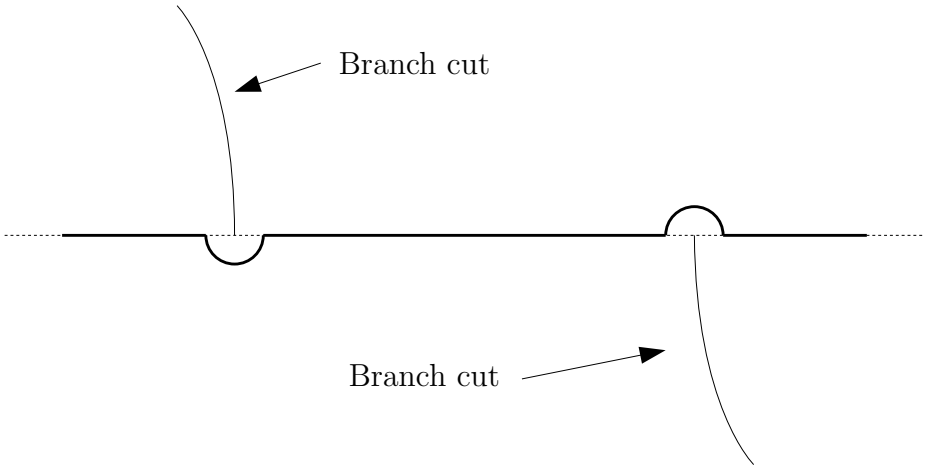

Figure 4.4: Path of the solution (in bold), showing detour around the turning points.

prescribe the solution as $\Re x \to \pm\infty$, and find the solution by following the path in Figure 4.4 and considering how the solution changes on crossing the Stokes lines.

For this method we need to recall that on traversing an anti-Stokes line for two solutions w_i and w_j, the subdominant solution becomes dominant and *vice versa*. On

traversing a Stokes line, if the only solution present on one side is subdominant, the solution on the other side is composed of the same subdominant solution. However, if the solution on one side contains a dominant component, the coefficient of the subdominant solution is changed on crossing the Stokes line, while the coefficient of the dominant solution remains the same. The amount by which the subdominant coefficient is changed is dependent on the nature of the turning point and is proportional to the dominant coefficient.

As previously noted, the turning points at $x = \pm 1$ give the solution in this vicinity the structure of an Airy function. For turning points of this form, consider Figure 4.5, which represents the solution in the vicinity of $x = +1$. The red and green arcs

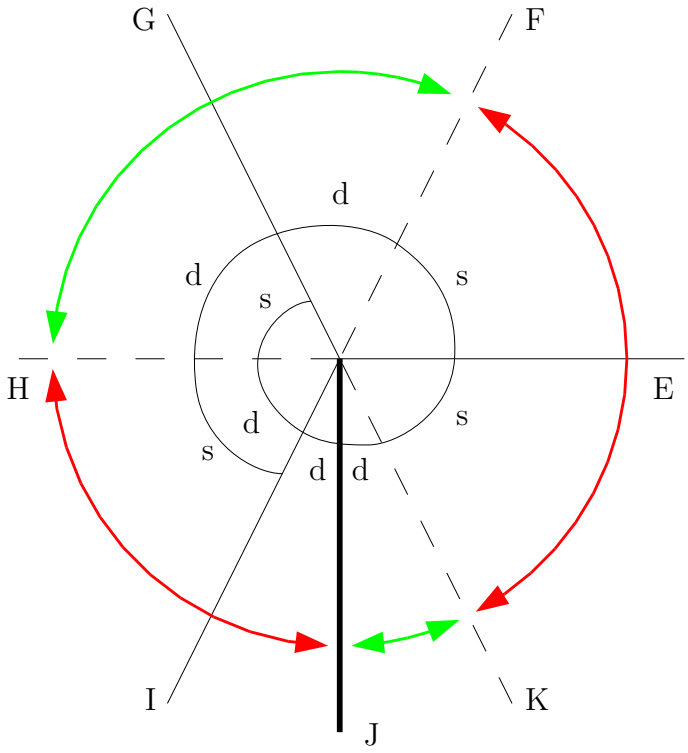

Figure 4.5: Schematic diagram of the Airy turning point. Please refer to the text for an explanation.

distinguish the regions in which different solutions are dominant. Considering the w_1 and w_2 solutions, the green arcs correspond to regions A in Figure 4.3 (near the turning point) and the red arcs to regions B. Stokes lines are represented as solid lines and anti-Stokes lines as broken lines. Line J is a branch cut.

Recall that in each Stokes region we have a different asymptotic solution, comprised of different combinations of the solutions w_1 and w_2. Suppose, therefore, that in the region between E and G, we have a solution $A_1 w_1 + A_2 w_2$. On crossing the

Stokes line G in an anticlockwise manner, the coefficient of the subdominant solution w_2 changes, so that the solution now becomes $A_1 w_1 + B_2 w_2$. In fact, it can be shown [13] that for the Airy turning point,

$$B_2 - A_2 \;=\; \mathrm{i}A_1 \;, \tag{4.81}$$

and that on traversing a Stokes line in an anticlockwise direction the coefficient of the subdominant solution is always increased by the coefficient of the dominant solution multiplied by i. The value i is the *Stokes multiplier* for the turning point.[4] Now, for the harmonic oscillator problem, we require an exponentially subdominant solution in the region $\Re x > 1$. Hence, with reference to Figure 4.5, the solution in the Stokes region E–G (and, indeed, in the region J–E) must be given by $C_+ w_1$. Circling the turning point anticlockwise from E, this solution becomes dominant on crossing the anti-Stokes line F. Therefore, on crossing the Stokes line G the coefficient of the subdominant solution, w_2, is increased from zero to $\mathrm{i}C_+$ according to equation (4.81). Thus, in the Stokes region G–I, the solution is comprised of $C_+ w_1 + \mathrm{i}C_+ w_2$. On crossing the Stokes line at I, we add $\mathrm{i} \times (\mathrm{i}C_+)$ to the coefficient of w_1, the subdominant solution, meaning that in the region I–J the solution is comprised solely of $\mathrm{i}C_+ w_2$. This solution then corresponds with the solution $C_+ w_1$ on the other side of the branch cut J.

Thus, the effect of the turning point is that if we have a solution $C_+ w_1$ in $\Re x > 1$, then for $\Re x < 1$ the solution comprises $C_+ w_1 + \mathrm{i}C_+ w_2$. The turning point at $x = -1$ has the same structure as the one at $x = 1$, but rotated by 180°. Therefore, if the solution for $\Re x < -1$ is $C_- w_2$, then for $\Re x > -1$ we have the solution $\mathrm{i}C_- w_1 + C_- w_2$.

Now, in the region $\Re x \in (-1, 1)$, we have two expressions for the asymptotic solution, which should match, *i.e.*

$$\mathrm{i}C_- w_1 + C_- w_2 \;=\; C_+ w_1 + \mathrm{i}C_+ w_2 \;. \tag{4.82}$$

The left-hand side of (4.82) becomes

$$L \;=\; C_- A_0(x) \left[\mathrm{i} \exp\left(\frac{\mathrm{i}}{\varepsilon} \int_{-1}^{x} \sqrt{1 - x^2}\, \mathrm{d}x \right) + \exp\left(-\frac{\mathrm{i}}{\varepsilon} \int_{-1}^{x} \sqrt{1 - x^2}\, \mathrm{d}x \right) \right] \;, \tag{4.83}$$

[4] This relies on the fact that the two solutions are normalised — we could multiply one solution by a constant, which would change the value of the Stokes multiplier. For the Airy function the two functions are defined as

$$\begin{aligned} w_1 &= x^{-1/4} \exp\left(-\tfrac{2}{3} x^{3/2}\right) \;, \\ w_2 &= x^{-1/4} \exp\left(\tfrac{2}{3} x^{3/2}\right) \;. \end{aligned}$$

with the right-hand side becoming

$$R \;=\; C_+ A_0(x)\left[\exp\left(\frac{\mathrm{i}}{\varepsilon}\int_1^x \sqrt{1-x^2}\,\mathrm{d}x\right) + \mathrm{i}\,\exp\left(-\frac{\mathrm{i}}{\varepsilon}\int_1^x \sqrt{1-x^2}\,\mathrm{d}x\right)\right]\ . \quad (4.84)$$

Written in terms of trigonometric functions, these become

$$L \;=\; 2C_- \mathrm{e}^{\mathrm{i}\pi/4} A_0(x)\cos\left(\frac{1}{\varepsilon}\int_{-1}^x \sqrt{1-x^2}\,\mathrm{d}x + \frac{\pi}{4}\right)\ , \quad (4.85)$$

and

$$\begin{aligned} R \;&=\; 2C_+ \mathrm{e}^{\mathrm{i}\pi/4} A_0(x)\cos\left(-\frac{1}{\varepsilon}\int_x^1 \sqrt{1-x^2}\,\mathrm{d}x - \frac{\pi}{4}\right) && (4.86)\\ &=\; 2C_+ \mathrm{e}^{\mathrm{i}\pi/4} A_0(x) \\ &\quad \times \cos\left(\frac{1}{\varepsilon}\int_{-1}^x \sqrt{1-x^2}\,\mathrm{d}x + \frac{\pi}{4} - \left[\frac{1}{\varepsilon}\int_{-1}^1 \sqrt{1-x^2}\,\mathrm{d}x + \frac{\pi}{2}\right]\right). && (4.87)\end{aligned}$$

If L and R are to be equated, we must have

$$\frac{1}{\varepsilon}\int_{-1}^1 \sqrt{1-x^2}\,\mathrm{d}x + \frac{\pi}{2} \;=\; n\pi \quad (4.88)$$

for $n \in \mathbb{Z}$. In other words,

$$\varepsilon \;=\; \frac{1}{2n+1} \quad (4.89)$$

for integer $n = 0, 1, 2, \ldots$, as $\varepsilon > 0$. Correspondingly, the eigenvalues λ_n to equation (4.54) are

$$\lambda_n \;=\; \frac{1}{\varepsilon} \;=\; 2n+1\ . \quad (4.90)$$

In fact it transpires that these energy levels are *exact*, with eigenfunctions given by

$$y_n \;=\; \mathrm{e}^{-x^2/2} H_n(x)\ , \quad (4.91)$$

where $H_n(x)$ are Hermite polynomials.

4.3.2 Return to the beam equation

We now return to the equation (4.25) for the beam on an elastic foundation. Into this we substitute the WKB ansatz, so that from (4.51)–(4.53) we obtain, at leading order,

$$\begin{aligned} \left(\phi'(x)^4 - 2\lambda\phi'(x)^2 + k(x)\right) A(x) \;&=\; 0 && (4.92)\\ \Rightarrow \qquad \phi'(x)^4 - 2\lambda\phi'(x)^2 + k(x) \;&=\; 0 && (4.93)\end{aligned}$$

as an eikonal equation. This equation will give us $\phi'(x)$ in terms of λ and $k(x)$. Let us assume that this problem is solved, and proceed to the next order in the equation. Expanding the amplitude $A(x)$ as in equation (4.57), the $O(\varepsilon)$ terms in equation (4.25) following the WKB substitution become

$$-\mathrm{i}(4A_0'\phi'^3 + 6A_0\phi''\phi'^2) + 2\lambda\mathrm{i}(A_0\phi'' + 2A_0'\phi') \;=\; 0\,, \tag{4.94}$$

which can be rearranged to give

$$\begin{aligned}
\frac{A_0'}{A_0} &= -\frac{\phi''(3\phi'^2-\lambda)}{2\phi'(\phi'^2-\lambda)} && (4.95)\\
\Rightarrow \qquad \log A_0(x) &= -\int \frac{\phi''(3\phi'^2-\lambda)}{2\phi'(\phi'^2-\lambda)}\,\mathrm{d}x + \text{constant} && (4.96)\\
&= -\int \left[\frac{\phi''}{2\phi'} + \frac{\phi''\phi'}{\phi'^2-\lambda}\right]\mathrm{d}x + \text{constant} && (4.97)\\
&= -\frac{1}{2}\log\left(\phi'(x)\left[\phi'(x)^2-\lambda\right]\right) + \text{constant} && (4.98)\\
\Rightarrow \qquad A_0(x) &= \frac{C}{\sqrt{\phi'(x)\big(\phi'(x)^2-\lambda\big)}}\,, && (4.99)
\end{aligned}$$

where C is a constant.

We now return to the eikonal equation (4.93) and solve it to get

$$\phi'(x) \;=\; \pm\sqrt{\lambda \pm \sqrt{\lambda^2 - k(x)}}\,. \tag{4.100}$$

The variable x refers to the real line, but as for the harmonic oscillator it is necessary to allow x to vary over the whole complex plane. This leads us to consider the four branches of $\phi'(x)$, which we denote by

$$\begin{aligned}
\phi_1'(x) &= \sqrt{\lambda + \sqrt{\lambda^2 - k(x)}}\,, && (4.101)\\
\phi_2'(x) &= \sqrt{\lambda - \sqrt{\lambda^2 - k(x)}}\,, && (4.102)\\
\phi_3'(x) &= -\sqrt{\lambda - \sqrt{\lambda^2 - k(x)}}\,, && (4.103)\\
\phi_4'(x) &= -\sqrt{\lambda + \sqrt{\lambda^2 - k(x)}}\,, && (4.104)
\end{aligned}$$

with $x \in \mathbb{C}$. Before we proceed further, we will make the simplifying assumption that $k(x)$ is of the form

$$k(x) \;=\; \kappa + l(x - x_0)^2\,, \tag{4.105}$$

where κ and l are both strictly positive. Thus, from the analysis on page 92, there are only nonzero solutions to (4.25)–(4.26) for $\lambda > k(x_0)^{1/2} = \sqrt{\kappa}$. This simplifies the

following algebra greatly without modifying the behaviour of the system. Thus

$$\phi_1'(x) = \sqrt{\lambda + \sqrt{\lambda^2 - \kappa - l(x-x_0)^2}}\,, \tag{4.106}$$

$$\phi_2'(x) = \sqrt{\lambda - \sqrt{\lambda^2 - \kappa - l(x-x_0)^2}}\,, \tag{4.107}$$

$$\phi_3'(x) = -\sqrt{\lambda - \sqrt{\lambda^2 - \kappa - l(x-x_0)^2}}\,, \tag{4.108}$$

$$\phi_4'(x) = -\sqrt{\lambda + \sqrt{\lambda^2 - \kappa - l(x-x_0)^2}}\,. \tag{4.109}$$

In order to analyse ϕ' in the complex plane, we need to identify the branch points of the function. In our case, these occur when the argument of a square-root term is zero. So, assuming that $\lambda \in \mathbb{R}^+$, we have branch points when

$$\lambda^2 - \kappa - l(x-x_0)^2 = 0\,, \tag{4.110}$$

and also when

$$\lambda + \sqrt{\lambda^2 - \kappa - l(x-x_0)^2} = 0\,, \tag{4.111}$$

$$\lambda - \sqrt{\lambda^2 - \kappa - l(x-x_0)^2} = 0\,. \tag{4.112}$$

Consider equation (4.110). Solving for x gives

$$x = x_0 \pm \sqrt{\frac{\lambda^2 - \kappa}{l}}\,, \tag{4.113}$$

which defines two branch points for each value of $\lambda \neq \sqrt{\kappa} = \lambda_c$. Thus we see that λ_c is the value of λ for which these branch points coincide. For equations (4.111)–(4.112) we find (squaring the equation) that

$$\lambda^2 = \lambda^2 - \kappa - l(x-x_0)^2 \tag{4.114}$$

$$\Rightarrow \qquad x = x_0 \pm \mathrm{i}\sqrt{\frac{\kappa}{l}}\,. \tag{4.115}$$

However, on substituting this back into equations (4.111)–(4.112) we find that it only satisfies the latter, implying that there are no values of x that satisfy equation (4.111).

Armed with this information we can proceed to describe the Riemann surface of the solution. The four solution sheets are numbered 1–4 as in equations (4.106)–(4.109). The branch points that link sheets 1 and 2 are located at x given by equation (4.113). The branch points that link sheets 3 and 4 are also located here. Meanwhile sheets 2 and 3 are linked by branch points located at x given in equation (4.115).

The branch cuts linking sheets 2 and 3 are assumed to follow a path parallel to the imaginary axis from each branch point in equation (4.115) to infinity. On the other hand, the other two sets of branch cuts, connecting sheets 1 and 2, and sheets

3 and 4, emanate from the branch points in equation (4.113) and proceed to infinity along the path of a hyperbola, for ease of computation. The hyperbola is defined by the equation

$$\left(\Re(x-x_0)\right)^2 - \left(\Im(x-x_0)\right)^2 \;=\; \frac{\lambda^2-\kappa}{l} \tag{4.116}$$

in the complex plane. A plot of these branch cuts can be seen in Figures 4.6 and 4.7, for the values

$$\kappa \;=\; l \;=\; 1\,, \qquad\qquad x_0 \;=\; 0\,, \tag{4.117}$$

and where λ takes the values 0.9 and 1.3 respectively. While there are no non-trivial solutions to (4.25)–(4.26) in the former case, we include it here for completeness. A representation of the Riemann surface can be seen in Figure 4.8, taking a cross-section along a line parallel to the real axis with $\Im x < -\sqrt{\kappa/l}$. In the diagram the sheets are numbered 1 to 4, from top to bottom.

Given any two solutions $w_i(x)$, we can now find the turning points and the Stokes and anti-Stokes lines that give the relative dominance of these solutions. Because the turning points are the same as the branch points, we find that there are turning points only between sheets 1 and 2, sheets 2 and 3, and sheets 3 and 4. Moreover, the families of Stokes and anti-Stokes lines for solutions w_1 and w_2, and for solutions w_3 and w_4, coincide. The results for representative values of $\lambda \lessgtr \lambda_{\rm c}$ are shown in Figures 4.9 and 4.10. The solid thick black lines are branch cuts (the branch cuts from $x = x_0 \pm \mathrm{i}\sqrt{\kappa/l}$ are omitted for clarity). The remaining solid lines are Stokes lines while anti-Stokes lines are broken lines on the plot; the thin red lines refer to the Stokes and anti-Stokes lines for solutions w_2 and w_3, and the thick green lines to those for solutions w_1 and w_2 (and also for solutions w_3 and w_4). The values of the constants are as given for Figures 4.6 and 4.7.

Next we will proceed to interpret the Stokes diagrams in order to predict the behaviour of the asymptotic solution to (4.25) along the real line, assuming as before that $\lambda > \lambda_{\rm c} = \sqrt{\kappa}$. We will consider the dominance of each of the solutions w_i with respect to the others. Taking any two solutions, recall that in regions delimited by anti-Stokes lines (and branch cuts), one solution is going to be exponentially dominant over the other. Consider first the relative dominance of w_1 and w_2. The anti-Stokes lines for these two solutions are shown as the thick green broken lines on Figure 4.10. We can find the relative dominance along the real axis as $\Re x \to \pm\infty$ by considering the behaviour of $\Im(\phi_1' - \phi_2')$. For $\Re x > x_0 + \sqrt{(\lambda^2-\kappa)/l}$ we have $\Im(\phi_1' - \phi_2') < 0$ and decreasing to $-\infty$ as $\Re x$ increases. Similarly, for $\Re x < x_0 - \sqrt{(\lambda^2-\kappa)/l}$ we have

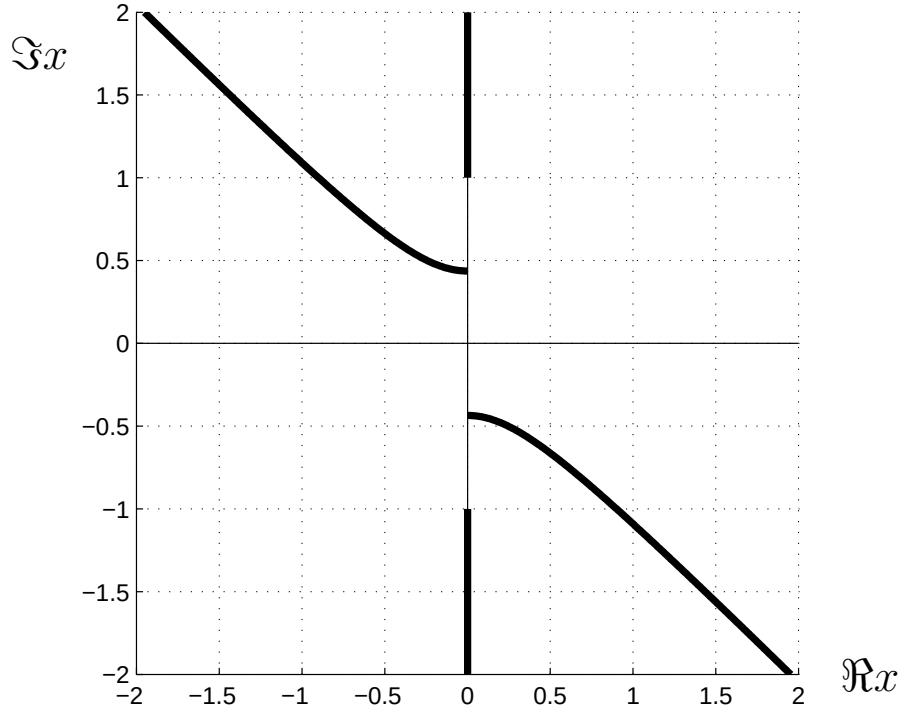

Figure 4.6: The branch cuts of $\phi(x)$ when $\lambda < \lambda_c$.

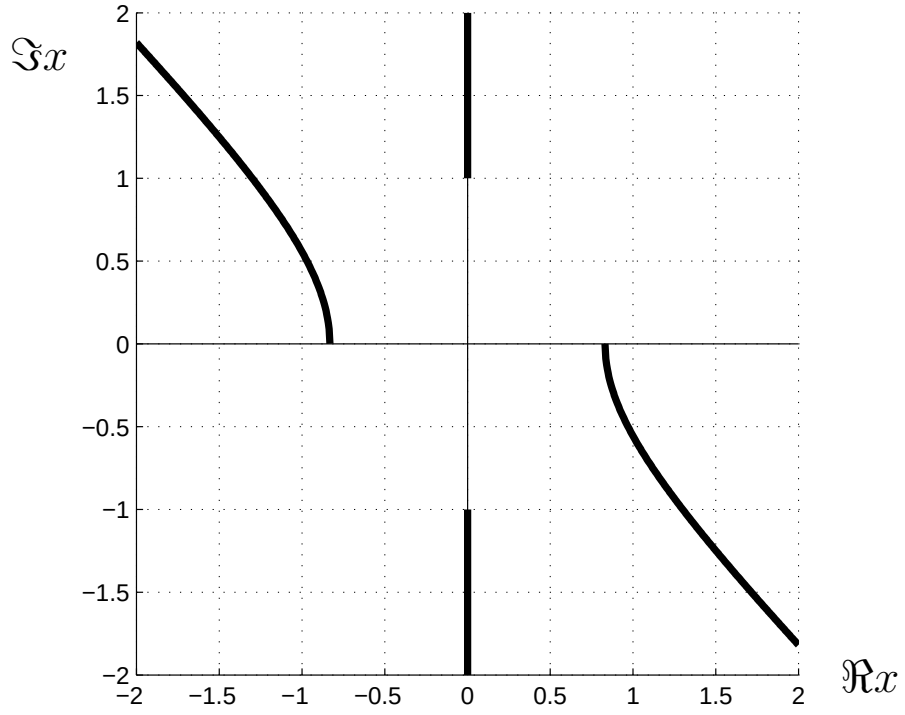

Figure 4.7: The branch cuts of $\phi(x)$ when $\lambda > \lambda_c$.

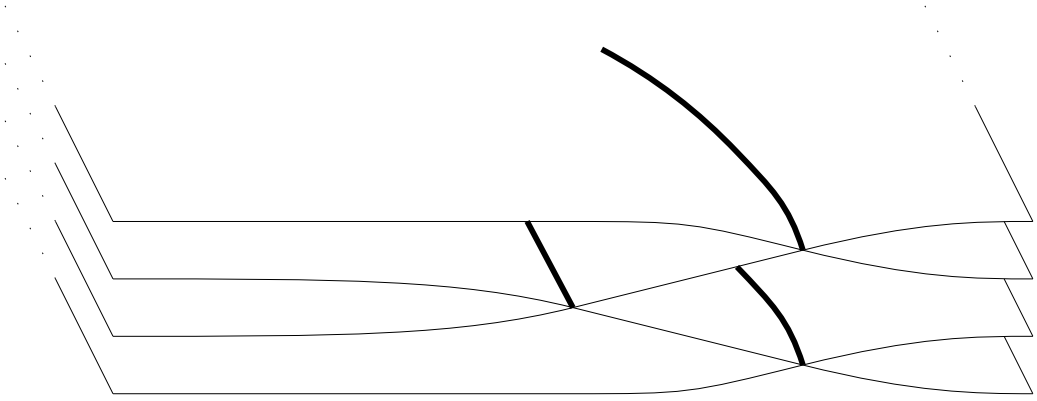

Figure 4.8: A pictorial representation of the Riemann surface of $\phi(x)$.

$\Im(\phi_1' - \phi_2') < 0$, decreasing to $-\infty$ as $\Re x \to -\infty$. Thus by equation (4.80),

$$\frac{w_1}{w_2} \to \infty \qquad \text{exponentially as } \Re x \to \infty \,, \tag{4.118}$$

$$\frac{w_1}{w_2} \to 0 \qquad \text{exponentially as } \Re x \to -\infty \,. \tag{4.119}$$

Knowing the relative dominance of w_1 and w_2 in two of the regions delimited by anti-Stokes lines allows us to determine the relative dominance in the whole of the complex plane, by realising that on traversing anti-Stokes lines the relative dominance switches.

In addition, knowledge of the relative dominance of w_1 and w_2 gives us the relative dominance of w_3 and w_4, given that

$$\phi_3' = -\phi_2' \,, \tag{4.120}$$

$$\phi_4' = -\phi_1' \,, \tag{4.121}$$

by equations (4.106)–(4.109). Thus, where w_1 is dominant over w_2, we also have w_3 dominant over w_4. Therefore, from Figure 4.10 we can divide the complex plane into two types of region:

- A: $w_1 \gg w_2$ and $w_3 \gg w_4$,
- B: $w_2 \gg w_1$ and $w_4 \gg w_3$.

The regions are shown in Figure 4.11.

To find the relative dominance of w_2 and w_3 we use the same process, namely by finding the behaviour of $\Im(\phi_2' - \phi_3')$ as $\Re x$ tends to $\pm\infty$. However,

$$\Im(\phi_2' - \phi_3') = 2\Im\phi_2' \tag{4.122}$$

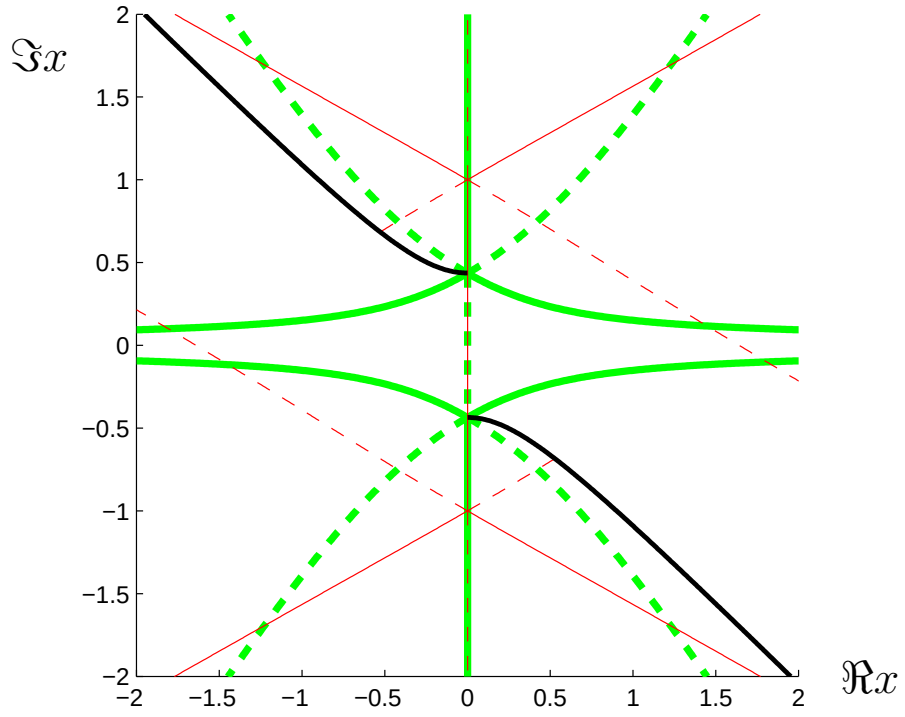

Figure 4.9: The Stokes diagram for $\phi(x)$ when $\lambda < \lambda_c$.

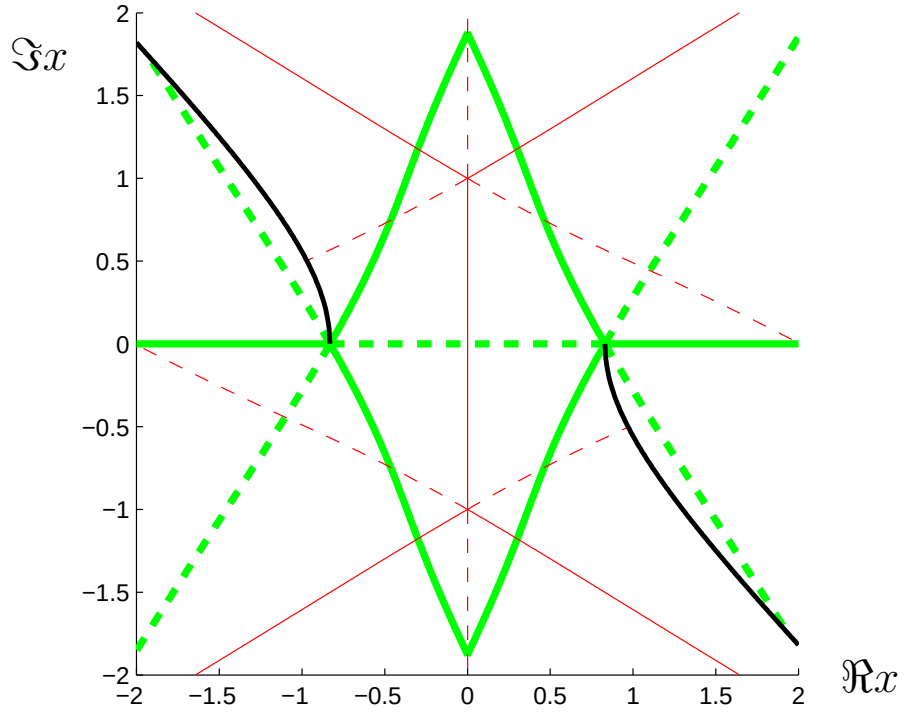

Figure 4.10: The Stokes diagram for $\phi(x)$ when $\lambda > \lambda_c$.

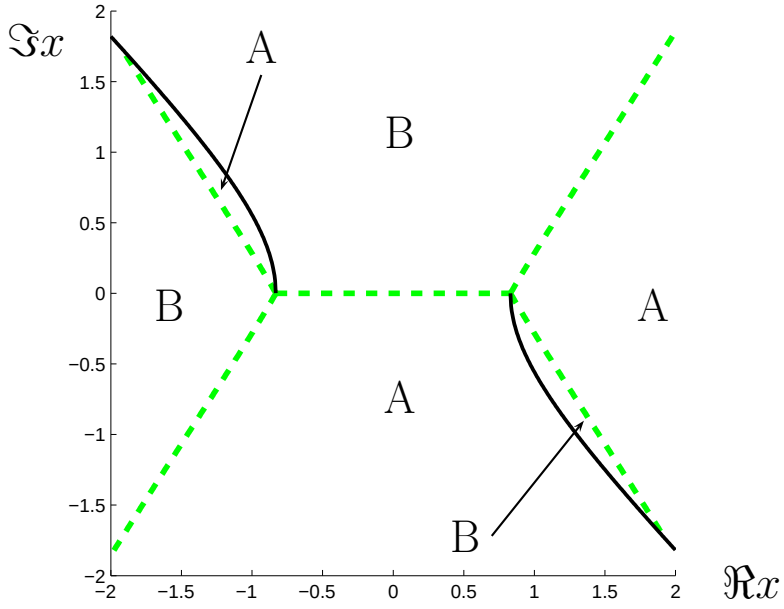

Figure 4.11: Regions of dominance for w_1 and w_2.

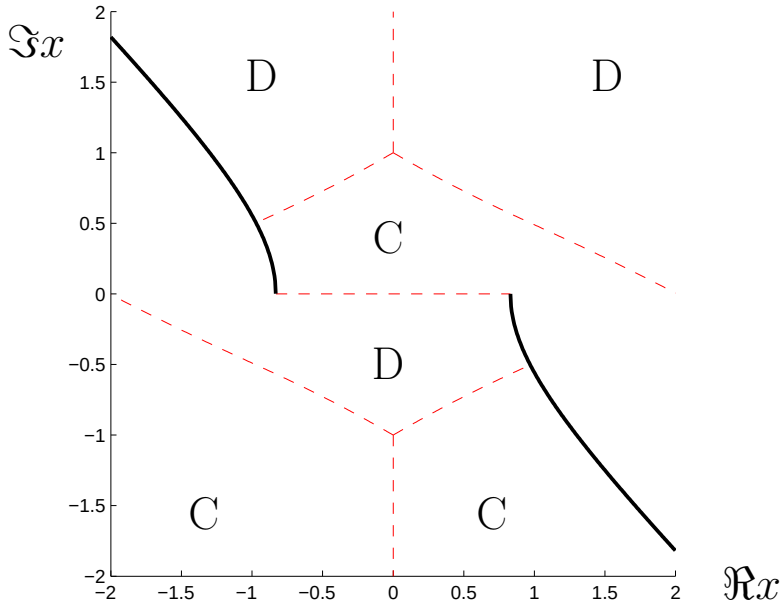

Figure 4.12: Regions of dominance for w_2 and w_3.

by equation (4.120), and $\Im\phi_2' \to +\infty$ as $\Re x \to \pm\infty$. This gives us the relative dominance of w_2 and w_3 in those limits, and hence (by considering the anti-Stokes lines) in the whole complex plane. The regions are shown in Figure 4.12, where the two regions are

- C: $w_2 \gg w_3$,
- D: $w_3 \gg w_2$,

recalling that there are branch cuts following the anti-Stokes lines on the imaginary axis from the turning points to infinity.

We are interested in the form of the solution w along the real axis. As stated earlier, in each Stokes region we will have a different asymptotic formula for w. In our case the different formulae will be different combinations of the four solutions w_i.

Consider Figures 4.10 and 4.11. Along the segment of the real line from $-\infty$ to $x_0 - \sqrt{(\lambda^2 - \kappa)/l}$, which we will denote (I), we have that w_2 and w_4 are dominant respectively over w_1 and w_3. Thus along (I) the solution must be a combination of the solutions w_1 and w_3, since we want the solution to decay at $-\infty$. For the same reason, the solution in (III), which is the segment of the real line from $x_0 + \sqrt{(\lambda^2 - \kappa)/l}$ to $+\infty$, the solution must be formed from the subdominant solutions w_2 and w_4. The region (II), along the real line between the values $x_0 \pm \sqrt{(\lambda^2 - \kappa)/l}$, must contain some combination of all four of the solutions, where the coefficients are dependent on the coefficients in regions (I) and (III).

With reference to Figure 4.10, we need to mention the Stokes line which crosses the real axis at $x = x_0$. Recall that on crossing a Stokes line, the coefficient of the subdominant solution is changed. By Figures 4.11 and 4.12, the four solutions are in balance along this section of the real axis. Thus, in order to analyse the behaviour of the full solution on crossing the Stokes line we must deform the contour slightly. Two paths, denoted P and Q, are shown in Figure 4.13; P is above the real axis while Q is below. Suppose that to the left of the Stokes line the solution is given by

$$w = C_1 w_1 + C_2 w_2 + C_3 w_3 + C_4 w_4 \,. \tag{4.123}$$

On traversing the Stokes line along path P, the solution w_2 is dominant over solution w_3, by Figure 4.12. Thus on crossing this line with all four solutions present, the dominant solution w_2 would modify the coefficient of the solution w_3. Conversely, along path Q the dominance is reversed, meaning that along this path it is the solution w_2 that is modified. Thus, to the right of the Stokes line we have the two solutions

$$L = C_1 w_1 + C_2 w_2 + \widetilde{C}_3 w_3 + C_4 w_4 \,, \tag{4.124}$$

$$R = C_1 w_1 + \widetilde{C}_2 w_2 + C_3 w_3 + C_4 w_4 \,, \tag{4.125}$$

where $\widetilde{C}_i \neq C_i$ for $i = 2, 3$. There is an obvious discrepancy between the solutions following the two paths, and thus we must conclude that the Stokes line in question is an *inactive* Stokes line. In other words, it satisfies the condition (4.62) but the asymptotic solutions of the equation in question either side of the line coincide.

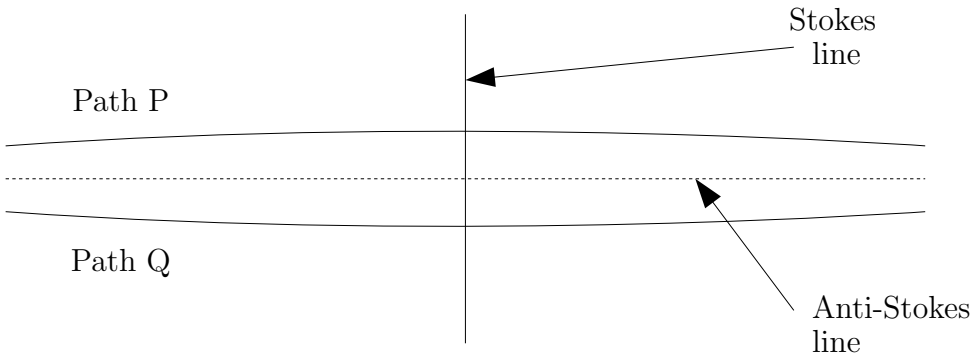

Figure 4.13: Paths for analysis of the Stokes line crossing $x = x_0$ in Figure 4.10.

The fact that this Stokes line is inactive means that there is no interaction between the two pairs of solutions $\{w_1, w_2\}$ and $\{w_3, w_4\}$. Thus, on analysing the full problem in the three regions (I)–(III), we can consider *either* the pair $\{w_1, w_2\}$ or $\{w_3, w_4\}$ for the eigenvalue calculation. The structure of the Stokes diagram for either of these pairs is that of the harmonic oscillator, so effectively we have two decoupled harmonic oscillator problems.

However, making the same calculation as for the harmonic oscillator is rather unwieldy, so we can take advantage of the fact that we are only interested in the *lowest* eigenvalue λ, in which case the turning points are positioned close together. This fact allows us to consider a local problem for the critical stress and resulting buckling pattern, which will be easier to apply to other related problems — such as the shell buckling problem of Chapter 3. This local problem should give us a solution related to the harmonic oscillator problem, given the similarities in their Stokes diagrams.

4.3.3 A general method of solution

Consider the beam equation, with the simplified foundation stiffness $k(x)$ given by equation (4.105),

$$\varepsilon^4 w'''' + 2\lambda\varepsilon^2 w'' + \left(\kappa + l(x - x_0)^2\right) w \;=\; 0\,. \tag{4.126}$$

Without loss of generality we can consider $x_0 = 0$, and we know that buckling will occur around this value of x. Therefore scale

$$x \;=\; \varepsilon^{\alpha}\bar{x} \tag{4.127}$$

to find

$$\varepsilon^{4(1-\alpha)}w'''' + 2\lambda\varepsilon^{2(1-\alpha)}w'' + \left(\kappa + l\varepsilon^{2\alpha}\bar{x}^2\right)w \;=\; 0\,, \tag{4.128}$$

where $'$ corresponds to differentiation with respect to $\bar{x}$. Matching terms gives $\alpha = 1$, and

$$w'''' + 2\lambda w'' + \kappa w \;=\; 0\,. \tag{4.129}$$

Subsitution of $w = \mathrm{e}^{m\bar{x}}$ gives

$$m^4 + 2\lambda m^2 + \kappa \;=\; 0\,, \tag{4.130}$$

or

$$m^2 \;=\; -\lambda \pm \sqrt{\lambda^2 - \kappa}\,. \tag{4.131}$$

This quantity has a double root at $\lambda = \sqrt{\kappa}$. But as we saw earlier, this is the critical value of λ at which the system undergoes a bifurcation. In other words, the two turning points coalesce at $x = x_0 = 0$ and move apart along the real axis. Thus the leading-order value of the buckling parameter λ is $\sqrt{\kappa}$, with a small correction since λ must be *greater* than λ_{c} for a buckling pattern to emerge. So we set

$$\lambda \;=\; \sqrt{\kappa} + \varepsilon^{\beta}\lambda_1 \tag{4.132}$$

for some unknown (as yet) exponent β, and then the exponent m becomes

$$m \;=\; \pm\mathrm{i}\kappa^{1/4} \tag{4.133}$$

at leading order. Thus, one possible solution of equation (4.129) is

$$w \;=\; \exp\left(\frac{\mathrm{i}\kappa^{1/4}x}{\varepsilon}\right)\,, \tag{4.134}$$

in terms of x rather than $\bar{x}$. This will be the leading order behaviour of w near $x = 0$.

We now wish to find the envelope of this oscillatory buckling pattern. To do this, we write

$$w \;=\; \exp\left(\frac{\mathrm{i}\kappa^{1/4}x}{\varepsilon}\right) f(x) \tag{4.135}$$

from equation (4.134). Substituting this and (4.132) into equation (4.126), we find that

$$\begin{aligned}\varepsilon^4 f'''' + 4\mathrm{i}\varepsilon^3\kappa^{1/4} f''' + (-4\varepsilon^2\sqrt{\kappa} + 2\varepsilon^{2+\beta}\lambda_1) f'' \\ +4\mathrm{i}\varepsilon^{1+\beta}\lambda_1\kappa^{1/4} f' + (lx^2 - 2\varepsilon^\beta\sqrt{\kappa}\lambda_1) f &= 0\,. \end{aligned} \tag{4.136}$$

We need to search on a scale intermediate between $x = O(1)$ and the $x = O(\varepsilon)$ scale which gave us the oscillatory pattern. Setting

$$x = \varepsilon^\gamma \widehat{x}\,, \tag{4.137}$$

we find that

$$\begin{aligned}\varepsilon^{4-4\gamma} f'''' + 4\mathrm{i}\varepsilon^{3-3\gamma}\kappa^{1/4} f''' + (-4\varepsilon^{2-2\gamma}\sqrt{\kappa} + 2\varepsilon^{2+\beta-2\gamma}\lambda_1) f'' \\ +4\mathrm{i}\varepsilon^{1+\beta-\gamma}\lambda_1\kappa^{1/4} f' + (\varepsilon^{2\gamma} l\widehat{x}^2 - 2\varepsilon^\beta\sqrt{\kappa}\lambda_1) f &= 0\,, \end{aligned} \tag{4.138}$$

where a prime now denotes differentiation with respect to $\widehat{x}$. We match the largest term in the coefficient of f'' together with both terms in the coefficient of f, or

$$2 - 2\gamma = 2\gamma = \beta\,, \tag{4.139}$$

giving

$$\gamma = \frac{1}{2}\,, \qquad \beta = 1\,, \tag{4.140}$$

with the leading order equation

$$f'' + \left(\frac{\lambda_1}{2} - \frac{l\widehat{x}^2}{4\sqrt{\kappa}}\right) f = 0\,. \tag{4.141}$$

Now if we rescale

$$\widehat{x} = \frac{\sqrt{2}\kappa^{1/8}}{l^{1/4}}\widetilde{x}\,, \tag{4.142}$$

$$\lambda_1 = \frac{\sqrt{l}}{\kappa^{1/4}}\Lambda\,, \tag{4.143}$$

we obtain the equation

$$f'' + (\Lambda - \widetilde{x}^2) f = 0\,, \tag{4.144}$$

which is the equation for the harmonic oscillator, for which the *exact* solutions are given by equations (4.90) and (4.91). In terms of $\widehat{x}$,

$$\lambda_1 = \frac{\sqrt{l}}{\kappa^{1/4}}(2n+1)\,, \tag{4.145}$$

$$f = \exp\left(-\frac{\sqrt{l}}{4\kappa^{1/4}}\widehat{x}^2\right) H_n\left(\frac{l^{1/4}}{\sqrt{2}\kappa^{1/8}}\widehat{x}\right)\,. \tag{4.146}$$

By equations (4.132), (4.135) and (4.137), we find that

$$w = \exp\left[\frac{1}{\varepsilon}\left(\mathrm{i}\kappa^{1/4}x - \frac{\sqrt{l}x^2}{4\kappa^{1/4}}\right)\right] H_n\left(\frac{l^{1/4}x}{\sqrt{2\varepsilon}\kappa^{1/8}}\right) , \tag{4.147}$$

$$\lambda = \sqrt{\kappa} + \frac{\varepsilon(2n+1)\sqrt{l}}{\kappa^{1/4}} . \tag{4.148}$$

This corresponds exactly to Coman's results given earlier. Effectively the solution is highly oscillatory, modulated by a function which is given by the solutions to the harmonic oscillator eigenvalue problem.

We now therefore have a general mechanism for taking a problem similar to the beam on a substrate of variable stiffness, and reducing it to the harmonic oscillator problem. Briefly:

- We obtain the Euler–Lagrange equation.
- To find the oscillation wavelength we substitute $x = \varepsilon^{\alpha}\bar{x}$ where x is the independent variable of the equation.
- We find the leading order equation by matching leading order terms and finding α, giving us a solution $w_0(\bar{x})$. The leading order λ, given by λ_0, is found by choosing the value of λ in this equation so that two roots coincide.
- We substitute $w = w_0(\bar{x})f(x)$ into the Euler–Lagrange equation.
- We set $\lambda = \lambda_0 + \varepsilon^{\beta}\lambda_1$ and $x = \varepsilon^{\gamma}\widehat{x}$. By judicious choice of β and γ we obtain an equation that can be scaled to give an eigenvalue problem for the amplitude f.
- The buckling pattern is then given by $w = w_0(\bar{x})f(x)$, where $f(x)$ and the correction λ_1 to the critical parameter λ are given by the solution to the eigenvalue problem for f.

4.4 Application to the shell problem

We now attempt to apply the solution method found in the previous section to the problem given in Chapter 3. Firstly, we need to find the Euler–Lagrange equation for the energy integral ΔW_2 defined in equation (3.20) in terms of three integrals $\mathscr{I}_i$

given by equations (3.133), (3.163) and (3.204). Combining these gives

$$\begin{aligned}\Delta W_2 &= \iint_{\text{shell}} \left\{ \frac{q_\infty}{2} \left(p_0 P_0^{(0)}(\mu) + p_2 P_2^{(0)}(\mu) \right) (1-\mu^2) \left(\frac{\mathrm{d}w}{\mathrm{d}\mu} \right)^2 \right. \\ &\quad + \frac{hG_{\mathrm{s}}}{1-\nu_{\mathrm{s}}} \left[\left(\nabla^2\psi - (1+\nu_{\mathrm{s}}) \frac{w}{\widehat{R}} \right)^2 + (1-\nu_{\mathrm{s}}^2) \frac{w^2}{\widehat{R}^2} + \frac{h^2}{12} (\nabla^2 w)^2 \right] \\ &\quad \left. - \frac{1}{2} \tau_{RR}(w,\psi) w + \frac{\sqrt{1-\mu^2}}{2\widehat{R}} \tau_{R\theta}(w,\psi) \frac{\partial \psi}{\partial \mu} \right\} \mathrm{d}S \,, \end{aligned} \tag{4.149}$$

assuming that the traction terms are evaluated on the mid-surface of the shell rather than the outer surface. Finding the Euler–Lagrange equations for this energy functional is not a simple task. One simplifiation that can be made is to suppose that

$$\psi = 0 \,, \tag{4.150}$$

which is equivalent to assuming that $v_\theta = 0$, meaning that we consider only radial displacements w of the shell. This can be motivated by looking at the numerical results of Chapter 3, which show that the ratio v_θ / w tends to zero in the limit $h/\widehat{R} \to 0$. We obtain

$$\begin{aligned}\Delta W_2 &= \iint_{\text{shell}} \left\{ \frac{q_\infty}{2} \left(p_0 P_0^{(0)}(\mu) + p_2 P_2^{(0)}(\mu) \right) (1-\mu^2) \left(\frac{\mathrm{d}w}{\mathrm{d}\mu} \right)^2 \right. \\ &\quad \left. + \frac{hG_{\mathrm{s}}}{1-\nu_{\mathrm{s}}} \left[2(1+\nu_{\mathrm{s}}) \frac{w^2}{\widehat{R}^2} + \frac{h^2}{12} (\nabla^2 w)^2 \right] - \frac{1}{2} \tau_{RR}(w) w \right\} \mathrm{d}S \,. \end{aligned} \tag{4.151}$$

However, there is still one complicating factor. The one stress component remaining, τ_{RR}, can not be found *explicitly* in terms of w (and ψ), which is why we found the stress component as an expansion in Legendre polynomials in Chapter 3. However, once we look at the limit of a highly-oscillatory displacement pattern, it becomes possible to find an asymptotic expression for the stress component. This will be analysed next.

4.4.1 WKB analysis of the Navier equations

Recall that in the limit being considered, the region over which buckling occurs becomes smaller. Thus, as shown in Figure 4.14, we can consider the region over which buckling occurs as a half-space. The displacement components (u, v) in the elastic medium then satisfy the equations of plane strain, which are the Navier equations,

$$(\lambda + 2G) \frac{\partial^2 u}{\partial x^2} + G \frac{\partial^2 u}{\partial y^2} + (\lambda + G) \frac{\partial^2 v}{\partial x \partial y} = 0 \,, \tag{4.152}$$

$$G \frac{\partial^2 v}{\partial x^2} + (\lambda + 2G) \frac{\partial^2 v}{\partial y^2} + (\lambda + G) \frac{\partial^2 u}{\partial x \partial y} = 0 \,, \tag{4.153}$$

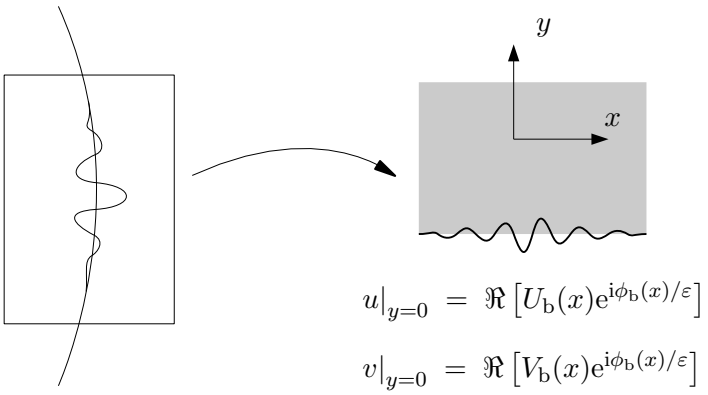

Figure 4.14: Approximation of the buckling region by a half-space.

where the material constants take their value in the matrix.

Now, as the wavelength of the buckling pattern is assumed to be small, we may consider the case where the displacement boundary conditions at the boundary of the half-space are given by modulated highly-oscillatory functions,

$$u|_{y=0} = \Re\left[\left(U_{\mathrm{b}}^0(x) + \varepsilon U_{\mathrm{b}}^1(x) + \cdots\right)\mathrm{e}^{\mathrm{i}\phi_{\mathrm{b}}(x)/\varepsilon}\right] , \tag{4.154}$$

$$v|_{y=0} = \Re\left[\left(V_{\mathrm{b}}^0(x) + \varepsilon V_{\mathrm{b}}^1(x) + \cdots\right)\mathrm{e}^{\mathrm{i}\phi_{\mathrm{b}}(x)/\varepsilon}\right] , \tag{4.155}$$

where we have expanded the modulating functions U_{b} and V_{b} in asymptotic series. The displacements and stresses in the half-space, in the limit $\varepsilon \to 0$, can be found by substituting the WKB ansatz

$$u = U(x,y)\mathrm{e}^{\mathrm{i}\phi(x,y)/\varepsilon} , \tag{4.156}$$

$$v = V(x,y)\mathrm{e}^{\mathrm{i}\phi(x,y)/\varepsilon} \tag{4.157}$$

into the Navier equations (4.152)–(4.153), where[5]

$$U(x,y) = \frac{1}{\varepsilon}U_0(x,y) + U_1(x,y) + \varepsilon U_2(x,y) + O(\varepsilon^2) , \tag{4.158}$$

$$V(x,y) = \frac{1}{\varepsilon}V_0(x,y) + V_1(x,y) + \varepsilon V_2(x,y) + O(\varepsilon^2) . \tag{4.159}$$

[5]The scaling of the first term with $1/\varepsilon$ is made with the benefit of hindsight. Had we set the leading order term to be $O(1)$, we would not be able to match the terms to the boundary conditions.

We obtain

$$\begin{aligned}
u_{xx} &= \left\{ -\frac{\phi_x^2}{\varepsilon^3} U_0 + \frac{1}{\varepsilon^2}\left[-\phi_x^2 U_1 + 2\mathrm{i}\phi_x U_{0x} + \mathrm{i}\phi_{xx} U_0 \right] \right. \\
&\qquad \left. + \frac{1}{\varepsilon}\left[-\phi_x^2 U_2 + 2\mathrm{i}\phi_x U_{1x} + \mathrm{i}\phi_{xx} U_1 + U_{0xx} \right] + O(1) \right\} \mathrm{e}^{\mathrm{i}\phi/\varepsilon} \,, \qquad (4.160) \\
u_{xy} &= \left\{ -\frac{\phi_x \phi_y}{\varepsilon^3} U_0 + \frac{1}{\varepsilon^2}\left[-\phi_x \phi_y U_1 + \mathrm{i}\phi_x U_{0y} + \mathrm{i}\phi_y U_{0x} + \mathrm{i}\phi_{xy} U_0 \right] \right. \\
&\qquad \left. + \frac{1}{\varepsilon}\left[-\phi_x \phi_y U_2 + \mathrm{i}\phi_x U_{1y} + \mathrm{i}\phi_y U_{1x} + \mathrm{i}\phi_{xy} U_1 + U_{0xy} \right] + O(1) \right\} \mathrm{e}^{\mathrm{i}\phi/\varepsilon} \,, \qquad (4.161) \\
u_{yy} &= \left\{ -\frac{\phi_y^2}{\varepsilon^3} U_0 + \frac{1}{\varepsilon^2}\left[-\phi_y^2 U_1 + 2\mathrm{i}\phi_y U_{0y} + \mathrm{i}\phi_{yy} U_0 \right] \right. \\
&\qquad \left. + \frac{1}{\varepsilon}\left[-\phi_y^2 U_2 + 2\mathrm{i}\phi_y U_{1y} + \mathrm{i}\phi_{yy} U_1 + U_{0yy} \right] + O(1) \right\} \mathrm{e}^{\mathrm{i}\phi/\varepsilon} \,, \qquad (4.162)
\end{aligned}$$

and equivalent formulae for v_{xx}, v_{xy} and v_{yy}.

These are substituted into Navier's equations, and to leading order we find that the two equations can be written as

$$\begin{bmatrix} (\lambda+2G)\phi_x^2 + G\phi_y^2 & (\lambda+G)\phi_x\phi_y \\ (\lambda+G)\phi_x\phi_y & G\phi_x^2 + (\lambda+2G)\phi_y^2 \end{bmatrix} \begin{bmatrix} U_0 \\ V_0 \end{bmatrix} = 0 \,. \qquad (4.163)$$

We require a non-trivial solution, so the determinant of the matrix on the left is set to zero. This results in the equation

$$\begin{aligned}
G(\lambda+2G)\left(\phi_x^2+\phi_y^2\right)^2 &= 0 \qquad (4.164) \\
\Rightarrow \qquad \phi_x^2+\phi_y^2 &= 0 \,. \qquad (4.165)
\end{aligned}$$

Now, in order to solve this equation we recall the boundary conditions at $y = 0$, (4.154)–(4.155), together with the requirement that the elastic displacement decays to zero as $y \to \infty$. This tells us that we must solve equation (4.165) with the conditions

$$\begin{aligned}
\phi(x,0) &= \phi_{\mathrm{b}}(x) \,, \qquad (4.166) \\
\Im\phi(x,y) &\to +\infty \qquad \text{as } y \to \infty \,. \qquad (4.167)
\end{aligned}$$

The solution becomes

$$\phi(x,y) = \phi_{\mathrm{b}}(x + \mathrm{i}ay) \,, \qquad (4.168)$$

where $a = \pm 1$ is chosen in order to satisfy equation (4.167). We substitute the resulting fact that

$$\phi_y = \mathrm{i}a\phi_x \qquad (4.169)$$

into equation (4.163) to find that

$$V_0 \;=\; \mathrm{i}aU_0\;. \tag{4.170}$$

We now proceed to the next order in the Navier equations, using equations (4.169) and (4.170) to simplify the resulting expressions. The two equations are found to be multiples of each other, both equivalent to

$$\frac{\partial U_0}{\partial x}+\mathrm{i}a\frac{\partial U_0}{\partial y} \;=\; -\mathrm{i}\frac{(\lambda+G)\phi_x}{(\lambda+3G)}(U_1+\mathrm{i}aV_1)\;. \tag{4.171}$$

The same process occurs at the third order in the Navier equations, resulting in the two equations

$$\begin{aligned}(\lambda+G)\phi_x^2(U_2+\mathrm{i}aV_2) \;=\;& (\lambda+G)a\phi_{xy}(U_1+\mathrm{i}aV_1)+(\lambda+2G)U_{0xx}+GU_{0yy}\\ &+\mathrm{i}a(\lambda+G)U_{0xy}+2\mathrm{i}(\lambda+2G)\phi_x\frac{\partial U_1}{\partial x}-2aG\phi_x\frac{\partial U_1}{\partial y}\\ &+\mathrm{i}(\lambda+G)\phi_x\frac{\partial V_1}{\partial y}-a(\lambda+G)\phi_x\frac{\partial V_1}{\partial x}\;, \end{aligned}\tag{4.172}$$

$$\begin{aligned}\mathrm{i}a(\lambda+G)\phi_x^2(U_2+\mathrm{i}aV_2) \;=\;& \mathrm{i}(\lambda+G)\phi_{xy}(U_1+\mathrm{i}aV_1)+\mathrm{i}aGU_{0xx}+\mathrm{i}a(\lambda+2G)U_{0yy}\\ &+(\lambda+G)U_{0xy}+2G\mathrm{i}\phi_x\frac{\partial V_1}{\partial x}-2a(\lambda+2G)\phi_x\frac{\partial V_1}{\partial y}\\ &+\mathrm{i}(\lambda+G)\phi_x\frac{\partial U_1}{\partial y}-a(\lambda+G)\phi_x\frac{\partial U_1}{\partial x}\;. \end{aligned}\tag{4.173}$$

These equations must be consistent, so that the right-hand side of the first equation added to ia times the right-hand side of the second equation must be zero. This eventually gives us another equation,

$$(\lambda+G)\left(\frac{\partial}{\partial x}+\mathrm{i}a\frac{\partial}{\partial y}\right)^2U_0+\mathrm{i}(\lambda+3G)\phi_x\left(\frac{\partial}{\partial x}+\mathrm{i}a\frac{\partial}{\partial y}\right)(U_1+\mathrm{i}aV_1) \;=\; 0\;. \tag{4.174}$$

Substituting for $U_{0x}+\mathrm{i}aU_{0y}$ from equation (4.171), we find that

$$\left(\frac{\partial}{\partial x}+\mathrm{i}a\frac{\partial}{\partial y}\right)(U_1+\mathrm{i}aV_1) \;=\; 0\;. \tag{4.175}$$

Now define

$$\xi \;=\; \mathrm{i}ay-x\;, \tag{4.176}$$

$$\eta \;=\; \mathrm{i}ay+x\;, \tag{4.177}$$

so that equation (4.175) becomes

$$\frac{\partial}{\partial\xi}(U_1+\mathrm{i}aV_1) \;=\; 0\;, \tag{4.178}$$

which we solve to get

$$U_1 + \mathrm{i}aV_1 \;=\; f(\eta)\;, \tag{4.179}$$

where $f(\eta)$ is an arbitrary function. We substitute this result into equation (4.171) to find

$$\left(\frac{\partial}{\partial x} + \mathrm{i}a\frac{\partial}{\partial y}\right) U_0 \;=\; -\mathrm{i}\frac{(\lambda+G)\phi_x}{(\lambda+3G)} f(\eta)\;. \tag{4.180}$$

Now, we have

$$\phi \;=\; \phi_{\mathrm{b}}(x+\mathrm{i}ay) \;=\; \phi_{\mathrm{b}}(\eta)\;, \tag{4.181}$$

so that the equation (4.180) becomes

$$-2\frac{\partial U_0}{\partial \xi} \;=\; -\mathrm{i}\frac{(\lambda+G)\phi'_{\mathrm{b}}(\eta) f(\eta)}{(\lambda+3G)} \tag{4.182}$$

$$\Rightarrow \qquad U_0 \;=\; \frac{\mathrm{i}\xi(\lambda+G)\phi'_{\mathrm{b}}(\eta) f(\eta)}{2(\lambda+3G)} + g(\eta)\;. \tag{4.183}$$

We can then find V_0 by equation (4.170).

Finally we will need to analyse the fourth order term in the Navier equations. We have

$$\begin{aligned}(\lambda+G)\phi_x^2(U_3+\mathrm{i}aV_3) \;=\;& (\lambda+G)a\phi_{xy}(U_2+\mathrm{i}aV_2) + (\lambda+2G)U_{1xx} + GU_{1yy} \\ &+(\lambda+G)V_{1xy} + 2\mathrm{i}(\lambda+2G)\phi_x\frac{\partial U_2}{\partial x} - 2aG\phi_x\frac{\partial U_2}{\partial y} \\ &+\mathrm{i}(\lambda+G)\phi_x\frac{\partial V_2}{\partial y} - a(\lambda+G)\phi_x\frac{\partial V_2}{\partial x}\;, \end{aligned} \tag{4.184}$$

$$\begin{aligned}\mathrm{i}a(\lambda+G)\phi_x^2(U_3+\mathrm{i}aV_3) \;=\;& \mathrm{i}(\lambda+G)\phi_{xy}(U_2+\mathrm{i}aV_2) + GV_{1xx} + (\lambda+2G)V_{1yy} \\ &+(\lambda+G)U_{1xy} + 2G\mathrm{i}\phi_x\frac{\partial V_2}{\partial x} - 2a(\lambda+2G)\phi_x\frac{\partial V_2}{\partial y} \\ &+\mathrm{i}(\lambda+G)\phi_x\frac{\partial U_2}{\partial y} - a(\lambda+G)\phi_x\frac{\partial U_2}{\partial x}\;. \end{aligned} \tag{4.185}$$

In a similar manner to the process at the third order, we take ia times the second equation and add it to the first, obtaining the equation

$$\begin{aligned}&(\lambda+2G)U_{1xx} + \mathrm{i}a(\lambda+G)U_{1xy} + GU_{1yy} + \mathrm{i}aGV_{1xx} + (\lambda+G)V_{1xy} \\ &\quad +\mathrm{i}a(\lambda+2G)V_{1yy} + \mathrm{i}\phi_x(\lambda+3G)\left(\frac{\partial}{\partial x} + \mathrm{i}a\frac{\partial}{\partial y}\right)(U_2+\mathrm{i}aV_2) \;=\; 0\;. \end{aligned} \tag{4.186}$$

Substituting for V_1 from equation (4.179), and changing to coordinates ξ, η, we find that

$$4(\lambda+G)\frac{\partial^2 U_1}{\partial \xi^2} - 2\mathrm{i}\phi_x(\lambda+3G)\frac{\partial}{\partial \xi}(U_2+\mathrm{i}aV_2) \;=\; 0 \tag{4.187}$$

$$\Rightarrow \qquad \frac{\partial U_1}{\partial \xi} \;=\; \frac{\mathrm{i}\phi_x}{2}\left(\frac{\lambda+3G}{\lambda+G}\right)(U_2+\mathrm{i}aV_2) + h(\eta) \tag{4.188}$$

where $h(\eta)$ is an arbitrary function. However, we can find $U_2 + \mathrm{i}aV_2$ from equation (4.172). Substituting for V_1 from equation (4.179) and for U_0 from equation (4.183), the equation simplifies to give

$$\phi_x(U_2 + \mathrm{i}aV_2) \;=\; \mathrm{i}f'(\eta) - 2\mathrm{i}\left(\frac{\lambda+3G}{\lambda+G}\right)\frac{\partial U_1}{\partial \xi}\,. \tag{4.189}$$

If this is substituted into equation (4.188), we find that $\partial U_1/\partial\xi$ is an arbitrary function of η, or

$$\frac{\partial U_1}{\partial \xi} \;=\; \widehat{h}(\eta)\,. \tag{4.190}$$

Thus

$$U_1 \;=\; \xi\widehat{h}(\eta) + j(\eta)\,, \tag{4.191}$$

where $j(\eta)$ is an arbitrary function.

Now, in our definitions of U_0, V_0, U_1 and V_1 we have four arbitrary functions, namely $f(\eta)$, $g(\eta)$, $\widehat{h}(\eta)$ and $j(\eta)$. To determine these functions we apply the boundary conditions on $y = 0$. We know that $U(x,y)$ and $V(x,y)$ are given by equations (4.158)–(4.159), but on the boundary we have

$$U(x,y)|_{y=0} \;=\; U_{\mathrm{b}}^0(x) + \varepsilon U_{\mathrm{b}}^1(x) + \cdots\,, \tag{4.192}$$

$$V(x,y)|_{y=0} \;=\; V_{\mathrm{b}}^0(x) + \varepsilon V_{\mathrm{b}}^1(x) + \cdots\,, \tag{4.193}$$

which are given. Matching at $O(\varepsilon^{-1})$, we have that

$$U_0|_{y=0} \;=\; V_0|_{y=0} \;=\; 0\,. \tag{4.194}$$

Substituting this into equation (4.183), we find that

$$-\frac{\mathrm{i}x(\lambda+G)\phi_{\mathrm{b}}'(x)f(x)}{2(\lambda+3G)} + g(x) \;=\; 0\,, \tag{4.195}$$

which determines $g(\eta)$. This is substituted back into equation (4.183) to give

$$U_0 \;=\; \frac{\mathrm{i}(\xi+\eta)(\lambda+G)\phi_{\mathrm{b}}'(\eta)f(\eta)}{2(\lambda+3G)}\,. \tag{4.196}$$

At the next order in the boundary conditions, we have

$$U_1|_{y=0} \;=\; U_{\mathrm{b}}^0(x)\,, \qquad V_1|_{y=0} \;=\; V_{\mathrm{b}}^0(x)\,. \tag{4.197}$$

In particular,

$$(U_1 + \mathrm{i}aV_1)|_{y=0} \;=\; U_{\mathrm{b}}^0(x) + \mathrm{i}aV_{\mathrm{b}}^0(x)\,. \tag{4.198}$$

From equation (4.179), this gives us

$$f(x) \;=\; U_{\rm b}^0(x) + {\rm i}aV_{\rm b}^0(x)\;. \tag{4.199}$$

Now, from equation (4.191),

$$U_1|_{y=0} \;=\; -x\widehat{h}(x) + j(x)\;, \tag{4.200}$$

which equals $U_{\rm b}(x)$. Hence

$$j(x) \;=\; U_{\rm b}^0(x) + x\widehat{h}(x) \tag{4.201}$$

$$\Rightarrow \qquad U_1 \;=\; (\xi+\eta)\widehat{h}(\eta) + U_{\rm b}^0(\eta)\;. \tag{4.202}$$

To find the remaining arbitrary function $\widehat{h}(\eta)$, we match the boundary conditions at the next level, giving

$$U_2|_{y=0} \;=\; U_{\rm b}^1(x)\;, \qquad V_2|_{y=0} \;=\; V_{\rm b}^1(x)\;, \tag{4.203}$$

so that

$$(U_2 + {\rm i}aV_2)|_{y=0} \;=\; U_{\rm b}^1(x) + {\rm i}aV_{\rm b}^1(x)\;. \tag{4.204}$$

Substituting this into the restriction of (4.189) to $y=0$, we obtain

$$\widehat{h}(x) \;=\; \frac{1}{2}\left(\frac{\lambda+G}{\lambda+3G}\right)\left[f'(x) + {\rm i}\phi_{\rm b}'(x)\left(U_{\rm b}^1(x) + {\rm i}aV_{\rm b}^1(x)\right)\right]\;. \tag{4.205}$$

Gathering the preceding results together, we have

$$U_0 \;=\; \frac{{\rm i}(\xi+\eta)(\lambda+G)\phi_{\rm b}'(\eta)\left[U_{\rm b}^0(\eta) + {\rm i}aV_{\rm b}^0(\eta)\right]}{2(\lambda+3G)}\;, \tag{4.206}$$

$$V_0 \;=\; {\rm i}aU_0\;, \tag{4.207}$$

$$\begin{aligned} U_1 \;=\; & U_{\rm b}^0(\eta) + \frac{\xi+\eta}{2}\left(\frac{\lambda+G}{\lambda+3G}\right)\Big[U_{\rm b}^{0\prime}(\eta) + {\rm i}aV_{\rm b}^{0\prime}(\eta) \\ & \qquad + {\rm i}\phi_{\rm b}'(\eta)\left(U_{\rm b}^1(\eta) + {\rm i}aV_{\rm b}^1(\eta)\right)\Big]\;, \end{aligned} \tag{4.208}$$

$$V_1 \;=\; V_{\rm b}^0(\eta) + {\rm i}a\left(U_1 - U_{\rm b}^0(\eta)\right)\;. \tag{4.209}$$

Combining these, we obtain our asymptotic formulae for $U(\xi,\eta)$ and $V(\xi,\eta)$:

$$U \;=\; U_{\rm b}^0(\eta) - {\rm i}a\frac{\xi+\eta}{2}F(\eta) + O(\varepsilon)\;, \tag{4.210}$$

$$V \;=\; V_{\rm b}^0(\eta) + \frac{\xi+\eta}{2}F(\eta) + O(\varepsilon)\;, \tag{4.211}$$

where

$$\begin{aligned} F(\eta) \;=\; & {\rm i}a\left(\frac{\lambda+G}{\lambda+3G}\right)\left\{\frac{1}{\varepsilon}\left[U_{\rm b}^0(\eta) + {\rm i}aV_{\rm b}^0(\eta)\right]{\rm i}\phi_{\rm b}'(\eta) + \left[U_{\rm b}^{0\prime}(\eta) + {\rm i}aV_{\rm b}^{0\prime}(\eta)\right]\right. \\ & \left. + \left[U_{\rm b}^1(\eta) + {\rm i}aV_{\rm b}^1(\eta)\right]{\rm i}\phi_{\rm b}'(\eta)\right\}\;. \end{aligned} \tag{4.212}$$

In terms of the original variables x and y,

$$U(x,y) = U_{\rm b}^0(x+{\rm i}ay) + yF(x+{\rm i}ay) + O(\varepsilon)\,, \tag{4.213}$$

$$V(x,y) = V_{\rm b}^0(x+{\rm i}ay) + {\rm i}ayF(x+{\rm i}ay) + O(\varepsilon)\,. \tag{4.214}$$

Then the displacement field in the medium is given by

$$u(x,y) = \left[U_{\rm b}(x+{\rm i}ay) + yF(x+{\rm i}ay)\right]{\rm e}^{{\rm i}\phi_{\rm b}(x+{\rm i}ay)/\varepsilon} + O(\varepsilon)\,, \tag{4.215}$$

$$v(x,y) = \left[V_{\rm b}(x+{\rm i}ay) + {\rm i}ayF(x+{\rm i}ay)\right]{\rm e}^{{\rm i}\phi_{\rm b}(x+{\rm i}ay)/\varepsilon} + O(\varepsilon)\,. \tag{4.216}$$

Now, consider the quantity $F{\rm e}^{{\rm i}\phi/\varepsilon}$. On setting $y=0$, we find that

$${\rm e}^{{\rm i}\phi_{\rm b}(x)/\varepsilon}F(x) = \left(\frac{{\rm i}a(\lambda+G)}{\lambda+3G}\right)\frac{\rm d}{{\rm d}x}\left[(U_{\rm b}(x)+{\rm i}aV_{\rm b}(x))\,{\rm e}^{{\rm i}\phi_{\rm b}(x)/\varepsilon}\right] + O(\varepsilon)\,, \tag{4.217}$$

$$\sim \frac{{\rm i}a(\lambda+G)}{\lambda+3G}\frac{\rm d}{{\rm d}x}\left[(u+{\rm i}av)\big|_{y=0}\right]\,. \tag{4.218}$$

Therefore, on defining

$$u_{\rm b}(x) = u(x,y)\big|_{y=0} = U_{\rm b}{\rm e}^{{\rm i}\phi_{\rm b}(x)/\varepsilon}\,, \tag{4.219}$$

$$v_{\rm b}(x) = v(x,y)\big|_{y=0} = V_{\rm b}{\rm e}^{{\rm i}\phi_{\rm b}(x)/\varepsilon}\,, \tag{4.220}$$

we find that

$$u(x,y) \sim u_{\rm b}(x+{\rm i}ay) + \frac{{\rm i}a(\lambda+G)y}{\lambda+3G}\left[u_{\rm b}'(x+{\rm i}ay) + {\rm i}av_{\rm b}'(x+{\rm i}ay)\right]\,, \tag{4.221}$$

$$v(x,y) \sim v_{\rm b}(x+{\rm i}ay) - \frac{(\lambda+G)y}{\lambda+3G}\left[u_{\rm b}'(x+{\rm i}ay) + {\rm i}av_{\rm b}'(x+{\rm i}ay)\right]\,, \tag{4.222}$$

where $a=\pm1$ is chosen so that $u,v\to0$ as $y\to\infty$.

Now that we have an analytic expression for the displacement, we can find the traction components on $y=0$, in particular the normal traction $\tau_{yy}|_{y=0}$. We have

$$\tau_{yy} = \lambda\left(\frac{\partial u}{\partial x}+\frac{\partial v}{\partial y}\right)+2G\frac{\partial v}{\partial y} \tag{4.223}$$

$$= \lambda\frac{\partial u}{\partial x}+(\lambda+2G)\frac{\partial v}{\partial y} \tag{4.224}$$

$$\begin{aligned} = {}& \lambda\left[u_{\rm b}'(x+{\rm i}ay) + \frac{{\rm i}a(\lambda+G)y}{\lambda+3G}\left(u_{\rm b}''(x+{\rm i}ay)+{\rm i}av_{\rm b}''(x+{\rm i}ay)\right)\right] \\ & +(\lambda+2G)\left[{\rm i}av_{\rm b}'(x+{\rm i}ay) - \frac{\lambda+G}{\lambda+3G}\left(u_{\rm b}'(x+{\rm i}ay)+{\rm i}av_{\rm b}'(x+{\rm i}ay)\right)\right. \\ & \left. -\frac{{\rm i}ay(\lambda+G)}{\lambda+3G}\left(u_{\rm b}''(x+{\rm i}ay)+{\rm i}av_{\rm b}''(x+{\rm i}ay)\right)\right]\,, \end{aligned} \tag{4.225}$$

so that

$$\begin{aligned} \tau_{yy}\big|_{y=0} = {}& \lambda u_{\rm b}'(x)+{\rm i}a(\lambda+2G)v_{\rm b}'(x) \\ & -\frac{(\lambda+G)(\lambda+2G)}{\lambda+3G}\left(u_{\rm b}'(x)+{\rm i}av_{\rm b}'(x)\right) \end{aligned} \tag{4.226}$$

$$= -\left(\frac{2G^2}{\lambda+3G}\right)u_{\rm b}'(x)+{\rm i}a\left(\frac{2G(\lambda+2G)}{\lambda+3G}\right)v_{\rm b}'(x)\,. \tag{4.227}$$

4.4.2 The Euler–Lagrange equation

Before returning to the energy functional (4.151), we will apply the result (4.227) from the previous section to find $\tau_{RR}(w)$. The variable x in that result corresponds to the arc-length parameter $\widehat{R}\theta$ in our problem, and $y = 0$ corresponds to $R = \widehat{R}$. Finally the displacements $u_{\rm b}(x)$, $v_{\rm b}(x)$ correspond to the shell displacements v_θ and w respectively. The values of the Lamé constants used are the values $\lambda_{\rm m}$ and $G_{\rm m}$ in the matrix. Hence

$$\begin{aligned} \tau_{RR}|_{R=\widehat{R}} &\approx \tau_{yy}|_{y=0} && (4.228)\\ &\approx -\left(\frac{2G_{\rm m}^2}{(\lambda_{\rm m}+3G_{\rm m})\widehat{R}}\right)\frac{\rm d}{{\rm d}\theta}(v_\theta|_{R=\widehat{R}}) \\ &\qquad +{\rm i}a\left(\frac{2G_{\rm m}(\lambda_{\rm m}+2G_{\rm m})}{(\lambda_{\rm m}+3G_{\rm m})\widehat{R}}\right)\frac{\rm d}{{\rm d}\theta}(w|_{R=\widehat{R}})\ . && (4.229)\end{aligned}$$

We set $v_\theta = 0$ and rewrite

$$\frac{2G_{\rm m}(\lambda_{\rm m}+2G_{\rm m})}{(\lambda_{\rm m}+3G_{\rm m})} = \frac{4G_{\rm m}(1-\nu_{\rm m})}{3-4\nu_{\rm m}}\ , \qquad (4.230)$$

and

$$\frac{\rm d}{{\rm d}\theta} = -\sqrt{1-\mu^2}\frac{\rm d}{{\rm d}\mu}\ , \qquad (4.231)$$

so that

$$\tau_{RR}|_{R=\widehat{R}} \approx -\sqrt{1-\mu^2}\frac{4{\rm i}a(1-\nu_{\rm m})G_{\rm m}}{(3-4\nu_{\rm m})\widehat{R}}\frac{{\rm d}w}{{\rm d}\mu}\ . \qquad (4.232)$$

However, this can not be substituted directly into equation (4.151), because that functional contains terms which are the *real* parts of w and τ_{RR}, while equation (4.232) refers to a complex quantity, due to the derivation method by WKB analysis. So, set $w_{\rm R}$ and $w_{\rm I}$ to be respectively the real and imaginary components of w. Thus

$$\begin{aligned} \tau_{RR}|_{R=\widehat{R}} &= -\sqrt{1-\mu^2}\frac{4{\rm i}a(1-\nu_{\rm m})G_{\rm m}}{(3-4\nu_{\rm m})\widehat{R}}\frac{\rm d}{{\rm d}\mu}(w_{\rm R}+{\rm i}w_{\rm I}) && (4.233)\\ \Rightarrow \qquad \Re\,\tau_{RR}|_{R=\widehat{R}} &= \sqrt{1-\mu^2}\frac{4a(1-\nu_{\rm m})G_{\rm m}}{(3-4\nu_{\rm m})\widehat{R}}\frac{{\rm d}w_{\rm I}}{{\rm d}\mu}\ . && (4.234)\end{aligned}$$

Substituting this into equation (4.151) eventually gives

$$\begin{aligned} \Delta W_2 = \iint_{\rm shell}\Bigg\{ &\frac{q_\infty}{2}\left(p_0P_0^{(0)}(\mu)+p_2P_2^{(0)}(\mu)\right)(1-\mu^2)\left(\frac{{\rm d}w_{\rm R}}{{\rm d}\mu}\right)^2 \\ &+\frac{hG_{\rm s}}{1-\nu_{\rm s}}\left[2(1+\nu_{\rm s})\frac{w_{\rm R}^2}{\widehat{R}^2}+\frac{h^2}{12}(\nabla^2 w_{\rm R})^2\right] \\ &-\frac{2a(1-\nu_{\rm m})G_{\rm m}}{(3-4\nu_{\rm m})\widehat{R}}\sqrt{1-\mu^2}w_{\rm R}\frac{{\rm d}w_{\rm I}}{{\rm d}\mu}\Bigg\}\,{\rm d}S\ . \end{aligned} \qquad (4.235)$$

Now, we set

$$\mathrm{d}S \;=\; \widehat{R}^2 \sin\theta \,\mathrm{d}\theta \,\mathrm{d}\phi \;, \tag{4.236}$$

and after integrating over ϕ and changing coordinate to μ by equation (3.141) we find

$$\begin{aligned}\Delta W_2 \;=\; \int_{-1}^{1} \Bigg\{ & \pi \widehat{R}^2 q_\infty \left(p_0 P_0^{(0)}(\mu) + p_2 P_2^{(0)}(\mu) \right) (1-\mu^2) \left(\frac{\mathrm{d}w_\mathrm{R}}{\mathrm{d}\mu} \right)^2 \\ & + \frac{2\pi \widehat{R}^2 h G_\mathrm{s}}{1-\nu_\mathrm{s}} \left[2(1+\nu_\mathrm{s}) \frac{w_\mathrm{R}^2}{\widehat{R}^2} + \frac{h^2}{12} (\nabla^2 w_\mathrm{R})^2 \right] \\ & - \frac{4\pi \widehat{R} a (1-\nu_\mathrm{m}) G_\mathrm{m}}{(3-4\nu_\mathrm{m})} \sqrt{1-\mu^2}\, w_\mathrm{R} \frac{\mathrm{d}w_\mathrm{I}}{\mathrm{d}\mu} \Bigg\} \,\mathrm{d}\mu \;. \end{aligned} \tag{4.237}$$

Now, the in-surface Laplacian operator is given by equation (3.169),

$$\nabla^2 w \;=\; \frac{1}{\widehat{R}^2} \left[\frac{\mathrm{d}^2 w}{\mathrm{d}\theta^2} + \cot\theta \frac{\mathrm{d}w}{\mathrm{d}\theta} \right] \tag{4.238}$$

$$\;=\; \frac{1}{\widehat{R}^2 \sin\theta} \frac{\mathrm{d}}{\mathrm{d}\theta} \left(\sin\theta \frac{\mathrm{d}w}{\mathrm{d}\theta} \right) \tag{4.239}$$

$$\;=\; \frac{1}{\widehat{R}^2} \frac{\mathrm{d}}{\mathrm{d}\mu} \left((1-\mu^2) \frac{\mathrm{d}w}{\mathrm{d}\mu} \right) \;. \tag{4.240}$$

Thus the energy integral becomes

$$\begin{aligned}\Delta W_2 \;=\; \int_{-1}^{1} \Bigg\{ & \frac{\pi h^3 G_\mathrm{s}}{6(1-\nu_\mathrm{s}) \widehat{R}^2} \left[\frac{\mathrm{d}}{\mathrm{d}\mu} \left((1-\mu^2) \frac{\mathrm{d}w_\mathrm{R}}{\mathrm{d}\mu} \right) \right]^2 + \frac{4\pi(1+\nu_\mathrm{s}) h G_\mathrm{s}}{1-\nu_\mathrm{s}} w_\mathrm{R}^2 \\ & + \pi \widehat{R}^2 q_\infty \left(p_0 P_0^{(0)}(\mu) + p_2 P_2^{(0)}(\mu) \right) (1-\mu^2) \left(\frac{\mathrm{d}w_\mathrm{R}}{\mathrm{d}\mu} \right)^2 \\ & - \frac{4\pi \widehat{R} a (1-\nu_\mathrm{m}) G_\mathrm{m}}{(3-4\nu_\mathrm{m})} \sqrt{1-\mu^2}\, w_\mathrm{R} \frac{\mathrm{d}w_\mathrm{I}}{\mathrm{d}\mu} \Bigg\} \,\mathrm{d}\mu \;. \end{aligned} \tag{4.241}$$

Now, we set about nondimensionalising the components. Note that from equations (3.135)–(3.136) that we can write

$$p_0 \;=\; \frac{h G_\mathrm{s}}{\widehat{R}^2 G_\mathrm{m}} \widetilde{p}_0 \;, \tag{4.242}$$

where $\widetilde{p}_0$ depends only on the Poisson ratios of the shell and matrix. The same relation holds for p_2. We find that

$$\widetilde{p}_0 \;=\; \frac{(1-\nu_\mathrm{m})(-5\nu_\mathrm{m} + 15\nu_\mathrm{m}\nu_\mathrm{s} - 17 + 3\nu_\mathrm{s})}{2(1-\nu_\mathrm{s})(7-5\nu_\mathrm{s})(1+\nu_\mathrm{m})} \;, \tag{4.243}$$

$$\widetilde{p}_2 \;=\; \frac{10(1-\nu_\mathrm{m})}{(1-\nu_\mathrm{s})(7-5\nu_\mathrm{m})} \;, \tag{4.244}$$

for the case of a uniaxial stress field at infinity. We also nondimensionalise

$$w \;=\; \widehat{R}\widetilde{w}\,, \tag{4.245}$$

and

$$q_\infty \;=\; \left(\frac{G_{\rm s}}{G_{\rm m}}\right)^{\alpha} G_{\rm s}\widetilde{q}_\infty\,. \tag{4.246}$$

This additional factor of $(G_{\rm s}/G_{\rm m})^\alpha$ in the scaling of q_∞ is introduced to enable us to write the equation (almost) entirely in terms of our small parameter, which will be chosen shortly. The energy functional that results from this analysis is given by

$$\begin{aligned}\Delta W_2 \;=\; \pi\widehat{R}^3 G_{\rm m}\int_{-1}^{1}\Bigg\{&\frac{h^3}{\widehat{R}^3}\frac{G_{\rm s}}{G_{\rm m}}\frac{1}{6(1-\nu_{\rm s})}\left[\frac{\rm d}{{\rm d}\mu}\left((1-\mu^2)\frac{{\rm d}\widetilde{w}_{\rm R}}{{\rm d}\mu}\right)\right]^2\\ &+\frac{h}{\widehat{R}}\left(\frac{G_{\rm s}}{G_{\rm m}}\right)^{2+\alpha}\widetilde{q}_\infty\left(\widetilde{p}_0+\widetilde{p}_2P_2^{(0)}(\mu)\right)(1-\mu^2)\left(\frac{{\rm d}\widetilde{w}_{\rm R}}{{\rm d}\mu}\right)^2\\ &-\frac{4a(1-\nu_{\rm m})}{3-4\nu_{\rm m}}\sqrt{1-\mu^2}\widetilde{w}_{\rm R}\frac{{\rm d}\widetilde{w}_{\rm I}}{{\rm d}\mu}+\frac{h}{\widehat{R}}\frac{G_{\rm s}}{G_{\rm m}}\frac{4(1+\nu_{\rm s})}{1-\nu_{\rm s}}\widetilde{w}_{\rm R}^2\Bigg\}\,{\rm d}\mu\,.\end{aligned} \tag{4.247}$$

At this stage we can identify

$$\varepsilon^3 \;:=\; \frac{h^3}{\widehat{R}^3}\frac{G_{\rm s}}{G_{\rm m}} \tag{4.248}$$

to define the small parameter ε. The exponent α is defined by setting

$$\frac{h}{\widehat{R}}\left(\frac{G_{\rm s}}{G_{\rm m}}\right)^{2+\alpha} \;=\; \varepsilon\,, \tag{4.249}$$

which gives

$$\alpha \;=\; -\frac{5}{3}\,. \tag{4.250}$$

We note that this rescaling of our buckling parameter q_∞ is made for the same reason as the rescaling of P in the Euler strut problem at equation (4.24).

By setting

$$P(\mu) \;=\; 6(1-\nu_{\rm s})\left(\widetilde{p}_0+\widetilde{p}_2P_2^{(0)}(\mu)\right) \tag{4.251}$$

$$\;=\; -A+\frac{B\mu^2}{2}\,, \tag{4.252}$$

where

$$A \;=\; -6(1-\nu_{\rm s})\left(\widetilde{p}_0-\frac{\widetilde{p}_2}{2}\right) \tag{4.253}$$

$$\;=\; \frac{9(1-\nu_{\rm m})(9+5\nu_{\rm m}-5\nu_{\rm m}\nu_{\rm s}-\nu_{\rm s})}{(7-5\nu_{\rm m})(1+\nu_{\rm m})} \;>\; 0\,, \tag{4.254}$$

$$B \;=\; 18(1-\nu_{\rm s})\widetilde{p}_2 \tag{4.255}$$

$$\;=\; \frac{180(1-\nu_{\rm m})}{7-5\nu_{\rm m}} \;>\; 0\,, \tag{4.256}$$

and

$$C = -\frac{24a(1-\nu_{\rm m})(1-\nu_{\rm s})}{3-4\nu_{\rm m}}\,, \tag{4.257}$$

$$D = 24\left(\frac{G_{\rm s}}{G_{\rm m}}\right)^{2/3}(1+\nu_{\rm s})\,, \tag{4.258}$$

we find, on rearranging equation (4.247), and dropping the tilde notation, that

$$\Delta W_2 = \frac{\pi\widehat{R}^3 G_{\rm m}}{6(1-\nu_{\rm s})}\int_{-1}^{1}\left\{\varepsilon^3\left[\frac{\rm d}{{\rm d}\mu}\left((1-\mu^2)\frac{{\rm d}w_{\rm R}}{{\rm d}\mu}\right)\right]^2+\varepsilon q_\infty P(\mu)(1-\mu^2)\left(\frac{{\rm d}w_{\rm R}}{{\rm d}\mu}\right)^2 + C\sqrt{1-\mu^2}w_{\rm R}\frac{{\rm d}w_{\rm I}}{{\rm d}\mu}+\varepsilon D w_{\rm R}^2\right\}{\rm d}\mu\,. \tag{4.259}$$

We will treat the constant D as an $O(1)$ parameter even though it contains the ratio of shear moduli. It is possible to find a parameter regime in which ε is small but $G_{\rm s}/G_{\rm m}$ is large, but for simplicity we will assume that this is not the case here.

Recall that we have effectively made the assumption that

$$w \sim A(\mu){\rm e}^{{\rm i}\phi/\varepsilon} = A(\mu)\left(\cos(\phi/\varepsilon)+{\rm i}\sin(\phi/\varepsilon)\right) \tag{4.260}$$

in finding the approximation to the stress term τ_{RR}. Thus we have

$$\frac{{\rm d}w}{{\rm d}\mu} \sim \frac{{\rm i}\phi'}{\varepsilon}{\rm e}^{{\rm i}\phi/\varepsilon}\,, \tag{4.261}$$

which allows us to make the assumption that

$$\frac{{\rm d}w_{\rm I}}{{\rm d}\mu} = Q(\mu)w_{\rm R} \tag{4.262}$$

for the purposes of minimising (4.259), for some function $Q(\mu)$. Thus equation (4.259) becomes

$$\Delta W_2 = \frac{\pi\widehat{R}^3 G_{\rm m}}{6(1-\nu_{\rm s})}\int_{-1}^{1}\left\{\varepsilon^3\left[\frac{\rm d}{{\rm d}\mu}\left((1-\mu^2)\frac{{\rm d}w_{\rm R}}{{\rm d}\mu}\right)\right]^2+\varepsilon q_\infty P(\mu)(1-\mu^2)\left(\frac{{\rm d}w_{\rm R}}{{\rm d}\mu}\right)^2 + \left[C\sqrt{1-\mu^2}Q(\mu)+\varepsilon D\right]w_{\rm R}^2\right\}{\rm d}\mu\,. \tag{4.263}$$

Now, denoting the integrand by $F(w_{\rm R}, w_{\rm R}', w_{\rm R}'')$, the Euler–Lagrange equation is given by

$$\frac{{\rm d}^2}{{\rm d}\mu^2}\left(\frac{\partial F}{\partial w_{\rm R}''}\right)-\frac{\rm d}{{\rm d}\mu}\left(\frac{\partial F}{\partial w_{\rm R}'}\right)+\frac{\partial F}{\partial w_{\rm R}} = 0\,. \tag{4.264}$$

Applying this to ΔW_2, we find that

$$\varepsilon^3\frac{\rm d}{{\rm d}\mu}\left\{(1-\mu^2)\frac{{\rm d}^2}{{\rm d}\mu^2}\left[(1-\mu^2)\frac{{\rm d}w_{\rm R}}{{\rm d}\mu}\right]\right\} -\varepsilon q_\infty\frac{\rm d}{{\rm d}\mu}\left[P(\mu)(1-\mu^2)\frac{{\rm d}w_{\rm R}}{{\rm d}\mu}\right]+\left[C\sqrt{1-\mu^2}Q(\mu)+\varepsilon D\right]w_{\rm R} = 0\,, \tag{4.265}$$

or, on using (4.262),

$$\begin{aligned} \varepsilon^3 \frac{\mathrm{d}}{\mathrm{d}\mu}\left\{(1-\mu^2)\frac{\mathrm{d}^2}{\mathrm{d}\mu^2}\left[(1-\mu^2)\frac{\mathrm{d}w}{\mathrm{d}\mu}\right]\right\} \\ -\varepsilon q_\infty \frac{\mathrm{d}}{\mathrm{d}\mu}\left[P(\mu)(1-\mu^2)\frac{\mathrm{d}w}{\mathrm{d}\mu}\right] - \mathrm{i}C\sqrt{1-\mu^2}\frac{\mathrm{d}w}{\mathrm{d}\mu} + \varepsilon D w &= 0\,, \end{aligned} \tag{4.266}$$

where we take the real part of the equation.

4.4.3 Analysis of the equation

We now apply the asymptotic method of Section 4.3.3 to equation (4.266). The first step is to let $\mu = \varepsilon^\alpha \bar{\mu}$, and find the leading order terms. For each term the leading order components are

$$\varepsilon^{3-4\alpha}\frac{\mathrm{d}^4 w}{\mathrm{d}\bar{\mu}^4} - 8\varepsilon^{3-2\alpha}\bar{\mu}\frac{\mathrm{d}^3 w}{\mathrm{d}\bar{\mu}^3} + \varepsilon^{1-2\alpha}(q_\infty)_0 A\frac{\mathrm{d}^2 w}{\mathrm{d}\bar{\mu}^2} - \varepsilon^{-\alpha}\mathrm{i}C\frac{\mathrm{d}w}{\mathrm{d}\bar{\mu}} + \varepsilon D w = 0\,, \tag{4.267}$$

where $(q_\infty)_0$ is the leading-order value of q_∞. The largest three terms are matched by setting $\alpha = 1$. Then the linear equation to solve becomes

$$\frac{\mathrm{d}^4 w}{\mathrm{d}\bar{\mu}^4} + (q_\infty)_0 A\frac{\mathrm{d}^2 w}{\mathrm{d}\bar{\mu}^2} - \mathrm{i}C\frac{\mathrm{d}w}{\mathrm{d}\bar{\mu}} = 0\,. \tag{4.268}$$

We substitute $w = \mathrm{e}^{m\bar{\mu}}$ to find the auxiliary equation

$$m^4 + (q_\infty)_0 A m^2 - \mathrm{i}C m = 0\,, \tag{4.269}$$

or (discounting the $m = 0$ root),

$$m^3 + (q_\infty)_0 A m - \mathrm{i}C = 0\,. \tag{4.270}$$

Now, $(q_\infty)_0$ is identified by demanding that two of the roots coincide, by Section 4.3.3. A cubic equation with three roots α_i is written as,

$$(m-\alpha_1)(m-\alpha_2)(m-\alpha_3) = 0\,. \tag{4.271}$$

Matching coefficients with equation (4.270), we have

$$-(\alpha_1+\alpha_2+\alpha_3) = 0\,, \tag{4.272}$$

$$\alpha_1\alpha_2 + \alpha_2\alpha_3 + \alpha_3\alpha_1 = (q_\infty)_0 A\,, \tag{4.273}$$

$$-\alpha_1\alpha_2\alpha_3 = -\mathrm{i}C\,. \tag{4.274}$$

As we are searching for coincident roots at this order, we let $\alpha_1 = \alpha_2$. Then from equation (4.272) we have

$$\alpha_3 = -2\alpha_1\,, \tag{4.275}$$

which is then substituted into equations (4.273)–(4.274) to find

$$-3\alpha_1^2 = (q_\infty)_0 A \,, \tag{4.276}$$

$$2\alpha_1^3 = -\mathrm{i}C \,. \tag{4.277}$$

Eliminating α_1 between these two equations gives

$$(q_\infty)_0 = \frac{3}{A}\left(\frac{C}{2}\right)^{2/3} \,, \tag{4.278}$$

whereby the double root becomes

$$\alpha_1 = \mathrm{i}\left(\frac{C}{2}\right)^{1/3} \,. \tag{4.279}$$

Therefore, by defining

$$\kappa = \left(\frac{C}{2}\right)^{1/3} \,, \tag{4.280}$$

we have $\alpha_1 = \mathrm{i}\kappa$ and hence we obtain the oscillatory solution to (4.268),

$$w_0(\bar{\mu}) = \mathrm{e}^{\mathrm{i}\kappa\bar{\mu}} \,, \tag{4.281}$$

and the leading order buckling stress,

$$(q_\infty)_0 = \frac{3\kappa^2}{A} \,. \tag{4.282}$$

We need to choose the constant a appropriately in the definition (4.257) of C. Recall that a was chosen in Section 4.4.1 so that the displacement in the matrix was zero at infinity, or equivalently so that the WKB exponent $\phi(x, y)$ satisfied (4.167). Now, to put our solution in the form required by the work of that section, notice that

$$\mu = \cos\theta \tag{4.283}$$

$$= -\sin(\theta - \pi/2) \tag{4.284}$$

$$\approx \frac{\pi}{2} - \theta \,, \tag{4.285}$$

for $\theta \approx \pi/2$. Then

$$w_0 = \mathrm{e}^{\mathrm{i}\kappa\mu/\varepsilon} \tag{4.286}$$

$$\approx \alpha \mathrm{e}^{-\mathrm{i}\kappa\theta/\varepsilon} \tag{4.287}$$

$$= \alpha \exp\left(-\frac{\mathrm{i}\kappa s}{\varepsilon \widehat{R}}\right) \,, \tag{4.288}$$

where s is the arc-length parameter $\widehat{R}\theta$ and α is a constant. Now, as stated previously, s corresponds to the coordinate x in Section 4.4.1, thus the corresponding value of ϕ on the boundary, from (4.288), becomes

$$\phi_{\mathrm{b}}(x) \;=\; -\frac{\kappa x}{\widehat{R}}\,. \tag{4.289}$$

By (4.257) and (4.280), we have $\kappa = -a|\kappa|$, so

$$\phi_{\mathrm{b}}(x) \;=\; \frac{a|\kappa|x}{\widehat{R}}\,. \tag{4.290}$$

Next we use (4.168) to find

$$\mathrm{i}\phi(x,y) \;=\; \frac{|\kappa|y}{\widehat{R}}\,, \tag{4.291}$$

which tends to $+\infty$ as $y \to \infty$ *whatever* the value of a, thus satisfying (4.167) automatically. Henceforth we will therefore choose $a = -1$ without loss of generality so that $C > 0$; the other choice $a = +1$ would be equivalent to writing $w_0(\bar{\mu}) = \mathrm{e}^{-\mathrm{i}\kappa\bar{\mu}}$.

Returning to the shell problem, we now need to set

$$w \;=\; w_0(\mu/\varepsilon)f(\mu) \tag{4.292}$$

$$\;=\; \mathrm{e}^{\mathrm{i}\kappa\mu/\varepsilon}f(\mu)\,, \tag{4.293}$$

and substitute it into the Euler–Lagrange equation, (4.266). Furthermore, we must rescale $\mu = \varepsilon^\gamma\widehat{\mu}$ and set

$$q_\infty \;=\; \frac{3\kappa^2}{A} + \varepsilon^\beta\lambda\,, \tag{4.294}$$

where λ is the correction to the buckling stress. This is a long computation which eventually gives us a linear differential equation for $f(\widehat{\mu})$,

$$\begin{aligned}
&\varepsilon^{3-4\gamma}f'''' + 4\mathrm{i}\kappa\varepsilon^{2-3\gamma}f''' - 3\varepsilon^{1-2\gamma}\kappa^2 f'' \\
&\quad + \left[3\varepsilon^\gamma\mathrm{i}\kappa^3\widehat{\mu}^2\left(1-\frac{B}{A}\right) + 3\varepsilon\kappa^2\widehat{\mu}\left(6-\frac{B}{A}\right) + 2\varepsilon^{\beta-\gamma}\mathrm{i}\kappa\lambda A\right]f' \\
&+ \left[\varepsilon^{2\gamma-1}\frac{3B}{2A}\kappa^4\widehat{\mu}^2 + \varepsilon^\gamma\mathrm{i}\kappa^3\widehat{\mu}\left(2-\frac{3B}{A}\right) - \varepsilon^{\beta-1}\lambda\kappa^2 A + \varepsilon(6\kappa^2+D)\right]f \;=\; 0\,,
\end{aligned} \tag{4.295}$$

where only the largest coefficients are shown. We choose the exponents β and γ so that the terms in f'', $\widehat{\mu}^2 f$ and λf remain at the leading order, or

$$\beta \;=\; 1\,, \qquad \gamma \;=\; \frac{1}{2}\,. \tag{4.296}$$

Thus the leading order equation becomes

$$\frac{\mathrm{d}^2 f}{\mathrm{d}\widehat{\mu}^2} + \left[\frac{\lambda A}{3} - \frac{B\kappa^2}{2A}\widehat{\mu}^2\right]f \;=\; 0\,. \tag{4.297}$$

The equation can clearly be transformed to the equation for the harmonic oscillator. In fact, by setting

$$\widehat{\mu} \;=\; \gamma\widetilde{\mu}\,, \qquad \lambda \;=\; \frac{3}{\gamma^2 A}\Lambda\,, \tag{4.298}$$

where

$$\gamma^2 \;=\; \sqrt{\frac{2A}{B\kappa^2}}\,, \tag{4.299}$$

we obtain

$$\frac{\mathrm{d}^2 f}{\mathrm{d}\widetilde{\mu}^2} + (\Lambda - \widetilde{\mu}^2) f \;=\; 0\,. \tag{4.300}$$

The expression for γ is well-defined since $B > 0$ and $A > 0$ by the definitions (4.254) and (4.256).

The solutions to the harmonic oscillator equation are given by

$$f_n \;=\; \mathrm{e}^{-\widetilde{\mu}^2/2} H_n(\widetilde{\mu})\,, \tag{4.301}$$

$$\Lambda_n \;=\; 2n + 1\,. \tag{4.302}$$

We will require the lowest eigenvalue, $\Lambda_0 = 1$. Given that $H_0(x) = 1$, the corresponding eigenfunction to Λ_0 is

$$f_0 \;=\; \mathrm{e}^{-\widetilde{\mu}^2/2}\,. \tag{4.303}$$

Transforming back to $\widehat{\mu}$ and λ, we find that the lowest eigenvalue and corresponding eigenfunction are

$$\lambda \;=\; \frac{3|\kappa|}{A}\sqrt{\frac{B}{2A}}\,, \qquad f \;=\; \exp\left[-\frac{|\kappa|}{2}\sqrt{\frac{B}{2A}}\,\widehat{\mu}^2\right]\,. \tag{4.304}$$

Substituting these back into the expressions for the critical stress (4.294) and the buckling pattern (4.293), we find

$$q_\infty \;=\; \frac{3\kappa^2}{A} + \frac{3\varepsilon|\kappa|}{A}\sqrt{\frac{B}{2A}}\,, \tag{4.305}$$

$$w(\mu) \;=\; \exp\left(\frac{\mathrm{i}\kappa\mu}{\varepsilon}\right)\exp\left(-\frac{|\kappa|}{2\varepsilon}\sqrt{\frac{B}{2A}}\,\mu^2\right)\,. \tag{4.306}$$

These are, of course, the nondimensionalised quantities. Using equation (4.246), we find that the full asymptotic expression for the critical stress at infinity is

$$q_\infty \;=\; \left(\frac{G_\mathrm{m}}{G_\mathrm{s}}\right)^{5/3} G_\mathrm{s}\left[\frac{3\kappa^2}{A} + \frac{3\varepsilon|\kappa|}{A}\sqrt{\frac{B}{2A}}\right]\,. \tag{4.307}$$

We could equally find the dimensional buckling pattern $w(\mu)$. However, given that this is an eigenfunction, any constant multiple of w is also a solution. Thus redimensionalising is unnecessary and (4.306) can be regarded as the dimensional buckling pattern.

4.4.4 Comparison with numerical results

We will first compare the asymptotic result for q_∞, (4.307) with the numerical results found in Section 3. The results are shown in Figures 4.15 and 4.16. The first graph shows how the critical stress q_∞ changes as the shear stress ratio $G_\mathrm{s}/G_\mathrm{m}$ tends to zero. The points are the numerical results while the unbroken curve denotes the asymptotic result in (4.307). The Poisson ratios in Table 1.1 are used, $h/\widehat{R}$ is kept constant at 0.01 and G_m is set to 1. A very good agreement is seen.

The second graph shows the equivalent result from (4.307) in the limit as the thickness ratio $h/\widehat{R}$ tends to zero. The same constants are used, with $G_\mathrm{s}/G_\mathrm{m}$ kept constant at 100. At first sight the agreement seems to be inferior, but in fact the error is only around 4.4 % at most, and the result at $h/\widehat{R} = 0.01$ is the same as the result in the previous graph at $G_\mathrm{s}/G_\mathrm{m} = 100$.

We now consider how the buckling patterns agree with the progression in Figure 4.1. The results are shown in Figure 4.17. Here, only for the largest value of $h/\widehat{R}$ can we easily discern a difference between the asymptotic (red) and numerical (blue) results. This is a strong validation of our asymptotic expression (4.306) for w.

Having established that the asymptotic solution is correct for increasingly small values of ε, we would now like to evaluate it for the values given in Table 1.1, for which $\varepsilon = 0.093$. Recall from Section 3.6 that the true value of q_∞ for these values is 0.0550, with odd and even buckling patterns[6] given in Figures 3.3–3.4. Substituting the relevant values into (4.307) gives the asymptotic value of q_∞ to be 0.0481. This is the correct order of magnitude, but is not especially accurate. The buckling pattern comparison is shown in Figure 4.18, where the red curve is the asymptotic solution and the blue curve is the even buckling pattern from Figure 3.3. We observe a good qualitative agreement.

One possible reason for the discrepancy in these values is that the constant D given by equation (4.258) becomes 698.0, which means that we may not be justified in neglecting it. We can introduce it back into the analysis by scaling $\bar{D} = \varepsilon^2 D$, which will be an $O(1)$ constant on using the values in Table 1.1. The equation (4.270) now becomes the quartic

$$m^4 + (q_\infty)_0 A m^2 - \mathrm{i}Cm + \bar{D} \;=\; 0\,. \tag{4.308}$$

By setting the discriminant of this polynomial to zero [62], we can find the $(q_\infty)_0$ corresponding to two roots being repeated. We denote this repeated root by $m = \mathrm{i}\kappa$, for $\kappa \in \mathbb{R}$. The quantities κ and $(q_\infty)_0$ will be related — but not according to the

[6] In order to compare odd buckling patterns, we simply multiply w in equation (4.306) by a multiple of i, since w is an eigenfunction. The real part is taken in order to plot the buckling patterns.

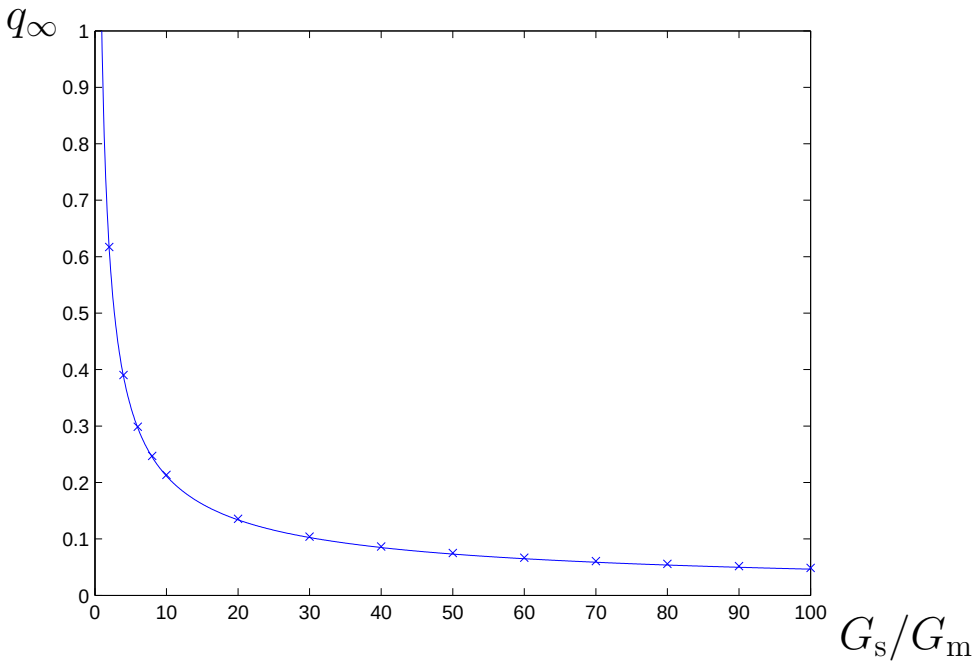

Figure 4.15: Comparison of asymptotic and numerical results for q_∞ in the limit $G_\mathrm{s}/G_\mathrm{m} \to 0$.

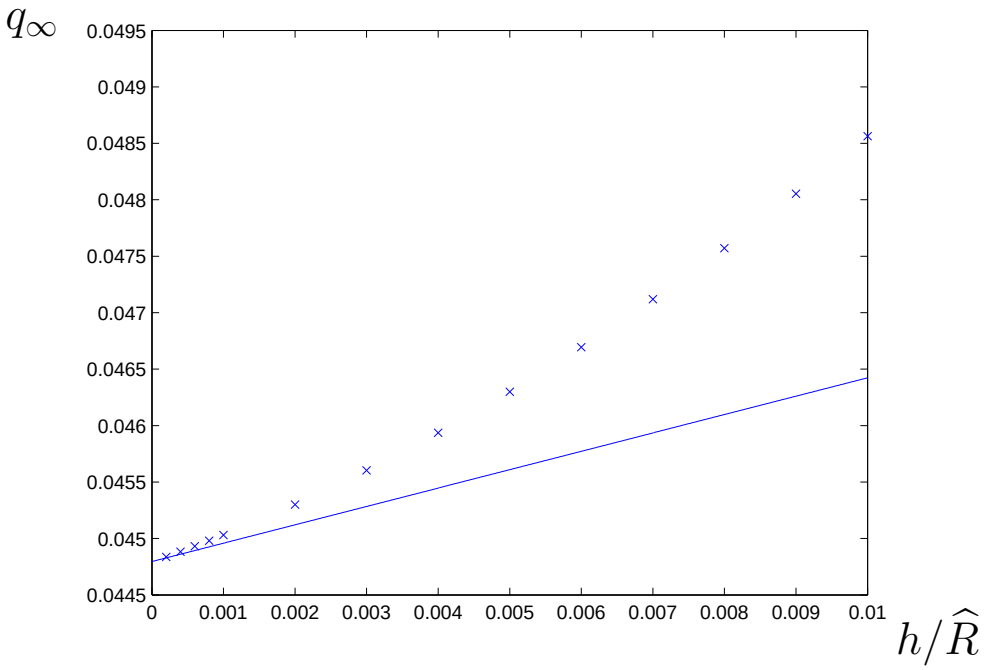

Figure 4.16: Comparison of asymptotic and numerical results for q_∞ in the limit $h/\widehat{R} \to 0$.

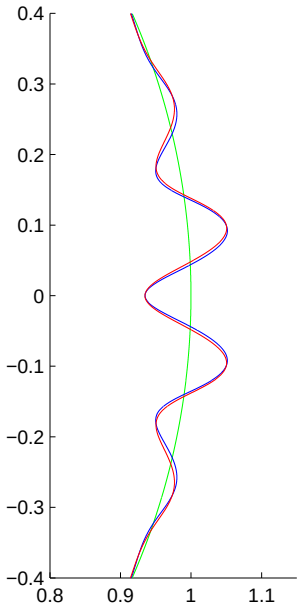

$h/\widehat{R} \;=\; 0.01$

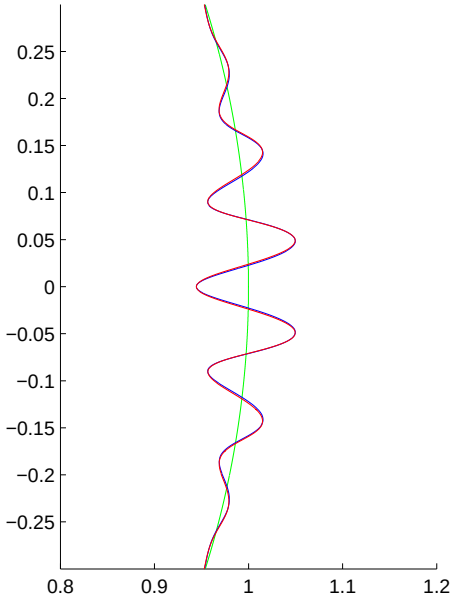

$h/\widehat{R} \;=\; 0.005$

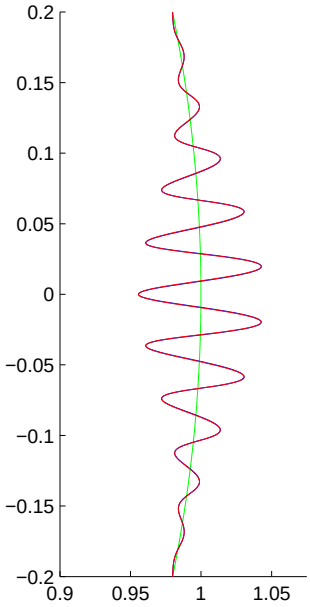

$h/\widehat{R} \;=\; 0.002$

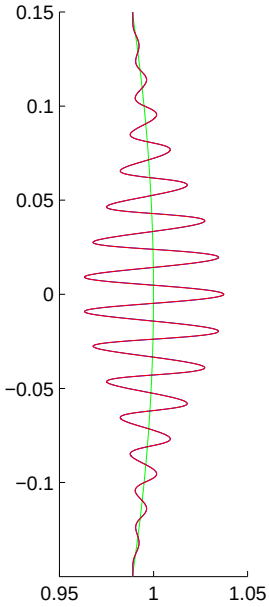

$h/\widehat{R} \;=\; 0.001$

Figure 4.17: Comparison of the asymptotic buckling pattern with the numerical as $h/\widehat{R} \to 0$.

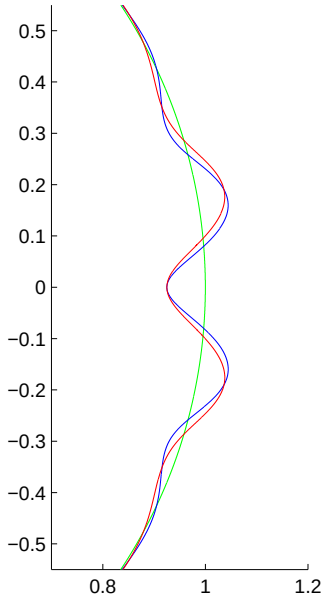

Figure 4.18: Comparison of the asymptotic and numerical buckling pattern for values in Table 1.1.

relation (4.282), which held in the absence of $\bar{D}$. Next, in place of equation (4.297), we have

$$\frac{\mathrm{d}^2 f}{\mathrm{d}\widehat{\mu}^2} + \left[\left(\frac{\kappa^2 A}{6\kappa^2 - A(q_\infty)_0} \right) \lambda - \left(\frac{\kappa^2 (q_\infty)_0 (A + B/2) - \frac{1}{2}\kappa C - 2\kappa^4}{6\kappa^2 - A(q_\infty)_0} \right) \widehat{\mu}^2 \right] f \;=\; 0\,. \tag{4.309}$$

We can scale this equation to obtain the correction to the critical stress as before. Solving numerically, however, we find that the dimensional critical stress becomes $q_\infty = 0.0617$, which is as inaccurate as the approximation having not taken D into account. We suspect therefore that the discrepancy is in fact due to the omission of terms involving ψ in the original energy integral (4.149). This is verified by numerical solutions of the eigenvalue problem (4.266), which gave $q_\infty = 0.0619$. This compares well with the asymptotic solution given previously.[7]

One final useful calculation that can be made is to find the number of oscillations appearing in the buckling pattern. From equation (4.306) we can see that the buckling pattern is formed from an oscillatory part multipled by a strictly positive envelope. The region of buckling is defined by the envelope, which is never zero, but let us define the buckling region as the range of μ over which the envelope is greater than some proportion s of the maximum value, 1. The buckling region is therefore defined

[7]The numerical scheme was a pseudospectral method using Hermite polynomials scaled with a Gaussian profile, as implemented in a Matlab program by Weideman and Reddy [95].

as

$$\exp\left(-\frac{|\kappa|}{2\varepsilon}\sqrt{\frac{B}{2A}}\mu^2\right) > s \tag{4.310}$$

$$\Rightarrow \quad \mu^2 < -\log s\left(\frac{2\varepsilon}{|\kappa|}\right)\sqrt{\frac{2A}{B}} \tag{4.311}$$

$$\Rightarrow \quad |\mu| < \sqrt{\frac{2\varepsilon}{|\kappa|}\log\left(\frac{1}{s}\right)}\left(\frac{2A}{B}\right)^{1/4} . \tag{4.312}$$

Thus we can define the *disturbance length* as

$$L = 2\sqrt{\frac{2\varepsilon}{|\kappa|}\log\left(\frac{1}{s}\right)}\left(\frac{2A}{B}\right)^{1/4} . \tag{4.313}$$

Now, the oscillatory part of the buckling pattern is given by $e^{i\kappa\mu/\varepsilon}$, or $\cos(\kappa\mu/\varepsilon)$ so that the wavelength is

$$\lambda = \frac{2\pi\varepsilon}{|\kappa|} . \tag{4.314}$$

Thus to find the number of oscillations within the buckled region, we divide the disturbance length by the wavelength, or

$$N = \frac{1}{\pi}\sqrt{\frac{2|\kappa|}{\varepsilon}\log\left(\frac{1}{s}\right)}\left(\frac{2A}{B}\right)^{1/4} . \tag{4.315}$$

For the values in Table 1.1, we find that

$$A = 7.27 , \tag{4.316}$$

$$B = 20.8 , \tag{4.317}$$

$$\kappa = 1.53 , \tag{4.318}$$

$$\varepsilon = 0.0928 , \tag{4.319}$$

and we use a representative value for s of 0.05. The number of oscillations N in the buckling region is calculated to be 2.890, which agrees with Figure 4.18.

4.5 Conclusion

The key result from this chapter that will be used in the homogenisation process of Chapter 6 is the analytic expression (4.307) for the critical buckling stress. Given a distribution of differently-sized shells embedded in a matrix, this expression will be used to predict the proportion of those shells which have buckled as the stress on the composite material is increased.

However, before we can approach the homogenisation problem we need to analyse the behaviour of the shell once it has buckled. This will be examined in the next chapter.

Chapter 5

Post-buckling Analysis

In this chapter we investigate a model for the behaviour of a single embedded spherical shell, which has been weakened due to buckling. In Chapter 3 we found that the buckling occurred in a band around the shell's equator. To model this we introduce a crack in the shell around the equator, to account for the loss of stiffness which occurs here. The components of displacement in the shell and the matrix are found in terms of Love stress functions, which are expanded in series of Legendre functions. An infinite system of equations is found for the coefficients of the functions, which is then solved numerically.

5.1 Basic modelling

The post-buckled shell and the surrounding matrix are, as before, modelled as linear elastic materials. The spherical shell occupies the region $R_0 < R < R_1$, with the surrounding region $R > R_1$ being the matrix. As in previous chapters, the shell has elastic constants G_{s} and ν_{s}, and the matrix has elastic constants G_{m} and ν_{m}.

As stated in the preamble, we are interested in the *post*-buckling behaviour of the shell, in other words its behaviour once the stress at infinity has increased beyond the value calculated in Chapter 3 and determined analytically in Chapter 4. To model the fact that the shell buckles in a band around the equator, we introduce an imperfection here, namely that the shell is *split* along the plane $\theta = \pi/2$, with zero traction on that plane. The flaw in the shell is depicted in Figure 5.1. Any interpenetration of the two hemispheres of the shell is ignored.

This model for the buckled shell is clearly not what the shell would in reality experience. However, all we require for the purposes of our report is that the shell is somehow weakened around the equator, and introducing this crack would seem to be a simple way of achieving this aim.

As in previous chapters, the geometry is axisymmetric, so the problem is immediately simplified. However, in contrast to the pre-buckled shell of Chapter 3, where

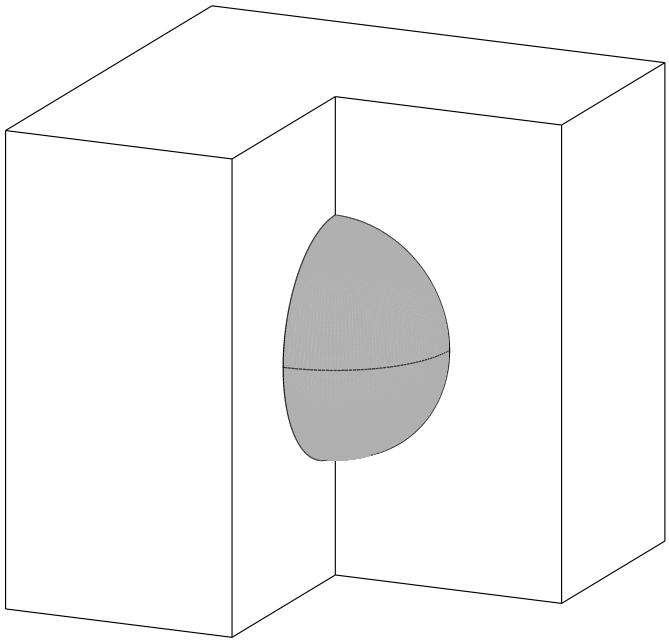

Figure 5.1: Depiction of the split in the embedded shell around its equator.

a solution method had been found previously, the split shell is not one that has been considered in the literature. The axisymmetry enables us to consider the problem in one quadrant only, described by polar coordinates R and θ (which we will write in terms of $\mu = \cos\theta$ as before). The conditions on the boundaries of the shell and the matrix are

$$\tau^{(\mathrm{s})}_{RR}\Big|_{R=R_0} = 0\,, \tag{5.1}$$

$$\tau^{(\mathrm{s})}_{R\theta}\Big|_{R=R_0} = 0\,, \tag{5.2}$$

$$\tau^{(\mathrm{s})}_{RR}\Big|_{R=R_1} - \tau^{(\mathrm{m})}_{RR}\Big|_{R=R_1} = 0\,, \tag{5.3}$$

$$\tau^{(\mathrm{s})}_{R\theta}\Big|_{R=R_1} - \tau^{(\mathrm{m})}_{R\theta}\Big|_{R=R_1} = 0\,, \tag{5.4}$$

$$u^{(\mathrm{s})}_{R}\Big|_{R=R_1} - u^{(\mathrm{m})}_{R}\Big|_{R=R_1} = 0\,, \tag{5.5}$$

$$u^{(\mathrm{s})}_{\theta}\Big|_{R=R_1} - u^{(\mathrm{m})}_{\theta}\Big|_{R=R_1} = 0\,, \tag{5.6}$$

$$\tau^{(\mathrm{s})}_{R\theta}\Big|_{\mu=0} = 0\,, \tag{5.7}$$

$$\tau^{(\mathrm{s})}_{\theta\theta}\Big|_{\mu=0} = 0\,, \tag{5.8}$$

$$\tau^{(\mathrm{m})}_{R\theta}\Big|_{\mu=0} = 0\,, \tag{5.9}$$

$$u^{(\mathrm{m})}_{\theta}\Big|_{\mu=0} = 0\,, \tag{5.10}$$

where a superscript (s) or (m) corresponds to the quantity in the shell or the matrix

respectively. A diagram is shown in Figure 5.2.

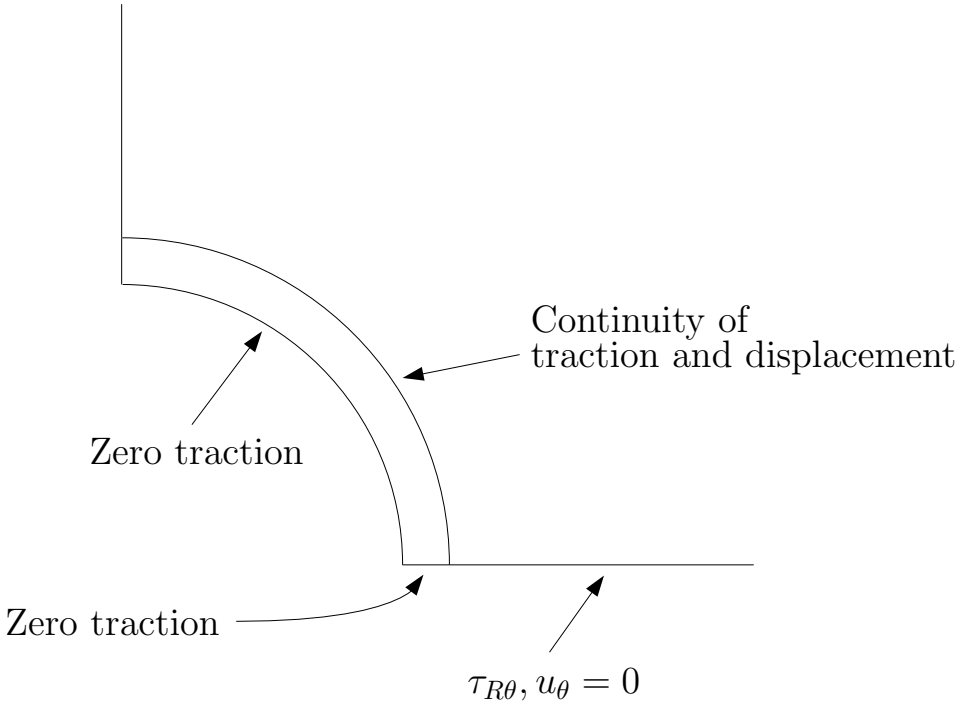

Figure 5.2: Diagram of the solution quadrant for the split shell problem.

We also have a condition on the stress at infinity. As in Chapter 3, we consider an axisymmetric state of stress at infinity, composed of the superposition of the two states of stress

$$\tau_{zz} = -q_z \,, \tag{5.11}$$

$$\tau_{RR} = \tau_{\theta\theta} = \tau_{\phi\phi} = -q_R \,. \tag{5.12}$$

To combine these two states, consider the total stress state at infinity, which is given by

$$\boldsymbol{\tau} = -q_z \boldsymbol{e}_z \otimes \boldsymbol{e}_z - q_R(\boldsymbol{e}_R \otimes \boldsymbol{e}_R + \boldsymbol{e}_\theta \otimes \boldsymbol{e}_\theta + \boldsymbol{e}_\phi \otimes \boldsymbol{e}_\phi) \tag{5.13}$$

which, on writing $\boldsymbol{e}_z$ in terms of $\boldsymbol{e}_R$ and $\boldsymbol{e}_\theta$ by equation (A.102), gives us

$$\begin{aligned} \boldsymbol{\tau} = {} & (-q_R - q_z \cos^2\theta)\boldsymbol{e}_R \otimes \boldsymbol{e}_R + (-q_R - q_z \sin^2\theta)\boldsymbol{e}_\theta \otimes \boldsymbol{e}_\theta \\ & -q_R \boldsymbol{e}_\phi \otimes \boldsymbol{e}_\phi + q_z \cos\theta \sin\theta (\boldsymbol{e}_R \otimes \boldsymbol{e}_\theta + \boldsymbol{e}_\theta \otimes \boldsymbol{e}_R) \,. \end{aligned} \tag{5.14}$$

This corresponds to a state of stress at infinity given by

$$\begin{aligned}
\tau_{RR} &= -q_R - q_z \cos^2\theta && (5.15)\\
&= \left(-q_R - \frac{q_z}{3}\right) P_0^{(0)}(\mu) - \frac{2q_z}{3} P_2^{(0)}(\mu)\ , && (5.16)\\
\tau_{R\theta} &= q_z \cos\theta \sin\theta && (5.17)\\
&= -\frac{q_z}{3} P_2^{(1)}(\mu)\ . && (5.18)
\end{aligned}$$

Strictly speaking, we should consider the problem where the matrix occupies the region $R_1 < R < R_2$, where $R_2 \gg R_1$, with traction components τ_{RR}, $\tau_{R\theta}$ given by (5.16) and (5.18) applied at $R = R_2$. Then the problem described earlier is the limiting case where $R_2 \to \infty$. This is why only two stress components are prescribed at infinity in the formulation presented here.

The hemispherical shell is not modelled by the thin shell equations of Chapter 3, for two reasons. Firstly, the boundary conditions at $\theta = \pi/2$ are not simple to determine, and would make the equations less tractable. Secondly, the full linear elastic equations in this axisymmetric geometry are readily solvable by expanding the displacements in harmonic functions, via the biharmonic Love stress functions, which would not necessarily be the case on using shell equations. Thus, for this problem we have neglected the effect of geometric nonlinearity.

5.2 Love stress functions

Introduced by Love [64], Love stress functions are biharmonic functions which describe the solution to the equations of elasticity for axisymmetric problems. Ling and Yang [61] derived the expressions for the displacement and stress components in spherical polar coordinates. If the Love stress function is given by $\mathscr{L}$ then the displacement and stress components in a material of shear modulus G and Poisson ratio ν are given by

$$\begin{aligned}
u_R &= \frac{1-\nu}{G}\mu\nabla^2\mathscr{L} - \frac{1}{2G}\frac{\partial}{\partial R}\left(\mathrm{D}\mathscr{L}\right)\ , && (5.19)\\
u_\theta &= \frac{\sqrt{1-\mu^2}}{2G}\left\{-2(1-\nu)\nabla^2\mathscr{L} + \frac{1}{R}\frac{\partial}{\partial\mu}\left(\mathrm{D}\mathscr{L}\right)\right\}\ , && (5.20)\\
\tau_{RR} &= \left\{(2-\nu)\mu\frac{\partial}{\partial R} + \frac{\nu(1-\mu^2)}{R}\frac{\partial}{\partial\mu}\right\}\nabla^2\mathscr{L} - \frac{\partial^2}{\partial R^2}\left(\mathrm{D}\mathscr{L}\right)\ , && (5.21)\\
\tau_{R\theta} &= \sqrt{1-\mu^2}\left\{-(1-\nu)\left(\frac{\partial}{\partial R} + \frac{\mu}{R}\frac{\partial}{\partial\mu}\right)\nabla^2\mathscr{L}\right.\\
&\qquad \left. + \frac{\partial}{\partial R}\left(\frac{1}{R}\frac{\partial}{\partial\mu}\right)\left(\mathrm{D}\mathscr{L}\right)\right\}\ , && (5.22)
\end{aligned}$$

$$\tau_{\theta\theta} = -(1-\nu)\left(\mu\frac{\partial}{\partial R} - \frac{1-\mu^2}{R}\frac{\partial}{\partial \mu}\right)\nabla^2\mathscr{L} + \frac{\partial^2}{\partial R^2}(\mathrm{D}\mathscr{L}) + \left(\mu\frac{\partial}{\partial R} + \frac{1-\mu^2}{R}\frac{\partial}{\partial \mu}\right)\left(\frac{1}{R}\frac{\partial \mathscr{L}}{\partial R} - \frac{\mu}{R^2}\frac{\partial \mathscr{L}}{\partial \mu}\right) , \quad (5.23)$$

$$\tau_{\phi\phi} = \left(\mu\frac{\partial}{\partial R} + \frac{1-\mu^2}{R}\frac{\partial}{\partial \mu}\right)\left[\nu\nabla^2\mathscr{L} - \left(\frac{1}{R}\frac{\partial \mathscr{L}}{\partial R} - \frac{\mu}{R^2}\frac{\partial \mathscr{L}}{\partial \mu}\right)\right] , \quad (5.24)$$

where

$$\nabla^2\mathscr{L} = \frac{1}{R^2}\frac{\partial}{\partial R}\left(R^2\frac{\partial \mathscr{L}}{\partial R}\right) + \frac{1}{R^2}\frac{\partial}{\partial \mu}\left[(1-\mu^2)\frac{\partial \mathscr{L}}{\partial \mu}\right] , \quad (5.25)$$

$$\mathrm{D}\mathscr{L} = \mu\frac{\partial \mathscr{L}}{\partial R} + \frac{1-\mu^2}{R}\frac{\partial \mathscr{L}}{\partial \mu} . \quad (5.26)$$

Now, the Love stress functions are biharmonic, so that they satisfy the biharmonic equation

$$\nabla^4\mathscr{L} = 0 . \quad (5.27)$$

It can be shown that axisymmetric solutions to this equation are of the form

$$\mathscr{L} = \left(\alpha R^{n+2} + \beta R^n + \gamma R^{-(n-1)} + \delta R^{-(n+1)}\right)\left(AP_n^{(0)}(\mu) + BQ_n(\mu)\right) , \quad (5.28)$$

where α, β, γ, δ, A and B are arbitrary constants, $Q_n(\mu)$ is a Legendre function of the second kind, and $n \geqslant 0$ is an integer. Now, using the fact that

$$P_n^{(0)}(\mu) = P_{-(n+1)}^{(0)}(\mu) , \quad (5.29)$$

we can consider two general types of Love stress function:

$$\mathscr{L}_n = (\alpha_n + R^2\beta_n)R^n P_n^{(0)}(\mu) \quad (5.30)$$

for any $n \in \mathbb{Z}$, and

$$\widetilde{\mathscr{L}_n} = (A_n R^{n+2} + B_n R^n + C_n R^{-(n-1)} + D_n R^{-(n+1)})Q_n(\mu) \quad (5.31)$$

for $n \geqslant 0$. This form of stress function is chosen for $Q_n(\mu)$ since these functions are undefined for $n < 0$.

We will first find the components of displacement and stress derived from $\mathscr{L}_n$. Using equation (5.25), we find that

$$\nabla^2\mathscr{L}_n = \left[n(n+1)\alpha_n + (n+2)(n+3)\beta_n R^2\right]R^{n-2}P_n^{(0)}(\mu) - (\alpha_n + R^2\beta_n)R^{n-2}n(n+1)P_n^{(0)}(\mu) \quad (5.32)$$

$$= 2(2n+3)\beta_n R^n P_n^{(0)}(\mu) . \quad (5.33)$$

Secondly, from equation (5.26), we find

$$\begin{aligned}
\mathrm{D}\mathscr{L}_n &= \left[n\alpha_n + (n+2)R^2\beta_n\right] R^{n-1}\mu P_n^{(0)}(\mu) \\
&\qquad +(\alpha_n + R^2\beta_n)R^{n-1}(1-\mu^2)\frac{\mathrm{d}P_n^{(0)}}{\mathrm{d}\mu} \qquad (5.34)\\
&= \frac{2(n+1)}{2n+1}R^{n+1}\beta_n P_{n+1}^{(0)}(\mu) + \left[n\alpha_n + \frac{n(2n+3)}{2n+1}R^2\beta_n\right] R^{n-1}P_{n-1}^{(0)}(\mu)\ , \qquad (5.35)
\end{aligned}$$

on using identities in Appendix B.

Next we substitute the values in equations (5.33) and (5.35) into equations (5.19)–(5.22). We obtain, after some algebra,

$$\begin{aligned}
u_R &= \frac{1}{G}\left\{-\frac{n(n-1)}{2}\alpha_n + \frac{n(2n+3)}{2(2n+1)}\left[4(1-\nu)-(n+1)\right]\beta_n R^2\right\} R^{n-2}P_{n-1}^{(0)}(\mu) \\
&\qquad +\frac{1}{G}\left\{\frac{2(1-\nu)(2n+3)(n+1)-(n+1)^2}{2n+1}\right\} R^n\beta_n P_{n+1}^{(0)}(\mu)\ , \qquad (5.36)\\
u_\theta &= \frac{1}{2G}\left\{-n\alpha_n - \left[\frac{n(2n+3)+4(1-\nu)(2n+3)}{2n+1}\right] R^2\beta_n\right\} R^{n-2}P_{n-1}^{(1)}(\mu) \\
&\qquad +\frac{1}{2G}\left\{\frac{4(1-\nu)(2n+3)-2(n+1)}{2n+1}\right\} R^n\beta_n P_{n+1}^{(1)}(\mu)\ , \qquad (5.37)\\
\tau_{RR} &= \left\{-n(n-1)(n-2)\alpha_n - \frac{n(2n+3)(n^2-3n-2\nu)}{2n+1}R^2\beta_n\right\} R^{n-3}P_{n-1}^{(0)}(\mu) \\
&\qquad +\left[\frac{4(1-\nu)n(2n+3)(n+1)-2n(n+1)^2}{2n+1}\right] R^{n-1}\beta_n P_{n+1}^{(0)}(\mu)\ , \qquad (5.38)\\
\tau_{R\theta} &= \left\{-n(n-2)\alpha_n + \frac{2(1-\nu)(2n+3)-n^2(2n+3)}{2n+1}R^2\beta_n\right\} R^{n-3}P_{n-1}^{(1)}(\mu) \\
&\qquad +\left[\frac{4(1-\nu)n(2n+3)-2n(n+1)}{2n+1}\right] R^{n-1}\beta_n P_{n+1}^{(1)}(\mu)\ . \qquad (5.39)
\end{aligned}$$

Finally, we will find that we need to calculate $\tau_{\theta\theta}$ for the Love stress function $\mathscr{L}_n$. However, this would not yield a concise expression. It is much simpler merely to calculate the value of $\tau_{\theta\theta}$ at $\mu = 0$, given that this is where we will be using the condition involving this stress component.

Setting $\mu = 0$ in equation (5.23), and using the expression (5.26) for $\mathrm{D}\mathscr{L}_n$, we find

$$\tau_{\theta\theta}\big|_{\mu=0} = \left\{(1-\mu^2)\frac{\partial}{\partial\mu}\left[\frac{1-\nu}{R}\nabla^2\mathscr{L}_n + \frac{\partial^2}{\partial R^2}\left(\frac{\mathscr{L}_n}{R}\right) + \frac{1}{R^2}\frac{\partial\mathscr{L}_n}{\partial R} - \frac{\mu}{R^3}\frac{\partial\mathscr{L}_n}{\partial\mu}\right]\right\}\Bigg|_{\mu=0}. \qquad (5.40)$$

This expression can be simplified on using the product rule for derivatives, to give

$$\tau_{\theta\theta}\big|_{\mu=0} = \left\{(1-\mu^2)\frac{\partial}{\partial\mu}\left[\frac{1-\nu}{R}\nabla^2\mathscr{L}_n + \frac{1}{R^3}\mathscr{L}_n - \frac{1}{R^2}\frac{\partial\mathscr{L}_n}{\partial R} + \frac{1}{R}\frac{\partial^2\mathscr{L}_n}{\partial R^2}\right]\right\}\Bigg|_{\mu=0}. \qquad (5.41)$$

Substituting the expressions from equations (5.30) and (5.33), and simplifying, gives us

$$\begin{aligned}\tau_{\theta\theta}\big|_{\mu=0} &= \left\{(n-1)^2\alpha_n + \left[(n+1)^2 + 2(1-\nu)(2n+3)\right] R^2\beta_n\right\} \\ &\quad \times R^{n-3}\left[(1-\mu^2)\frac{\mathrm{d}P_n^{(0)}}{\mathrm{d}\mu}\right]\Bigg|_{\mu=0} . \end{aligned} \tag{5.42}$$

However,

$$\left[(1-\mu^2)\frac{\mathrm{d}P_n^{(0)}}{\mathrm{d}\mu}\right]\Bigg|_{\mu=0} = \frac{n(n+1)}{2n+1}\left(P_{n-1}^{(0)}(0) - P_{n+1}^{(0)}(0)\right) , \tag{5.43}$$

and

$$0 = \left(\mu P_n^{(0)}\right)\big|_{\mu=0} = \frac{n+1}{2n+1}P_{n+1}^{(0)}(0) + \frac{n}{2n+1}P_{n-1}^{(0)}(0) \tag{5.44}$$

$$\Rightarrow \quad (n+1)P_{n+1}^{(0)}(0) = -nP_{n-1}^{(0)}(0) \tag{5.45}$$

so that

$$\left[(1-\mu^2)\frac{\mathrm{d}P_n^{(0)}}{\mathrm{d}\mu}\right]\Bigg|_{\mu=0} = \frac{n(n+1)}{2n+1}\left(P_{n-1}^{(0)}(0) + \frac{n}{n+1}P_{n-1}^{(0)}(0)\right) \tag{5.46}$$

$$= nP_{n-1}^{(0)}(0) . \tag{5.47}$$

Therefore,

$$\begin{aligned}\tau_{\theta\theta}\big|_{\mu=0} &= \left\{(n-1)^2\alpha_n + \left[(n+1)^2 + 2(1-\nu)(2n+3)\right] R^2\beta_n\right\} \\ &\quad \times nR^{n-3}P_{n-1}^{(0)}(0) . \end{aligned} \tag{5.48}$$

Finally it is worth noting that in the expression (5.30) for $\mathscr{L}_n$, the constants α_0 and α_1 do not give rise to any displacement or stresses in the material: in other words, they are arbitrary. Therefore we may set them to be zero without loss of generality.

Next we will consider the Love stress function $\widetilde{\mathscr{L}_n}$ from equation (5.31). It can be shown that only one function of this form gives rise to displacement components which are non-singular at $\mu = 1$, which is $\widetilde{\mathscr{L}_0}$ with only the constant A_0 non-zero. Define $\chi = A_0$, and denote the stress function by

$$\mathscr{L}^{\mathrm{comp}} = \chi Q_0(\mu) = \frac{\chi}{2}\log\left(\frac{1+\mu}{1-\mu}\right) , \tag{5.49}$$

because the deformation described by this function is also known as a centre of compression.[1] We find, on using equations (5.19)–(5.23), that the displacements and

[1] Ling and Yang [61] state that it is 'convenient' to include this term in the general expression for the stress, whereas in fact it is *necessary* since a centre of compression cannot be constructed by Love stress functions of the form (5.30).

stress components arising from this stress function are

$$u_R = \frac{\chi}{2GR^2} , \tag{5.50}$$

$$u_\theta = 0 , \tag{5.51}$$

$$\tau_{RR} = -\frac{2\chi}{R^3} , \tag{5.52}$$

$$\tau_{R\theta} = 0 , \tag{5.53}$$

$$\tau_{\theta\theta} = \frac{\chi}{R^3} . \tag{5.54}$$

We will finally consider a third Love stress function, which we will denote $\mathscr{L}^\infty$. This will describe the response of an infinite expanse of material to a given homogeneous stress field. By incorporating this term into the deformation field of the matrix, with the homogeneous stress field given by the applied stress at infinity of the problem, we can assume that the remaining terms in the matrix deformation field decay at infinity. The function $\mathscr{L}^\infty$ is a specific solution of the type $\mathscr{L}_n$, but will be treated separately for convenience. As noted before, the state of stress at infinity in our problem will be given by equations (5.16) and (5.18). The appropriate Love stress function is found by using the functions $\mathscr{L}_n$ from equation (5.30) and choosing the terms whose stress components have no dependence on R. This is achieved by choosing $\mathscr{L}_1$ and $\mathscr{L}_3$, with $\alpha_1 = 0$ (as it is arbitrary, as mentioned previously), and $\beta_3 = 0$ (as it has the wrong dependence on R). Thus

$$\mathscr{L}^\infty = \left(\alpha_3 P_3^{(0)}(\mu) + \beta_1 P_1^{(0)}(\mu)\right) R^3 , \tag{5.55}$$

giving us stress components at infinity

$$\tau_{RR} = \frac{10(1+\nu_\mathrm{m})}{3}\beta_1 P_0^{(0)}(\mu) + \left[\frac{8(4-5\nu_\mathrm{m})\beta_1}{3} - 6\alpha_3\right] P_2^{(0)}(\mu) , \tag{5.56}$$

$$\tau_{R\theta} = \left[\frac{4(4-5\nu_\mathrm{m})\beta_1}{3} - 3\alpha_3\right] P_2^{(1)}(\mu) . \tag{5.57}$$

Comparing these with equations (5.16) and (5.18), we find that

$$\beta_1 = = -\frac{(3q_R + q_z)}{10(1+\nu_\mathrm{m})} , \tag{5.58}$$

$$\alpha_3 = \frac{1}{9}\left[q_z - \frac{4(4-5\nu_\mathrm{m})(3q_R+q_z)}{10(1+\nu_\mathrm{m})}\right] . \tag{5.59}$$

We can now determine the displacement components described by the Love stress function $\mathscr{L}^\infty$:

$$u_R = -\frac{R}{G_\mathrm{m}}\left[\frac{(3q_R+q_z)(1-2\nu_\mathrm{m})}{6(1+\nu_\mathrm{m})}P_0^{(0)}(\mu) + \frac{q_z}{3}P_2^{(0)}(\mu)\right] , \tag{5.60}$$

$$u_\theta = -\frac{Rq_z}{6G_\mathrm{m}}P_2^{(1)}(\mu) . \tag{5.61}$$

5.3 Analysis

We will choose appropriate Love stress functions in the matrix and the shell. Recall that we had three types of function: $\mathscr{L}_n(\alpha_n, \beta_n)$, $\mathscr{L}^{\text{comp}}(\chi)$ and $\mathscr{L}^{\infty}$. Where superscripts (s) and (m) refer to the shell and matrix respectively, we have

$$\mathscr{L}^{(\text{m})} = \sum_{n=-\infty}^{\infty} \mathscr{L}_n(\alpha_n, \beta_n) + \mathscr{L}^{\text{comp}}(\chi_{\text{m}}) + \mathscr{L}^{\infty} , \tag{5.62}$$

$$\mathscr{L}^{(\text{s})} = \sum_{n=-\infty}^{\infty} \mathscr{L}_n(\gamma_n, \delta_n) + \mathscr{L}^{\text{comp}}(\chi_{\text{s}}) , \tag{5.63}$$

so that the constants α_n, β_n and χ_{m} refer to the matrix, and γ_n, δ_n and χ_{s} to the shell.

One simplification we can make immediately is to note that in the matrix, by design, the only stress at infinity should be that due to the term $\mathscr{L}^{\infty}$. By analysing the stress fields produced by $\mathscr{L}_n$, we find that we need

$$\alpha_n = 0 \quad \text{for } n = 3, 4, 5, \ldots \tag{5.64}$$

$$\beta_n = 0 \quad \text{for } n = 1, 2, 3, \ldots . \tag{5.65}$$

We also set $\beta_0 = 0$ and $\alpha_2 = 0$ to omit the rigid body displacement field that would result from these coefficients. Additionally, α_0 and α_1 are arbitrary, so to ensure the correct behaviour of the stress field at infinity, we remove the $\mathscr{L}_n$ terms in equation (5.62) for $n = 0, 1, 2, \ldots$, giving

$$\mathscr{L}^{(\text{m})} = \sum_{n=-\infty}^{-1} \mathscr{L}_n(\alpha_n, \beta_n) + \mathscr{L}^{\text{comp}}(\chi_{\text{m}}) + \mathscr{L}^{\infty} . \tag{5.66}$$

5.3.1 Conditions along the equatorial plane

We will now consider separately the conditions which are applied at $\mu = 0$, namely equations (5.7)–(5.10). We consider first of all the conditions in the matrix. The displacement condition (5.10) becomes, on using our choice of $\mathscr{L}^{(\text{m})}$,

$$\begin{aligned} 0 = \sum_{n=-\infty}^{-1} R^n \Bigg[& -\frac{n(2n+3) + 4(1-\nu_{\text{m}})(2n+3)}{2n+1} \beta_n P_{n-1}^{(1)}(0) \\ & + \frac{4(1-\nu_{\text{m}})(2n+3) - 2(n+1)}{2n+1} \beta_n P_{n+1}^{(1)}(0) \Bigg] \\ & - \sum_{n=-\infty}^{-3} R^n \alpha_{n+2}(n+2) P_{n+1}^{(1)}(0) . \end{aligned} \tag{5.67}$$

Recall the relationship (5.45) between Legendre functions of order zero. The equivalent expression for Legendre functions of order 1, from equation (B.7), is

$$nP_{n+1}^{(1)}(0) \;=\; -(n+1)P_{n-1}^{(1)}(0)\;. \tag{5.68}$$

This equation implies that $P_m^{(1)}(0)$ is zero if $m \geqslant 0$ is even, or if $m < 0$ is odd. Equation (5.67) thus becomes

$$\begin{aligned} 0 \;=\; \sum_{\substack{n=-\infty \\ n \text{ odd}}}^{-1} R^n \Bigg\{ & \frac{4(1-\nu_{\mathrm{m}})(2n+3)-2(n+1)}{2n+1}\beta_n P_{n+1}^{(1)}(0) \\ & -\frac{n(2n+3)+4(1-\nu_{\mathrm{m}})(2n+3)}{2n+1}\beta_n P_{n-1}^{(1)}(0) \\ & -\alpha_{n+2}(n+2)P_{n+1}^{(1)}(0)\Bigg\}\;. \end{aligned} \tag{5.69}$$

Now, the above equation holds for $R > R_1$, and over this interval the functions R^n form a linearly independent set. We can therefore set the coefficients of each R^n to be zero. This tells us that

$$\beta_{-1} \;=\; 0\;, \tag{5.70}$$

and that

$$\begin{aligned} \alpha_{n+2} \;=\; \frac{1}{n+2}\Bigg\{ & \frac{4(1-\nu_{\mathrm{m}})(2n+3)-2(n+1)}{2n+1} \\ & -\frac{n(2n+3)+4(1-\nu_{\mathrm{m}})(2n+3)}{2n+1}\frac{P_{n-1}^{(1)}(0)}{P_{n+1}^{(1)}(0)}\Bigg\}\beta_n \end{aligned} \tag{5.71}$$

for $n = -3, -5, -7, \ldots$.

By applying the same process to equation (5.9), we obtain the relation

$$\begin{aligned} \alpha_{n+2} \;=\; \frac{1}{n(n+2)}\Bigg\{ & \frac{4(1-\nu_{\mathrm{m}})n(2n+3)-2n(n+1)}{2n+1} \\ & +\frac{2(1-\nu_{\mathrm{m}})(2n+3)-n^2(2n+3)}{2n+1}\frac{P_{n-1}^{(1)}(0)}{P_{n+1}^{(1)}(0)}\Bigg\}\beta_n \end{aligned} \tag{5.72}$$

for $n = -3, -5, -7, \ldots$.

Combining these two results gives us

$$\alpha_n \;=\; \beta_n \;=\; 0 \qquad \text{for } n = -1, -3, -5, \ldots\;. \tag{5.73}$$

Thus

$$\mathscr{L}^{(\mathrm{m})} \;=\; \sum_{\substack{n=-\infty \\ n \text{ even}}}^{-2} \mathscr{L}_n(\alpha_n, \beta_n) + \mathscr{L}^{\mathrm{comp}}(\chi_{\mathrm{m}}) + \mathscr{L}^{\infty}\;. \tag{5.74}$$

We will now consider the corresponding conditions in the shell, using equation (5.63). Condition (5.7) gives us

$$n(n+2)\gamma_{n+2}P^{(1)}_{n+1}(0) = \left\{\frac{4(1-\nu_{\rm s})n(2n+3)-2n(n+1)}{2n+1}P^{(1)}_{n+1}(0) + \frac{2(1-\nu_{\rm s})(2n+3)-n^2(2n+3)}{2n+1}P^{(1)}_{n-1}(0)\right\}\delta_n \ , \quad (5.75)$$

leading to

$$\delta_{-1} = 0 \quad (5.76)$$

and

$$\gamma_{n+2} = \frac{1}{n(n+2)}\left\{\frac{4(1-\nu_{\rm s})n(2n+3)-2n(n+1)}{2n+1} + \frac{2(1-\nu_{\rm s})(2n+3)-n^2(2n+3)}{2n+1}\frac{P^{(1)}_{n-1}(0)}{P^{(1)}_{n+1}(0)}\right\}\delta_n \quad (5.77)$$

for $n = 2, 4, 6, \ldots$ and for $n = -3, -5, -7, \ldots$. The equation (5.75) is identically zero for other values of n.

Finally we consider equation (5.8), which together with equations (5.54) and (5.48) gives

$$0 = \sum_{n=-\infty}^{\infty}\left\{\left[(n+1)^2+2(1-\nu_{\rm s})(2n+3)\right]R^2\delta_n + (n-1)^2\gamma_n\right\}R^{n-3}nP^{(0)}_{n-1}(0) + \frac{\chi_{\rm s}}{R^3} \ . \quad (5.78)$$

Collecting terms in R^{n-1} and equating the coefficients to zero, we get

$$(n+1)^2(n+2)\gamma_{n+2}P^{(0)}_{n+1}(0) + n\left[(n+1)^2+2(1-\nu_{\rm s})(2n+3)\right]\delta_nP^{(0)}_{n-1}(0) + \chi_{\rm s}\delta_{n,-2} = 0 \ , \quad (5.79)$$

where the last term involves Kronecker's delta. This equation is trivially satisfied if $n = 0$ or $n = -1$. For $n = -2$, we obtain

$$\chi_{\rm s} = (1-2\nu_{\rm s})\delta_{-2} \ , \quad (5.80)$$

and

$$\gamma_{n+2} = -\frac{\left[(n+1)^2+2(1-\nu_{\rm s})(2n+3)\right]n}{(n+1)^2(n+2)}\frac{P^{(0)}_{n-1}(0)}{P^{(0)}_{n+1}(0)}\delta_n \quad (5.81)$$

for $n = 1, 3, 5, 7, \ldots$ and $n = -4, -6, -8, \ldots$. Taking equations (5.77) and (5.81), we have found all components γ_n in terms of components δ_n, except for γ_0, γ_1 and γ_2.

The first two of these, as noted before, are arbitrary so can be set to zero without loss of generality. Finally, we note that the displacement field resulting from a Love stress function involving only γ_2 is exactly equivalent (modulo a multiplicative constant) to the displacement field resulting from a Love stress function involving only δ_0. Both these fields correspond to a rigid body displacement parallel to the z-axis in the problem. Therefore, we can also set $\gamma_2 = 0$ without loss of generality.

From equations (5.45) and (5.68), we can write

$$\frac{P^{(0)}_{n-1}(0)}{P^{(0)}_{n+1}(0)} = -\frac{n+1}{n} , \tag{5.82}$$

$$\frac{P^{(1)}_{n-1}(0)}{P^{(1)}_{n+1}(0)} = -\frac{n}{n+1} . \tag{5.83}$$

Using these, we define

$$\gamma_{n+2} = \lambda_n \delta_n \tag{5.84}$$

where

$$\lambda_n = \begin{cases} \dfrac{2(1-\nu_{\rm s})(2n+3)+(n+1)^2}{(n+1)(n+2)} \\ \qquad \text{for } n = \ldots, -8, -6, -4, 1, 3, 5, \ldots \\ \dfrac{2(1-\nu_{\rm s})(2n+3)+n^2-2}{(n+1)(n+2)} \\ \qquad \text{for } n = \ldots, -7, -5, -3, 2, 4, 6, \ldots \\ 0 \\ \qquad \text{for } n = -2, -1, 0 . \end{cases} \tag{5.85}$$

Then

$$\mathscr{L}^{(\rm s)} = \sum_{n=-\infty}^{\infty} \mathscr{L}_n(\lambda_{n-2}\delta_{n-2}, \delta_n) + \mathscr{L}^{\rm comp}(\chi_{\rm s}) , \tag{5.86}$$

where $\chi_{\rm s}$ is given by equation (5.80).

5.3.2 The remaining boundary conditions

In equation (5.86), we split the sum in two:

$$\mathscr{L}^{(\rm s)} = \mathscr{L}^{+} + \mathscr{L}^{-} + \mathscr{L}^{\rm comp} \tag{5.87}$$

where

$$\mathscr{L}^{-} = \sum_{n=-\infty}^{-1} \mathscr{L}_n(\lambda_{n-2}\delta_{n-2}, \delta_n) \tag{5.88}$$

$$\mathscr{L}^{+} = \sum_{n=0}^{\infty} \mathscr{L}_n(\lambda_{n-2}\delta_{n-2}, \delta_n) . \tag{5.89}$$

In $\mathscr{L}^-$ we replace n by $-(m+1)$, so that

$$\mathscr{L}^- \;=\; \sum_{m=0}^{\infty} R^{-(m+1)}(\lambda_{-m-3}\delta_{-m-3} + R^2\delta_{-m-1})P_m^{(0)}(\mu)\;, \tag{5.90}$$

using the fact that

$$P_{-n-1}^{(m)}(\mu) \;=\; P_n^{(m)}(\mu)\;. \tag{5.91}$$

We then define

$$\zeta_m \;=\; \delta_{-m-1}\;, \tag{5.92}$$

resulting in

$$\mathscr{L}^- \;=\; \sum_{m=0}^{\infty} R^{-m-1}(\lambda_{-m-3}\zeta_{m+2} + R^2\zeta_m)P_m^{(0)}(\mu)\;. \tag{5.93}$$

By applying equations (5.36)–(5.39) to $\mathscr{L}^{\pm}$ separately, making the substitution (5.92) and rearranging, we can write the displacement and traction components in the shell as

$$\begin{aligned}
\tau_{RR}^{(\mathrm{s})} \;=\; & -\frac{2\chi_{\mathrm{s}}}{R^3} + \sum_{n=0}^{\infty} P_n^{(0)}(\mu)\left\{\left[-(n+1)n(n-1)\lambda_{n-1}\right.\right. \\
& \qquad \left. + \frac{[4(1-\nu_{\mathrm{s}})(2n+1)-2n]\,n(n-1)}{2n-1}\right] R^{n-2}\delta_{n-1} \\
& + \frac{(n+1)(2n+5)\,[2\nu_{\mathrm{s}}-(n-2)(n+1)]}{2n+3} R^{n}\delta_{n+1} \\
& + \frac{n(2n-3)\,[n(n+3)-2\nu_{\mathrm{s}}]}{2n-1} R^{-n-1}\zeta_{n-1} \\
& + \left[n(n+1)(n+2)\lambda_{-(n+2)} \right. \\
& \qquad \left.\left. + \frac{2(n+2)(n+1)\,[2(1-\nu_{\mathrm{s}})(2n+1)-(n+1)]}{2n+3}\right] R^{-n-3}\zeta_{n+1}\right\}\;,
\end{aligned} \tag{5.94}$$

$$\begin{aligned}
\tau_{R\theta}^{(\mathrm{s})} \;=\; & \sum_{n=1}^{\infty} P_n^{(1)}(\mu)\left\{\left[-(n+1)(n-1)\lambda_{n-1}\right.\right. \\
& \qquad \left. + \frac{2(n-1)\,[2(1-\nu_{\mathrm{s}})(2n+1)-n]}{2n-1}\right] R^{n-2}\delta_{n-1} \\
& + \frac{(2n+5)\,[2(1-\nu_{\mathrm{s}})-(n+1)^2]}{2n+3} R^{n}\delta_{n+1} \\
& + \frac{(2n-3)\,[2(1-\nu_{\mathrm{s}})-n^2]}{2n-1} R^{-n-1}\zeta_{n-1} \\
& + \left[-n(n+2)\lambda_{-(n+2)} \right. \\
& \qquad \left.\left. - \frac{2(n+2)\,[2(1-\nu_{\mathrm{s}})(2n+1)-(n+1)]}{2n+3}\right] R^{-n-3}\zeta_{n+1}\right\}\;,
\end{aligned} \tag{5.95}$$

$$
\begin{aligned}
u_R^{(\mathrm{s})} &= \frac{\chi_{\mathrm{s}}}{2G_{\mathrm{s}}R^2} + \frac{1}{2G_{\mathrm{s}}}\sum_{n=0}^{\infty} P_n^{(0)}(\mu)\left\{\left[-n(n+1)\lambda_{n-1}\right.\right. \\
&\qquad \left.+\frac{2n\left[2(1-\nu_{\mathrm{s}})(2n+1)-n\right]}{2n-1}\right]R^{n-1}\delta_{n-1} \\
&\quad +\frac{(n+1)(2n+5)\left[4(1-\nu_{\mathrm{s}})-(n+2)\right]}{2n+3}R^{n+1}\delta_{n+1} \\
&\quad -\frac{n(2n-3)\left[4(1-\nu_{\mathrm{s}})+(n-1)\right]}{2n-1}R^{-n}\zeta_{n-1} \\
&\quad +\left[-n(n+1)\lambda_{-(n+2)}\right. \\
&\qquad \left.\left.+\frac{2(n+1)\left[(n+1)-2(1-\nu_{\mathrm{s}})(2n+1)\right]}{2n+3}\right]R^{-n-2}\zeta_{n+1}\right\}, \qquad (5.96)
\end{aligned}
$$

$$
\begin{aligned}
u_\theta^{(\mathrm{s})} &= \frac{1}{2G_{\mathrm{s}}}\sum_{n=1}^{\infty} P_n^{(1)}(\mu)\left\{\left[-(n+1)\lambda_{n-1}\right.\right. \\
&\qquad \left.+\frac{4(1-\nu_{\mathrm{s}})(2n+1)-2n}{2n-1}\right]R^{n-1}\delta_{n-1} \\
&\quad -\frac{(2n+5)\left[4(1-\nu_{\mathrm{s}})+(n+1)\right]}{2n+3}R^{n+1}\delta_{n+1} \\
&\quad -\frac{(2n-3)\left[4(1-\nu_{\mathrm{s}})-n\right]}{2n-1}R^{-n}\zeta_{n-1} \\
&\quad +\left[n\lambda_{-(n+2)}+\frac{4(1-\nu_{\mathrm{s}})(2n+1)-2(n+1)}{2n+3}\right]R^{-n-2}\zeta_{n+1}\right\}. \qquad (5.97)
\end{aligned}
$$

Now, we will split up the Love stress function in the matrix into the two components

$$
\mathscr{L}^{(\mathrm{m})} = \mathscr{L}^{\mathrm{P}} + \mathscr{L}^{\infty}\,, \qquad (5.98)
$$

where

$$
\mathscr{L}^{\mathrm{P}} = \mathscr{L}^{\mathrm{comp}}(\chi_{\mathrm{m}}) + \sum_{\substack{n=-\infty \\ n\ \mathrm{even}}}^{-2} \mathscr{L}_n(\alpha_n,\beta_n)\,. \qquad (5.99)
$$

Writing

$$
\phi_n = \alpha_{-(n+1)}\,, \qquad (5.100)
$$

$$
\psi_n = \beta_{-(n+1)}\,, \qquad (5.101)
$$

in the same way as for the shell coefficients, we find that the stress and displacement

components corresponding to $\mathscr{L}^{\rm P}$ are

$$\begin{aligned}
\tau^{\rm P}_{RR} &= -\frac{2\chi_{\rm m}}{R^3} + \sum_{\substack{n=0\\ n\ \text{even}}}^{\infty} P_n^{(0)}(\mu)\left\{\frac{n(2n-3)\left[n(n+3)-2\nu_{\rm m}\right]}{2n-1}R^{-n-1}\psi_{n-1}\right. \\
&\qquad +n(n+1)(n+2)R^{-n-3}\phi_{n-1} \\
&\qquad \left. + \frac{2(n+2)(n+1)\left[2(1-\nu_{\rm m})(2n+1)-n-1\right]}{2n+3}R^{-n-3}\psi_{n+1}\right\}, \qquad (5.102)\\
\tau^{\rm P}_{R\theta} &= \sum_{\substack{n=2\\ n\ \text{even}}}^{\infty} P_n^{(1)}(\mu)\left\{\frac{(2n-3)\left[2(1-\nu_{\rm m})-n^2\right]}{2n-1}R^{-n-1}\psi_{n-1}\right. \\
&\qquad -n(n+2)R^{-n-3}\phi_{n-1} \\
&\qquad \left. - \frac{2(n+2)\left[2(1-\nu_{\rm m})(2n+1)-(n+1)\right]}{2n+3}R^{-n-3}\psi_{n+1}\right\}, \qquad (5.103)\\
u^{\rm P}_{R} &= \frac{\chi_{\rm m}}{2G_{\rm m}R^2} + \frac{1}{2G_{\rm m}}\sum_{\substack{n=0\\ n\ \text{even}}}^{\infty} P_n^{(0)}(\mu)\left\{-\frac{n(2n-3)\left[4(1-\nu_{\rm m})+(n-1)\right]}{2n-1}R^{-n}\psi_{n-1}\right. \\
&\qquad -n(n+1)R^{-n-2}\phi_{n-1} \\
&\qquad \left. + \frac{2(n+1)\left[-2(1-\nu_{\rm m})(2n+1)+(n+1)\right]}{2n+3}R^{-n-2}\psi_{n+1}\right\}, \qquad (5.104)\\
u^{\rm P}_{\theta} &= \frac{1}{2G_{\rm m}}\sum_{\substack{n=2\\ n\ \text{even}}}^{\infty} P_n^{(1)}(\mu)\left\{-\frac{(2n-3)\left[4(1-\nu_{\rm m})-n\right]}{2n-1}R^{-n}\psi_{n-1}\right. \\
&\qquad +nR^{-n-2}\phi_{n-1} \\
&\qquad \left. + \frac{4(1-\nu_{\rm m})(2n+1)-2(n+1)}{2n+3}R^{-n-2}\psi_{n+1}\right\}. \qquad (5.105)
\end{aligned}$$

Applying (5.98), the conditions (5.1)–(5.6) become

$$\begin{aligned}
\tau^{(\rm s)}_{RR}\Big|_{R=R_0} &= 0\,, \qquad (5.106)\\
\tau^{(\rm s)}_{R\theta}\Big|_{R=R_0} &= 0\,, \qquad (5.107)\\
\left(\tau^{(\rm s)}_{RR}-\tau^{\rm P}_{RR}\right)\Big|_{R=R_1} &= \tau^{\infty}_{RR}|_{R=R_1}\,, \qquad (5.108)\\
\left(\tau^{(\rm s)}_{R\theta}-\tau^{\rm P}_{R\theta}\right)\Big|_{R=R_1} &= \tau^{\infty}_{R\theta}|_{R=R_1}\,, \qquad (5.109)\\
\left(u^{(\rm s)}_{R}-u^{\rm P}_{R}\right)\Big|_{R=R_1} &= u^{\infty}_{R}|_{R=R_1}\,, \qquad (5.110)\\
\left(u^{(\rm s)}_{\theta}-u^{\rm P}_{\theta}\right)\Big|_{R=R_1} &= u^{\infty}_{\theta}|_{R=R_1}\,, \qquad (5.111)
\end{aligned}$$

where τ^{∞}_{RR}, $\tau^{\infty}_{R\theta}$, u^{∞}_{R} and u^{∞}_{θ} are given by equations (5.16), (5.18), (5.60) and (5.61). The equations (5.106)–(5.111) can in turn be written in the form

$$\sum_{n=0}^{\infty}\left\{A^1_n\delta_{n-1}+A^2_n\delta_{n+1}+A^3_n\zeta_{n-1}+A^4_n\zeta_{n+1}\right\}P_n^{(0)}(\mu) = 0\,, \qquad (5.112)$$

$$\sum_{n=1}^{\infty}\left\{B_n^1\delta_{n-1}+B_n^2\delta_{n+1}+B_n^3\zeta_{n-1}+B_n^4\zeta_{n+1}\right\}P_n^{(1)}(\mu) \;=\; 0\,, \tag{5.113}$$

$$\sum_{n=0}^{\infty}\Bigg\{C_n^1\delta_{n-1}+C_n^2\delta_{n+1}+C_n^3\zeta_{n-1}+C_n^4\zeta_{n+1}+C_n^5\psi_{n-1} +C_n^6\phi_{n-1}+C_n^7\psi_{n+1}+\frac{2\chi_{\rm m}}{R_1^3}\delta_{n,0}\Bigg\}P_n^{(0)}(\mu) \;=\; C^8P_2^{(0)}+C^9P_0^{(0)}\,, \tag{5.114}$$

$$\sum_{n=1}^{\infty}\left\{D_n^1\delta_{n-1}+D_n^2\delta_{n+1}+D_n^3\zeta_{n-1}+D_n^4\zeta_{n+1}+D_n^5\psi_{n-1} +D_n^6\phi_{n-1}+D_n^7\psi_{n+1}\right\}P_n^{(1)}(\mu) \;=\; D^8P_2^{(1)}(\mu)\,, \tag{5.115}$$

$$\sum_{n=0}^{\infty}\Bigg\{E_n^1\delta_{n-1}+E_n^2\delta_{n+1}+E_n^3\zeta_{n-1}+E_n^4\zeta_{n+1}+E_n^5\psi_{n-1} +E_n^6\phi_{n-1}+E_n^7\psi_{n+1}-\frac{\chi_{\rm m}}{2G_{\rm m}R_1^2}\delta_{n,0}\Bigg\}P_n^{(0)}(\mu) \;=\; E^8P_2^{(0)}+E^9P_0^{(0)}\,, \tag{5.116}$$

$$\sum_{n=1}^{\infty}\left\{F_n^1\delta_{n-1}+F_n^2\delta_{n+1}+F_n^3\zeta_{n-1}+F_n^4\zeta_{n+1}+F_n^5\psi_{n-1} +F_n^6\phi_{n-1}+F_n^7\psi_{n+1}\right\}P_n^{(1)}(\mu) \;=\; F^8P_2^{(1)}(\mu)\,. \tag{5.117}$$

All these equations are only valid in the domain $\mu\in(0,1)$. The coefficients A_n^i to F_n^i are given in Appendix D for completeness.

5.3.3 Obtaining the linear system in general

All six of the equations (5.112)–(5.117) can be written in one of the forms

$$\sum_{n=0}^{\infty}\alpha_nP_n^{(0)}(\mu) \;=\; AP_2^{(0)}(\mu)+BP_0^{(0)}(\mu) \tag{5.118}$$

$$\sum_{n=1}^{\infty}\beta_nP_n^{(1)}(\mu) \;=\; CP_2^{(1)}(\mu)\,, \tag{5.119}$$

for $\mu\in(0,1)$. We will find the linear system arising from the six equations (5.112)–(5.117) by studying these canonical equations.

We will require the results

$$\int_0^1 P_m^{(0)}(\mu)P_n^{(0)}(\mu)\,\mathrm{d}\mu \;=\; \begin{cases}\dfrac{1}{2m+1} & m=n\\ f_{m,n} & m \text{ even, } n \text{ odd}\\ f_{n,m} & m \text{ odd, } n \text{ even}\\ 0 & m\neq n, \text{ same parity}\end{cases} \tag{5.120}$$

$$\int_0^1 P_m^{(1)}(\mu)P_n^{(1)}(\mu)\,\mathrm{d}\mu \;=\; \begin{cases} \dfrac{m(m+1)}{2m+1} & m=n \\ m(m+1)f_{m,n} & m \text{ even, } n \text{ odd} \\ n(n+1)f_{n,m} & m \text{ odd, } n \text{ even} \\ 0 & m\neq n, \text{ same parity} \end{cases} \tag{5.121}$$

where

$$f_{m,n} \;=\; \frac{(-1)^{(m+n+1)/2}\,m!\,n!}{2^{m+n-1}(m-n)(m+n+1)\left[\left(\frac{m}{2}\right)!\right]^2\left[\left(\frac{n-1}{2}\right)!\right]^2}\,. \tag{5.122}$$

The result for Legendre functions of order 0 is given by Byerly [17], but his method also holds for the order 1 functions.

The result above is not convenient for numerical calculations, given that the factorial terms soon become so large that they exceed the maximum number able to be held by the program. The quantities are said to *overflow*. To counter this we re-write equation (5.122) by considering, for even r,

$$s_r \;=\; \frac{r!}{2^r\left[\left(\frac{r}{2}\right)!\right]^2} \tag{5.123}$$

$$\;=\; \frac{r!}{\left[2^{r/2}\left(\frac{r}{2}\right)!\right]^2} \tag{5.124}$$

$$\;=\; \frac{1\cdot 2\cdot 3\cdots r}{\left[2\cdot 4\cdot 6\cdots r\right]^2} \tag{5.125}$$

$$\;=\; \frac{1\cdot 3\cdot 5\cdots (r-1)}{2\cdot 4\cdot 6\cdots r} \tag{5.126}$$

$$\;=\; \prod_{n=1}^{r/2}\left(\frac{2n-1}{2n}\right)\,. \tag{5.127}$$

Then

$$f_{m,n} \;=\; \frac{(-1)^{(m+n+1)/2}ns_ms_{n-1}}{(m-n)(m+n+1)}\,. \tag{5.128}$$

We will now consider equations (5.118) and (5.119) in turn, beginning with (5.118). We multiply the equation by $P_m^{(0)}(\mu)$ and integrate over $\mu\in(0,1)$. Considering even and odd m as separate cases, we obtain

$$\sum_{\substack{n=1\\ n \text{ odd}}}^{\infty}\alpha_n f_{m,n}+\frac{\alpha_m}{2m+1} \;=\; \frac{A}{5}\delta_{m,2}+B\delta_{m,0}$$

$$\text{for } m=0,2,4,6,\ldots \tag{5.129}$$

$$\sum_{\substack{n=0\\ n \text{ even}}}^{\infty}\alpha_n f_{n,m}+\frac{\alpha_m}{2m+1} \;=\; Af_{2,m}+Bf_{0,m}$$

$$\text{for } m=1,3,5,7,\ldots\,. \tag{5.130}$$

These two systems of equations should be equivalent. The reason for this is that, from (5.120), we can write any even Legendre polynomial over $(0,1)$ as a linear combination of odd Legendre polynomials, and vice versa. Thus, over $(0,1)$, the system (5.118) can be written either as a sum of odd or even Legendre polynomials. The two systems (5.129) and (5.130) are the result of considering even and odd series respectively. To analyse the two systems, we will split α_n into odd and even indices. Define

$$e_m = \alpha_{2m-2} \tag{5.131}$$

$$o_m = \alpha_{2m-1}\,, \tag{5.132}$$

then from equations (5.129) and (5.130) we obtain the systems

$$\sum_{r=1}^{\infty} f_{2s-2,2r-1} o_r + \frac{e_s}{4s-3} = \frac{A}{5}\delta_{s,2} + B\delta_{s,1} \qquad \text{for } s = 1,2,3,\ldots \tag{5.133}$$

$$\sum_{s=1}^{\infty} f_{2s-2,2r-1} e_s + \frac{o_r}{4r-1} = A f_{2,2r-1} + B f_{0,2r-1} \qquad \text{for } r = 1,2,3,\ldots\,. \tag{5.134}$$

Now define an infinite matrix $\boldsymbol{M}$ with entries

$$M_{rs} = f_{2s-2,2r-1} \tag{5.135}$$

and a vector

$$\widehat{a}_s = A\delta_{s,2} + B\delta_{s,1} \tag{5.136}$$

so that

$$\frac{A}{5}\delta_{s,2} + B\delta_{s,1} = \frac{1}{4s-3}\widehat{a}_s \tag{5.137}$$

$$A f_{2,2r-1} + B f_{0,2r-1} = \sum_{s=1}^{\infty} M_{rs}\widehat{a}_s\,. \tag{5.138}$$

Therefore, on defining the two diagonal matrices $\boldsymbol{\Delta}_1$ and $\boldsymbol{\Delta}_2$ with entries

$$(\boldsymbol{\Delta}_1)_{ss} = \frac{1}{4s-3}\,, \tag{5.139}$$

$$(\boldsymbol{\Delta}_2)_{rr} = \frac{1}{4r-1}\,, \tag{5.140}$$

the two systems can be written in the form

$$\boldsymbol{M}^{\mathrm{T}}\boldsymbol{o} + \boldsymbol{\Delta}_1\boldsymbol{e} = \boldsymbol{\Delta}_1\widehat{\boldsymbol{a}}\,, \tag{5.141}$$

$$\boldsymbol{\Delta}_2\boldsymbol{o} + \boldsymbol{M}\boldsymbol{e} = \boldsymbol{M}\widehat{\boldsymbol{a}}\,, \tag{5.142}$$

for the solution vectors $\boldsymbol{o}$ and $\boldsymbol{e}$.

We now turn to equation (5.119). As before, we multiply by $P_m^{(1)}(\mu)$ and integrate over $\mu \in (0,1)$, obtaining (for even and odd m in turn)

$$\sum_{\substack{n=1 \\ n \text{ odd}}}^{\infty} \beta_n m(m+1) f_{m,n} + \frac{m(m+1)\beta_m}{2m+1} = \frac{6C}{5}\delta_{m,2}$$
$$\text{for } m = 2, 4, 6, \ldots \tag{5.143}$$

$$\sum_{\substack{n=2 \\ n \text{ even}}}^{\infty} \beta_n n(n+1) f_{n,m} + \frac{m(m+1)\beta_m}{2m+1} = 6C f_{2,m}$$
$$\text{for } m = 1, 3, 5, \ldots \ . \tag{5.144}$$

Set

$$\widetilde{e}_m = \beta_{2m-2} \qquad \text{for } m = 2, 3, 4, \ldots \tag{5.145}$$
$$\widetilde{o}_m = \beta_{2m-1} \qquad \text{for } m = 1, 2, 3, \ldots \ , \tag{5.146}$$

noting that $\widetilde{e}_1$ is never determined by this system. Eventually we obtain

$$\sum_{r=1}^{\infty} g_{2s-2,2r-1}\widetilde{o}_r + \frac{2(s-1)(2s-1)}{4s-3}\widetilde{e}_s = \frac{6C}{5}\delta_{s,2}$$
$$\text{for } s = 2, 3, 4, \ldots \tag{5.147}$$

$$\sum_{s=2}^{\infty} g_{2s-2,2r-1}\widetilde{e}_s + \frac{2r(2r-1)}{4r-1}\widetilde{o}_r = C g_{2,2r-1}$$
$$\text{for } r = 1, 2, 3, \ldots \ , \tag{5.148}$$

where

$$g_{2s-2,2r-1} = 2(s-1)(2s-1) f_{2s-2,2r-1} \ . \tag{5.149}$$

Now, define the diagonal matrices $\boldsymbol{\Delta}_3$ and $\boldsymbol{\Delta}_4$ by

$$(\boldsymbol{\Delta}_3)_{ss} = 2(s-1)(2s-1) \ , \tag{5.150}$$
$$(\boldsymbol{\Delta}_4)_{rr} = 2r(2r-1) \ , \tag{5.151}$$

so that

$$(\boldsymbol{M}\boldsymbol{\Delta}_3)_{rs} = g_{2s-2,2r-1}. \tag{5.152}$$

Finally note that if

$$\widehat{c}_s = C\delta_{s,2} \tag{5.153}$$

then

$$\frac{6C}{5}\delta_{s,2} = \boldsymbol{\Delta}_3\boldsymbol{\Delta}_1\widehat{\boldsymbol{c}}\,, \tag{5.154}$$

$$Cg_{2,2r-1} = \boldsymbol{M}\boldsymbol{\Delta}_3\widehat{\boldsymbol{c}}\,. \tag{5.155}$$

This all results in the two systems

$$\boldsymbol{\Delta}_3\boldsymbol{M}^{\mathrm{T}}\widetilde{\boldsymbol{o}} + \boldsymbol{\Delta}_3\boldsymbol{\Delta}_1\widetilde{\boldsymbol{e}} = \boldsymbol{\Delta}_3\boldsymbol{\Delta}_1\widehat{\boldsymbol{c}}\,, \tag{5.156}$$

$$\boldsymbol{\Delta}_4\boldsymbol{\Delta}_2\widetilde{\boldsymbol{o}} + \boldsymbol{M}\boldsymbol{\Delta}_3\widetilde{\boldsymbol{e}} = \boldsymbol{M}\boldsymbol{\Delta}_3\widehat{\boldsymbol{c}}\,. \tag{5.157}$$

Now, the first row of equation (5.156) is empty, which will cause problems when we apply the results above. Therefore, we premultiply the equation with the matrix

$$\boldsymbol{\Gamma} = \begin{pmatrix} 0 & 1 & 0 & 0 & \\ 0 & 0 & 1 & 0 & \cdots \\ 0 & 0 & 0 & 1 & \\ & \vdots & & & \ddots \end{pmatrix} \tag{5.158}$$

which has the effect of moving all the rows up by one. Then define

$$\boldsymbol{\Delta}_5 = \boldsymbol{\Gamma}\boldsymbol{\Delta}_3\,, \tag{5.159}$$

so that equation (5.156) becomes

$$\boldsymbol{\Delta}_5\boldsymbol{M}^{\mathrm{T}}\widetilde{\boldsymbol{o}} + \boldsymbol{\Delta}_5\boldsymbol{\Delta}_1\widetilde{\boldsymbol{e}} = \boldsymbol{\Delta}_5\boldsymbol{\Delta}_1\widehat{\boldsymbol{c}}\,. \tag{5.160}$$

We cannot multiply throughout by $\boldsymbol{\Delta}_5^{-1}$ because the matrix $\boldsymbol{\Delta}_5$ is singular. This, however, will not cause any problems in the calculation of the solution to the split shell problem, as we shall see shortly.

5.3.4 Application to the split shell

In this section we will be applying the results of the previous section to equations (5.112)–(5.117). We will first consider the equations involving $P_n^{(0)}(\mu)$. Because they are all of the same form, we will analyse the canonical equation

$$\sum_{n=0}^{\infty}\Big\{V_n^1\delta_{n-1} + V_n^2\delta_{n+1} + V_n^3\zeta_{n-1} + V_n^4\zeta_{n+1} + V_n^5\psi_{n-1} + V_n^6\phi_{n-1} + V_n^7\psi_{n+1} + \widetilde{V}\chi_{\mathrm{m}}\delta_{n,0}\Big\}P_n^{(0)}(\mu) = V^8P_2^{(0)} + V^9P_0^{(0)} \tag{5.161}$$

where V is used here as a symbol which can be replaced by A, C or E, and $\widetilde{V}$ corresponds to the multiplier of $\chi_{\mathrm{m}}\delta_{n,0}$ in the sum. Comparing this to (5.118), we get

$$\alpha_n = V_n^1\delta_{n-1} + V_n^2\delta_{n+1} + V_n^3\zeta_{n-1} + V_n^4\zeta_{n+1} + V_n^5\psi_{n-1} + V_n^6\phi_{n-1} + V_n^7\psi_{n+1} + \widetilde{V}\chi_{\mathrm{m}}\delta_{n,0}\,, \tag{5.162}$$

$$A = V^8\,, \tag{5.163}$$

$$B = V^9\,. \tag{5.164}$$

At this stage we need to determine which coefficients are to be solved for. They are

$$\begin{aligned}
&\delta_0, \delta_1, \delta_2, \delta_3, \ldots , \\
&\zeta_1, \zeta_2, \zeta_3, \zeta_4, \ldots , \\
&\psi_1, \psi_3, \psi_5, \psi_7, \ldots , \\
&\phi_1, \phi_3, \phi_5, \phi_7, \ldots , \\
&\chi_{\mathrm{m}} \cdot
\end{aligned} \tag{5.165}$$

The coefficient ζ_0 is zero by equation (5.76). We find that it is convenient to write the coefficients above in terms of six solution vectors,

$$\boldsymbol{\delta}^{\mathrm{o}} = (\delta_1, \delta_3, \delta_5, \ldots) , \tag{5.166}$$

$$\boldsymbol{\zeta}^{\mathrm{o}} = (\zeta_1, \zeta_3, \zeta_5, \ldots) , \tag{5.167}$$

$$\boldsymbol{\psi} = (\psi_1, \psi_3, \psi_5, \ldots) , \tag{5.168}$$

$$\boldsymbol{\phi} = (\chi_{\mathrm{m}}, \phi_1, \phi_3, \ldots) , \tag{5.169}$$

$$\boldsymbol{\delta}^{\mathrm{e}} = (\delta_0, \delta_2, \delta_4, \ldots) , \tag{5.170}$$

$$\boldsymbol{\zeta}^{\mathrm{e}} = (\zeta_2, \zeta_4, \zeta_6, \ldots) . \tag{5.171}$$

The reason for this becomes clear when we perform the split into odd and even indices, as in equations (5.131)–(5.132). We eventually find that

$$\boldsymbol{e} = \boldsymbol{V}_1 \boldsymbol{\delta}^{\mathrm{o}} + \boldsymbol{V}_2 \boldsymbol{\zeta}^{\mathrm{o}} + \boldsymbol{V}_3 \boldsymbol{\psi} + \boldsymbol{V}_4 \boldsymbol{\phi} , \tag{5.172}$$

$$\boldsymbol{o} = \boldsymbol{V}_5 \boldsymbol{\delta}^{\mathrm{e}} + \boldsymbol{V}_6 \boldsymbol{\zeta}^{\mathrm{e}} , \tag{5.173}$$

where the six matrices $\boldsymbol{V}_i$ are given by

$$\boldsymbol{V}_1 = \begin{pmatrix} V_0^2 & 0 & 0 & \\ V_2^1 & V_2^2 & 0 & \cdots \\ 0 & V_4^1 & V_4^2 & \\ & \vdots & & \ddots \end{pmatrix} , \tag{5.174}$$

$$\boldsymbol{V}_2 = \begin{pmatrix} V_0^4 & 0 & 0 & \\ V_2^3 & V_2^4 & 0 & \cdots \\ 0 & V_4^3 & V_4^4 & \\ & \vdots & & \ddots \end{pmatrix} , \tag{5.175}$$

$$\boldsymbol{V}_3 = \begin{pmatrix} V_0^7 & 0 & 0 & \\ V_2^5 & V_2^7 & 0 & \cdots \\ 0 & V_4^5 & V_4^7 & \\ & \vdots & & \ddots \end{pmatrix} , \tag{5.176}$$

$$\boldsymbol{V}_4 = \begin{pmatrix} \widetilde{V} & 0 & 0 & \\ 0 & V_2^6 & 0 & \cdots \\ 0 & 0 & V_4^6 & \\ & \vdots & & \ddots \end{pmatrix} , \tag{5.177}$$

$$\boldsymbol{V}_5 = \begin{pmatrix} V_1^1 & V_1^2 & 0 & \\ 0 & V_3^1 & V_3^2 & \cdots \\ 0 & 0 & V_5^1 & \\ & \vdots & & \ddots \end{pmatrix} , \tag{5.178}$$

$$\boldsymbol{V}_6 = \begin{pmatrix} V_1^4 & 0 & 0 & \\ V_3^3 & V_3^4 & 0 & \cdots \\ 0 & V_5^3 & V_5^4 & \\ & \vdots & & \ddots \end{pmatrix} . \tag{5.179}$$

Given that V can stand for A, C or E, we have thus defined matrices $\boldsymbol{A}_i$, $\boldsymbol{C}_i$ and $\boldsymbol{E}_i$ for $i = 1, \ldots, 6$. Having found expressions for the vectors $\boldsymbol{o}$ and $\boldsymbol{e}$ in equations (5.141)–(5.142), we now only need to define the vectors $\widehat{\boldsymbol{a}}$ for the three choices of V. We find that

$$\widehat{\boldsymbol{a}}_V = \begin{pmatrix} V^9 \\ V^8 \\ 0 \\ 0 \\ \vdots \end{pmatrix} . \tag{5.180}$$

We next consider the same problem for the three equations of (5.112)–(5.117) that involve $P_n^{(1)}(\mu)$. Once again using V as a symbol, which this time could stand for B, D or F, the equation to be analysed is

$$\sum_{n=1}^{\infty} \left\{ V_n^1 \delta_{n-1} + V_n^2 \delta_{n+1} + V_n^3 \zeta_{n-1} + V_n^4 \zeta_{n+1} + V_n^5 \psi_{n-1} \right. \\ \left. + V_n^6 \phi_{n+1} + V_n^7 \psi_{n+1} \right\} P_n^{(1)}(\mu) = V^8 P_2^{(1)}(\mu) , \tag{5.181}$$

so that comparison with (5.119) yields

$$\beta_n = V_n^1 \delta_{n-1} + V_n^2 \delta_{n+1} + V_n^3 \zeta_{n-1} + V_n^4 \zeta_{n+1} \\ + V_n^5 \psi_{n-1} + V_n^6 \phi_{n+1} + V_n^7 \psi_{n+1} , \tag{5.182}$$

$$C = V^8 . \tag{5.183}$$

Performing the split (5.145)–(5.146) into even and odd indices, we find that

$$\widetilde{\boldsymbol{e}} = \boldsymbol{V}_1 \boldsymbol{\delta}^{\mathrm{o}} + \boldsymbol{V}_2 \boldsymbol{\zeta}^{\mathrm{o}} + \boldsymbol{V}_3 \boldsymbol{\psi} + \boldsymbol{V}_4 \boldsymbol{\phi} , \tag{5.184}$$

$$\widetilde{\boldsymbol{o}} = \boldsymbol{V}_5 \boldsymbol{\delta}^{\mathrm{e}} + \boldsymbol{V}_6 \boldsymbol{\zeta}^{\mathrm{e}} \tag{5.185}$$

for the same six matrices $\boldsymbol{V}_i$ given by (5.174)–(5.179). Additionally, the vector $\widehat{\boldsymbol{c}}$ for each equation is given by

$$\widehat{\boldsymbol{c}}_V \;=\; \begin{pmatrix} 0 \\ V^8 \\ 0 \\ 0 \\ \vdots \end{pmatrix} . \tag{5.186}$$

Now, the preceding expressions for $\boldsymbol{e}$, $\boldsymbol{o}$, $\widetilde{\boldsymbol{e}}$, $\widetilde{\boldsymbol{o}}$ and the vectors $\widehat{\boldsymbol{a}}_V$, $\widehat{\boldsymbol{c}}_V$ can be substituted either into (5.141) and (5.160), or into (5.142) and (5.157). In both cases we have six infinite systems of equations for six vectors of unknowns, (5.166)–(5.171). These six systems will be combined into one matrix equation, whose form will depend on whether we substitute the quantities into (5.141) and (5.160), or into (5.142) and (5.157). The first case we name the 'even' method, since this was the result of multiplying the original equations by $P_m^{(0)}(\mu)$ for even m. The second case is accordingly dubbed the 'odd' method.

In the 'even' method the matrix equation is given by

$$\boldsymbol{T}_{\rm e}\boldsymbol{X} \;=\; \boldsymbol{R}_{\rm e} \,, \tag{5.187}$$

where the solution vector is

$$\boldsymbol{X} \;=\; \begin{pmatrix} \boldsymbol{\delta}^{\rm o} \\ \boldsymbol{\zeta}^{\rm o} \\ \boldsymbol{\psi} \\ \boldsymbol{\phi} \\ \boldsymbol{\delta}^{\rm e} \\ \boldsymbol{\zeta}^{\rm e} \end{pmatrix} , \tag{5.188}$$

and the matrix is given by

$$\boldsymbol{T}_{\rm e} \;=\; \begin{pmatrix} \boldsymbol{\Delta}_1\boldsymbol{A}_1 & \boldsymbol{\Delta}_1\boldsymbol{A}_2 & \boldsymbol{O} & \boldsymbol{O} & \boldsymbol{M}^{\rm T}\boldsymbol{A}_5 & \boldsymbol{M}^{\rm T}\boldsymbol{A}_6 \\ \boldsymbol{\Delta}_5\boldsymbol{\Delta}_1\boldsymbol{B}_1 & \boldsymbol{\Delta}_5\boldsymbol{\Delta}_1\boldsymbol{B}_2 & \boldsymbol{O} & \boldsymbol{O} & \boldsymbol{\Delta}_5\boldsymbol{M}^{\rm T}\boldsymbol{B}_5 & \boldsymbol{\Delta}_5\boldsymbol{M}^{\rm T}\boldsymbol{B}_6 \\ \boldsymbol{\Delta}_1\boldsymbol{C}_1 & \boldsymbol{\Delta}_1\boldsymbol{C}_2 & \boldsymbol{\Delta}_1\boldsymbol{C}_3 & \boldsymbol{\Delta}_1\boldsymbol{C}_4 & \boldsymbol{M}^{\rm T}\boldsymbol{C}_5 & \boldsymbol{M}^{\rm T}\boldsymbol{C}_6 \\ \boldsymbol{\Delta}_5\boldsymbol{\Delta}_1\boldsymbol{D}_1 & \boldsymbol{\Delta}_5\boldsymbol{\Delta}_1\boldsymbol{D}_2 & \boldsymbol{\Delta}_5\boldsymbol{\Delta}_1\boldsymbol{D}_3 & \boldsymbol{\Delta}_5\boldsymbol{\Delta}_1\boldsymbol{D}_4 & \boldsymbol{\Delta}_5\boldsymbol{M}^{\rm T}\boldsymbol{D}_5 & \boldsymbol{\Delta}_5\boldsymbol{M}^{\rm T}\boldsymbol{D}_6 \\ \boldsymbol{\Delta}_1\boldsymbol{E}_1 & \boldsymbol{\Delta}_1\boldsymbol{E}_2 & \boldsymbol{\Delta}_1\boldsymbol{E}_3 & \boldsymbol{\Delta}_1\boldsymbol{E}_4 & \boldsymbol{M}^{\rm T}\boldsymbol{E}_5 & \boldsymbol{M}^{\rm T}\boldsymbol{E}_6 \\ \boldsymbol{\Delta}_5\boldsymbol{\Delta}_1\boldsymbol{F}_1 & \boldsymbol{\Delta}_5\boldsymbol{\Delta}_1\boldsymbol{F}_2 & \boldsymbol{\Delta}_5\boldsymbol{\Delta}_1\boldsymbol{F}_3 & \boldsymbol{\Delta}_5\boldsymbol{\Delta}_1\boldsymbol{F}_4 & \boldsymbol{\Delta}_5\boldsymbol{M}^{\rm T}\boldsymbol{F}_5 & \boldsymbol{\Delta}_5\boldsymbol{M}^{\rm T}\boldsymbol{F}_6 \end{pmatrix} \tag{5.189}$$

where $\boldsymbol{O}$ is the zero matrix, and the right-hand side vector is

$$\boldsymbol{R}_{\rm e} \;=\; \begin{pmatrix} \boldsymbol{0} \\ \boldsymbol{0} \\ \boldsymbol{\Delta}_1\widehat{\boldsymbol{a}}_C \\ \boldsymbol{\Delta}_5\boldsymbol{\Delta}_1\widehat{\boldsymbol{c}}_D \\ \boldsymbol{\Delta}_1\widehat{\boldsymbol{a}}_E \\ \boldsymbol{\Delta}_5\boldsymbol{\Delta}_1\widehat{\boldsymbol{c}}_F \end{pmatrix} . \tag{5.190}$$

The equivalent equation for the 'odd' method is

$$\boldsymbol{T}_{\mathrm{o}}\boldsymbol{X} \;=\; \boldsymbol{R}_{\mathrm{o}}\,, \tag{5.191}$$

where

$$\boldsymbol{T}_{\mathrm{o}} \;=\; \begin{pmatrix} \boldsymbol{M}\boldsymbol{A}_1 & \boldsymbol{M}\boldsymbol{A}_2 & \boldsymbol{O} & \boldsymbol{O} & \boldsymbol{\Delta}_2\boldsymbol{A}_5 & \boldsymbol{\Delta}_2\boldsymbol{A}_6 \\ \boldsymbol{M}\boldsymbol{\Delta}_3\boldsymbol{B}_1 & \boldsymbol{M}\boldsymbol{\Delta}_3\boldsymbol{B}_2 & \boldsymbol{O} & \boldsymbol{O} & \boldsymbol{\Delta}_4\boldsymbol{\Delta}_2\boldsymbol{B}_5 & \boldsymbol{\Delta}_4\boldsymbol{\Delta}_2\boldsymbol{B}_6 \\ \boldsymbol{M}\boldsymbol{C}_1 & \boldsymbol{M}\boldsymbol{C}_2 & \boldsymbol{M}\boldsymbol{C}_3 & \boldsymbol{M}\boldsymbol{C}_4 & \boldsymbol{\Delta}_2\boldsymbol{C}_5 & \boldsymbol{\Delta}_2\boldsymbol{C}_6 \\ \boldsymbol{M}\boldsymbol{\Delta}_3\boldsymbol{D}_1 & \boldsymbol{M}\boldsymbol{\Delta}_3\boldsymbol{D}_2 & \boldsymbol{M}\boldsymbol{\Delta}_3\boldsymbol{D}_3 & \boldsymbol{M}\boldsymbol{\Delta}_3\boldsymbol{D}_4 & \boldsymbol{\Delta}_4\boldsymbol{\Delta}_2\boldsymbol{D}_5 & \boldsymbol{\Delta}_4\boldsymbol{\Delta}_2\boldsymbol{D}_6 \\ \boldsymbol{M}\boldsymbol{E}_1 & \boldsymbol{M}\boldsymbol{E}_2 & \boldsymbol{M}\boldsymbol{E}_3 & \boldsymbol{M}\boldsymbol{E}_4 & \boldsymbol{\Delta}_2\boldsymbol{E}_5 & \boldsymbol{\Delta}_2\boldsymbol{E}_6 \\ \boldsymbol{M}\boldsymbol{\Delta}_3\boldsymbol{F}_1 & \boldsymbol{M}\boldsymbol{\Delta}_3\boldsymbol{F}_2 & \boldsymbol{M}\boldsymbol{\Delta}_3\boldsymbol{F}_3 & \boldsymbol{M}\boldsymbol{\Delta}_3\boldsymbol{F}_4 & \boldsymbol{\Delta}_4\boldsymbol{\Delta}_2\boldsymbol{F}_5 & \boldsymbol{\Delta}_4\boldsymbol{\Delta}_2\boldsymbol{F}_6 \end{pmatrix} \tag{5.192}$$

and

$$\boldsymbol{R}_{\mathrm{o}} \;=\; \begin{pmatrix} \boldsymbol{0} \\ \boldsymbol{0} \\ \boldsymbol{M}\widehat{\boldsymbol{a}}_C \\ \boldsymbol{M}\boldsymbol{\Delta}_3\widehat{\boldsymbol{c}}_D \\ \boldsymbol{M}\widehat{\boldsymbol{a}}_E \\ \boldsymbol{M}\boldsymbol{\Delta}_3\widehat{\boldsymbol{c}}_F \end{pmatrix}\,. \tag{5.193}$$

5.4 Numerical analysis

We now have two systems to solve, given by (5.187) and (5.191), which should give the same solution. The difficulty in finding these solutions lies in the fact that the systems are infinite.

The matrices $\boldsymbol{T}_{\mathrm{e}}$ and $\boldsymbol{T}_{\mathrm{o}}$ are composed of 36 infinite submatrices. We suppose that each of these submatrices is truncated to a size of $N \times N$, with the corresponding subvectors of $\boldsymbol{R}_{\mathrm{e}}$ and $\boldsymbol{R}_{\mathrm{o}}$ truncated to a length of N. Then the equations (5.187) and (5.191) form a system of $6N$ linear simultaneous equations for $6N$ of the coefficients in the vector $\boldsymbol{X}$. We will seek the solutions to these systems as $N \to \infty$. A number of issues will arise which we will now consider in turn.

During the course of this analysis, we will assume for the purposes of illustration that the material and geometric parameters are those of Table 1.1, apart from the choice of $\widehat{R} = 1$. We apply a uniaxial stress field at infinity, given by $q_z = q > 0$ and $q_R = 0$.

5.4.1 Scaling of the solution matrix

One observation that can be made on calculating the solution of the truncated systems (5.187) and (5.191) is that the matrices $\boldsymbol{T}_{\mathrm{e}}$ and $\boldsymbol{T}_{\mathrm{o}}$ are *badly scaled*. This implies that the solutions that are found can be less accurate than is expected. To counter this

effect, the matrix $\boldsymbol{T}$ must be scaled appropriately. Neumaier [75] suggests that the system (5.187) (for example) should be replaced by

$$\Rightarrow \qquad \widetilde{\boldsymbol{T}}_{\mathrm{e}}\widetilde{\boldsymbol{X}} \;=\; \boldsymbol{R}_{\mathrm{e}} \tag{5.194}$$

where

$$\widetilde{\boldsymbol{T}}_{\mathrm{e}} \;=\; \boldsymbol{T}_{\mathrm{e}}\boldsymbol{K}^{-1} \tag{5.195}$$

and

$$\widetilde{\boldsymbol{X}} \;=\; \boldsymbol{K}\boldsymbol{X} \tag{5.196}$$

for some matrix $\boldsymbol{K}$. It is readily verified that the system (5.194) is exactly equivalent to the original system (5.187). A 'natural' choice for $\boldsymbol{K}$ is suggested, which is given by the diagonal matrix with entries

$$(\boldsymbol{K})_{kk} \;=\; \sqrt{(\boldsymbol{T}_{\mathrm{e}}^{\mathrm{T}}\boldsymbol{T}_{\mathrm{e}})_{kk}}\,. \tag{5.197}$$

5.4.2 Comparison of the 'odd' and 'even' solutions

Recall that the two systems (5.187) and (5.191), having been derived from the same matching conditions, should give the same solution. However, on calculation, it transpires that the solutions given by the odd and even methods are different. This discrepancy between the two methods is obviously worrying. Which one of these solutions, if either, is closest to the true solution?

The answer to this question is found by the realisation that the system (5.191) is numerically singular. In other words, there exist nonzero solutions $\widetilde{\boldsymbol{X}}$ to the system

$$\widetilde{\boldsymbol{T}}_{\mathrm{o}}\widetilde{\boldsymbol{X}} \;=\; \boldsymbol{0}\,. \tag{5.198}$$

In practical terms, we should speak of nonzero vectors $\widetilde{\boldsymbol{X}}$ such that $\widetilde{\boldsymbol{T}}_{\mathrm{o}}\widetilde{\boldsymbol{X}}$ is negligible. In this context, 'negligible' refers to quantities which are smaller than a certain tolerance, which is determined from $\widetilde{\boldsymbol{T}}_{\mathrm{o}}$ and ε. Here, ε is a quantity referred to as 'machine epsilon' and essentially characterises the distance between successive numbers in floating point arithmetic [92].

Numerical experiments for certain values of the constants of the problem show that the numerical nullity of $\widetilde{\boldsymbol{T}}_{\mathrm{o}}$ (the number of solutions to (5.198)) is 1 for $N \lesssim 200$ while (in the same range of N) the nullity of $\widetilde{\boldsymbol{T}}_{\mathrm{e}}$ is 0. We thus conclude that it is the odd method which is incorrect. In fact, by taking an appropriate multiple of the solution to (5.198) and adding it to the calculated solution of (5.191), we can recover the solution as given by the even method. Given that the even method appears to be more numerically accurate, we will henceforth only consider this method.

Thus we will be seeking the solution to the system

$$\boldsymbol{T}\boldsymbol{X} \;=\; \boldsymbol{R} \tag{5.199}$$

where $\boldsymbol{T} = \boldsymbol{T}_{\mathrm{e}}$ and $\boldsymbol{R} = \boldsymbol{R}_{\mathrm{e}}$. The system is scaled according to the theory of Section 5.4.1 before calculation.

5.4.3 Convergence acceleration

Now, we wish to be able to determine the solution of the system in the limit as $N \to \infty$. We introduce the notation $\chi_{\mathrm{m}}^{(N)}$ to denote the coefficient χ_{m} found from the numerical scheme with the submatrices of $\boldsymbol{T}$ truncated to size $N \times N$. A similar notation will hold for the other coefficients, *viz.* $\delta_n^{(N)}$, $\zeta_n^{(N)}$ and so forth. Unfortunately, the coefficients do not converge before the system becomes too large to solve in a reasonable amount of time. As an example, Figure 5.3 shows the behaviour of $\chi_{\mathrm{m}}^{(N)}$ as N increases, for a certain combination of geometric and material constants.

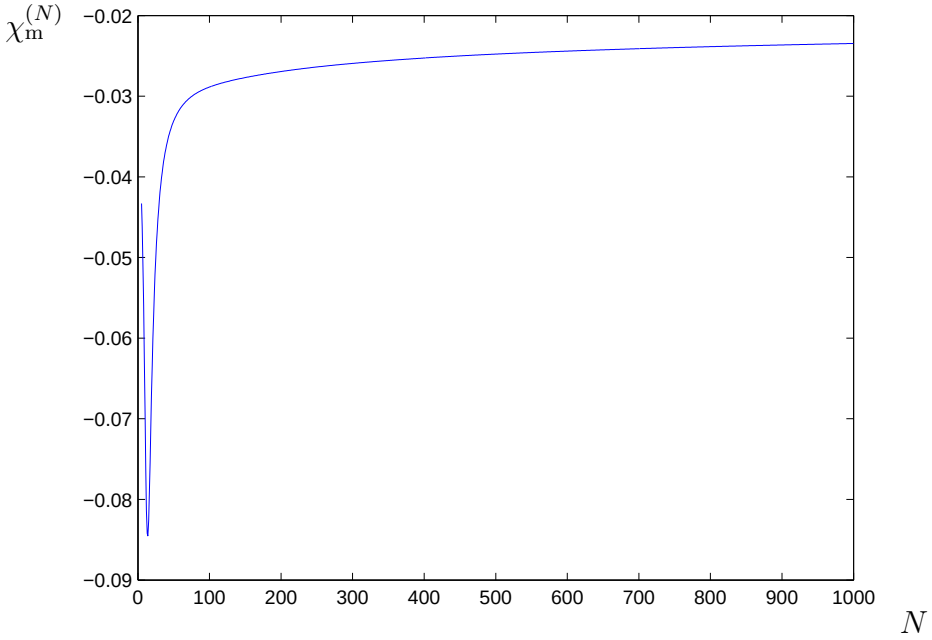

Figure 5.3: Plot of $\chi_{\mathrm{m}}^{(N)}$ for increasing N.

In this situation we must resort to using *convergence acceleration methods*. These methods take a sequence of the form

$$S_N \;=\; S + q_N \;, \tag{5.200}$$

where $q_N \to 0$ as $N \to \infty$. By taking the terms S_N and applying some transformation to them, a convergence acceleration method constructs a new sequence which is designed to converge more quickly to S.

Sequences can be categorised according to the behaviour of the sequence

$$\rho_N \quad := \quad \frac{S_{N+1} - S}{S_N - S} \quad = \quad \frac{q_{N+1}}{q_N} \,. \tag{5.201}$$

Defining

$$\rho \quad = \quad \lim_{N\to\infty} |\rho_N| \,, \tag{5.202}$$

we define sequences S_N which have $\rho = 0$ to be *hyperlinearly convergent*, those for which $0 < \rho < 1$ to be *linearly convergent*, and those for which $\rho = 1$ to be *logarithmically convergent* [45]. If $\rho > 1$, the sequence diverges.

Perhaps the best-known acceleration methods are the Shanks transformation and Richardson extrapolation [6]. However, in recent years a number of other acceleration methods have been developed. Smith and Ford [85] compared a number of these methods on a range of linearly and logarithmically convergent sequences for which the solutions are known. They showed that the best-performing schemes were the u and v Levin transforms and the Brezinski θ-method. However, applying these methods to our coefficients does not result in accelerated convergence. Thus our sequences must be especially hard to accelerate.

Logarithmically convergent sequences are known to be the most difficult to accelerate. A theorem by Delahaye and Germain-Bonne [26] shows that there is no one scheme that will accelerate every logarithmically convergent sequence. In general, the appropriate choice of scheme will depend on the form of the remainder terms q_N in (5.200). If the form of q_N is *not* known, as is the case for our coefficients, we must choose an acceleration scheme by other means. One way of doing so is by assuming that q_N is given by a certain expression, and apply a method which is designed for remainder terms of that form.

The form of q_N that we consider is given by

$$q_N \quad \sim \quad N^\sigma \left(c_0 + c_1 N^{-1} + c_2 N^{-2} + \cdots\right) \tag{5.203}$$

as $N \to \infty$, where $\sigma < 0$ is a constant. We know that the remainder terms of $\chi_{\mathrm{m}}^{(N)}$ and the other coefficients are not of this form, since Weniger [96] showed that sequences with this remainder term are accelerated by the Levin u-transform. However, we will search for other accelerating sequences designed for this form of q_N which also happen to accelerate the convergence of our coefficients. One such method is the *modified Aitken δ^2-method*, which was proposed by Bjørstad, Dahlquist and Grosse [9]. We will use the slightly modified method given by Osada [78].

Suppose that we are given a sequence S_N that satisfies $S_N - S = q_N$, where q_N is given in equation (5.203). Then define

$$s_0^0 = 0\,, \tag{5.204}$$

$$s_N^0 = S_N \qquad \text{for } N = 1, 2, \ldots, M. \tag{5.205}$$

Then, for $k = 0, 1, \ldots, \left\lfloor \frac{M}{2} \right\rfloor - 1$ we define

$$s_N^{k+1} = s_N^k - \left[\frac{2k+1-\sigma}{2k-\sigma} \right] \frac{(s_{N+1}^k - s_N^k)(s_N^k - s_{N-1}^k)}{s_{N+1}^k - 2s_N^k + s_{N-1}^k} \tag{5.206}$$

for $k+1 \leqslant N \leqslant M-(k+1)$. We find that

$$s_N^k - S = O(N^{\sigma-2k}) \tag{5.207}$$

as $N \to \infty$. Clearly, in order to use this method, the value of σ must be known beforehand. This causes problems if we want to apply it to the coefficients of $\boldsymbol{X}$, the solution of (5.199), as $N \to \infty$. Because we do not know the value of σ for this sequence (if indeed the sequence even satisfies (5.203)), we must determine it by other means.

For sequences that do satisfy (5.203), the constant σ can be constructed from the values of the sequence. Bjørstad, Dahlquist and Grosse [9] state that on defining

$$T_N = 1 + \frac{1}{\Delta\left(\dfrac{S_{N+1} - S_N}{S_{N+1} - 2S_N + S_{N-1}} \right)}\,, \tag{5.208}$$

where Δ is the forward difference operator, we have

$$T_N \sim \sigma + N^{-2}\left(t_0 + t_1 N^{-1} + t_2 N^{-2} + \cdots\right) \tag{5.209}$$

as $N \to \infty$. Thus σ can be found by applying the modified Aitken δ^2-method with $\sigma = -2$ to the sequence T_N.

However, given that the coefficients in our problem do not have remainder terms of the form (5.203), this method does not work as well as hoped. In addition, the values of the coefficients for large N have small errors in them, due to numerical inaccuracies in solving the original matrix system for $N \gtrsim 200$. These errors are magnified by the process of applying difference operators in the definition of the auxiliary sequence T_N.

Nevertheless, if we apply the modified Aitken δ^2-method to T_N, we find that for each coefficient ϕ_n, ψ_n, the resulting value of σ is broadly similar. The value of σ for the coefficients δ_n and ζ_n vary wildly (including obviously incorrect positive values), but as n increases the value tends to that for ψ_n and ϕ_n. These trends can be seen in Figure 5.4. Therefore, it is reasonable to assume that we can treat σ as a parameter of

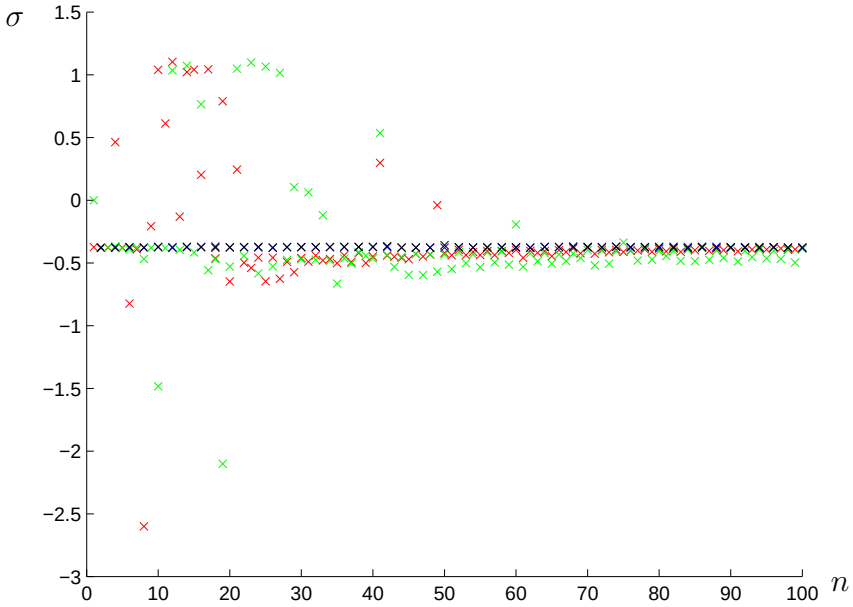

Figure 5.4: The value of σ as calculated by T_N for each coefficient: red (δ_n), green (ζ_n), blue (ψ_n), black (ϕ_n).

the whole problem, with each coefficient being found by applying the modified Aitken δ^2-method with the same value of σ. Unfortunately, this value is not determined by the sequence T_N — the limiting value found depends strongly on the number of terms taken in the acceleration process, and had not converged by the time we had taken the maximum number of terms.

However, by treating σ as a parameter of the problem, we can apply the δ^2-method to the whole problem, with differing values of σ, and determine the correct value by choosing the solution with the best behaviour. In this situation, 'best behaviour' is determined by the displacement of the outer boundary of the shell. We find that as we vary σ, the limiting values of the coefficients, as calculated by the δ^2-method, also vary. This results in a variation in the shell displacement components. In particular, we can evaluate the shell displacement component $u_\theta^{(\mathrm{s})}$, evaluated at $R = R_1$ and $\mu = 0$. Clearly this quantity should be zero. However, in general, this is not calculated to be the case. Denoting this offset by ℓ, we find that ℓ varies monotonically with σ. Using the same parameters as before, we find (through numerical experiments) that $\ell < 0$ when $\sigma = -0.5$, and that $\ell > 0$ when $\sigma = -0.05$. By a simple root-finding technique, we calculate that $\ell = 0$ is given by $\sigma = -0.119$ to three significant figures. These values were found by using the range of $N = 501, \ldots, 1000$.

Thus the correct coefficients for the problem should be given by the results of the δ^2-method with this value of σ. As a comparison with Figure 5.3, the value of

χ_{m} obtained by acceleration is -0.01044. Using these coefficients, we can determine the shell displacements. We can verify that the coefficients calculated are correct by overlaying the resulting plot of the deformed shell over the plot from a finite element computation.[2] For the uniaxial stress state at infinity that we have considered up to now, the overlay is shown in Figure 5.5. Note that it would not have been appropriate

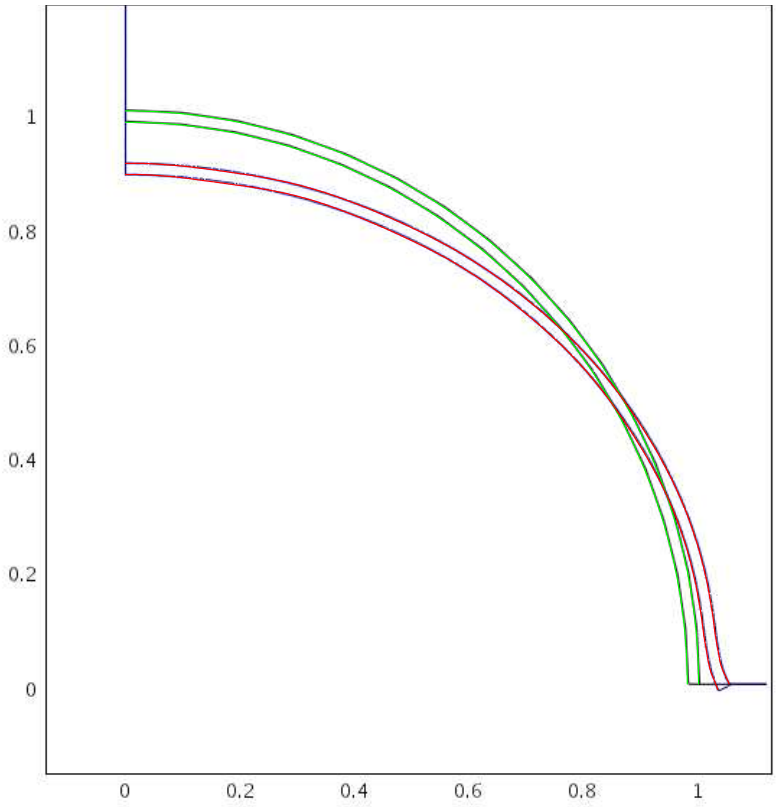

Figure 5.5: Overlay of the plot of the deformed shell found by using the convergence acceleration method (red) on the finite element result (blue).

to calculate the finite element result instead of the Love stress function calculation, because in Chapter 6 we will require the behaviour of the solution at infinity, which is readily found from the latter but impossible to measure from the finite element result.

We note that the parameter σ will depend on the material and geometric parameters of the problem. Thus, for each problem we consider, we must find σ separately. The problem under consideration is a *mixed boundary value problem*: in other words, along part of the boundary of the material, displacement boundary conditions apply whereas along the remainder, traction boundary conditions are imposed. It is known, for example from fracture mechanics problems, that there are in general singularities

[2]The finite element computation was made using the COMSOL Multiphysics package, formerly known as FEMLAB.

in the stress of the material near the points at which the two types of boundary condition meet. In linear elasticity, if the materials on either side of the transition point are the same, the singularity is an inverse square root singularity, as exemplified by Section 2.3 of this thesis. However, in this chapter the transition point between the boundary conditions is also the point at which two different materials meet. In this case, the singularity strength is a complicated function of the material and geometric parameters of the problem [24]. We speculate that the value of σ is in some way dependent on this singularity strength.

We can verify that the calculated value of σ is correct by considering that if

$$S_N \quad \sim \quad S + c_0 N^{\sigma} \tag{5.210}$$

as $N \to \infty$, then in the same limit we have

$$\log(|S_N - S|) \quad \sim \quad \sigma \log N + \text{constant}, \tag{5.211}$$

where S is the limiting value of the sequence as calculated by the convergence acceleration method. In Figure 5.6 we have plotted graphs of $\log(|S_N - S|)$ versus $\log(N)$, where S_N corresponds to $\delta_{20}^{(N)}$, $\zeta_{20}^{(N)}$, $\psi_{20}^{(N)}$ and $\phi_{20}^{(N)}$. Superimposed on these graphs are straight lines whose gradient is the calculated value of σ. We find that as $N \to \infty$ (so $\log N \to \infty$), the graphs agree, as expected. Thus our choice of σ appears to be validated.

5.5 Results for canonical stress states at infinity

Now that we have a method that finds the solution to the original problem in the limit as the size of the system of equations becomes infinite, we apply it to the case of two canonical stress states at infinity. We again choose the values given in Table 1.1, apart from the choice $\widehat{R} = 1$. These states are:

- Radial compression, or $q_z = 0$ and $q_R = q_{\mathrm{r}}$
- Pure shear, or $q_z = 3q_{\mathrm{s}}$ and $q_R = -q_{\mathrm{s}}$.

The reason for choosing these two states will become clear in Chapter 6, where these results will be used. The shell displacements which result from solving the linear system and accelerating the convergence are shown in Figures 5.7 and 5.8. As before, these were compared with finite element calculations and were shown to match. However, it is fair to note that if q is taken too large, numerical instabilities appear in the shell displacement plots. The values of σ for these calculations are, to three significant figures, $\sigma = -0.119$ for the radial case and $\sigma = -0.120$ for the pure shear case.

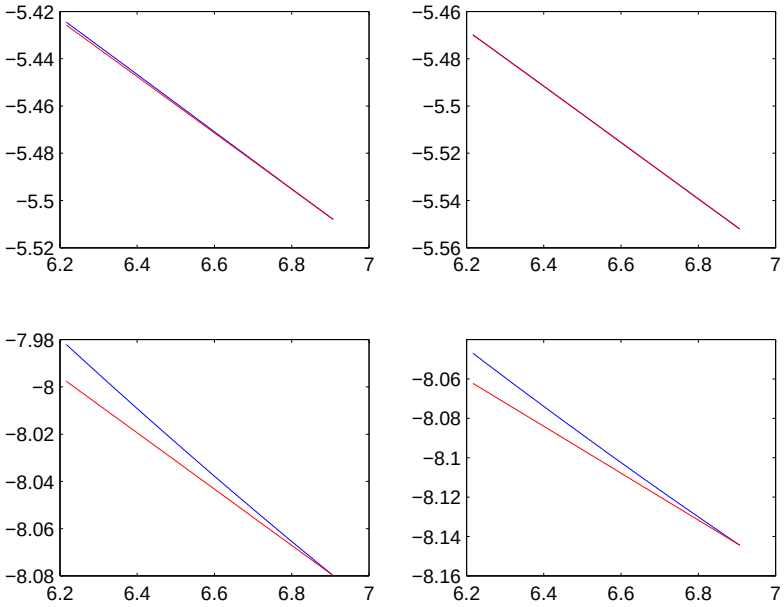

Figure 5.6: In blue: Comparison of $\log|S_N - S|$ (vertical axis) versus $\log N$, where (clockwise from top-left) $S_N = \delta_{20}^{(N)}$, $\zeta_{20}^{(N)}$, $\phi_{20}^{(N)}$ and $\psi_{20}^{(N)}$. In red: a straight line with gradient σ.

For the purposes of Chapter 6, we need to know the behaviour of the solution as $R \to \infty$. Referring to (5.98), we know that if $\mathscr{L}^\infty$ characterises the state of an infinite expanse of the matrix material undergoing a given applied stress, then $\mathscr{L}^{\rm P}$ is what needs to be added to this to account for the presence of the inclusion. By examining equations (5.102)–(5.105), we find that to leading-order these added terms are:

$$\tau_{RR}^{\rm P} = -\frac{2\chi_{\rm m}}{R^3} + \frac{4}{3}\left[(5-\nu_{\rm m})P_2^{(0)}(\mu) + (1-2\nu_{\rm m})P_0^{(0)}(\mu)\right]\frac{\psi_1}{R^3} + O(R^{-5}) \,, \quad (5.212)$$

$$\tau_{R\theta}^{\rm P} = -\frac{2}{3}(1+\nu_{\rm m})P_2^{(1)}(\mu)\frac{\psi_1}{R^3} + O(R^{-5}) \,, \quad (5.213)$$

$$u_R^{\rm P} = \frac{1}{2G_{\rm m}R^2}\left\{\chi_{\rm m} - \frac{2}{3}\left[(5-4\nu_{\rm m})P_2^{(0)}(\mu) + (1-2\nu_{\rm m})P_0^{(0)}(\mu)\right]\psi_1\right\} + O(R^{-4}) \,, \quad (5.214)$$

$$u_\theta^{\rm P} = -\frac{1}{2G_{\rm m}}\frac{2(1-2\nu_{\rm m})}{3}\frac{\psi_1}{R^2}P_2^{(1)}(\mu) + O(R^{-4}) \,. \quad (5.215)$$

Thus we can see that the leading order terms at infinity in the matrix depend on only two of the coefficients, namely $\chi_{\rm m}$ and ψ_1.

This means that we only need to calculate these two coefficients in both the radial compression and pure shear cases for the analysis of Chapter 6. Denoting the first

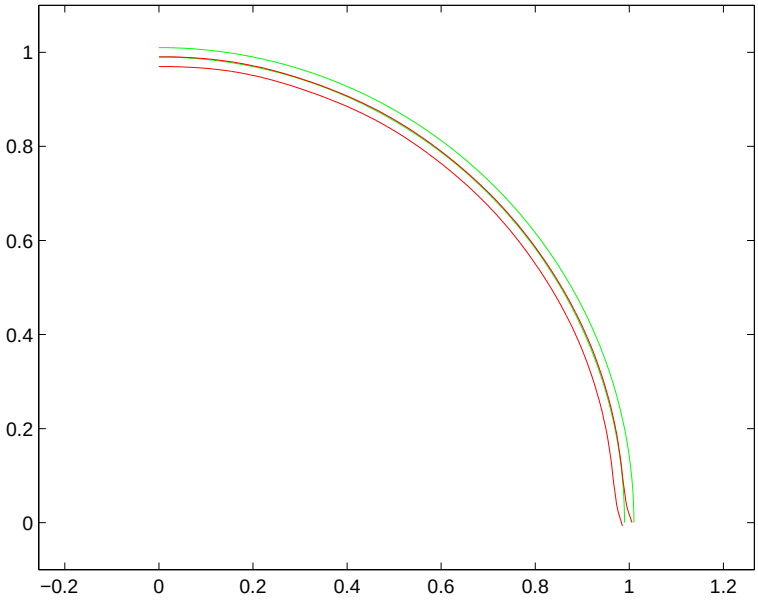

Figure 5.7: Shell displacement (red) for the radial compression case, where $q_{\mathrm{r}} = 0.3$.

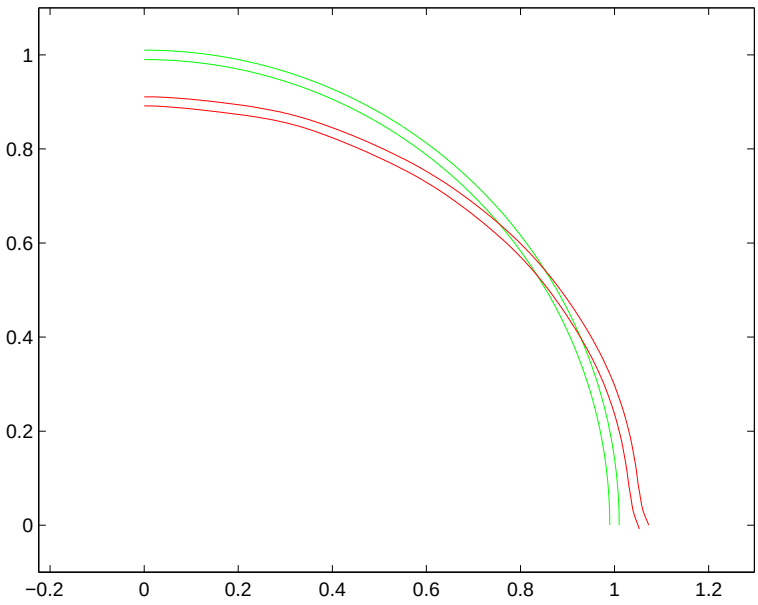

Figure 5.8: Shell displacement (red) for the pure shear case, where $q_{\mathrm{s}} = 0.1$.

case by a superscript 'r' and the second by a superscript 's', we find that

$$\chi_{\mathrm{m}}^{\mathrm{r}} = \widetilde{\chi}_{\mathrm{m}}^{\mathrm{r}} q_{\mathrm{r}} \,, \tag{5.216}$$

$$\psi_1^{\mathrm{r}} = \widetilde{\psi}_1^{\mathrm{r}} q_{\mathrm{r}} \,, \tag{5.217}$$

$$\chi_{\mathrm{m}}^{\mathrm{s}} = \widetilde{\chi}_{\mathrm{m}}^{\mathrm{s}} q_{\mathrm{s}} \,, \tag{5.218}$$

$$\psi_1^{\mathrm{s}} = \widetilde{\psi}_1^{\mathrm{s}} q_{\mathrm{s}} \,, \tag{5.219}$$

where

$$\widetilde{\chi}_{\mathrm{m}}^{\mathrm{r}} = -0.05014 \,, \tag{5.220}$$

$$\widetilde{\psi}_1^{\mathrm{r}} = 0.01761 \,, \tag{5.221}$$

$$\widetilde{\chi}_{\mathrm{m}}^{\mathrm{s}} = -0.06896 \,, \tag{5.222}$$

$$\widetilde{\psi}_1^{\mathrm{s}} = -0.5217 \,. \tag{5.223}$$

Finally, in the next chapter we will show that three of these coefficients will be related. In fact, from equation (6.311), we need that

$$4(1+\nu_{\mathrm{m}})\widetilde{\psi}_1^{\mathrm{r}} - 2(1-2\nu_{\mathrm{m}})\widetilde{\psi}_1^{\mathrm{s}} + 3\widetilde{\chi}_{\mathrm{m}}^{\mathrm{s}} = 0 \,. \tag{5.224}$$

Using the values in (5.220)–(5.223) and $\nu_{\mathrm{m}} = 0.45$, we calculate this quantity to be -3.90×10^{-4}. This is small in comparison with (5.220)–(5.223), so we suppose that it is the errors in the numerical method that cause it to be non-zero.

5.6 Discussion

During the course of this chapter, we have considered a problem which serves as a model of a shell which is weakened due to buckling around its equator. By considering Love stress functions in the matrix and shell, we were able to find a semi-analytical solution, which gave us the displacements and stresses as infinite series in Legendre polynomials, for which the coefficients had to be found by solving an infinite system of linear equations. This system was truncated to successively larger sizes, giving for each coefficient a sequence of values which didn't converge before the system became too large to solve. Instead we considered a convergence acceleration method which employed a parameter σ. This parameter was determined by demanding that the displacements of the shell and matrix matched at $\theta = \pi/2$.

Clearly, the one major weakness of this theory is the necessity of convergence acceleration methods. While the method seems to give results which match closely to finite element calculations, we cannot be sure if the coefficients obtained are correct, nor define how accurate they are. However, in the absence of knowledge about the true behaviour of the remainder terms q_N for the coefficients, and thus being able to

tailor an acceleration method for them, it appears that we must be content with the results obtained.

Further work, however, may be carried out to modify the solution method in such a way as to improve the convergence properties of the problem. Specifically, we suspect that the main culprit is the singularity in the material at the point where the crack in the shell meets the matrix. We have noted that the strength of this singularity is dependent on geometric and material parameters of the problem. If this strength is calculated, it may be feasible to consider the full solution as the sum of a singular field and a regular field, of which the latter may be calculated more easily using the approach of this chapter.

Asymptotic methods may also be used to simplify the problem in the limit as the shell thickness ratio $h/\widehat{R}$ tends to zero. However, Figure 5.5 shows that near the crack we would need to consider the full elastic solution, as the displacement varies over a lengthscale comparable with the shell thickness. This full solution would be obtained using numerical methods, leading to a hybrid asymptotic-numerical method for the solution of the problem.

Chapter 6

Homogenisation

In this chapter we will model the experiment described in Chapter 1. This will involve finding the displacement of the upper surface of a block of material undergoing uniaxial compression. Consequently we will require the elastic constants of the composite material, which will be found by a homogenisation process. This echoes the 'point-inclusion' process of Chapter 2, which calculated the shear modulus of a composite material undergoing antiplane shear, assuming that the inclusions were far apart. Section 6.2 reviews this work and applies it to arbitrarily-shaped inclusions, which introduces an element of anisotropy to the material. By this process we introduce the method which will be applied to three-dimensional inclusions.

The only information that we require for the homogenisation process is the behaviour of a single inclusion. If we know the leading-order displacement of an embedded inclusion which is experiencing an arbitrary stress field at infinity, then the behaviour of a dilute composite material composed of these inclusions can be deduced. This will be analysed in Section 6.3.1. Following this, in Section 6.3.2 we will determine the form of the elasticity tensor for such a material, if deformations are restricted to being axisymmetric. In Sections 6.3.3–6.3.4, we will specialise this result even further, namely to the pre-buckled shell described in Section 3.3 and the idealised post-buckled shell described in Chapter 5.

Finally we will model the experiment described in Chapter 1 by considering a block of the material which is experiencing a homogeneous stress field $\tau_{zz} = -q$. We will mirror the theory of Section 2.4.4 by using the results of Chapter 4 to determine at what stress q the inclusions buckle.

6.1 Homogenisation of composite materials

In the theory of homogenisation for linearly elastic materials, we consider a material whose elasticity tensor is variable in space,

$$A_{ijkl} \;=\; A_{ijkl}(\boldsymbol{x}) \;, \tag{6.1}$$

so that the stress–strain relation is given by

$$\tau_{ij}(\boldsymbol{x}) \;=\; A_{ijkl}(\boldsymbol{x})e_{kl}(\boldsymbol{x}) \;, \tag{6.2}$$

where τ_{ij} and e_{ij} are stress and strain tensors in the material. The variations in all the above quantities are assumed to be over a short lengthscale. Thus, on introducing an averaging process $\langle\cdot\rangle$, we can define an *effective elasticity tensor* $\widehat{A}_{ijkl}$ by

$$\langle\tau_{ij}\rangle \;=\; \widehat{A}_{ijkl}\langle e_{kl}\rangle \;, \tag{6.3}$$

which describes the deformation of the material on the macro-scale. The transition from (6.2) to (6.3) is non-trivial, and involves assumptions on the distribution and configuration of the microstructure of the material.

A material which consists of two or more phases of material — where the elasticity tensor $A_{ijkl}(\boldsymbol{x})$ is piecewise constant — is referred to as a *composite material*. Common examples of such materials are fibre-reinforced materials, lamellar materials and materials containing a certain proportion of inclusions of a different material. The analysis of such materials is relatively well-advanced [20, 69, 83].

We will be analysing materials for which the microstructure consists of a distribution of inclusions embedded in a continuous matrix. If these inclusions are spherical elastic bodies and dilutely dispersed in the matrix, the effective elasticity tensor was found by Hashin [42]. This result can be extended to ellipsoidal inclusions, using a method of Eshelby [30], who determined the state of deformation in a single ellipsoidal inclusion embedded in a matrix.

To find the elasticity tensor when the inclusions are *not* dilutely dispersed, we need to consider the interaction of inclusions with each other. Additionally it is necessary to describe the distribution of the inclusions. For identical randomly-dispersed spherical inclusions this problem was considered by Chen and Acrivos [19] and a better approximation was obtained.

The inclusions which we will study are not of the type that can by analysed by Eshelby's method, because they are not solid elastic inclusions. Instead, we will use the known solution of a single inclusion in the matrix, and determine the effective material properties for dilutely-dispersed inclusions by matching this solution to an 'outer' solution where the inclusions are regarded as points (hence the 'point-inclusion' model).

6.2 Return to antiplane strain

We begin, however, by reconsidering the point-inclusion method of Section 2.4.2. Recall that we solved the problem for a circular inclusion undergoing an antiplane shear at infinity. Where the stress at infinity was given by

$$G_{\mathrm{m}}\nabla f \;=\; \tau_0\widehat{\boldsymbol{p}}\,, \tag{6.4}$$

we found that the displacement field in the matrix was given by

$$f \;=\; \frac{\tau_0}{G_{\mathrm{m}}}\left(\widehat{\boldsymbol{p}}\cdot\boldsymbol{x}+\frac{a^2 s}{|\boldsymbol{x}|^2}\widehat{\boldsymbol{p}}\cdot\boldsymbol{x}\right)\,. \tag{6.5}$$

In this expression, G_{m} is the matrix shear modulus, a is the inclusion radius and s is the compliance parameter given by equation (2.273). We can consider this displacement field as a 'bulk' response which would be the solution in the absence of the inclusion, plus the 'perturbation' solution $\widetilde{f}$ which arises due to the presence of the inclusion. Here we have

$$\widetilde{f} \;=\; \frac{\tau_0}{G_{\mathrm{m}}}\frac{a^2 s}{|\boldsymbol{x}|^2}\widehat{\boldsymbol{p}}\cdot\boldsymbol{x}\,. \tag{6.6}$$

Subsequently, we took the corresponding outer displacement to this inner displacement and found that it was the solution to equation (2.297). This equation was then the basis of our homogenisation method. Now, while this homogenisation method gave a satisfactory result for the case of a distribution of circular inclusions, we cannot immediately transfer the result to three-dimensional inclusions without a deeper understanding of the homogenisation process. To illustrate this, we will consider the homogenisation of *non-circular* inclusions.

It can be shown [70] that if we had considered an arbitrarily-shaped inclusion in an infinite matrix undergoing antiplane shear at infinity, then the displacement field f in the matrix is again given by

$$f \;\sim\; \frac{\tau_0}{G_{\mathrm{m}}}\widehat{\boldsymbol{p}}\cdot\boldsymbol{x}+\widetilde{f}\,, \tag{6.7}$$

where the perturbation field in this case is given by

$$\widetilde{f} \;=\; \frac{\tau_0}{G_{\mathrm{m}}}M_{ij}\widehat{p}_i\frac{x_j}{|\boldsymbol{x}|^2}+O(|\boldsymbol{x}|^{-2}) \tag{6.8}$$

as $|\boldsymbol{x}|\to\infty$, applying the summation convention for $i,j=1,2$. The 2×2 symmetric matrix $-2\pi G_{\mathrm{m}}M_{ij}$ is referred to in [70] as the *Pólya–Szegő matrix*, and elsewhere as the *polarisability tensor*. For comparison we note that for the case of a circular inclusion we have

$$M_{ij} \;=\; a^2 s\delta_{ij}\,. \tag{6.9}$$

Now, we will naïvely apply the point-inclusion homogenisation process to equation (6.7). We readily find that f satisfies the equation

$$\nabla^2 f \;=\; 2\pi M_{ij}\left[\lim_{|\boldsymbol{x}|\to\infty}\frac{\partial f}{\partial x_i}\right]\frac{\partial \delta(\boldsymbol{x})}{\partial x_j}\,. \tag{6.10}$$

Homogenising to a distribution of inclusions in the manner of Section 2.4.2 gives

$$\nabla^2 f \;=\; 2\pi M_{ij}\frac{\partial f}{\partial x_i}\frac{\partial \omega}{\partial x_j}\,. \tag{6.11}$$

Now, if we consider a material with an effective modulus $\widehat{G}_{ij}$, then the displacement in such a material would satisfy the equation

$$\frac{\partial}{\partial x_i}\left(\widehat{G}_{ij}\frac{\partial f}{\partial x_j}\right) \;=\; 0 \tag{6.12}$$

$$\Rightarrow \qquad \widehat{G}_{ij}\frac{\partial^2 f}{\partial x_i \partial x_j} \;=\; -\frac{\partial \widehat{G}_{ij}}{\partial x_i}\frac{\partial f}{\partial x_j}\,. \tag{6.13}$$

However, we now notice that there is no way of comparing equations (6.11) and (6.13), unless $\widehat{G}_{ij}$ is a scalar multiple of δ_{ij}. We must therefore be a little more sophisticated in our analysis.

6.2.1 The inner and outer solutions

Before reappraising the homogenisation process, we will take into consideration the different scales in the problem. We note that the model assumes that the inclusions are of the order a in length, with their centres being separated by a length of order b, as shown in Figure 6.1. We choose the inclusions to be of size $2a$ so that circular inclusions have radius a. The ratio

$$\varepsilon \;=\; \frac{a}{b} \tag{6.14}$$

is assumed to be small. We refer to the two cases A and B in Figure 6.1 to be the inner and outer regimes respectively. The inner region considers the lengthscale to be that of the inclusions, with each inclusion being infinitely far apart. Conversely the outer region has the inclusion separation as its lengthscale and considers the inclusions to be points in the plane. We can thus construct nondimensional spatial variables in these two regimes. We will label the inclusions by d, which ranges over $1, 2, \ldots, D$. If $\boldsymbol{x}$ refers to the dimensional variable centred on an inclusion d, then the dimensionless inner variable $\widetilde{\boldsymbol{x}}^{(d)}$ near that inclusion can be found by

$$\widetilde{\boldsymbol{x}}^{(d)} \;=\; \frac{\boldsymbol{x}}{a}\,. \tag{6.15}$$

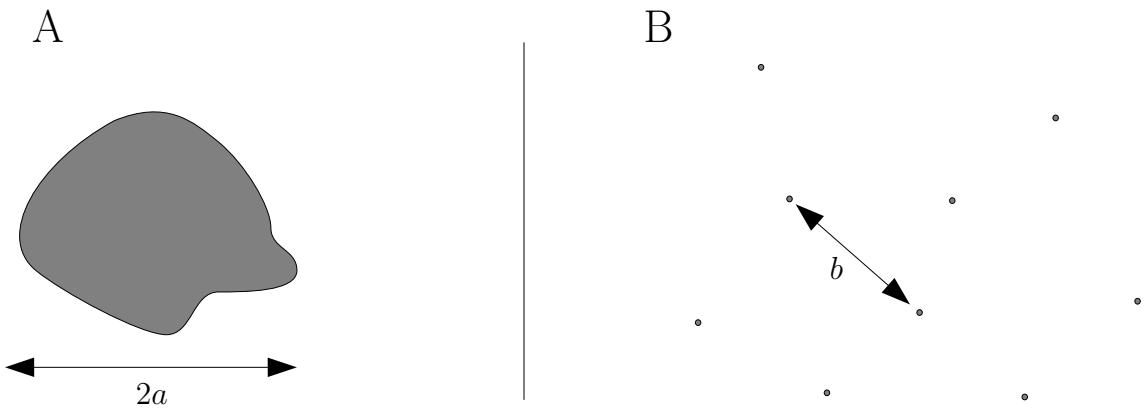

Figure 6.1: Length scales for one inclusion (A) and the separation (B).

Now, we will denote the dimensionless outer variable by $\widetilde{\boldsymbol{X}}$. If the inclusions in the outer region are placed at the points $\widetilde{\boldsymbol{X}}^d$ for $d = 1, \ldots, D$, then the inner variable around inclusion d is linked to the outer variable by the relation

$$\widetilde{\boldsymbol{X}} \;=\; \widetilde{\boldsymbol{X}}^d + \varepsilon \widetilde{\boldsymbol{x}}^{(d)} \,. \tag{6.16}$$

We can reconstruct a *dimensional* outer variable by scaling this quantity by b, or

$$\boldsymbol{X} \;=\; b\widetilde{\boldsymbol{X}} \,. \tag{6.17}$$

Now, we will analyse the displacement in both inner and outer regimes. Recall that the displacement in the inner problem satisfied

$$f \;=\; c_i \left(x_i + \frac{M_{ij} x_j}{|\boldsymbol{x}|^2} \right) + O(|\boldsymbol{x}|^{-2}) \,, \tag{6.18}$$

where c_i is the displacement gradient at infinity, or

$$c_i \;=\; \left. \frac{\partial f}{\partial x_i} \right|_{|\boldsymbol{x}| \to \infty} \,. \tag{6.19}$$

However, in general the constants c_i will be different for each inclusion. In addition, we note that the displacement can be made subject to a rigid body displacement β parallel to the z-axis without changing the nature of the deformation, because the inclusions which are attached to the matrix would also be subject to the same rigid body displacement. This β will also be different from inclusion to inclusion.

Labelling the inclusions by d, we thus have the inner solution f_{A}^d for the displacement,

$$f_{\mathrm{A}}^d \;=\; \beta^d + c_i^d x_i + \frac{c_i^d M_{ij} x_j}{|\boldsymbol{x}|^2} + O(|\boldsymbol{x}|^{-2}) \,, \tag{6.20}$$

in the vicinity of inclusion d. This expression can be nondimensionalised using the scaling (6.15) to give

$$f_{\rm A}^d \;=\; \beta^d + a c_i^d \widetilde{x}_i^{(d)} + \frac{c_i^d M_{ij}}{a} \frac{\widetilde{x}_j^{(d)}}{|\widetilde{\boldsymbol{x}}^{(d)}|^2} + O(|\widetilde{\boldsymbol{x}}^{(d)}|^{-2}) \;. \tag{6.21}$$

Writing

$$\widetilde{c}_i^d \;=\; a c_i^d \;, \tag{6.22}$$

$$\widetilde{M}_{ij} \;=\; \frac{1}{a^2} M_{ij} \;, \tag{6.23}$$

we have

$$f_{\rm A}^d \;=\; \beta^d + \widetilde{c}_i^d \widetilde{x}_i^{(d)} + \widetilde{c}_i^d \widetilde{M}_{ij} \frac{\widetilde{x}_j^{(d)}}{|\widetilde{\boldsymbol{x}}^{(d)}|^2} + O(|\widetilde{\boldsymbol{x}}^{(d)}|^{-2}) \;. \tag{6.24}$$

Now, we know from equation (6.10) that by taking the Laplacian of (6.24) in the inner variables $\widetilde{\boldsymbol{x}}^{(d)}$, we obtain

$$\nabla^2_{\widetilde{\boldsymbol{x}}} f_{\rm A}^d \;=\; 2\pi \widetilde{c}_i^d \widetilde{M}_{ij} \frac{\partial \delta(\widetilde{\boldsymbol{x}}^{(d)})}{\partial \widetilde{x}_j^{(d)}} \;. \tag{6.25}$$

Changing to outer variables according to (6.16), we find that the *outer* displacement $f_{\rm B}$ due to inclusion d satisfies

$$\varepsilon^2 \nabla^2_{\widetilde{\boldsymbol{X}}} f_{\rm B} \;=\; 2\pi \varepsilon^3 \widetilde{c}_i^d \widetilde{M}_{ij} \frac{\partial \delta(\widetilde{\boldsymbol{X}} - \widetilde{\boldsymbol{X}}^d)}{\partial \widetilde{X}_j} \;. \tag{6.26}$$

But this is true for each $d = 1, 2, \ldots, D$, so

$$\nabla^2_{\widetilde{\boldsymbol{X}}} f_{\rm B} \;=\; 2\pi \varepsilon \widetilde{M}_{ij} \sum_{d=1}^{D} \widetilde{c}_i^d \frac{\partial \delta(\widetilde{\boldsymbol{X}} - \widetilde{\boldsymbol{X}}^d)}{\partial \widetilde{X}_j} \;. \tag{6.27}$$

This equation can be solved to give

$$f_{\rm B} \;=\; Q(\widetilde{\boldsymbol{X}}) + \varepsilon \widetilde{M}_{ij} \sum_{d=1}^{D} \frac{\widetilde{c}_i^d (\widetilde{X}_j - \widetilde{X}_j^d)}{|\widetilde{\boldsymbol{X}} - \widetilde{\boldsymbol{X}}^d|^2} \;, \tag{6.28}$$

where $Q(\widetilde{\boldsymbol{X}})$ is some displacement field that satisfies

$$\nabla^2_{\widetilde{\boldsymbol{X}}} Q(\widetilde{\boldsymbol{X}}) \;=\; 0 \;. \tag{6.29}$$

Now that we have the displacement in the outer solution, we can find the coefficients β^d and $\widetilde{c}_i^d$ in terms of $Q(\widetilde{\boldsymbol{X}})$ by matching the inner solution (6.24) to the outer solution (6.28) using van Dyke's matching rule. This rule states that if we take m terms of the inner solution and expand them in n terms of the outer variable, the

resulting expression will equal n terms of the outer solution expanded in m terms of the inner variable. We write

$$(n\text{to})(m\text{ti}) \;=\; (m\text{ti})(n\text{to})\;, \tag{6.30}$$

where 'ti' stands for 'terms inner' and 'to' stands for 'terms outer'. Taking the outer solution (6.28) and expanding $Q(\widetilde{\boldsymbol{X}})$ in an asymptotic solution

$$Q(\widetilde{\boldsymbol{X}}) \;=\; Q^{(0)}(\widetilde{\boldsymbol{X}}) + \varepsilon Q^{(1)}(\widetilde{\boldsymbol{X}}) + \varepsilon^2 Q^{(2)}(\widetilde{\boldsymbol{X}}) + \cdots\;, \tag{6.31}$$

we find that

$$\begin{aligned}
(1\text{to}) \;&=\; Q^{(0)}(\widetilde{\boldsymbol{X}}) && (6.32)\\
&=\; Q^{(0)}(\widetilde{\boldsymbol{X}}^d + \varepsilon\widetilde{\boldsymbol{x}}^{(d)}) && (6.33)\\
&=\; Q^{(0)}(\widetilde{\boldsymbol{X}}^d) + \varepsilon\widetilde{\boldsymbol{x}}^{(d)}\cdot(\nabla_{\widetilde{\boldsymbol{X}}}Q^{(0)})\big|_{\widetilde{\boldsymbol{X}}=\widetilde{\boldsymbol{X}}^d} + \cdots\;, && (6.34)
\end{aligned}$$

so that

$$\begin{aligned}
(1\text{ti})(1\text{to}) \;&=\; Q^{(0)}(\widetilde{\boldsymbol{X}}^d)\;, && (6.35)\\
(2\text{ti})(1\text{to}) \;&=\; Q^{(0)}(\widetilde{\boldsymbol{X}}^d) + \varepsilon\widetilde{\boldsymbol{x}}^{(d)}\cdot(\nabla_{\widetilde{\boldsymbol{X}}}Q^{(0)})\big|_{\widetilde{\boldsymbol{X}}=\widetilde{\boldsymbol{X}}^d}\;. && (6.36)
\end{aligned}$$

These will be compared to the corresponding expansions of the inner solution in terms of outer variables. We expand β^d and $\widetilde{c}_i^d$ in asymptotic expansions,

$$\begin{aligned}
\beta^d \;&=\; (\beta^d)_0 + \varepsilon(\beta^d)_1 + \cdots\;, && (6.37)\\
\widetilde{c}_i^d \;&=\; (\widetilde{c}_i^d)_0 + \varepsilon(\widetilde{c}_i^d)_1 + \cdots\;. && (6.38)
\end{aligned}$$

For consistent matching, we find that we require $(\widetilde{c}_i^d)_0 = 0$. Then

$$\begin{aligned}
(1\text{to})(1\text{ti}) \;&=\; (\beta^d)_0\;, && (6.39)\\
(1\text{to})(2\text{ti}) \;&=\; (\beta^d)_0 + (\widetilde{c}_i^d)_1(\widetilde{X}_i - \widetilde{X}_i^d)\;. && (6.40)
\end{aligned}$$

Equating (6.35)–(6.36) with (6.39)–(6.40), we find that

$$\begin{aligned}
(\beta^d)_0 \;&=\; Q^{(0)}(\widetilde{\boldsymbol{X}}^d)\;, && (6.41)\\
(\widetilde{c}_i^d)_1 \;&=\; \frac{\partial Q^{(0)}}{\partial\widetilde{X}_i}\bigg|_{\widetilde{\boldsymbol{X}}=\widetilde{\boldsymbol{X}}^d}\;. && (6.42)
\end{aligned}$$

The result (6.42) is substituted into equation (6.28) to obtain the first three terms in the outer displacement,

$$\begin{aligned}
f_{\text{B}} \;=\;& Q^{(0)}(\widetilde{\boldsymbol{X}}) + \varepsilon Q^{(1)}(\widetilde{\boldsymbol{X}}) + \varepsilon^2 Q^{(2)}(\widetilde{\boldsymbol{X}})\\
&+\varepsilon^2\widetilde{M}_{ij}\sum_{d=1}^{D}\frac{\partial Q^{(0)}}{\partial\widetilde{X}_i}\bigg|_{\widetilde{\boldsymbol{X}}=\widetilde{\boldsymbol{X}}^d}\frac{(\widetilde{X}_j - \widetilde{X}_j^d)}{|\widetilde{\boldsymbol{X}} - \widetilde{\boldsymbol{X}}^d|^2}\;. \qquad (6.43)
\end{aligned}$$

Now that we have determined the first three terms in the outer displacement, we will now use this expansion to find the effective shear modulus of a material containing a distribution of inclusions.

6.2.2 The averaging operator

We first introduce an averaging operator, as used by Chapman [18] in the context of homogenising vortices in superconductors. Suppose that we have a material containing a discrete distribution of inclusions. Suppose also that we have a quantity $\Phi(\boldsymbol{X})$ which is defined on this domain, in terms of the *dimensional* spatial variable $\boldsymbol{X}$. Then the effective value of Φ in the material is defined by

$$\widehat{\Phi}(\boldsymbol{\xi}) \;=\; \langle \Phi(\boldsymbol{X}) \rangle \;, \tag{6.44}$$

where $\langle \cdot \rangle$ is an averaging operator given by

$$\langle \Phi(\boldsymbol{X}) \rangle \;=\; \lim_{c \to 0} \frac{1}{\pi c^2} \int_{|\boldsymbol{X}-\boldsymbol{\xi}|<c} \Phi(\boldsymbol{X}) \, \mathrm{d}^2 \boldsymbol{X} \;, \tag{6.45}$$

where $\boldsymbol{\xi}$ is the position of the centre of the circle over which the integration is performed. In the definition (6.45), the limiting process occurs in such a way that the separation b of the inclusions tends to zero at the same time as $c \to 0$, with $b \ll c$ at all times.

We define a *number density* of inclusions by

$$\omega(\boldsymbol{\xi}) \;=\; \lim_{c \to 0} \frac{1}{\pi c^2} \int_{|\boldsymbol{X}-\boldsymbol{\xi}|<c} \sum_{d=1}^{D} \delta(\boldsymbol{X} - \boldsymbol{X}^d) \, \mathrm{d}^2 \boldsymbol{X} \;, \tag{6.46}$$

where the summation is over all inclusions in the integration domain. The relationship between the separation b and the scale c of the integration region is the same as above.

All these quantities are defined for functions of the dimensional variable $\boldsymbol{X}$, whereas we will be averaging quantities which are defined in terms of the dimensionless spatial variable $\widetilde{\boldsymbol{X}}$. To find this, we take (6.45) and change variables to $\widetilde{\boldsymbol{X}}$ by equation (6.17). We find that

$$\langle \Phi(\widetilde{\boldsymbol{X}}) \rangle \;=\; \lim_{c \to 0} \frac{1}{\pi c^2} \int_{|\widetilde{\boldsymbol{X}}-\widetilde{\boldsymbol{\xi}}|<c/b} \Phi(\widetilde{\boldsymbol{X}}) b^2 \, \mathrm{d}^2 \widetilde{\boldsymbol{X}} \tag{6.47}$$

$$\;=\; \lim_{c \to 0} \frac{1}{\pi \rho^2} \int_{|\widetilde{\boldsymbol{X}}-\widetilde{\boldsymbol{\xi}}|<\rho} \Phi(\widetilde{\boldsymbol{X}}) \, \mathrm{d}^2 \widetilde{\boldsymbol{X}} \;, \tag{6.48}$$

where we have assumed that $c = \rho b$ for some $\rho \gg 1$. Then the expression above is independent of c, so that

$$\langle \Phi(\widetilde{\boldsymbol{X}}) \rangle \;=\; \frac{1}{\pi \rho^2} \int_{|\widetilde{\boldsymbol{X}}-\widetilde{\boldsymbol{\xi}}|<\rho} \Phi(\widetilde{\boldsymbol{X}}) \, \mathrm{d}^2 \widetilde{\boldsymbol{X}} \;. \tag{6.49}$$

Thus we are integrating over a large region, keeping the separation of the inclusions constant. In this formulation, we find that the dimensionless density function is given

by

$$\widetilde{\omega}(\widetilde{\boldsymbol{\xi}}) = \left\langle \sum_{d=1}^{D} \delta(\widetilde{\boldsymbol{X}} - \widetilde{\boldsymbol{X}}^d) \right\rangle \tag{6.50}$$

$$= b^2 \left\langle \sum_{d=1}^{D} \delta(\boldsymbol{X} - \boldsymbol{X}^d) \right\rangle \tag{6.51}$$

$$= b^2 \omega(\boldsymbol{\xi}) \, . \tag{6.52}$$

Finally, it can be shown that

$$\lim_{c \to 0} \frac{1}{\pi c^2} \sum_{d=1}^{D} \Phi(\boldsymbol{X}^d) = \left\langle \Phi(\boldsymbol{X}) \sum_{d=1}^{D} \delta(\boldsymbol{X} - \boldsymbol{X}^d) \right\rangle \tag{6.53}$$

$$\approx \langle \Phi(\boldsymbol{X}) \rangle \, \omega(\boldsymbol{\xi}) \, , \tag{6.54}$$

if ω is assumed to be slowly-varying in $\boldsymbol{\xi}$. Equivalently, for functions defined in terms of dimensionless variables,

$$\frac{1}{\pi \rho^2} \sum_{d=1}^{D} \Phi(\widetilde{\boldsymbol{X}}^d) = \left\langle \Phi(\widetilde{\boldsymbol{X}}) \sum_{d=1}^{D} \delta(\widetilde{\boldsymbol{X}} - \widetilde{\boldsymbol{X}}^d) \right\rangle \tag{6.55}$$

$$\approx \langle \Phi(\widetilde{\boldsymbol{X}}) \rangle \widetilde{\omega}(\widetilde{\boldsymbol{\xi}}) \, . \tag{6.56}$$

6.2.3 The homogenisation process

In this section we will write $\boldsymbol{X}$, M_{ij} and $\omega(\boldsymbol{\xi})$ instead of $\widetilde{\boldsymbol{X}}$, $\widetilde{M}_{ij}$ and $\widetilde{\omega}(\widetilde{\boldsymbol{\xi}})$, for clarity.

We take the displacement (6.43) and form its gradient e_i.[1] On differentiating, we obtain

$$e_i = \frac{\partial f_{\mathrm{B}}}{\partial X_i} = \frac{\partial Q^{(0)}}{\partial X_i} + \varepsilon \frac{\partial Q^{(1)}}{\partial X_i} + \varepsilon^2 \frac{\partial Q^{(2)}}{\partial X_i} + \varepsilon^2 M_{kj} \sum_{d=1}^{D} \left. \frac{\partial Q^{(0)}}{\partial X_k} \right|_{\boldsymbol{X} = \boldsymbol{X}^d} H_{ij}(\boldsymbol{X} - \boldsymbol{X}^d) \, , \tag{6.57}$$

where

$$H_{ij}(\boldsymbol{X}) = H_{ji}(\boldsymbol{X}) = \frac{\partial}{\partial X_i} \left(\frac{X_j}{|\boldsymbol{X}|^2} \right) \tag{6.58}$$

$$= \frac{\delta_{ij} |\boldsymbol{X}|^2 - 2 X_i X_j}{|\boldsymbol{X}|^4} \, . \tag{6.59}$$

The expressions (6.43) and (6.57) above comprise only the first two terms of an asymptotic expansion of those quantities, and they hold everywhere except for an arbitrarily small neighbourhood of the inclusions, *i.e.* for $\boldsymbol{X} \in \Omega^*$, where

$$\Omega^* = \bigcap_{d=1}^{D} \left\{ \boldsymbol{X} \, : \, |\boldsymbol{X} - \boldsymbol{X}^d| > \eta \right\} \tag{6.60}$$

[1] The strain field, which is a vector for antiplane deformations because the displacement is constrained to one direction, is given by $\frac{1}{2} e_i$.

for some arbitrarily small $\eta > 0$.

The stress field τ_i in the material will be given by

$$\tau_i \;=\; G_{ij}(\boldsymbol{X})e_j \;, \tag{6.61}$$

where $G_{ij}(\boldsymbol{X})$ is the shear modulus of the material. Considering $\boldsymbol{X} \in \Omega^*$, we have

$$G_{ij}(\boldsymbol{X})|_{\boldsymbol{X}\in\Omega^*} \;=\; G_{\mathrm{m}}\delta_{ij} \;, \tag{6.62}$$

since the material in Ω^* is the matrix (as the inclusions are considered to be points). The value of $G_{ij}(\boldsymbol{X})$ at the inclusions is not known, however we do know that the stress field τ_i is continuous throughout the material. The stress field also satisfies the equilibrium condition,

$$\frac{\partial \tau_i}{\partial X_i} \;=\; 0 \;. \tag{6.63}$$

We define the *polarisation* [69] to be the vector field given by

$$p_i(\boldsymbol{X}) \;=\; G_{ij}(\boldsymbol{X})e_j - G_{\mathrm{m}}e_i \tag{6.64}$$

$$\;=\; \tau_i - G_{\mathrm{m}}e_i \;. \tag{6.65}$$

If we apply the averaging operator to this quantity, we find that

$$\langle p_i \rangle \;=\; \langle \tau_i \rangle - G_{\mathrm{m}}\langle e_i \rangle \;. \tag{6.66}$$

However, the definition of an effective shear modulus $\widehat{G}_{ij}$, echoing (6.3), is that

$$\langle \tau_i \rangle \;=\; \widehat{G}_{ij}\langle e_j \rangle \;. \tag{6.67}$$

Hence

$$\widehat{G}_{ij}\langle e_j \rangle \;=\; G_{\mathrm{m}}\langle e_i \rangle + \langle p_i \rangle \;. \tag{6.68}$$

Thus, if we can determine the effective polarisation $\langle p_i \rangle$ as a multiple of the effective strain field $\langle e_i \rangle$, we can determine the effective shear modulus.

To analyse the effective polarisation, we recall from equation (6.49) that

$$\langle p_i \rangle \;=\; \frac{1}{\pi\rho^2}\int_{|\boldsymbol{X}-\boldsymbol{\xi}|<\rho} p_i \,\mathrm{d}^2\boldsymbol{X} \;, \tag{6.69}$$

since p_i is defined in terms of the nondimensional spatial coordinates. However, by the expressions (6.62) and (6.64), we have $p_i = 0$ for $\boldsymbol{X} \in \Omega^*$. Hence the integrand in (6.69) is zero apart from in a vicinity of each inclusion. Hence

$$\langle p_i \rangle \;=\; \frac{1}{\pi\rho^2}\sum_{d=1}^{D}\int_{|\boldsymbol{X}-\boldsymbol{X}^d|<\eta} p_i \,\mathrm{d}^2\boldsymbol{X} \;, \tag{6.70}$$

where the sum is over all inclusions in the domain of integration. We will write

$$\langle p_i \rangle \;=\; \frac{1}{\pi\rho^2}[p_i]\;, \tag{6.71}$$

where

$$[p_i] \;=\; \sum_{d=1}^{D} \int_{|\boldsymbol{X}-\boldsymbol{X}^d|<\eta} p_i \,\mathrm{d}^2\boldsymbol{X}\;. \tag{6.72}$$

Consider now the integral of p_i over an arbitrary domain Ω. We obtain, on using the divergence theorem and the equilibrium equation, (6.63),

$$\begin{aligned}
\int_\Omega p_i \,\mathrm{d}^2\boldsymbol{X} &= \int_\Omega (\tau_i - G_\mathrm{m} e_i)\,\mathrm{d}^2\boldsymbol{X} && (6.73)\\
&= \int_\Omega \left[\frac{\partial}{\partial X_j}(X_i\tau_j) - G_\mathrm{m}\frac{\partial f}{\partial X_i}\right]\,\mathrm{d}^2\boldsymbol{X} && (6.74)\\
&= \int_{\partial\Omega} [X_i\tau_j n_j - G_\mathrm{m} f n_i]\,\mathrm{d}S\;, && (6.75)
\end{aligned}$$

where n_i are the components of the unit outward normal to Ω. Thus, (6.72) becomes

$$[p_i] \;=\; \sum_{d=1}^{D} \int_{|\boldsymbol{X}-\boldsymbol{X}^d|=\eta} \left[(X_i - X_i^d)\tau_j n_j - G_\mathrm{m} f n_i\right]\,\mathrm{d}S\;. \tag{6.76}$$

However, because the stress is continuous throughout the material, we have $\tau_j = G_\mathrm{m} e_j$ along this contour. In addition, $(X_i - X_i^d) = \eta n_i$ here. Hence

$$[p_i] \;=\; G_\mathrm{m} \sum_{d=1}^{D} \int_{|\boldsymbol{X}-\boldsymbol{X}^d|=\eta} [\eta e_j n_i n_j - f n_i]\,\mathrm{d}S\;. \tag{6.77}$$

Given that η is arbitrarily small, we can analyse this expression in the limit $\eta \to 0$. At any singularity d, we can separate the expressions for strain and displacements into terms which are bounded and unbounded respectively. From (6.43) and (6.57), the leading part of the unbounded terms at the singularity d are given by

$$\begin{aligned}
f^* &= \varepsilon^2 M_{ij} \left.\frac{\partial Q^{(0)}}{\partial X_i}\right|_{\boldsymbol{X}=\boldsymbol{X}^d} \frac{(X_j - X_j^d)}{|\boldsymbol{X}-\boldsymbol{X}^d|^2}\;, && (6.78)\\
e_i^* &= \varepsilon^2 M_{kj} \left.\frac{\partial Q^{(0)}}{\partial X_k}\right|_{\boldsymbol{X}=\boldsymbol{X}^d} H_{ij}(\boldsymbol{X}-\boldsymbol{X}^d)\;. && (6.79)
\end{aligned}$$

Now, for each inclusion d, if the integrand in (6.77) is bounded as $\boldsymbol{X} \to \boldsymbol{X}^d$, then the integral tends to zero in the limit $\eta \to 0$. Thus we need only consider the unbounded terms in calculating the effective polarisation, so that

$$[p_i] \;=\; G_\mathrm{m} \sum_{d=1}^{D} \int_{|\boldsymbol{X}-\boldsymbol{X}^d|=\eta} \left[\eta e_j^* n_i n_j - f^* n_i\right]\,\mathrm{d}S\;. \tag{6.80}$$

Evaluating expressions (6.78) and (6.79) at $|\boldsymbol{X} - \boldsymbol{X}^d| = \eta$, we have

$$f^* = \varepsilon^2 M_{kl} \left.\frac{\partial Q^{(0)}}{\partial X_k}\right|_{\boldsymbol{X}=\boldsymbol{X}^d} \frac{n_l}{\eta} , \tag{6.81}$$

$$e_j^* = \varepsilon^2 M_{kl} \left.\frac{\partial Q^{(0)}}{\partial X_k}\right|_{\boldsymbol{X}=\boldsymbol{X}^d} \frac{\delta_{jl} - 2n_j n_l}{\eta^2} . \tag{6.82}$$

Substituting these into (6.80) gives

$$[p_i] = \varepsilon^2 G_{\rm m} M_{kl} \sum_{d=1}^{D} \left.\frac{\partial Q^{(0)}}{\partial X_k}\right|_{\boldsymbol{X}=\boldsymbol{X}^d} \int_0^{2\pi} (n_i n_j(\delta_{jl} - 2n_j n_l) - n_i n_l) \, {\rm d}\theta . \tag{6.83}$$

Simplifying this expression, using the fact that $n_j n_j = 1$, gives

$$[p_i] = \varepsilon^2 G_{\rm m} M_{kl} \sum_{d=1}^{D} \left.\frac{\partial Q^{(0)}}{\partial X_k}\right|_{\boldsymbol{X}=\boldsymbol{X}^d} \int_0^{2\pi} (-2n_i n_l) \, {\rm d}\theta . \tag{6.84}$$

However,

$$\int_0^{2\pi} n_i n_j \, {\rm d}\theta = \pi\delta_{ij} , \tag{6.85}$$

so that

$$[p_i] = -2\pi\varepsilon^2 G_{\rm m} M_{ki} \sum_{d=1}^{D} \left.\frac{\partial Q^{(0)}}{\partial X_k}\right|_{\boldsymbol{X}=\boldsymbol{X}^d} . \tag{6.86}$$

Then, from equation (6.71), we have

$$\langle p_i \rangle = -2\pi\varepsilon^2 G_{\rm m} M_{ki} \cdot \frac{1}{\pi\rho^2} \sum_{d=1}^{d} \left.\frac{\partial Q^{(0)}}{\partial X_k}\right|_{\boldsymbol{X}=\boldsymbol{X}^d} . \tag{6.87}$$

From equation (6.56), this becomes

$$\langle p_i \rangle = -2\pi\varepsilon^2 G_{\rm m} M_{ki} \omega(\boldsymbol{\xi}) \left\langle \frac{\partial Q^{(0)}}{\partial X_k} \right\rangle . \tag{6.88}$$

Now, from equation (6.57), we have that

$$e_i = \frac{\partial Q^{(0)}}{\partial X_i} + O(\varepsilon) \tag{6.89}$$

$$\Rightarrow \qquad \left\langle \frac{\partial Q^{(0)}}{\partial X_k} \right\rangle = \langle e_k \rangle + O(\varepsilon) . \tag{6.90}$$

Substituting into equation (6.88), we have

$$\langle p_i \rangle = -2\pi\varepsilon^2 G_{\rm m} M_{ki} \omega(\boldsymbol{\xi}) \langle e_k \rangle + O(\varepsilon^3) , \tag{6.91}$$

which we substitute into equation (6.68), obtaining

$$\widehat{G}_{ij}\langle e_j\rangle = G_{\rm m}\langle e_i\rangle - 2\pi\varepsilon^2 G_{\rm m} M_{ki}\omega(\boldsymbol{\xi})\langle e_k\rangle + O(\varepsilon^3) \tag{6.92}$$

$$\Rightarrow \quad \widehat{G}_{ij} = G_{\rm m}\delta_{ij} - 2\pi\varepsilon^2 G_{\rm m} M_{ij}\omega(\boldsymbol{\xi}) + O(\varepsilon^3)\ , \tag{6.93}$$

since the matrix M_{ij} is symmetric. However, recall that this is in terms of dimensionless quantities, or

$$\widehat{G}_{ij} = G_{\rm m}\delta_{ij} - 2\pi\varepsilon^2 G_{\rm m}\widetilde{M}_{ij}\widetilde{\omega}(\widetilde{\boldsymbol{\xi}}) + O(\varepsilon^3)\ . \tag{6.94}$$

Returning to dimensional quantities, using (6.23) and (6.52), we have

$$\widehat{G}_{ij} \sim G_{\rm m}\delta_{ij} - 2\pi(\varepsilon^2 b^2 a^{-2}) G_{\rm m} M_{ij}\omega(\boldsymbol{\xi}) \tag{6.95}$$

$$= G_{\rm m}\delta_{ij} - 2\pi G_{\rm m} M_{ij}\omega(\boldsymbol{\xi})\ . \tag{6.96}$$

This agrees with the equivalent result of Movchan and Serkov [70], who calculated the result for disperse periodic composites.

6.2.4 Matching stress at infinity and locally

Recall that in Chapter 2 we assumed that the stress at infinity in the inner problem near an inclusion was equal to the effective stress at a point in the composite material. This assumption was made in order to determine the criterion at which the inclusions turned from being attached to detached. To verify this assumption, we now return to the expressions (6.24) and (6.28) for the inner and outer displacements respectively and match them in a more systematic way.

First we note that, near an inclusion d, the inner displacement is given by an expression of the form

$$\begin{aligned} f_{\rm A}^d = {} & (\beta^d)_0 + \varepsilon(\beta^d)_1 + \varepsilon^2(\beta^d)_2 + \cdots \\ & + \left[(\widetilde{c}_i^d)_0 + \varepsilon(\widetilde{c}_i^d)_1 + \varepsilon^2(\widetilde{c}_i^d)_2 + \cdots\right]\left[\widetilde{x}_i^{(d)} + \frac{\widetilde{M}_{ij}\widetilde{x}_j^{(d)}}{|\widetilde{\boldsymbol{x}}^{(d)}|^2} + \frac{\widetilde{M}_{ikl}\widetilde{x}_k^{(d)}\widetilde{x}_l^{(d)}}{|\widetilde{\boldsymbol{x}}^{(d)}|^4} + \cdots\right] \\ & + \left[(\widetilde{g}_{ij}^d)_0 + \varepsilon(\widetilde{g}_{ij}^d)_1 + \varepsilon^2(\widetilde{g}_{ij}^d)_2 + \cdots\right]\left[\widetilde{x}_i^{(d)}\widetilde{x}_j^{(d)} + \frac{\widetilde{N}_{ijkl}\widetilde{x}_k^{(d)}\widetilde{x}_l^{(d)}}{|\widetilde{\boldsymbol{x}}^{(d)}|^4} + \cdots\right] \\ & + \cdots\ . \end{aligned} \tag{6.97}$$

As on page 179, we find that for consistent matching we must have $(\widetilde{c}_i^d)_0 = 0$, and additionally $(\widetilde{g}_{ij}^d)_0 = (\widetilde{g}_{ij}^d)_1 = 0$. We have included the possibility that the behaviour at infinity of the inner displacement is more general, in order to match fully into arbitrary outer displacements $Q(\widetilde{\boldsymbol{X}})$. It is assumed that, in antiplane strain, if the displacement behaves as $\Omega(r^n)$ at infinity, then the correction to this due to the presence of the

inclusion (what has been referred to as the 'perturbation' displacement) is $O(r^{-n})$ at infinity.

In the outer problem, the displacement field, including higher-order terms, is given by

$$\begin{aligned} f_{\rm B} &= Q^{(0)}(\widetilde{\boldsymbol{X}}) + \varepsilon Q^{(1)}(\widetilde{\boldsymbol{X}}) + \cdots + \varepsilon \widetilde{M}_{ij} \sum_{d=1}^{D} \frac{\left(\varepsilon(\widetilde{c}_i^d)_1 + \varepsilon^2(\widetilde{c}_i^d)_2 + \cdots\right)(\widetilde{X}_j - \widetilde{X}_j^d)}{|\widetilde{\boldsymbol{X}} - \widetilde{\boldsymbol{X}}^d|^2} \\ &\quad + \varepsilon^2 \sum_{d=1}^{D} \frac{\left(\varepsilon \widetilde{M}_{ikl}[(\widetilde{c}_i^d)_1 + \varepsilon(\widetilde{c}_i^d)_2] + \varepsilon^2 \widetilde{N}_{ijkl}(\widetilde{g}_{ij}^d)_2 + \cdots\right)(\widetilde{X}_k - \widetilde{X}_k^d)(\widetilde{X}_l - \widetilde{X}_l^d)}{|\widetilde{\boldsymbol{X}} - \widetilde{\boldsymbol{X}}^d|^4} \\ &\quad + \cdots, \end{aligned} \tag{6.98}$$

which is an extension of the result (6.28). If we split the sum into terms which are non-singular and singular at $\widetilde{\boldsymbol{X}} = \widetilde{\boldsymbol{X}}^d$, we can write this as

$$\begin{aligned} f_{\rm B} &= L^{(0)}(\widetilde{\boldsymbol{X}}) + \varepsilon L^{(1)}(\widetilde{\boldsymbol{X}}) + \cdots + \varepsilon^2 \widetilde{M}_{ij} \frac{\left((\widetilde{c}_i^d)_1 + \varepsilon(\widetilde{c}_i^d)_2 + \cdots\right)(\widetilde{X}_j - \widetilde{X}_j^d)}{|\widetilde{\boldsymbol{X}} - \widetilde{\boldsymbol{X}}^d|^2} \\ &\quad + \varepsilon^3 \frac{\left(\widetilde{M}_{ikl}(\widetilde{c}_i^d)_1 + \varepsilon \widetilde{N}_{ijkl}(\widetilde{g}_{ij}^d)_2 + \cdots\right)(\widetilde{X}_k - \widetilde{X}_k^d)(\widetilde{X}_l - \widetilde{X}_l^d)}{|\widetilde{\boldsymbol{X}} - \widetilde{\boldsymbol{X}}^d|^4} + \cdots, \end{aligned} \tag{6.99}$$

where $L(\widetilde{\boldsymbol{X}}) = L^{(0)}(\widetilde{\boldsymbol{X}}) + \varepsilon L^{(1)}(\widetilde{\boldsymbol{X}}) + \cdots$ is the finite part of the displacement at $\widetilde{\boldsymbol{X}} = \widetilde{\boldsymbol{X}}^d$. Matching the inner and outer solutions by Van Dyke's method, we find that

$$(\widetilde{c}_i^d)_k = \left.\frac{\partial L^{(k-1)}}{\partial \widetilde{X}_i}\right|_{\widetilde{\boldsymbol{X}}^d}, \tag{6.100}$$

$$(\widetilde{g}_{ij}^d)_k = \frac{1}{2} \left.\frac{\partial^2 L^{(k-2)}}{\partial \widetilde{X}_i \partial \widetilde{X}_j}\right|_{\widetilde{\boldsymbol{X}}^d}, \tag{6.101}$$

and so forth. This agrees with the theory given previously since $L^{(0)}(\widetilde{\boldsymbol{X}}) = Q^{(0)}(\widetilde{\boldsymbol{X}})$.

If (6.100)–(6.101) are substituted into (6.97), the limit of the inner displacement at infinity becomes

$$\begin{aligned} f_{\rm A}^d\big|_\infty &= L^{(0)}(\widetilde{\boldsymbol{X}}^d) + \varepsilon L^{(1)}(\widetilde{\boldsymbol{X}}^d) + \cdots \\ &\quad + \varepsilon \widetilde{x}_i^{(d)} \left.\frac{\partial L^{(0)}}{\partial \widetilde{X}_i}\right|_{\widetilde{\boldsymbol{X}}^d} + \varepsilon^2 \widetilde{x}_i^{(d)} \left.\frac{\partial L^{(1)}}{\partial \widetilde{X}_i}\right|_{\widetilde{\boldsymbol{X}}^d} + \cdots \\ &\quad + \frac{\varepsilon^2 \widetilde{x}_i^{(d)} \widetilde{x}_j^{(d)}}{2} \left.\frac{\partial^2 L^{(0)}}{\partial \widetilde{X}_i \partial \widetilde{X}_j}\right|_{\widetilde{\boldsymbol{X}}^d} + \cdots \end{aligned} \tag{6.102}$$

$$= \left[L^{(0)} + \varepsilon L^{(1)} + \cdots\right]\big|_{\widetilde{\boldsymbol{X}} = \widetilde{\boldsymbol{X}}^d + \varepsilon \widetilde{\boldsymbol{x}}^{(d)}}. \tag{6.103}$$

Hence the (dimensional) stress at infinity in the inner problem is

$$\tau_i^{\text{inner}}\big|_\infty = G_{\text{m}}\frac{\partial f_{\text{A}}^d}{\partial x_i} \tag{6.104}$$

$$= \frac{G_{\text{m}}}{a}\frac{\partial f_{\text{A}}^d}{\partial \widetilde{x}_i^{(d)}} \tag{6.105}$$

$$= \frac{G_{\text{m}}}{a}\left[\varepsilon\frac{\partial L^{(0)}}{\partial \widetilde{X}_i} + \varepsilon^2\frac{\partial L^{(1)}}{\partial \widetilde{X}_i} + \cdots\right]\Bigg|_{\widetilde{\boldsymbol{X}}=\widetilde{\boldsymbol{X}}^d+\varepsilon\widetilde{\boldsymbol{x}}^{(d)}} \tag{6.106}$$

$$= \frac{G_{\text{m}}}{b}\left[\frac{\partial}{\partial \widetilde{X}_i}(L^{(0)} + \varepsilon L^{(1)} + \cdots)\right]\Bigg|_{\widetilde{\boldsymbol{X}}=\widetilde{\boldsymbol{X}}^d+\varepsilon\widetilde{\boldsymbol{x}}^{(d)}} . \tag{6.107}$$

On the other hand the (dimensional) effective stress in the composite material is given by the finite part of the outer stress,

$$\tau_i^{\text{eff}} = G_{\text{m}}\frac{\partial f_{\text{B}}}{\partial X_i} \tag{6.108}$$

$$= \frac{G_{\text{m}}}{b}\frac{\partial}{\partial \widetilde{X}_i}(L^{(0)} + \varepsilon L^{(1)} + \cdots) , \tag{6.109}$$

so that the stress at infinity in the inner problem equals the effective stress in the composite material at a point near that inclusion.

6.3 Three-dimensional inclusions

We will now consider the homogenisation problem for three-dimensional inclusions embedded in a matrix. Recall that in the previous section for antiplane strain, we analysed the slowest-decaying solutions at infinity for an embedded inclusion experiencing a certain strain field at infinity.

In the case of spherical shell inclusions, the analogue of the perturbation field $\widetilde{f}$ in antiplane strain can be found from Chapters 3 and 5. We saw in Chapter 3 that the perturbation displacement for both uniaxial and radial stress fields decayed as $O(R^{-2})$ to leading order at infinity: see equations (3.63), (3.64) and (3.89). Similarly, in Chapter 5, the perturbation displacement field was denoted by $\boldsymbol{u}^{\text{P}}$ in equations (5.104)–(5.105), whose leading order solution at infinity decayed as $O(R^{-2})$.

Now, for the antiplane deformations, we identified displacement solutions that decayed as $O(r^{-1})$ at infinity with solutions of

$$\nabla^2 f = \frac{\partial \delta}{\partial x_j} . \tag{6.110}$$

We now wish to find the equivalent singular solutions of the elasticity equations in the matrix that decay as $O(R^{-2})$ at infinity. These are the *unit doublet states*. These states are shown by Gurtin [39] to be

$$\boldsymbol{u}^{ij} = \frac{1}{kR^3}\left[\boldsymbol{x}\delta_{ij} + x_i\boldsymbol{e}_j - \frac{3x_ix_j}{R^2}\boldsymbol{x} - (3-4\nu_{\text{m}})x_j\boldsymbol{e}_i\right] \tag{6.111}$$

with Cartesian components

$$u_l^{ij} = \frac{1}{kR^3}\left[x_l\delta_{ij} + x_i\delta_{jl} - (3-4\nu_{\rm m})x_j\delta_{il} - \frac{3x_ix_jx_l}{R^2}\right] , \tag{6.112}$$

where

$$\boldsymbol{x} = (x_1, x_2, x_3) , \tag{6.113}$$

$$R = \sqrt{x_1^2 + x_2^2 + x_3^2} , \tag{6.114}$$

$$k = 16\pi G_{\rm m}(1-\nu_{\rm m}) . \tag{6.115}$$

The state $\boldsymbol{u}^{ij}$ is the solution to

$$\nabla\cdot\boldsymbol{\tau}^{ij} + \boldsymbol{e}_i\frac{\partial}{\partial x_j}\delta(\boldsymbol{x}) = 0 , \tag{6.116}$$

or

$$\frac{\partial\tau_{rm}^{ij}}{\partial x_m} + \delta_{ir}\frac{\partial\delta}{\partial x_j} = 0 \tag{6.117}$$

$$\Rightarrow \qquad A_{rmkl}^{\rm m}\frac{\partial e_{kl}^{ij}}{\partial x_m} + \delta_{ir}\frac{\partial\delta}{\partial x_j} = 0 , \tag{6.118}$$

where $A_{ijkl}^{\rm m}$ is the standard elasticity tensor in the matrix.

Thus, in order to construct a singular solution that decays as $O(R^{-2})$ at infinity, we take a linear combination of these unit doublet states. Define a perturbation displacement field in the matrix to have Cartesian components

$$u_l = P_{ij}u_l^{ij} \tag{6.119}$$

$$= \frac{P_{ij}}{kR^3}\left[x_l\delta_{ij} + x_i\delta_{jl} - \frac{3x_ix_jx_l}{R^2} - (3-4\nu_{\rm m})x_j\delta_{il}\right] , \tag{6.120}$$

applying the summation convention. We will suppose that the matrix P_{ij} is known, given by a linear transformation of the applied strain field at infinity, or

$$P_{ij} = M_{ijmn}\, e_{mn}|_\infty , \tag{6.121}$$

so that the tensor M_{ijmn} plays the same part as the polarisability tensor M_{ij} in the previous work for antiplane strain deformations.

In addition to this perturbation field, there will be a homogeneous displacement field due to the applied stress at infinity. Suppose that this is given by

$$u_i = (E_{ij} + K_{ij})x_j \tag{6.122}$$

where E_{ij} is symmetric and K_{ij} is skew-symmetric. Then the strain field at infinity is given by

$$e_{ij}|_\infty = E_{ij} . \tag{6.123}$$

This is substituted into equation (6.121), so that the total displacement field is now given by the sum of the homogeneous displacement field (6.122), the perturbation field (6.119), and a rigid body displacement F_k:

$$u_k = F_k + (E_{kl} + K_{kl})x_l + M_{ijmn}E_{mn}u_k^{ij} \tag{6.124}$$

$$= F_k + (E_{mn} + K_{mn})\left(\delta_{km}\delta_{ln}x_l + M_{ijmn}u_k^{ij}\right) , \tag{6.125}$$

since $M_{ijmn} = M_{ijnm}$ from equation (6.121). The tensors E_{mn}, K_{mn} and the rigid displacement F_k will in general be different for each inclusion, which as before we will label with d for $d = 1, \ldots, D$. Thus

$$u_k = F_k^d + (E_{mn}^d + K_{mn}^d)\left(\delta_{km}\delta_{ln}x_l + M_{ijmn}u_k^{ij}\right) . \tag{6.126}$$

As for antiplane deformations, we now nondimensionalise this displacement, for inclusions of size a. We set

$$\widetilde{\boldsymbol{x}}^{(d)} = \frac{1}{a}\boldsymbol{x} , \tag{6.127}$$

so that

$$u_k^{ij}(\widetilde{\boldsymbol{x}}^{(d)}) = a^{-2}u_k^{ij}(\boldsymbol{x}) . \tag{6.128}$$

Writing

$$\widetilde{M}_{ijmn} = a^{-3}M_{ijmn} , \tag{6.129}$$

$$\widetilde{E}_{mn}^d = aE_{mn}^d , \tag{6.130}$$

$$\widetilde{K}_{mn}^d = aK_{mn}^d , \tag{6.131}$$

we find that the dimensionless inner displacement becomes

$$u_k^{\mathrm{A}} = F_k^d + (\widetilde{E}_{mn}^d + \widetilde{K}_{mn}^d)\left(\delta_{km}\delta_{ln}\widetilde{x}_l^{(d)} + \widetilde{M}_{ijmn}u_k^{ij}(\widetilde{\boldsymbol{x}}^{(d)})\right) . \tag{6.132}$$

Now, the unit doublet states satisfy equation (6.118). Thus,

$$A_{rmkl}^{\mathrm{m}}\frac{\partial}{\partial\widetilde{x}_m^{(d)}}\left[\frac{1}{2}\left(\frac{\partial u_k^{\mathrm{A}}}{\partial\widetilde{x}_l^{(d)}} + \frac{\partial u_l^{\mathrm{A}}}{\partial\widetilde{x}_k^{(d)}}\right)\right] = -\widetilde{E}_{mn}^d\widetilde{M}_{ijmn}\delta_{ir}\frac{\partial\delta(\widetilde{\boldsymbol{x}}^{(d)})}{\partial\widetilde{x}_j^{(d)}} . \tag{6.133}$$

Changing to outer variables $\widetilde{\boldsymbol{X}}$, given by

$$\widetilde{\boldsymbol{x}}^{(d)} = \frac{1}{\varepsilon}(\widetilde{\boldsymbol{X}} - \widetilde{\boldsymbol{X}}^d) , \tag{6.134}$$

we find that

$$\varepsilon^2 A_{rmkl}^{\mathrm{m}}\frac{\partial}{\partial\widetilde{X}_m}\left[\frac{1}{2}\left(\frac{\partial u_k^{\mathrm{B}}}{\partial\widetilde{X}_l} + \frac{\partial u_l^{\mathrm{B}}}{\partial\widetilde{X}_k}\right)\right] = -\varepsilon^4\widetilde{E}_{mn}^d\widetilde{M}_{ijmn}\delta_{ir}\frac{\partial\delta(\widetilde{\boldsymbol{X}} - \widetilde{\boldsymbol{X}}^d)}{\partial\widetilde{X}_j} . \tag{6.135}$$

This is true for each $d = 1, \ldots, D$, so

$$\varepsilon^2 A^{\rm m}_{rmkl} \frac{\partial}{\partial \widetilde{X}_m} \left[\frac{1}{2} \left(\frac{\partial u^{\rm B}_k}{\partial \widetilde{X}_l} + \frac{\partial u^{\rm B}_l}{\partial \widetilde{X}_k} \right) \right] \;=\; -\varepsilon^4 \widetilde{M}_{ijmn} \delta_{ir} \sum_{d=1}^{D} \widetilde{E}^d_{mn} \frac{\partial \delta(\widetilde{\boldsymbol{X}} - \widetilde{\boldsymbol{X}}^d)}{\partial \widetilde{X}_j} \; . \quad (6.136)$$

Integrating, we find that

$$u^{\rm B}_k \;=\; Q_k(\widetilde{\boldsymbol{X}}) + \varepsilon^2 \widetilde{M}_{ijmn} \sum_{d=1}^{D} \widetilde{E}^d_{mn} u^{ij}_k (\widetilde{\boldsymbol{X}} - \widetilde{\boldsymbol{X}}^d) \; , \quad (6.137)$$

where $Q_k(\widetilde{\boldsymbol{X}})$ is some admissable displacement, that satisfies

$$A^{\rm m}_{rmkl} \frac{\partial}{\partial \widetilde{X}_m} \left[\frac{1}{2} \left(\frac{\partial Q_k}{\partial \widetilde{X}_l} + \frac{\partial Q_l}{\partial \widetilde{X}_k} \right) \right] \;=\; 0 \; . \quad (6.138)$$

We now need an expression for $\widetilde{E}^d_{mn}$. This is found by matching the inner and outer displacements (6.132) and (6.137) respectively. The method is exactly analogous to that for antiplane strain deformations. We suppose that $Q_k(\widetilde{\boldsymbol{X}})$ is expanded in an asymptotic series,

$$Q_k(\widetilde{\boldsymbol{X}}) \;=\; Q^{(0)}_k(\widetilde{\boldsymbol{X}}) + \varepsilon Q^{(1)}_k(\widetilde{\boldsymbol{X}}) + \cdots \; , \quad (6.139)$$

so that

$$(1{\rm ti})(1{\rm to}) \;=\; Q^{(0)}_k(\widetilde{\boldsymbol{X}}^d) \; , \quad (6.140)$$

$$(2{\rm ti})(1{\rm to}) \;=\; Q^{(0)}_k(\widetilde{\boldsymbol{X}}^d) + \varepsilon \widetilde{x}^{(d)}_l \left. \frac{\partial Q^{(0)}_k}{\partial \widetilde{X}_l} \right|_{\widetilde{\boldsymbol{X}}^d} \; . \quad (6.141)$$

For the inner solution, we expand $\widetilde{F}_k$, $\widetilde{E}_{kl}$ and $\widetilde{K}_{kl}$ in asymptotic expansions,

$$\widetilde{F}_k \;=\; (\widetilde{F}_k)_0 + \varepsilon (\widetilde{F}_k)_1 + \cdots \; , \quad (6.142)$$

$$\widetilde{E}_{kl} \;=\; (\widetilde{E}_{kl})_0 + \varepsilon (\widetilde{E}_{kl})_1 + \cdots \; , \quad (6.143)$$

$$\widetilde{K}_{kl} \;=\; (\widetilde{K}_{kl})_0 + \varepsilon (\widetilde{K}_{kl})_1 + \cdots \; . \quad (6.144)$$

Analogously to the antiplane strain case, we assume that both $(\widetilde{E}_{kl})_0$ and $(\widetilde{K}_{kl})_0$ are zero. Then

$$(1{\rm to})(1{\rm ti}) \;=\; (F^d_k)_0 \; , \quad (6.145)$$

$$(1{\rm to})(2{\rm ti}) \;=\; (F^d_k)_0 + \Big((\widetilde{E}_{kl})_1 + (\widetilde{K}_{kl})_1 \Big) (\widetilde{X}_l - \widetilde{X}^d_l) \; . \quad (6.146)$$

This implies, on using van Dyke's matching rule, that

$$(F^d_k)_0 \;=\; Q^{(0)}_k(\widetilde{\boldsymbol{X}}^d) \; , \quad (6.147)$$

$$(\widetilde{E}^d_{kl})_1 \;=\; \frac{1}{2} \left(\frac{\partial Q^{(0)}_k}{\partial \widetilde{X}_l} + \frac{\partial Q^{(0)}_l}{\partial \widetilde{X}_k} \right) \Bigg|_{\widetilde{\boldsymbol{X}}^d} \; , \quad (6.148)$$

$$(\widetilde{K}^d_{kl})_1 \;=\; \frac{1}{2} \left(\frac{\partial Q^{(0)}_k}{\partial \widetilde{X}_l} - \frac{\partial Q^{(0)}_l}{\partial \widetilde{X}_k} \right) \Bigg|_{\widetilde{\boldsymbol{X}}^d} \; . \quad (6.149)$$

Thus the first four terms of the outer displacement become

$$u_k^{\mathrm{B}} \;=\; \bar{Q}_k(\widetilde{\boldsymbol{X}}) + \varepsilon^3 \widetilde{M}_{ijmn} \sum_{d=1}^{D} \frac{1}{2} \left(\frac{\partial Q_m^{(0)}}{\partial \widetilde{X}_n} + \frac{\partial Q_n^{(0)}}{\partial \widetilde{X}_m} \right) \Bigg|_{\widetilde{\boldsymbol{X}}^d} u_k^{ij}(\widetilde{\boldsymbol{X}} - \widetilde{\boldsymbol{X}}^d) \;, \tag{6.150}$$

where we use the notation

$$\bar{Q}_k \;=\; Q_k^{(0)} + \varepsilon Q_k^{(1)} + \varepsilon^2 Q_k^{(2)} + \varepsilon^3 Q_k^{(3)} \;. \tag{6.151}$$

We now denote the strain field caused by the displacement Q_k by

$$\Phi_{kl}(\widetilde{\boldsymbol{X}}) \;=\; \frac{1}{2} \left(\frac{\partial Q_k}{\partial \widetilde{X}_l} + \frac{\partial Q_l}{\partial \widetilde{X}_k} \right) \;, \tag{6.152}$$

so that

$$u_k^{\mathrm{B}} \;=\; \bar{Q}_k(\widetilde{\boldsymbol{X}}) + \varepsilon^3 \widetilde{M}_{ijmn} \sum_{d=1}^{D} \Phi_{mn}^{(0)}(\widetilde{\boldsymbol{X}}^d) u_k^{ij}(\widetilde{\boldsymbol{X}} - \widetilde{\boldsymbol{X}}^d) \;, \tag{6.153}$$

and the corresponding strain field is

$$e_{kl}^{\mathrm{B}} \;=\; \bar{\Phi}_{kl}(\widetilde{\boldsymbol{X}}) + \varepsilon^3 \widetilde{M}_{ijmn} \sum_{d=1}^{D} \Phi_{mn}^{(0)}(\widetilde{\boldsymbol{X}}^d) H_{ijkl}(\widetilde{\boldsymbol{X}} - \widetilde{\boldsymbol{X}}^d) \;, \tag{6.154}$$

using the same notation as (6.151). In this expression,

$$H_{ijkl}(\widetilde{\boldsymbol{X}}) \;=\; \frac{1}{2} \left(\frac{\partial u_k^{ij}(\widetilde{\boldsymbol{X}})}{\partial \widetilde{X}_l} + \frac{\partial u_l^{ij}(\widetilde{\boldsymbol{X}})}{\partial \widetilde{X}_k} \right) \;. \tag{6.155}$$

6.3.1 The homogenisation process for three-dimensional inclusions

In three dimensions, the averaging operator analogous to the two-dimensional version (6.45) is defined by

$$\langle \Phi(\boldsymbol{X}) \rangle \;=\; \lim_{c \to 0} \frac{3}{4\pi c^3} \int_{|\boldsymbol{X} - \boldsymbol{\xi}| < c} \Phi(\boldsymbol{X}) \, \mathrm{d}^3 \boldsymbol{X} \;, \tag{6.156}$$

since the averaging region is now a sphere. The limiting operation, as before, occurs in such a way that the separation b is much smaller than c at all times. The number density $\omega(\boldsymbol{\xi})$ of inclusions is now

$$\omega(\boldsymbol{\xi}) \;=\; \left\langle \sum_{d=1}^{D} \delta(\boldsymbol{X} - \boldsymbol{X}^d) \right\rangle \;, \tag{6.157}$$

where the summation is over all inclusions in the integration domain.

The above definitions are for quantities defined in terms of the dimensional coordinate $\boldsymbol{X}$. For quantities defined in terms of *non*-dimensional coordinates $\widetilde{\boldsymbol{X}}$ we have, analogously to (6.49),

$$\langle \Phi(\widetilde{\boldsymbol{X}}) \rangle \;=\; \frac{3}{4\pi\rho^3} \int_{|\widetilde{\boldsymbol{X}}-\widetilde{\boldsymbol{\xi}}|<\rho} \Phi(\widetilde{\boldsymbol{X}})\, \mathrm{d}^3\widetilde{\boldsymbol{X}} \;, \tag{6.158}$$

for some $\rho \gg 1$. Then

$$\widetilde{\omega}(\widetilde{\boldsymbol{\xi}}) \;=\; \left\langle \sum_{d=1}^{D} \delta(\widetilde{\boldsymbol{X}} - \widetilde{\boldsymbol{X}}^d) \right\rangle \;=\; b^3 \omega(\boldsymbol{\xi}) \;. \tag{6.159}$$

We now proceed to find an expression for the effective elasticity tensor of the material. As in the antiplane strain case, we will write $\boldsymbol{X}$, M_{ijkl} and $\omega(\boldsymbol{\xi})$ instead of $\widetilde{\boldsymbol{X}}$, $\widetilde{M}_{ijkl}$ and $\widetilde{\omega}(\widetilde{\boldsymbol{\xi}})$, to avoid cumbersome notation, with the implicit understanding that these are the *dimensionless* quantities. The displacement and strain fields are given by equations (6.153) and (6.154), for $\boldsymbol{X}$ not close to the inclusions, or $\boldsymbol{X} \in \Omega^*$, where

$$\Omega^* \;=\; \bigcap_{d=1}^{D} \left\{ \boldsymbol{X} \;:\; |\boldsymbol{X} - \boldsymbol{X}^d| > \eta \right\} \tag{6.160}$$

for some arbitrarily small $\eta > 0$. Let the stress and strain be linked in the material by the equation

$$\tau_{ij}(\boldsymbol{X}) \;=\; A_{ijkl}(\boldsymbol{X}) e_{kl}(\boldsymbol{X}) \;, \tag{6.161}$$

where A_{ijkl} is the elasticity tensor. This is equal to the matrix elasticity tensor A^{m}_{ijkl} for $\boldsymbol{X} \in \Omega^*$, and not known in a region near each inclusion — however we do assume that the stress field is continuous. Then the *effective* elasticity tensor is defined by equation (6.3). We find $\widehat{A}_{ijkl}$ through a method based on the polarisation tensor as shown in Section 6.2.3. Analogously to the work in that section, we define the polarisation tensor to be

$$p_{ij} \;=\; \tau_{ij} - A^{\mathrm{m}}_{ijkl} e_{kl} \;. \tag{6.162}$$

Hence

$$\begin{aligned} \langle p_{ij} \rangle \;&=\; \langle \tau_{ij} \rangle - A^{\mathrm{m}}_{ijkl} \langle e_{kl} \rangle & (6.163) \\ &=\; \widehat{A}_{ijkl} \langle e_{kl} \rangle - A^{\mathrm{m}}_{ijkl} \langle e_{kl} \rangle \;, & (6.164) \end{aligned}$$

so that

$$\widehat{A}_{ijkl} \langle e_{kl} \rangle \;=\; A^{\mathrm{m}}_{ijkl} \langle e_{kl} \rangle + \langle p_{ij} \rangle \;. \tag{6.165}$$

We thus need to determine $\langle p_{ij} \rangle$. This is given by

$$\langle p_{ij} \rangle \;=\; \frac{3}{4\pi\rho^3}[p_{ij}]\;, \tag{6.166}$$

where

$$[p_{ij}] \;=\; \int_{|\boldsymbol{X}-\boldsymbol{\xi}|<\rho} p_{ij}\,\mathrm{d}^3\boldsymbol{X}\;. \tag{6.167}$$

However, since $A_{ijkl}(\boldsymbol{X}) = A^{\mathrm{m}}_{ijkl}$ for $\boldsymbol{X} \in \Omega^*$, we have that $p_{ij}|_{\boldsymbol{X}\in\Omega^*} = 0$. Thus p_{ij} is only nonzero for a small region surrounding each inclusion. Hence

$$[p_{ij}] \;=\; \sum_{d=1}^{D} \int_{|\boldsymbol{X}-\boldsymbol{X}^d|<\eta} p_{ij}\,\mathrm{d}^3\boldsymbol{X}\;. \tag{6.168}$$

However, for a given region $\Omega \in \mathbb{R}^3$, we have

$$\begin{aligned}
\int_\Omega p_{ij}\,\mathrm{d}^3\boldsymbol{X} \;&=\; \int_\Omega (\tau_{ij} - A^{\mathrm{m}}_{ijkl}e_{kl})\,\mathrm{d}^3\boldsymbol{X} && (6.169)\\
&=\; \int_\Omega \left[\frac{\partial}{\partial X_k}(X_j\tau_{ik}) - \frac{1}{2}A^{\mathrm{m}}_{ijkl}\left(\frac{\partial u_k}{\partial X_l} + \frac{\partial u_l}{\partial X_k}\right)\right]\mathrm{d}^3\boldsymbol{X} && (6.170)\\
&=\; \int_{\partial\Omega} \left[X_j\tau_{ik}n_k - \frac{1}{2}A^{\mathrm{m}}_{ijkl}\,(u_k n_l + u_l n_k)\right]\mathrm{d}S\;, && (6.171)
\end{aligned}$$

on using $\tau_{ik,k} = 0$ and where n_i are the Cartesian components of the normal vector to the surface. Thus

$$[p_{ij}] \;=\; \sum_{d=1}^{D} \int_{|\boldsymbol{X}-\boldsymbol{X}^d|=\eta} \left[(X_j - X^d_j)\tau_{ik}n_k - \frac{1}{2}A^{\mathrm{m}}_{ijkl}\,(u_k n_l + u_l n_k)\right]\mathrm{d}S\;. \tag{6.172}$$

By the continuity of the stress field, we use $\tau_{ik} = A^{\mathrm{m}}_{iklm}e_{lm}$ on each contour, so that

$$[p_{ij}] \;=\; A^{\mathrm{m}}_{iklm}\sum_{d=1}^{D} \int_{|\boldsymbol{X}-\boldsymbol{X}^d|=\eta} \left[\eta n_j e_{lm}n_k - \frac{1}{2}\delta_{jk}(u_l n_m + u_m n_l)\right]\mathrm{d}S\;, \tag{6.173}$$

since $X_j - X^d_j = \eta n_j$ along the contour.

This expression will be analysed in the limit $\eta \to 0$, since η is an arbitrarily small constant. As for antiplane strain, at any singularity d we can separate the expressions (6.153) and (6.154) for the displacement and strain fields respectively into bounded and unbounded terms. Integrating the bounded terms results in zero in the limit $\eta \to 0$, so we will consider only the unbounded terms, so that

$$[p_{ij}] \;=\; A^{\mathrm{m}}_{iklm}\sum_{d=1}^{D} \int_{|\boldsymbol{X}-\boldsymbol{X}^d|=\eta} \left[\eta n_j e^*_{lm}n_k - \frac{1}{2}\delta_{jk}(u^*_l n_m + u^*_m n_l)\right]\mathrm{d}S\;. \tag{6.174}$$

For the inclusion d, the unbounded parts of the displacement and strain fields are given by

$$u_k^* = \varepsilon^3 M_{ijmn}\Phi_{mn}^{(0)}(\boldsymbol{X}^d)u_k^{ij}(\boldsymbol{X}-\boldsymbol{X}^d)\,, \tag{6.175}$$

$$e_{kl}^* = \varepsilon^3 M_{ijmn}\Phi_{mn}^{(0)}(\boldsymbol{X}^d)H_{ijkl}(\boldsymbol{X}-\boldsymbol{X}^d) \tag{6.176}$$

respectively, from (6.153) and (6.154). Substituting equations (6.175)–(6.176) into equation (6.174), we obtain

$$[p_{ij}] = \varepsilon^3 A^{\mathrm{m}}_{iklm}M_{pquv}\sum_{d=1}^{D}\Phi_{uv}^{(0)}(\boldsymbol{X}^d)\int_{|\boldsymbol{X}-\boldsymbol{X}^d|=\eta}\Big\{\eta n_j n_k H_{pqlm}(\eta\boldsymbol{n}) - \frac{1}{2}\delta_{jk}\left[u_l^{pq}(\eta\boldsymbol{n})n_m + u_m^{pq}(\eta\boldsymbol{n})n_l\right]\Big\}\,\mathrm{d}S\,. \tag{6.177}$$

Evaluating u_k^{ij} and H_{ijkl} from equations (6.112) and (6.155) at $X_j - X_j^d = \eta n_j$, we find that

$$u_l^{ij}(\eta\boldsymbol{n}) = \frac{1}{k\eta^2}\left[n_l\delta_{ij} + n_i\delta_{jl} - (3-4\nu_{\mathrm{m}})n_j\delta_{il} - 3n_in_jn_l\right]\,, \tag{6.178}$$

$$H_{ijlm}(\eta\boldsymbol{n}) = \frac{1}{k\eta^3}\Big\{\delta_{ij}\delta_{lm} - (1-2\nu_{\mathrm{m}})(\delta_{il}\delta_{jm}+\delta_{im}\delta_{jl}) - 3\Big[\delta_{ij}n_ln_m - (1-2\nu_{\mathrm{m}})(\delta_{im}n_jn_l+\delta_{il}n_jn_m) + \delta_{jm}n_in_l + \delta_{lm}n_in_j + \delta_{jl}n_in_m\Big] \tag{6.179}$$

$$+15n_in_jn_ln_m\Big\}\,. \tag{6.180}$$

Now, if we define the integrals

$$I_{ij} = \int_0^{2\pi}\int_0^{\pi} n_in_j\sin\theta\,\mathrm{d}\theta\mathrm{d}\phi\,, \tag{6.181}$$

$$I_{ijkl} = \int_0^{2\pi}\int_0^{\pi} n_in_jn_kn_l\sin\theta\,\mathrm{d}\theta\mathrm{d}\phi\,, \tag{6.182}$$

$$I_{ijklpq} = \int_0^{2\pi}\int_0^{\pi} n_in_jn_kn_ln_pn_q\sin\theta\,\mathrm{d}\theta\mathrm{d}\phi\,, \tag{6.183}$$

then equation (6.177) becomes

$$
\begin{aligned}
[p_{ij}] \;=\; & \frac{\varepsilon^3 M_{pquv} A^{\mathrm{m}}_{ilmn}}{2k} \sum_{d=1}^{D} \left[\frac{1}{2} \left(\frac{\partial Q^{(0)}_u}{\partial X_v} + \frac{\partial Q^{(0)}_v}{\partial X_u} \right) \right] \Bigg|_{\boldsymbol{X}^d} \\
& \times \Big\{ 2\delta_{pq}\delta_{mn} I_{jl} - (2 - 4\nu_{\mathrm{m}})(\delta_{pm}\delta_{qn} I_{jl} + \delta_{pn}\delta_{qm} I_{jl}) \\
& \quad -6 \Big[\delta_{pq} I_{jlmn} - (1 - 2\nu_{\mathrm{m}})(\delta_{pn} I_{jlqm} + \delta_{pm} I_{jlqn}) \\
& \qquad + \delta_{qn} I_{pmjl} + \delta_{mn} I_{pqjl} + \delta_{qm} I_{pnjl} \Big] \\
& \quad + 30 I_{pqmnjl} - 2\delta_{jl}\delta_{pq} I_{mn} - \delta_{jl}\delta_{qm} I_{pn} - \delta_{jl}\delta_{qn} I_{pm} \\
& \quad + (3 - 4\nu_{\mathrm{m}})(\delta_{jl}\delta_{pm} I_{qn} + \delta_{jl}\delta_{pn} I_{qm}) + 6\delta_{jl} I_{pqmn} \Big\} \; . \qquad (6.184)
\end{aligned}
$$

In evaluating the integrals (6.181)–(6.183), we note that they are *isotropic* tensors, in that a rotation of the axis doesn't change the components of the tensor.[2] Moreover, interchanging any two indices in the integrals yields the same result, making the tensors *symmetric*. Now, Suiker and Chang [90] give the general form for isotropic Cartesian tensors. The tensors of ranks 2 and 4 can be written, for constants C_i, as

$$
\begin{aligned}
T_{ij} &= C_1 \delta_{ij} \; , & (6.185) \\
T_{ijkl} &= C_1 \delta_{ij}\delta_{kl} + C_2 \delta_{ik}\delta_{jl} + C_3 \delta_{il}\delta_{jk} \; , & (6.186)
\end{aligned}
$$

and T_{ijklpq} is a linear combination of the 15 possible products of three Kronecker delta symbols. Now, the symmetry property identified earlier means that these expressions can be simplified to give

$$
\begin{aligned}
T_{ij} &= C\delta_{ij} \; , & (6.187) \\
T_{ijkl} &= C\left(\delta_{ij}\delta_{kl} + \delta_{ik}\delta_{jl} + \delta_{il}\delta_{jk}\right) \; , & (6.188) \\
T_{ijklpq} &= C \Big[\delta_{ij}\left(\delta_{kl}\delta_{pq} + \delta_{kp}\delta_{lq} + \delta_{kq}\delta_{lp}\right) \\
&\qquad + \delta_{ik}\left(\delta_{jl}\delta_{pq} + \delta_{jp}\delta_{lq} + \delta_{jq}\delta_{lp}\right) \\
&\qquad + \delta_{il}\left(\delta_{jk}\delta_{pq} + \delta_{jp}\delta_{kq} + \delta_{jq}\delta_{kp}\right) \\
&\qquad + \delta_{ip}\left(\delta_{jk}\delta_{lq} + \delta_{jl}\delta_{kq} + \delta_{jq}\delta_{kl}\right) \\
&\qquad + \delta_{iq}\left(\delta_{jk}\delta_{lp} + \delta_{jl}\delta_{kp} + \delta_{jp}\delta_{kl}\right) \Big] \; , & (6.189)
\end{aligned}
$$

where C is some constant in each case. Thus, we only need to calculate the tensors

[2] If the axes of n_i were changed, we would simply change the integration variables, given that integration occurs over the whole surface of the unit sphere.

I_{ij} to I_{ijklpq} for *one* choice of index. We have that

$$\begin{aligned} I_{\underbrace{33\cdots3}_{n}} &= \int_0^{2\pi}\int_0^{\pi} \cos^n\theta \sin\theta \,\mathrm{d}\theta\mathrm{d}\phi && (6.190)\\ &= 2\pi\int_0^{\pi} \cos^n\theta\sin\theta\,\mathrm{d}\theta && (6.191)\\ &= -2\pi\left[\frac{\cos^{n+1}\theta}{n+1}\right]_0^{\pi} && (6.192)\\ &= \frac{2\pi}{n+1}\left(1-(-1)^{n+1}\right) . && (6.193) \end{aligned}$$

Thus

$$\begin{aligned} I_{33} &= \frac{4\pi}{3} , && (6.194)\\ I_{3333} &= \frac{4\pi}{5} , && (6.195)\\ I_{333333} &= \frac{4\pi}{7} . && (6.196) \end{aligned}$$

Hence

$$\begin{aligned} I_{ij} &= \frac{4\pi}{3}\delta_{ij} && (6.197)\\ I_{ijkl} &= \frac{4\pi}{15}\left(\delta_{ij}\delta_{kl}+\delta_{ik}\delta_{jl}+\delta_{il}\delta_{jk}\right) && (6.198)\\ I_{ijklpq} &= \frac{4\pi}{105}\Big[\delta_{ij}\left(\delta_{kl}\delta_{pq}+\delta_{kp}\delta_{lq}+\delta_{kq}\delta_{lp}\right)\\ &\quad +\delta_{ik}\left(\delta_{jl}\delta_{pq}+\delta_{jp}\delta_{lq}+\delta_{jq}\delta_{lp}\right)\\ &\quad +\delta_{il}\left(\delta_{jk}\delta_{pq}+\delta_{jp}\delta_{kq}+\delta_{jq}\delta_{kp}\right)\\ &\quad +\delta_{ip}\left(\delta_{jk}\delta_{lq}+\delta_{jl}\delta_{kq}+\delta_{jq}\delta_{kl}\right)\\ &\quad +\delta_{iq}\left(\delta_{jk}\delta_{lp}+\delta_{jl}\delta_{kp}+\delta_{jp}\delta_{kl}\right)\Big] . && (6.199) \end{aligned}$$

Using these integrals, we eventually find that

$$\begin{aligned} [p_{ij}] &= \frac{8\pi\varepsilon^3}{35k}M_{pquv}A^{\mathrm{m}}_{ilmn}\sum_{d=1}^{D}\left[\frac{1}{2}\left(\frac{\partial Q_u^{(0)}}{\partial X_v}+\frac{\partial Q_v^{(0)}}{\partial X_u}\right)\right]\Bigg|_{\boldsymbol{X}^d}\\ &\quad\times\Big\{\delta_{jl}\left[-\delta_{mn}\delta_{pq}+(6-7\nu_{\mathrm{m}})\delta_{mp}\delta_{nq}+(6-7\nu_{\mathrm{m}})\delta_{mq}\delta_{np}\right]\\ &\quad +\delta_{jm}\left[-\delta_{ln}\delta_{pq}-\delta_{lp}\delta_{nq}+(6-7\nu_{\mathrm{m}})\delta_{lq}\delta_{np}\right]\\ &\quad +\delta_{jn}\left[-\delta_{lm}\delta_{pq}-\delta_{lp}\delta_{mq}+(6-7\nu_{\mathrm{m}})\delta_{lq}\delta_{mp}\right]\\ &\quad +\delta_{jp}\left[-\delta_{lm}\delta_{nq}-\delta_{ln}\delta_{mq}-\delta_{lq}\delta_{mn}\right]\\ &\quad +\delta_{jq}\left[(6-7\nu_{\mathrm{m}})\delta_{lm}\delta_{np}+(6-7\nu_{\mathrm{m}})\delta_{ln}\delta_{mp}-\delta_{lp}\delta_{mn}\right]\Big\} . \quad (6.200) \end{aligned}$$

Furthermore, if we multiply the sixth-order tensor in the braces with the tensor A^{m}_{iklm}, we obtain

$$70G_{\mathrm{m}}(1-\nu_{\mathrm{m}})\delta_{ip}\delta_{jq}\ . \tag{6.201}$$

Thus

$$\begin{aligned}
[p_{ij}] &= \frac{16\pi\varepsilon^3 G_{\mathrm{m}}(1-\nu_{\mathrm{m}})}{k} M_{pquv}\delta_{ip}\delta_{jq}\sum_{d=1}^{D}\left[\frac{1}{2}\left(\frac{\partial Q_u^{(0)}}{\partial X_v}+\frac{\partial Q_v^{(0)}}{\partial X_u}\right)\right]\Bigg|_{\boldsymbol{X}^d} && (6.202)\\
&= \varepsilon^3 M_{ijuv}\sum_{d=1}^{D}\left[\frac{1}{2}\left(\frac{\partial Q_u^{(0)}}{\partial X_v}+\frac{\partial Q_v^{(0)}}{\partial X_u}\right)\right]\Bigg|_{\boldsymbol{X}^d}\ , && (6.203)
\end{aligned}$$

by the definition (6.115) of k.

Now,

$$\begin{aligned}
\langle p_{ij}\rangle &= \frac{3}{4\pi\rho^3}[p_{ij}] && (6.204)\\
&= \varepsilon^3 M_{ijuv}\cdot\frac{3}{4\pi\rho^3}\sum_{d=1}^{D}\left[\frac{1}{2}\left(\frac{\partial Q_u^{(0)}}{\partial X_v}+\frac{\partial Q_v^{(0)}}{\partial X_u}\right)\right]\Bigg|_{\boldsymbol{X}^d} && (6.205)\\
&= \varepsilon^3 M_{ijuv}\left\langle\frac{1}{2}\left(\frac{\partial Q_u^{(0)}}{\partial X_v}+\frac{\partial Q_v^{(0)}}{\partial X_u}\right)\sum_{d=1}^{D}\delta(\boldsymbol{X}-\boldsymbol{X}^d)\right\rangle && (6.206)\\
&\approx \varepsilon^3 M_{ijuv}\omega(\boldsymbol{\xi})\left\langle\frac{1}{2}\left(\frac{\partial Q_u^{(0)}}{\partial X_v}+\frac{\partial Q_v^{(0)}}{\partial X_u}\right)\right\rangle && (6.207)\\
&= \varepsilon^3 M_{ijuv}\omega(\boldsymbol{\xi})\langle e_{uv}\rangle + O(\varepsilon^4)\ . && (6.208)
\end{aligned}$$

Substituting into equation (6.165), we find that

$$\widehat{A}_{ijkl}\langle e_{kl}\rangle = \left(A^{\mathrm{m}}_{ijkl}+\varepsilon^3 M_{ijkl}\omega(\boldsymbol{\xi})\right)\langle e_{kl}\rangle + O(\varepsilon^4)\ , \tag{6.209}$$

so that

$$\widehat{A}_{ijkl} = A^{\mathrm{m}}_{ijkl}+\varepsilon^3 M_{ijkl}\omega(\boldsymbol{\xi}) + o(\varepsilon^3)\ . \tag{6.210}$$

However, recall that this expression is in terms of dimensionless quantites, or

$$\widehat{A}_{ijkl} = A^{\mathrm{m}}_{ijkl}+\varepsilon^3\widetilde{M}_{ijkl}\widetilde{\omega}(\widetilde{\boldsymbol{\xi}})\ . \tag{6.211}$$

Changing to dimensional coordinates, we have

$$\begin{aligned}
\widehat{A}_{ijkl} &\approx A^{\mathrm{m}}_{ijkl}+(\varepsilon^3 b^3 a^{-3})M_{ijkl}\omega(\boldsymbol{\xi}) && (6.212)\\
&= A^{\mathrm{m}}_{ijkl}+M_{ijkl}\omega(\boldsymbol{\xi})\ . && (6.213)
\end{aligned}$$

6.3.2 The polarisability tensor for axisymmetric deformations

The previous section showed that in order to find the effective elasticity tensor of the composite material, we need to determine the polarisability tensor M_{ijkl}. We will do this for the situation where the individual inclusions undergo axisymmetric deformations.

Recall that the polarisability tensor satisfies

$$M_{ijkl}\, e_{kl}|_{\infty} \;=\; P_{ij}\ . \tag{6.214}$$

We will determine M_{ijkl} by first finding the canonical form of $e_{kl}|_{\infty}$ for axisymmetric deformations. Secondly, we will find P_{ij} from a representation of the axisymmetric form of the perturbation deformation $\boldsymbol{u}$. This will give us a system of equations to solve for the tensor M_{ijkl}.

To find the state of strain at infinity for axisymmetric deformations, we will assume that the state of stress at infinity is given by a superposition of two states. The overall stress tensor at infinity, in Cartesian components, becomes

$$\boldsymbol{\tau}|_{\infty} \;=\; \begin{pmatrix} q_{\rm s}-q_{\rm r} & 0 & 0 \\ 0 & q_{\rm s}-q_{\rm r} & 0 \\ 0 & 0 & -2q_{\rm s}-q_{\rm r} \end{pmatrix} \tag{6.215}$$

for two stress parameters $q_{\rm r}$ and $q_{\rm s}$. Now, consider an isotropic material experiencing a state of stress τ_{ij} and a state of strain e_{ij}. Any second order tensor can be uniquely split up into *hydrostatic* and *deviatoric* parts. For instance, define

$$\widehat{e} \;=\; e_{kk} \tag{6.216}$$

to be the dilatation, then

$$e_{ij} \;=\; \frac{\widehat{e}}{3}\delta_{ij} + \widetilde{e}_{ij}\ , \tag{6.217}$$

where $\widetilde{e}_{ij}$ is the deviatoric strain tensor (satisfying $\widetilde{e}_{kk}=0$). Similarly, we can write

$$\tau_{ij} \;=\; \widehat{\tau}\delta_{ij} + \widetilde{\tau}_{ij}\ , \tag{6.218}$$

where $\widehat{\tau} = \frac{1}{3}\tau_{kk}$ is known as the *mean stress*. Substituting (6.217) into the stress–strain relation for isotropic materials,

$$\tau_{ij} \;=\; \lambda e_{kk}\delta_{ij} + 2Ge_{ij}\ , \tag{6.219}$$

we find that

$$\tau_{ij} \;=\; \left(\lambda + \frac{2G}{3}\right)\widehat{e}\delta_{ij} + 2G\widetilde{e}_{ij}\ . \tag{6.220}$$

Comparing this with (6.218), we find that

$$\widehat{\tau} = K\widehat{e}\,, \tag{6.221}$$

$$\widetilde{\tau}_{ij} = 2G\widetilde{e}_{ij}\,, \tag{6.222}$$

where $K = \lambda + \frac{2}{3}G$ is the bulk modulus of the material.

Now, considering the state of stress (6.215), we obtain

$$\widehat{\tau}|_{\infty} = -q_{\mathrm{r}}\,, \tag{6.223}$$

$$\widetilde{\tau}_{ij}|_{\infty} = q_{\mathrm{s}}A_{ij}\,, \tag{6.224}$$

where A_{ij} are the components of the matrix

$$\boldsymbol{A} = \begin{pmatrix} 1 & 0 & 0 \\ 0 & 1 & 0 \\ 0 & 0 & -2 \end{pmatrix}. \tag{6.225}$$

Hence

$$\widehat{e}|_{\infty} = -\frac{q_{\mathrm{r}}}{K}\,, \tag{6.226}$$

$$\widetilde{e}_{ij}|_{\infty} = \frac{q_{\mathrm{s}}}{2G}A_{ij}\,, \tag{6.227}$$

and from (6.217) we can write the state of strain at infinity for general axisymmetric deformations as

$$e_{kl}|_{\infty} = -\frac{q_{\mathrm{r}}}{3K}\delta_{kl} + \frac{q_{\mathrm{s}}}{2G}A_{kl}\,. \tag{6.228}$$

In order to determine P_{ij} in (6.214), we note that for axisymmetric deformations, the leading-order terms of the perturbation displacement at infinity are of the form

$$\begin{aligned}\boldsymbol{u} = \frac{1}{R^2}\left[\xi P_0^{(0)}(\mu) + \left(\frac{5-4\nu_{\mathrm{m}}}{1-2\nu_{\mathrm{m}}}\right)\eta P_2^{(0)}(\mu)\right]\boldsymbol{e}_R \\ + \frac{1}{R^2}\eta P_2^{(1)}(\mu)\boldsymbol{e}_\theta\end{aligned} \tag{6.229}$$

for some constants ξ and η. These constants will be linearly dependent on the stress field at infinity. We note that we have decomposed this stress field into hydrostatic and deviatoric parts, represented by q_{r} and q_{s} respectively. Thus we can write

$$\xi = q_{\mathrm{r}}\xi^{\mathrm{r}} + q_{\mathrm{s}}\xi^{\mathrm{s}}\,, \tag{6.230}$$

$$\eta = q_{\mathrm{r}}\eta^{\mathrm{r}} + q_{\mathrm{s}}\eta^{\mathrm{s}}\,. \tag{6.231}$$

Therefore the leading-order part to the perturbation displacement in any axisymmetric problem is given by

$$\begin{aligned}\boldsymbol{u} = \frac{1}{R^2}\left[(q_{\mathrm{r}}\xi^{\mathrm{r}} + q_{\mathrm{s}}\xi^{\mathrm{s}})P_0^{(0)}(\mu) + \left(\frac{5-4\nu_{\mathrm{m}}}{1-2\nu_{\mathrm{m}}}\right)(q_{\mathrm{r}}\eta^{\mathrm{r}} + q_{\mathrm{s}}\eta^{\mathrm{s}})P_2^{(0)}(\mu)\right]\boldsymbol{e}_R \\ + \frac{1}{R^2}(q_{\mathrm{r}}\eta^{\mathrm{r}} + q_{\mathrm{s}}\eta^{\mathrm{s}})P_2^{(1)}(\mu)\boldsymbol{e}_\theta\,,\end{aligned} \tag{6.232}$$

and is thus characterised by the four constants $\xi^{\rm r}$, $\xi^{\rm s}$, $\eta^{\rm r}$ and $\eta^{\rm s}$. These constants will be found for both the pre-buckled and post-buckled shell in Sections 6.3.3–6.3.4.

We now suppose that P_{ij} is a matrix of the form

$$P_{ij} \;=\; \alpha\delta_{ij} + \beta A_{ij} \;, \tag{6.233}$$

where α and β are to be found. We substitute this into equation (6.120) and equate the result to the general expression (6.232) for a uniaxial response to an applied stress field. Eventually, we find that $\boldsymbol{u} = P_{ij}\boldsymbol{u}^{ij}$ becomes

$$\boldsymbol{u} \;=\; -\frac{2(1-2\nu_{\rm m})\alpha}{kR^2}\boldsymbol{e}_R + \frac{2(5-4\nu_{\rm m})\beta}{kR^2}P_2^{(0)}(\mu)\boldsymbol{e}_R + \frac{2(1-2\nu_{\rm m})\beta}{kR^2}P_2^{(1)}(\mu)\boldsymbol{e}_\theta \;. \tag{6.234}$$

On comparison with (6.232), we obtain

$$\alpha \;=\; -\frac{k(q_{\rm r}\xi^{\rm r} + q_{\rm s}\xi^{\rm s})}{2(1-2\nu_{\rm m})} \;, \tag{6.235}$$

$$\beta \;=\; \frac{k(q_{\rm r}\eta^{\rm r} + q_{\rm s}\eta^{\rm s})}{2(1-2\nu_{\rm m})} \;. \tag{6.236}$$

Thus

$$P_{ij} \;=\; \frac{k}{2(1-2\nu_{\rm m})}\left[-(q_{\rm r}\xi^{\rm r} + q_{\rm s}\xi^{\rm s})\delta_{ij} + (q_{\rm r}\eta^{\rm r} + q_{\rm s}\eta^{\rm s})A_{ij}\right] \;, \tag{6.237}$$

and, from (6.214) it remains to find the M_{ijkl} that satisfies

$$M_{ijkl}\left(-\frac{q_{\rm r}}{3K_{\rm m}}\delta_{kl} + \frac{q_{\rm s}}{2G_{\rm m}}A_{kl}\right) \;=\; \frac{k}{2(1-2\nu_{\rm m})}\left[-(q_{\rm r}\xi^{\rm r} + q_{\rm s}\xi^{\rm s})\delta_{ij} + (q_{\rm r}\eta^{\rm r} + q_{\rm s}\eta^{\rm s})A_{ij}\right] \;. \tag{6.238}$$

The equation (6.238) has to be true for any values of $q_{\rm r}$ and $q_{\rm s}$. Thus the equation can be decomposed into two:

$$-\frac{1}{3K_{\rm m}}M_{ijkl}\delta_{kl} \;=\; \frac{k}{2(1-2\nu_{\rm m})}\left(-\xi^{\rm r}\delta_{ij} + \eta^{\rm r}A_{ij}\right) \;, \tag{6.239}$$

$$\frac{1}{2G_{\rm m}}M_{ijkl}A_{kl} \;=\; \frac{k}{2(1-2\nu_{\rm m})}\left(-\xi^{\rm s}\delta_{ij} + \eta^{\rm s}A_{ij}\right) \;. \tag{6.240}$$

This tensor M_{ijkl} has to satisfy the restrictions applied to all elasticity tensors, because the effective elasticity tensor (6.213) is linear in M_{ijkl}. Thus we require

$$M_{ijkl} \;=\; M_{jikl} \;=\; M_{ijlk} \;=\; M_{klij} \;. \tag{6.241}$$

Alternatively, we could use the symmetry of the problem to prescribe a form of M_{ijkl}, and then solve for its components. Certainly, if $\xi^{\rm s} = \eta^{\rm r} = 0$, then we can assume that M_{ijkl} has the form of an isotropic elasticity tensor, i.e.

$$M_{ijkl} \;=\; \lambda'\delta_{ij}\delta_{kl} + G'(\delta_{ik}\delta_{jl} + \delta_{il}\delta_{jk}) \;, \tag{6.242}$$

for constants λ' and G'. With this form of M_{ijkl}, we find that

$$M_{ijkl}\delta_{kl} = (3\lambda' + 2G')\delta_{ij} \tag{6.243}$$

$$M_{ijkl}A_{kl} = 2G'A_{ij} \; . \tag{6.244}$$

Thus, defining $K' = \lambda' + \frac{2}{3}G'$, we have from equations (6.239)–(6.240) that

$$K' = K_{\rm m}\frac{k\xi^{\rm r}}{2(1-2\nu_{\rm m})} \; , \tag{6.245}$$

$$G' = G_{\rm m}\frac{k\eta^{\rm s}}{2(1-2\nu_{\rm m})} \; . \tag{6.246}$$

If, on the other hand, one or both of $\xi^{\rm s}$ and $\eta^{\rm r}$ are nonzero, the tensor M_{ijkl} will have the form of an *anisotropic* elasticity tensor. All elasticity tensors can be represented as a 6×6 symmetric matrix, satisfying

$$\begin{pmatrix} \tau_{11} \\ \tau_{22} \\ \tau_{33} \\ \tau_{23} \\ \tau_{31} \\ \tau_{12} \end{pmatrix} = \begin{pmatrix} C_{11} & C_{12} & C_{13} & C_{14} & C_{15} & C_{16} \\ & C_{22} & C_{23} & C_{24} & C_{25} & C_{26} \\ & & C_{33} & C_{34} & C_{35} & C_{36} \\ & & & C_{44} & C_{45} & C_{46} \\ & & & & C_{55} & C_{56} \\ & & & & & C_{66} \end{pmatrix} \begin{pmatrix} e_{11} \\ e_{22} \\ e_{33} \\ e_{23} \\ e_{31} \\ e_{12} \end{pmatrix} \; , \tag{6.247}$$

where the missing components are found from the fact that C_{ij} is symmetric. We will assume that M_{ijkl} has the form of an elasticity tensor for a *transversely isotropic* material. Such an elasticity tensor has the 6×6 form

$$\begin{pmatrix} C_1 & C_2 & C_4 & 0 & 0 & 0 \\ & C_1 & C_4 & 0 & 0 & 0 \\ & & C_3 & 0 & 0 & 0 \\ & & & C_5 & 0 & 0 \\ & & & & C_5 & 0 \\ & & & & & (C_1 - C_2) \end{pmatrix} \tag{6.248}$$

if the z-axis is taken to be the axis of symmetry, where C_i are material constants. Isotropic materials are a subset of transversely isotropic materials, with material constants given by

$$C_1 = C_3 = \lambda + 2G \; , \tag{6.249}$$

$$C_2 = C_4 = \lambda \; , \tag{6.250}$$

$$C_5 = 2G \; , \tag{6.251}$$

where λ and G are the usual Lamé elastic moduli.

Because both matrices δ_{ij} and A_{ij} are diagonal, the tensor M_{ijkl} can in fact be represented by the 3×3 submatrix

$$\begin{pmatrix} C_1 & C_2 & C_4 \\ C_2 & C_1 & C_4 \\ C_4 & C_4 & C_3 \end{pmatrix} \; . \tag{6.252}$$

The reason for this is that we do not consider simple shear deformations in our assumption of axisymmetry. Thus the material constant C_5 will be indeterminate. This will not cause difficulties, because the composite material will not be subjected to simple shear deformations, rather only deformations whose strain tensor will be a linear combination of δ_{ij} and A_{ij}.

Thus, considering equation (6.239), we find that

$$\begin{pmatrix} C_1 & C_2 & C_4 \\ C_2 & C_1 & C_4 \\ C_4 & C_4 & C_3 \end{pmatrix} \begin{pmatrix} 1 \\ 1 \\ 1 \end{pmatrix} = -\frac{3kK_{\rm m}}{2(1-2\nu_{\rm m})} \left[-\xi^{\rm r} \begin{pmatrix} 1 \\ 1 \\ 1 \end{pmatrix} + \eta^{\rm r} \begin{pmatrix} 1 \\ 1 \\ -2 \end{pmatrix} \right] . \quad (6.253)$$

Similarly for equation (6.240),

$$\begin{pmatrix} C_1 & C_2 & C_4 \\ C_2 & C_1 & C_4 \\ C_4 & C_4 & C_3 \end{pmatrix} \begin{pmatrix} 1 \\ 1 \\ -2 \end{pmatrix} = \frac{2kG_{\rm m}}{2(1-2\nu_{\rm m})} \left[-\xi^{\rm s} \begin{pmatrix} 1 \\ 1 \\ 1 \end{pmatrix} + \eta^{\rm s} \begin{pmatrix} 1 \\ 1 \\ -2 \end{pmatrix} \right] . \quad (6.254)$$

In each of these equations, the first two rows are equivalent, so that we have four equations for the four constants C_1–C_4. These are written as the system

$$\begin{pmatrix} 1 & 1 & 0 & 1 \\ 0 & 0 & 1 & 2 \\ 1 & 1 & 0 & -2 \\ 0 & 0 & -2 & 2 \end{pmatrix} \begin{pmatrix} C_1 \\ C_2 \\ C_3 \\ C_4 \end{pmatrix} = \begin{pmatrix} \alpha_1 \\ \alpha_2 \\ \alpha_3 \\ \alpha_4 \end{pmatrix} , \quad (6.255)$$

where

$$\alpha_1 = \frac{3kK_{\rm m}(\xi^{\rm r} - \eta^{\rm r})}{2(1-2\nu_{\rm m})} , \quad (6.256)$$

$$\alpha_2 = \frac{3kK_{\rm m}(\xi^{\rm r} + 2\eta^{\rm r})}{2(1-2\nu_{\rm m})} , \quad (6.257)$$

$$\alpha_3 = -\frac{2kG_{\rm m}(\xi^{\rm s} - \eta^{\rm s})}{2(1-2\nu_{\rm m})} , \quad (6.258)$$

$$\alpha_4 = -\frac{2kG_{\rm m}(\xi^{\rm s} + 2\eta^{\rm s})}{2(1-2\nu_{\rm m})} . \quad (6.259)$$

The system (6.255) for the coefficients is singular, in that the matrix has zero determinant. Thus, in order for a solution to exist we must have a condition on the right-hand side, by the Fredholm Alternative. This theorem states that, given a system $\boldsymbol{M}\boldsymbol{x} = \boldsymbol{f}$, *either* there exists a unique solution $\boldsymbol{x}$, *or* $\boldsymbol{M}$ is not invertible, so that there exists a nonzero vector $\boldsymbol{y}$ satisfying $\boldsymbol{y}^{\rm T}\boldsymbol{M} = \boldsymbol{0}^{\rm T}$. In this latter case, for existence of solutions $\boldsymbol{x}$ to the original system we must have $\boldsymbol{y}^{\rm T}\boldsymbol{f} = 0$ for all such $\boldsymbol{y}$. The solutions $\boldsymbol{x}$ in this case will necessarily be non-unique.

For the system (6.255), the left-eigenvector $\boldsymbol{y}$ defined above is

$$\boldsymbol{y}^{\rm T} = (-2 \;\; 2 \;\; 2 \;\; 1) . \quad (6.260)$$

Thus, for solutions to exist, we must have

$$-2\alpha_1 + 2\alpha_2 + 2\alpha_3 + \alpha_4 \;=\; 0\,. \tag{6.261}$$

Substituting from equations (6.256)–(6.259), we obtain the relation which must hold in order for M_{ijkl} to have the form of an elasticity tensor,

$$3K_{\mathrm{m}}\eta^{\mathrm{r}} \;=\; G_{\mathrm{m}}\xi^{\mathrm{s}}\,. \tag{6.262}$$

We would like to ensure that this relationship holds for the split shell system of Chapter 5. This can be shown by using the *reciprocity* principle,[3] which can be found in Sokolnikoff's treatise [88]. For the unbuckled shell, (6.262) will be seen to be trivially satisfied. If we have two states of deformation, with displacement fields u_i, u'_i and stress fields τ_{ij}, τ'_{ij} respectively, then for any region Ω we have

$$\int_{\partial\Omega} u_i(\tau'_{ij}n_j)\,\mathrm{d}S \;=\; \int_{\partial\Omega} u'_i(\tau_{ij}n_j)\,\mathrm{d}S\,, \tag{6.263}$$

in the absence of body forces. The two deformation states that we will choose both have the form of a homogeneous deformation together with the resulting perturbation deformation due to the inclusion, as given by (6.232). We denote the first by $\boldsymbol{u}^{\mathrm{r}}$, where we take $q_{\mathrm{s}} = 0$, and $\boldsymbol{u}^{\mathrm{s}}$, for which $q_{\mathrm{r}} = 0$. Then, including the non-decaying term at infinity, we have that

$$\begin{aligned}
\boldsymbol{u}^{\mathrm{r}} \;=\;& -\frac{Rq_{\mathrm{r}}}{3K_{\mathrm{m}}}P_0^{(0)}(\mu)\boldsymbol{e}_R + \frac{1}{R^2}\left[q_{\mathrm{r}}\xi^{\mathrm{r}}P_0^{(0)}(\mu) + \left(\frac{5-4\nu_{\mathrm{m}}}{1-2\nu_{\mathrm{m}}}\right)q_{\mathrm{r}}\eta^{\mathrm{r}}P_2^{(0)}(\mu)\right]\boldsymbol{e}_R \\
&+\frac{q_{\mathrm{r}}\eta^{\mathrm{r}}}{R^2}P_2^{(1)}(\mu)\boldsymbol{e}_\theta\,, \qquad (6.264)\\
\boldsymbol{u}^{\mathrm{s}} \;=\;& -\frac{Rq_{\mathrm{s}}}{G_{\mathrm{m}}}P_2^{(0)}(\mu)\boldsymbol{e}_R - \frac{Rq_{\mathrm{s}}}{2G_{\mathrm{m}}}P_2^{(1)}(\mu)\boldsymbol{e}_\theta \\
&+\frac{1}{R^2}\left[q_{\mathrm{s}}\xi^{\mathrm{s}}P_0^{(0)}(\mu) + \left(\frac{5-4\nu_{\mathrm{m}}}{1-2\nu_{\mathrm{m}}}\right)q_{\mathrm{s}}\eta^{\mathrm{s}}P_2^{(0)}(\mu)\right]\boldsymbol{e}_R \\
&+\frac{q_{\mathrm{s}}\eta^{\mathrm{s}}}{R^2}P_2^{(1)}(\mu)\boldsymbol{e}_\theta\,. \qquad (6.265)
\end{aligned}$$

We will choose as our domain Ω the region

$$\left\{\boldsymbol{X} \;:\; R_0 < |\boldsymbol{X}| < \bar{R}\right\} \setminus \left\{\boldsymbol{X} \;:\; X_3 = 0 \text{ and } R_0 \leqslant |\boldsymbol{X}| \leqslant R_1\right\}\,. \tag{6.266}$$

This characterises the hollow sphere with internal and external radii R_0, $\bar{R}$ (where $\bar{R} > R_1$, so that the outer surface of the set lies in the matrix) respectively, having subtracted the cut in the split shell from the set. Then, $\partial\Omega$ is composed of the inner surface together with the cut (along which $\tau_{ij}n_j$ is zero, so that there are no

[3] This is also known as the Betti–Rayleigh theorem and the Betti theorem.

contributions to (6.263) from here), and the sphere of radius $\bar{R}$. On this surface, the normal vector $\boldsymbol{n}$ will be given by $\boldsymbol{e}_R$, and the quantity $\tau_{ij}n_j$ will be given by the components of $\boldsymbol{\tau}\boldsymbol{e}_R$. From (6.264)–(6.265), we have that

$$\begin{aligned}\boldsymbol{\tau}^{\mathrm{r}}\boldsymbol{e}_R &= -q_{\mathrm{r}}P_0^{(0)}(\mu)\boldsymbol{e}_R - \frac{4G_{\mathrm{m}}}{R^3}\left[q_{\mathrm{r}}\xi^{\mathrm{r}} + \frac{5-\nu_{\mathrm{m}}}{1-2\nu_{\mathrm{m}}}q_{\mathrm{r}}\eta^{\mathrm{r}}P_2^{(0)}(\mu)\right]\boldsymbol{e}_R \\ &\quad + \frac{2q_{\mathrm{r}}\eta^{\mathrm{r}}G_{\mathrm{m}}}{R^3}\left(\frac{1+\nu_{\mathrm{m}}}{1-2\nu_{\mathrm{m}}}\right)P_2^{(1)}(\mu)\boldsymbol{e}_\theta\ , \qquad (6.267)\\ \boldsymbol{\tau}^{\mathrm{s}}\boldsymbol{e}_R &= -2q_{\mathrm{s}}P_2^{(0)}(\mu)\boldsymbol{e}_R - q_{\mathrm{s}}P_2^{(1)}(\mu)\boldsymbol{e}_\theta \\ &\quad - \frac{4G_{\mathrm{m}}}{R^3}\left[q_{\mathrm{s}}\xi^{\mathrm{s}} + \frac{5-\nu_{\mathrm{m}}}{1-2\nu_{\mathrm{m}}}q_{\mathrm{s}}\eta^{\mathrm{s}}P_2^{(0)}(\mu)\right]\boldsymbol{e}_R \\ &\quad + \frac{2q_{\mathrm{s}}\eta^{\mathrm{s}}G_{\mathrm{m}}}{R^3}\left(\frac{1+\nu_{\mathrm{m}}}{1-2\nu_{\mathrm{m}}}\right)P_2^{(1)}(\mu)\boldsymbol{e}_\theta\ . \qquad (6.268)\end{aligned}$$

By the reciprocity relation (6.263), we now have

$$\int_{R=\bar{R}} \boldsymbol{u}^{\mathrm{r}}\cdot(\boldsymbol{\tau}^{\mathrm{s}}\boldsymbol{e}_R)\,\mathrm{d}S \;=\; \int_{R=\bar{R}} \boldsymbol{u}^{\mathrm{s}}\cdot(\boldsymbol{\tau}^{\mathrm{r}}\boldsymbol{e}_R)\,\mathrm{d}S\ . \qquad (6.269)$$

We take the leading order term as $\bar{R}\to\infty$, and evaluate the integrals. On using the orthogonality condition (B.12) for the Legendre functions, we have that

$$\frac{6\xi^{\mathrm{s}}}{1+\nu_{\mathrm{m}}} - \frac{12\eta^{\mathrm{r}}}{1-2\nu_{\mathrm{m}}} \;=\; 0\ , \qquad (6.270)$$

which is equivalent to equation (6.262).

With this relation in place, the equation (6.255) becomes a 3×3 system for the three variables C_1+C_2, C_3 and C_4. Setting $C_1=C_2$, we solve the equation to give

$$\begin{aligned}C_1 &= \frac{k}{6(1-2\nu_{\mathrm{m}})}\left[3K_{\mathrm{m}}(\xi^{\mathrm{r}}-\eta^{\mathrm{r}}) - G_{\mathrm{m}}(\xi^{\mathrm{s}}-\eta^{\mathrm{s}})\right]\ , \qquad (6.271)\\ C_3 &= \frac{k}{6(1-2\nu_{\mathrm{m}})}\left[3K_{\mathrm{m}}(\xi^{\mathrm{r}}+2\eta^{\mathrm{r}}) + 2G_{\mathrm{m}}(\xi^{\mathrm{s}}+2\eta^{\mathrm{s}})\right]\ , \qquad (6.272)\\ C_4 &= \frac{k}{6(1-2\nu_{\mathrm{m}})}\left[3K_{\mathrm{m}}(\xi^{\mathrm{r}}-\eta^{\mathrm{r}}) + 2G_{\mathrm{m}}(\xi^{\mathrm{s}}-\eta^{\mathrm{s}})\right]\ . \qquad (6.273)\end{aligned}$$

In summary, the polarisability tensor M_{ijkl} is given by

$$M_{ijkl} \;=\; \left(K' - \frac{2G'}{3}\right)\delta_{ij}\delta_{kl} + G'(\delta_{ik}\delta_{jl}+\delta_{il}\delta_{jk}) \qquad (6.274)$$

if $\xi^{\mathrm{s}}=\eta^{\mathrm{r}}=0$, where K' and G' are given by (6.245)–(6.246). If ξ^{s} and η^{r} are not zero, then the tensor M_{ijkl} has the form of a transversely isotropic elasticity tensor, whose action on a vector of strains e_{ij} is given by

$$\begin{pmatrix} C_1 & C_1 & C_3 & & & \\ C_1 & C_1 & C_3 & & & \\ C_3 & C_3 & C_4 & & & \\ & & & * & & \\ & & & & * & \\ & & & & & * \end{pmatrix}\begin{pmatrix} e_{11}\\ e_{22}\\ e_{33}\\ e_{23}\\ e_{31}\\ e_{12}\end{pmatrix} \qquad (6.275)$$

with C_1, C_3 and C_4 given by equations (6.271)–(6.273). The terms denoted $*$ in the relation above are not needed because the material that we will consider will never be subjected to simple shear deformations.

We will now proceed to determine the effective elasticity tensor for both unbuckled and buckled shells, by evaluating the tensor M_{ijkl} in each case.

6.3.3 The effective elasticity tensor pre-buckling

We recall that the effective elasticity tensor, in general, is given by equation (6.213). We first wish to find the polarisability tensor for the unbuckled shell. Recall from Chapter 3 that we had considered two types of stress field at infinity, namely uniaxial,

$$\tau_{ij}|_{\infty} = -q_z\delta_{i3}\delta_{j3} \,, \tag{6.276}$$

and radial,

$$\tau_{ij}|_{\infty} = -q_R\delta_{ij} \,. \tag{6.277}$$

The resulting displacement fields in the matrix were given by equations (3.63)–(3.64) for the uniaxial stress field, and by (3.89) for the radial stress field. The leading order parts of these fields at infinity are given by

$$\boldsymbol{u} = \left[-\frac{A}{R^2}P_0^{(0)}(\mu) + \frac{C(\alpha_{-3}-3)}{R^2}P_2^{(0)}(\mu)\right]\boldsymbol{e}_R + \frac{C}{R^2}P_2^{(1)}(\mu)\boldsymbol{e}_\theta \tag{6.278}$$

for the uniaxial stress field at infinity, and

$$\boldsymbol{u} = \frac{B_{\rm m}}{R^2}\boldsymbol{e}_R \tag{6.279}$$

for the radial stress field. The constants A and C are given by the solution to the system (3.77)–(3.85) and are proportional to q_z, whereas $B_{\rm m}$ is given by (3.93) with $q_{\rm in} = 0$, (we will assume this for simplicity) and is linear in q_R. Thus, if we define

$$\widetilde{A} = q_z^{-1}A \,, \tag{6.280}$$

$$\widetilde{C} = q_z^{-1}C \,, \tag{6.281}$$

$$\widetilde{B} = q_R^{-1}B_{\rm m} \,, \tag{6.282}$$

then these are independent of the stress at infinity and we can write the leading order perturbation displacement at infinity as

$$\boldsymbol{u} = \frac{1}{R^2}\left[\left(\widetilde{B}q_R - \widetilde{A}q_z\right)P_0^{(0)}(\mu) + \widetilde{C}q_z\left(\frac{5-4\nu_{\rm m}}{1-2\nu_{\rm m}}\right)P_2^{(0)}(\mu)\right]\boldsymbol{e}_R + \frac{\widetilde{C}q_z}{R^2}P_2^{(1)}(\mu)\boldsymbol{e}_\theta \,, \tag{6.283}$$

when the stress field at infinity is a superposition of the two states (6.276) and (6.277), and where we have substituted for α_{-3} from (3.45).

Now, we wish to consider a stress state at infinity as given by equation (6.215), involving the parameters $q_{\rm r}$ and $q_{\rm s}$. Then we have

$$\tau_{ij}|_{\infty} \;=\; (q_{\rm s}-q_{\rm r})\delta_{ij} - 3q_{\rm s}\delta_{i3}\delta_{j3}\;, \tag{6.284}$$

so that, on comparing with the superposition of the two states (6.276) and (6.277) we require

$$q_R \;=\; q_{\rm r}-q_{\rm s}\;, \tag{6.285}$$

$$q_z \;=\; 3q_{\rm s}\;. \tag{6.286}$$

Substituting into equation (6.283), we find that

$$\begin{aligned}\boldsymbol{u} \;=\; \frac{1}{R^2}\left[\left(\widetilde{B}q_{\rm r}-(\widetilde{B}+3\widetilde{A})q_{\rm s}\right)P_0^{(0)}(\mu)+3\widetilde{C}q_{\rm s}\left(\frac{5-4\nu_{\rm m}}{1-2\nu_{\rm m}}\right)P_2^{(0)}(\mu)\right]\boldsymbol{e}_R \\ +\frac{3\widetilde{C}q_{\rm s}}{R^2}P_2^{(1)}(\mu)\boldsymbol{e}_\theta\;.\end{aligned} \tag{6.287}$$

In order to find the parameters $\xi^{\rm r}$, $\xi^{\rm s}$, $\eta^{\rm r}$ and $\eta^{\rm s}$ for unbuckled shells, we need to compare this to equation (6.232), yielding

$$\xi^{\rm r} \;=\; \widetilde{B}\;, \tag{6.288}$$

$$\xi^{\rm s} \;=\; -\widetilde{B}-3\widetilde{A}\;, \tag{6.289}$$

$$\eta^{\rm r} \;=\; 0\;, \tag{6.290}$$

$$\eta^{\rm s} \;=\; 3\widetilde{C}\;. \tag{6.291}$$

However, on calculating the constants it is found that $\widetilde{B}=-3\widetilde{A}$ so that $\xi^{\rm s}=0$. Hence, by the theory of Section 6.3.2, we find that the polarisability tensor for unbuckled inclusions has the form of an isotropic elasticity tensor. Thus, where a superscript '$-$' reminds us that we are analysing the pre-buckling polarisability tensor,

$$M^{-}_{ijkl} \;=\; \left(K'-\frac{2G'}{3}\right)\delta_{ij}\delta_{kl}+G'(\delta_{ik}\delta_{jl}+\delta_{il}\delta_{jk})\;, \tag{6.292}$$

where K' and G' are given by equations (6.245)–(6.246). On substituting for the values of $\xi^{\rm r}$ and $\eta^{\rm s}$, we find that

$$K' \;=\; K_{\rm m}\frac{k\widetilde{B}}{2(1-2\nu_{\rm m})}\;, \tag{6.293}$$

$$G' \;=\; G_{\rm m}\frac{3k\widetilde{C}}{2(1-2\nu_{\rm m})}\;. \tag{6.294}$$

Substituting this into (6.213), we find that the effective elastic tensor for unbuckled shells is isotropic. Thus we can say that

$$\widehat{A}_{ijkl} = \left(\widehat{K} - \frac{2\widehat{G}}{3}\right)\delta_{ij}\delta_{kl} + \widehat{G}(\delta_{ik}\delta_{jl} + \delta_{il}\delta_{jk}) \,, \tag{6.295}$$

where $\widehat{K}$ and $\widehat{G}$ are the effective bulk modulus and shear modulus, respectively. These are given by

$$\widehat{K} = K_{\mathrm{m}} + \omega(\boldsymbol{\xi})K_{\mathrm{m}}\frac{k\widetilde{B}}{2(1-2\nu_{\mathrm{m}})} \,, \tag{6.296}$$

$$\widehat{G} = G_{\mathrm{m}} + \omega(\boldsymbol{\xi})G_{\mathrm{m}}\frac{3k\widetilde{C}}{2(1-2\nu_{\mathrm{m}})} \,. \tag{6.297}$$

6.3.3.1 Comparison with spherical elastic inclusions

In the expressions above for the effective bulk and shear moduli, the constants $\widetilde{B}$ and $\widetilde{C}$ are dependent on R_0 and R_1, the radii of the shell inner and outer surfaces, in a complicated way. However, by setting $R_0 \to 0$ and $R_1 \to \widehat{R}$, we can compare the results (6.296)–(6.297) to the well-known results that were originally derived by Hashin.

Analysis in a symbolic computation package such as Maple shows that in the limits described above we find that

$$\widetilde{B} \to \frac{\widehat{R}^3(K_{\mathrm{s}} - K_{\mathrm{m}})}{K_{\mathrm{m}}(4G_{\mathrm{m}} + 3K_{\mathrm{s}})} \,, \tag{6.298}$$

$$\widetilde{C} \to \frac{5\widehat{R}^3}{6G_{\mathrm{m}}}\left[\frac{(G_{\mathrm{s}} - G_{\mathrm{m}})(1-2\nu_{\mathrm{m}})}{G_{\mathrm{m}}(7-5\nu_{\mathrm{m}}) + G_{\mathrm{s}}(8-10\nu_{\mathrm{m}})}\right] \,. \tag{6.299}$$

Substituting these values into (6.296)–(6.297) gives the effective moduli as

$$\widehat{K} = K_{\mathrm{m}}\left[1 + \frac{4\pi\widehat{R}^3\omega}{3}\,\gamma_1\left(1 + \frac{4G_{\mathrm{m}}}{3K_{\mathrm{m}}}\right)\right] \,, \tag{6.300}$$

$$\widehat{G} = G_{\mathrm{m}}\left[1 + \frac{4\pi\widehat{R}^3\omega}{3}\,15\gamma_2(1-\nu_{\mathrm{m}})\right] \,, \tag{6.301}$$

where

$$\gamma_1 = \frac{3(K_{\mathrm{s}} - K_{\mathrm{m}})}{3K_{\mathrm{s}} + 4G_{\mathrm{m}}} \,, \tag{6.302}$$

$$\gamma_2 = \frac{G_{\mathrm{s}} - G_{\mathrm{m}}}{2G_{\mathrm{s}}(4-5\nu_{\mathrm{m}}) + G_{\mathrm{m}}(7-5\nu_{\mathrm{m}})} \,. \tag{6.303}$$

Now, given that the quantity $4\pi\widehat{R}^3\omega/3$ represents the volume fraction of the composite material occupied by the inclusions, these effective moduli correspond exactly with those found by Hashin [42].

6.3.4 The effective elasticity tensor post-buckling

In order to determine the effective elasticity tensor which results from a dispersion of *split* shells, we need to compare the leading order displacements (5.214)–(5.215) found in Chapter 5 to the general case (6.232), in order to find the coefficients ξ and η from the Love stress function coefficients $\chi_{\rm m}$ and ψ_1. Considering a superposition of the two stress states at infinity given on page 167, which is the same as (6.215), we find that

$$\begin{aligned}\boldsymbol{u} &= \frac{1}{2G_{\rm m}R^2}\left[\left(\chi_{\rm m}-\frac{2(1-2\nu_{\rm m})}{3}\psi_1\right)P_0^{(0)}(\mu)-\frac{2(5-4\nu_{\rm m})}{3}\psi_1 P_2^{(0)}(\mu)\right]\boldsymbol{e}_R \\ &\quad -\frac{1}{2G_{\rm m}R^2}\cdot\frac{2(1-2\nu_{\rm m})}{3}\psi_1 P_2^{(1)}(\mu)\boldsymbol{e}_\theta\ , \end{aligned} \tag{6.304}$$

where

$$\chi_{\rm m} = q_{\rm r}\widetilde{\chi}_{\rm m}^{\rm r}+q_{\rm s}\widetilde{\chi}_{\rm m}^{\rm s}\ , \tag{6.305}$$

$$\psi_1 = q_{\rm r}\widetilde{\psi}_1^{\rm r}+q_{\rm s}\widetilde{\psi}_1^{\rm s}\ . \tag{6.306}$$

The coefficients $\widetilde{\chi}_{\rm m}^{\rm r}$, $\widetilde{\chi}_{\rm m}^{\rm s}$, $\widetilde{\psi}_1^{\rm r}$ and $\widetilde{\psi}_1^{\rm s}$ are defined by (5.216)–(5.219). Therefore, comparing (6.304) with (6.232), we find that

$$\xi^{\rm r} = \frac{1}{2G_{\rm m}}\left(\widetilde{\chi}_{\rm m}^{\rm r}-\frac{2(1-2\nu_{\rm m})}{3}\widetilde{\psi}_1^{\rm r}\right)\ , \tag{6.307}$$

$$\eta^{\rm r} = -\frac{(1-2\nu_{\rm m})\widetilde{\psi}_1^{\rm r}}{3G_{\rm m}}\ , \tag{6.308}$$

$$\xi^{\rm s} = \frac{1}{2G_{\rm m}}\left(\widetilde{\chi}_{\rm m}^{\rm s}-\frac{2(1-2\nu_{\rm m})}{3}\widetilde{\psi}_1^{\rm s}\right)\ , \tag{6.309}$$

$$\eta^{\rm s} = -\frac{(1-2\nu_{\rm m})\widetilde{\psi}_1^{\rm s}}{3G_{\rm m}}\ . \tag{6.310}$$

Note that we have not yet made any restrictions on the values of $\widetilde{\chi}_{\rm m}$ and $\widetilde{\psi}_1$ between the radial and shear cases. However, the coefficients $\eta^{\rm r}$ and $\xi^{\rm s}$ must be related according to equation (6.262). This leads to a condition on the four Love stress function coefficients. This condition is

$$4(1+\nu_{\rm m})\widetilde{\psi}_1^{\rm r}-2(1-2\nu_{\rm m})\widetilde{\psi}_1^{\rm s}+3\widetilde{\chi}_{\rm m}^{\rm s} = 0\ . \tag{6.311}$$

For the values in Table 1.1, the values of the four Love stress function coefficents were given in (5.220)–(5.223) and were subsequently shown to agree with (6.311) satisfactorily.

Therefore, the tensor M_{ijkl} in this case — which we will denote M^+_{ijkl} to remind us that we are analysing the post-buckled case — is transversely isotropic with a form given by (6.275), where C_1–C_4 are given by (6.271)–(6.273). The effective elasticity tensor, from (6.213), is then given by

$$\widehat{A}_{ijkl} = A^{\rm m}_{ijkl}+\omega(\boldsymbol{\xi})M^+_{ijkl}\ . \tag{6.312}$$

6.4 Modelling the uniaxial displacement experiment

For the two cases that we will consider, namely buckled and unbuckled shells, we note that the effective elasticity tensor in each case can be written as

$$\widehat{A}_{ijkl} \;=\; \bar{A}_{ijkl} + \bar{M}_{ijkl} \tag{6.313}$$

where $\bar{A}_{ijkl}$ has the form of an isotropic elasticity tensor,

$$\bar{A}_{ijkl} \;=\; \bar{\lambda}\delta_{ij}\delta_{kl} + \bar{G}(\delta_{ik}\delta_{jl} + \delta_{il}\delta_{jk}) \;, \tag{6.314}$$

and $\bar{M}_{ijkl}$ has the form of a transversely isotropic elasticity tensor, which is given as in equation (6.275) with coefficients $\bar{C}_1$, $\bar{C}_3$ and $\bar{C}_4$. Thus, if we consider a slab of a material with this given effective elasticity tensor, undergoing a homogeneous axisymmetric state of strain (e_{11}, e_{11}, e_{33}) and a corresponding state of stress, they are related by

$$\begin{pmatrix} \tau_{11} \\ \tau_{11} \\ \tau_{33} \end{pmatrix} \;=\; \begin{pmatrix} \bar{C}_1 + \bar{\lambda} + 2\bar{G} & \bar{C}_1 + \bar{\lambda} & \bar{C}_3 + \bar{\lambda} \\ \bar{C}_1 + \bar{\lambda} & \bar{C}_1 + \bar{\lambda} + 2\bar{G} & \bar{C}_3 + \bar{\lambda} \\ \bar{C}_3 + \bar{\lambda} & \bar{C}_3 + \bar{\lambda} & \bar{C}_4 + \bar{\lambda} + 2\bar{G} \end{pmatrix} \begin{pmatrix} e_{11} \\ e_{11} \\ e_{33} \end{pmatrix} \;. \tag{6.315}$$

The experiment described in Chapter 1 involved a slab of the material undergoing a state of stress of the above form, with $\tau_{11} = 0$, $\tau_{33} = -q$. The equation (6.315) now becomes a system of two equations for the strain components e_{11} and e_{33}. The displacement of the top surface of the slab is then proportional to $-e_{33}$. We find that the two equations to be solved are

$$2(\bar{C}_1 + \bar{\lambda} + \bar{G})e_{11} + (\bar{C}_3 + \bar{\lambda})e_{33} \;=\; 0 \;, \tag{6.316}$$

$$2(\bar{C}_3 + \bar{\lambda})e_{11} + (\bar{C}_4 + \bar{\lambda} + 2\bar{G})e_{33} \;=\; -q \;. \tag{6.317}$$

Eliminating e_{11}, we find that

$$-\,e_{33} \;=\; q\left[(\bar{C}_4 + \bar{\lambda} + 2\bar{G}) - \frac{(\bar{C}_3 + \bar{\lambda})^2}{\bar{C}_1 + \bar{\lambda} + \bar{G}}\right]^{-1} \;. \tag{6.318}$$

We will now consider what the resulting displacement is for unbuckled shells, and buckled shells separately. For unbuckled shells, we apply the above formula with $\bar{C}_1 = \bar{C}_3 = \bar{C}_4 = 0$, and

$$\bar{\lambda} \;=\; \widehat{K} - \frac{2\widehat{G}}{3} \;, \tag{6.319}$$

$$\bar{G} \;=\; \widehat{G} \;, \tag{6.320}$$

for $\widehat{K}$ and $\widehat{G}$ from equations (6.296)–(6.297). We obtain

$$-e_{33} = \frac{q}{9}\left(\frac{3}{\widehat{G}}+\frac{1}{\widehat{K}}\right) . \tag{6.321}$$

For buckled shells, from equation (6.312), we use the values

$$\bar{C}_1 = \omega(\boldsymbol{\xi})C_1 , \qquad \bar{C}_3 = \omega(\boldsymbol{\xi})C_3 , \qquad \bar{C}_4 = \omega(\boldsymbol{\xi})C_4 , \tag{6.322}$$

$$\bar{\lambda} = \lambda_{\rm m} , \qquad \bar{G} = G_{\rm m} . \tag{6.323}$$

This gives us the resulting displacement

$$-e_{33} = q\left[(\omega(\boldsymbol{\xi})C_4+\lambda_{\rm m}+2G_{\rm m})-\frac{(\omega(\boldsymbol{\xi})C_3+\lambda_{\rm m})^2}{\omega(\boldsymbol{\xi})C_1+\lambda_{\rm m}+G_{\rm m}}\right]^{-1} . \tag{6.324}$$

6.4.1 A size-distribution of inclusions

We now follow the theory of Section 2.4.4, and consider a composite material which contains a range of differently-sized inclusions. These inclusions will buckle at different values of the applied stress, leading to a gradual softening of the material.

In general, the effective elasticity tensor of the composite material can be written as

$$\widehat{A}_{ijkl} = A^{\rm m}_{ijkl}+\omega(\boldsymbol{\xi})M_{ijkl} , \tag{6.325}$$

where the tensor M_{ijkl} has a different form for each inclusion, before and after buckling. We have denoted these two cases by M^{-}_{ijkl} and M^{+}_{ijkl} respectively, in equations (6.292) and (6.312).

It is necessary to work with the dimensionless forms of these tensors, given as in (6.129) by

$$\widetilde{M}^{\pm}_{ijkl} = a^{-3}M^{\pm}_{ijkl} , \tag{6.326}$$

where a is the radius of the inclusion, which was denoted in Chapters 3–5 by $\widehat{R}$. Henceforth we will replace the notation a by the shell mid-surface radius $\widehat{R}$. Then we have that

$$\widehat{A}^{\pm}_{ijkl} = A^{\rm m}_{ijkl}+\omega\widehat{R}^3\widetilde{M}^{\pm}_{ijkl} , \tag{6.327}$$

for both cases under consideration.

Now we'll suppose that the radii of the inclusions are distributed according to a random variable with probability density function $\mathscr{F}(\widehat{R})$. We will also assume that the inclusions are not buckled for $\widehat{R}<\widehat{R}_{\rm crit}$, but buckled for $\widehat{R}>\widehat{R}_{\rm crit}$, where $\widehat{R}_{\rm crit}$ is a critical value of the radius which is dependent on the applied stress q at infinity.

The stress at infinity is uniaxial as explained earlier, so that $\tau_{11} = 0$ and $\tau_{33} = -q$ throughout the material. Then, following the theory of Section 2.4.4, we have that the composite material with the above properties and experiencing the stress at infinity q, has the elasticity tensor

$$\widehat{A}_{ijkl}(q) \;=\; A^{\mathrm{m}}_{ijkl} + \omega \left[\widetilde{M}^{-}_{ijkl} \mathscr{Q}^{-}(q) + \widetilde{M}^{+}_{ijkl} \mathscr{Q}^{+}(q) \right] , \tag{6.328}$$

where

$$\mathscr{Q}^{+}(q) \;=\; \int_{\widehat{R}_{\mathrm{crit}}(q)}^{\infty} \widehat{R}^3 \mathscr{F}(\widehat{R}) \, \mathrm{d}\widehat{R} \, , \tag{6.329}$$

$$\mathscr{Q}^{-}(q) \;=\; \int_{0}^{\widehat{R}_{\mathrm{crit}}(q)} \widehat{R}^3 \mathscr{F}(\widehat{R}) \, \mathrm{d}\widehat{R} \, . \tag{6.330}$$

To find $\widehat{R}_{\mathrm{crit}}$ we note that, analogously to Section 6.2.4, the stress field locally at any point in the composite material is the same as the stress at infinity for the local problem of a single inclusion. Correspondingly, the *critical* stress for any inclusion in the composite material is the same as the critical stress for that inclusion considered in isolation. This critical stress was given by equation (4.307) in Chapter 4. We will redefine the constants in this expression, due to the subsequent duplication of notation. Writing the small parameter ε of that chapter in terms of its components, we have

$$q \;=\; \left(\frac{G_{\mathrm{m}}}{G_{\mathrm{s}}} \right)^{5/3} G_{\mathrm{s}} \left[\frac{3\kappa^2}{\alpha} + \frac{3h|\kappa|}{\widehat{R}\alpha} \left(\frac{G_{\mathrm{s}}}{G_{\mathrm{m}}} \right)^{1/3} \sqrt{\frac{\beta}{2\alpha}} \right] \tag{6.331}$$

for buckling, where α and β are the A and B of (4.254) and (4.256), κ is given by equation (4.280), h is the shell thickness and $\widehat{R}$ is the shell radius.

The thickness and radii of the spheres in the composite material will be distributed according to some joint probability distribution, where the two variables are not necessarily independent. However, in the absence of any data about this distribution, we will assume that the thickness h is kept constant for each inclusion, regardless of its size, so that we have a variation in the critical stress for differently-sized inclusions.

The critical radius $\widehat{R}_{\mathrm{crit}}$ is found by inverting (6.331) to become a function of q. We obtain

$$\widehat{R}_{\mathrm{crit}} \;=\; \begin{cases} \infty & q \leqslant q_{\min} \\ \dfrac{3h|\kappa|}{\alpha} \left(\dfrac{G_{\mathrm{s}}}{G_{\mathrm{m}}} \right)^{1/3} \sqrt{\dfrac{\beta}{2\alpha}} \left[\left(\dfrac{G_{\mathrm{s}}}{G_{\mathrm{m}}} \right)^{5/3} \dfrac{q}{G_{\mathrm{s}}} - \dfrac{3\kappa^2}{\alpha} \right]^{-1} & q > q_{\min} \, , \end{cases} \tag{6.332}$$

where

$$q_{\min} \;=\; \frac{3\kappa^2}{\alpha} G_{\mathrm{s}} \left(\frac{G_{\mathrm{m}}}{G_{\mathrm{s}}} \right)^{5/3} \tag{6.333}$$

represents the lowest value of the stress at infinity for which any inclusions buckle. A plot of $\widehat{R}_{\text{crit}}(q)$ for values of the constants as given in Table 1.1 is shown in Figure 6.2.

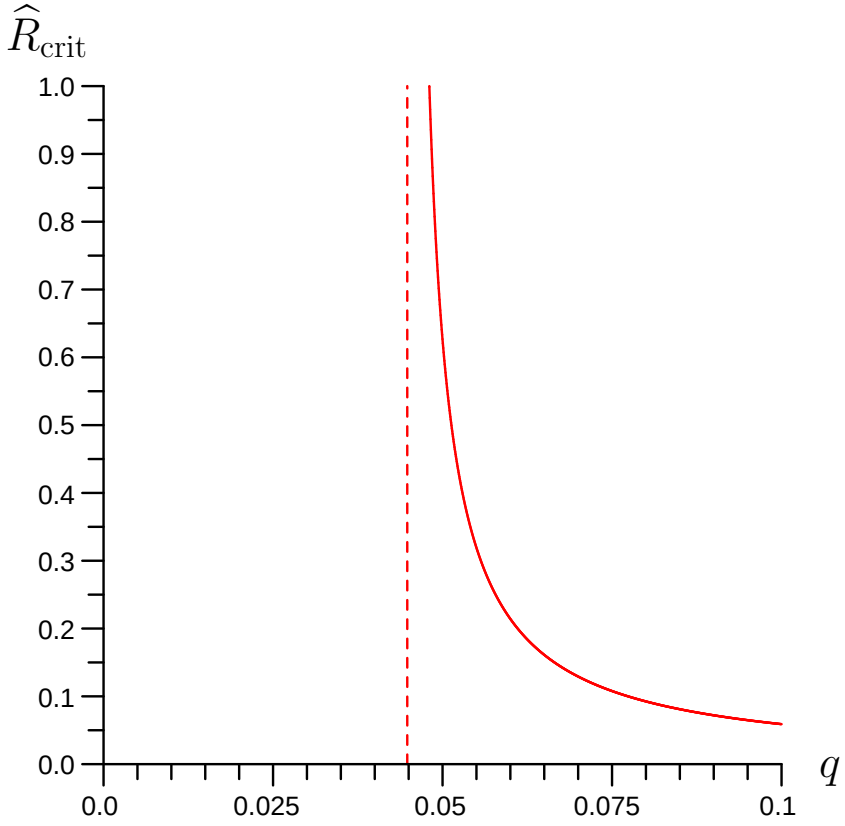

Figure 6.2: A plot of $\widehat{R}_{\text{crit}}(q)$ for typical parameter values, with asymptote $q = q_{\text{min}}$.

Now, we know that the effective elasticity tensor of the composite material is given by equation (6.328). Writing this in the form (6.313), we have that

$$\bar{A}_{ijkl} = A^{\text{m}}_{ijkl} + \omega \mathscr{Q}^{-}(q) \widetilde{M}^{-}_{ijkl} \,, \tag{6.334}$$

$$\bar{M}_{ijkl} = \omega \mathscr{Q}^{+}(q) \widetilde{M}^{+}_{ijkl} \,. \tag{6.335}$$

We can find $\widetilde{M}^{\pm}_{ijkl}$ from

$$\widetilde{M}^{\pm}_{ijkl} = M^{\pm}_{ijkl}\big|_{\widehat{R}=1} \;; \tag{6.336}$$

in other words the constants $\widetilde{B}$ and $\widetilde{C}$ from Chapter 3 and the quantities $\widetilde{\chi}^{\text{r}}_{\text{m}}$, $\widetilde{\psi}^{\text{r}}_{1}$, $\widetilde{\chi}^{\text{s}}_{\text{m}}$, $\widetilde{\psi}^{\text{s}}_{1}$ from Chapter 5 (that give the quantities K' and G' from (6.293)–(6.294) and C_1–C_4 from (6.271)–(6.273) via (6.307)–(6.310)) are calculated for a shell radius of 1.

Now we can find the displacement in a composite material undergoing uniaxial

compression, given by (6.318), where

$$\bar{\lambda} = \left(K_{\rm m} - \frac{2G_{\rm m}}{3}\right) + \omega\mathscr{Q}^{-}(q)\left(K' - \frac{2G'}{3}\right)\Big|_{\widehat{R}=1} , \tag{6.337}$$

$$\bar{G} = G_{\rm m} + \omega\mathscr{Q}^{-}(q)\, G'|_{\widehat{R}=1} , \tag{6.338}$$

$$\bar{C}_1 = \omega\mathscr{Q}^{+}(q)\, C_1|_{\widehat{R}=1} , \tag{6.339}$$

$$\bar{C}_3 = \omega\mathscr{Q}^{+}(q)\, C_3|_{\widehat{R}=1} , \tag{6.340}$$

$$\bar{C}_4 = \omega\mathscr{Q}^{+}(q)\, C_4|_{\widehat{R}=1} . \tag{6.341}$$

We calculate the displacement for two distributions of inclusions. Firstly we assume that there is only one size of inclusions, with a radius $\widehat{R}_0$. The probability density function $\mathscr{F}(\widehat{R})$ is then given by

$$\mathscr{F}(\widehat{R}) = \delta(\widehat{R} - \widehat{R}_0) , \tag{6.342}$$

and so the functions $\mathscr{Q}^{\pm}(q)$ are given by

$$\mathscr{Q}^{-}(q) = \begin{cases} \widehat{R}_0^3 & \text{if } \widehat{R}_0 < \widehat{R}_{\rm crit}(q) \\ 0 & \text{if } \widehat{R}_0 \geqslant \widehat{R}_{\rm crit}(q) , \end{cases} \tag{6.343}$$

$$\mathscr{Q}^{-}(q) = \begin{cases} 0 & \text{if } \widehat{R}_0 < \widehat{R}_{\rm crit}(q) \\ \widehat{R}_0^3 & \text{if } \widehat{R}_0 \geqslant \widehat{R}_{\rm crit}(q) . \end{cases} \tag{6.344}$$

The resulting stress–displacement graph is shown in Figure 6.4, displaying an instantaneous transition from a stiff material to a softer material on exceeding a critical stress. The values used were $\widehat{R}_0 = 1$, $\omega = 0.1$ and those in Table 1.1.

Secondly, we suppose that the sizes of the inclusions are distributed according to a gamma distribution [38], so that

$$\mathscr{F}(\widehat{R}) = \frac{1}{\Gamma(\Upsilon)}\Lambda^{\Upsilon}\widehat{R}^{\Upsilon-1}{\rm e}^{-\Lambda\widehat{R}} , \tag{6.345}$$

where Υ and Λ are shape parameters of the distribution. The mean and variance of such a distribution are located at Υ/Λ and Υ/Λ^2 respectively. Thus, if we set the mean radius to be $\widehat{R}_0$ to match with the previous distribution, then $\Upsilon = \widehat{R}_0\Lambda$ and the variance becomes $\widehat{R}_0/\Lambda$, so that we take a large value of Λ for a small variance and vice versa. We choose $\Lambda = 4$ and $\widehat{R}_0 = 1$, for which the probability density function is shown in Figure 6.3. The corresponding stress–displacement graph for this distribution of inclusions is shown in Figure 6.5.

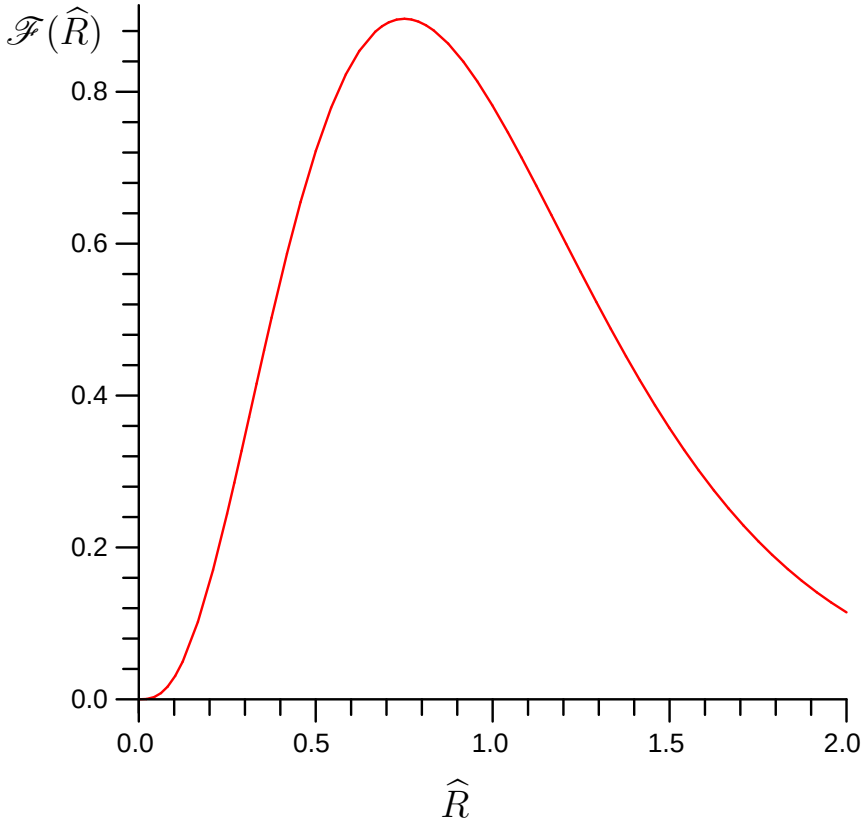

Figure 6.3: The gamma probability density function.

6.4.2 Modelling buckled shells as voids

Finally, we propose another model for the buckled shells, which is as voids rather than damaged shells, so that the buckling causes them to lose all stiffness. Voids can be modelled as elastic inclusions with zero stiffness, so that we can use the theory of Section 6.3.3.1. Setting $G_{\rm s} = K_{\rm s} = 0$ in (6.298)–(6.299), we find that

$$\widetilde{B} = -\frac{\widehat{R}^3}{4G_{\rm m}} , \tag{6.346}$$

$$\widetilde{C} = -\frac{5\widehat{R}^3(1-2\nu_{\rm m})}{6G_{\rm m}(7-5\nu_{\rm m})} \tag{6.347}$$

for void inclusions. Thus, if we model buckled shells as voids, then the post-buckling polarisation tensor M^+_{ijkl} becomes

$$M^+_{ijkl} = \left(K^+ - \frac{2G^+}{3}\right)\delta_{ij}\delta_{kl} + G^+(\delta_{ik}\delta_{jl} + \delta_{il}\delta_{jk}) , \tag{6.348}$$

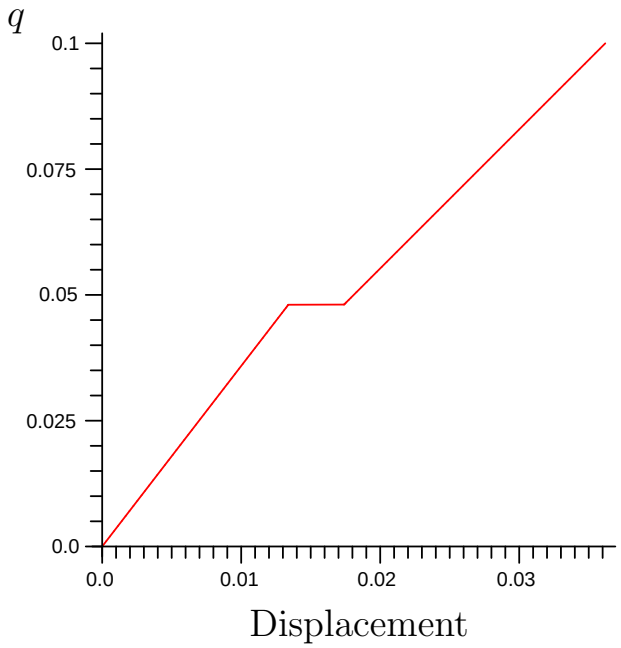

Figure 6.4: Displacement–stress graph for a composite material with one size of inclusion.

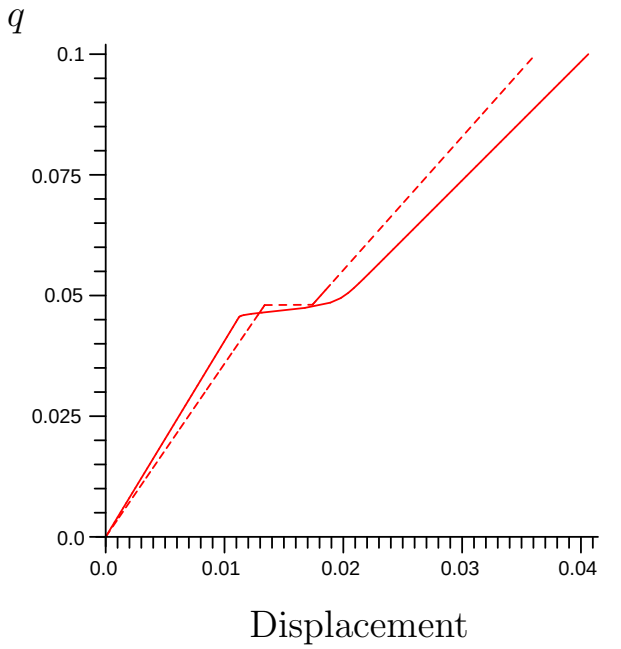

Figure 6.5: Displacement–stress graph for a composite material with a gamma distribution of inclusions, superimposed on Figure 6.4 (dashed).

where

$$K^+ = -2\pi K_{\rm m}\widehat{R}^3\frac{(1-\nu_{\rm m})}{(1-2\nu_{\rm m})}\,, \tag{6.349}$$

$$G^+ = -20\pi G_{\rm m}\widehat{R}^3\frac{(1-\nu_{\rm m})}{(7-5\nu_{\rm m})}\,. \tag{6.350}$$

Thus, the effective elasticity tensor is isotropic, and from (6.328), the effective bulk and shear moduli respectively are given by

$$\widehat{K} = K_{\rm m} + \omega\left[\mathscr{Q}^-(q)\,K'|_{\widehat{R}=1} + \mathscr{Q}^+(q)\,K^+\big|_{\widehat{R}=1}\right]\,, \tag{6.351}$$

$$\widehat{G} = G_{\rm m} + \omega\left[\mathscr{Q}^-(q)\,G'|_{\widehat{R}=1} + \mathscr{Q}^+(q)\,G^+\big|_{\widehat{R}=1}\right]\,, \tag{6.352}$$

where K' and G' are given by (6.293)–(6.294), and K^+, G^+ are given by (6.349)–(6.350). A plot of the resulting displacement–stress graph, where we have only considered one size of inclusions so that $\mathscr{F}(\widehat{R})$ is as given in (6.342), is shown in Figure 6.6.

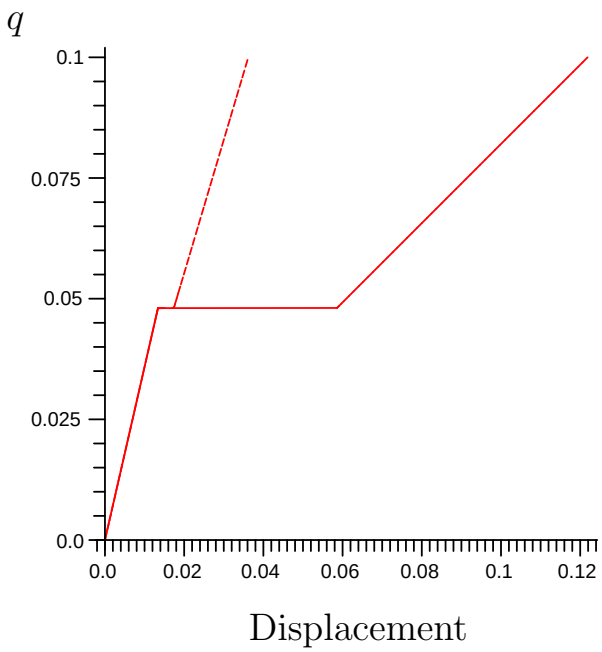

Figure 6.6: Displacement–stress graph for a composite material, modelling buckled shells as voids, superimposed on Figure 6.4 (dashed).

6.5 Discussion

In this chapter we have taken ideas from the four preceding chapters and formulated a theory for modelling the composite material such that a greater number of inclusions

are buckled at progressively greater stresses, which has the effect of softening the material.

Despite the fact that we are restricted to materials with a dilute dispersion of inclusions, the resulting stress–displacement graph for a distribution of differently-sized inclusion in Figure 6.5 is nevertheless reasonably similar to the loading part of the graph in Figure 1.3. On unloading the composite material discussed in this chapter, the inclusions would not regain stiffness as the stress on them is relieved, so the unloading curve is merely a straight line towards the origin.

Our final conclusions, drawbacks of the model, and possible improvements to it, are discussed in the following chapter.

Chapter 7

Conclusions and Further Work

7.1 Review

This thesis attempted to explain one of the features of the graph seen in Figure 1.3. We hypothesised that the 'kink' in that graph was due to buckling of the spheres at a specific critical stress in the material. Our aim, therefore, was to consider a composite material consisting of spherical shell inclusions. These inclusions would buckle as the stress on the material was increased, thus softening the material.

We began by considering a paradigm problem in Chapter 2, which embodied the basic features of the composite material to be studied. This problem was the antiplane shear at infinity of a composite material containing cylindrical inclusions. We considered an isolated inclusion and showed that the matrix effectively debonded fully from the inclusion at a particular critical stress, corresponding to the buckling of the microspheres. We considered two homogenisation methods, namely multiple-scales homogenisation (placing the inclusions in a regular grid) and the point-inclusion approach (assuming that the inclusions are infinitely far apart). These approaches agreed with each other. Finally in that chapter we extended the point inclusion approach to consider a distribution of differently-sized inclusions, so that the proportion of debonded inclusions in the composite material depended on the greatest previous stress on the material.

With this process in mind, we then proceeded to consider the problem of embedded shell inclusions. To emulate the process of Chapter 2, we needed to find the behaviour of an isolated shell at infinity before buckling, the criterion for buckling of that shell, and the behaviour of the shell after buckling. The pre-buckling behaviour was found in Chapter 3 by using Love's harmonic function method. In the same chapter we discussed the buckling criterion by using Koiter's theory of shallow shells and the assumption of axisymmetry to derive the energy functional relating to infinitesimal virtual displacements describing the buckling pattern. This energy functional was minimised by the Rayleigh–Ritz method, which assumed that the buckling

patterns were expanded as series of Legendre functions. This method gives rise to an infinite system of equations for the coefficients of these Legendre functions, which are truncated and solved (numerically) as an eigenvalue problem for the critical stress at infinity. The increasingly oscillatory behaviour of the buckling patterns, in the limit that the shell's thickness ratio tended to zero, allowed us to derive in Chapter 4 an asymptotic formula for the critical stress at infinity, and the resulting buckling pattern.

The numerical results of Chapter 3 gave us a buckling pattern that indicated that the buckled shell had lost its stiffness around the equator. Thus in Chapter 5, as a simplified model of the post-buckled shell, we considered a shell with a *crack* around the equator. Modelling the shell as linearly elastic without assuming anything about its thickness, the displacements in the matrix and shell were expanded in terms of Love stress functions. We matched displacements and tractions at the shell-matrix interface, set the traction on the inner surface and the crack of the shell to be zero, and set the stress to be constant and axisymmetric at infinity. The result was a sequence of equations in terms of Legendre polynomials. Integrating these over the half-shell led to two systems of equations for the coefficients of the Love stress functions. These systems were shown to be equivalent but only one was numerically stable, so this system was then solved for increasing truncation point. The rate of convergence as the truncation point increased was very slow, so that we resorted to a convergence acceleration process. We obtained the coefficients of the Love stress functions and the results compared well to a finite element solution of the problem.

Finally in Chapter 6 we drew the strands of the previous three chapters together to model a composite material consisting of shell inclusions. We began by reconsidering the point-inclusion method of Chapter 2, extending the results to arbitrarily-shaped cylindrical inclusions in antiplane strain. Using this as a guide, we considered the homogenisation of spherical inclusions placed far apart from each other, whose behaviour in isolation with a constant axisymmetric stress field at infinity was known. We then specialised our result to the two cases which were of interest, namely a certain statistical distribution of unbuckled shells and of buckled shells. We obtained the effective elasticity tensor for both cases, and also for the case where only a certain proportion of the shells were buckled. Finally we used the results of Chapter 4 to find the relation between the proportion of buckled shells and the stress in the composite material, and used this information to model the gradual uniaxial loading of a slab of the composite material, as described in Chapter 1.

7.2 Possible improvements to the model

The model that we have considered in Chapters 3–6 is by necessity rather simplified, yet several improvements can be considered. We will therefore revisit the assumptions made in these chapters and discuss the feasibility of their revision.

The assumption of linear elasticity is the key to obtaining analytical results and this has been assumed throughout the thesis. It is clear that under the high pressures experienced by the material in application, the material would be more accurately modelled by using nonlinear elasticity. However, any prediction of the behaviour of the material would then require finite element modelling and no dependence of the elastic properties on the microstructure would be obtainable.

7.2.1 The buckling model

The model for the shell chosen in Chapter 3 in order to analyse buckling was Koiter's shallow shell theory. This is the simplest nonlinear shell theory and the underlying assumption is that the wavelength of the buckling patterns is small compared to the radius of curvature of the shell. While this assumption seems to be confirmed *a posteriori* by the buckling patterns obtained, it may be worthwhile investigating more comprehensive nonlinear shell theories to verify that the observed buckling pattern justifies the use of the shallow shell assumption.

Another assumption made in the buckling problem is that the buckling patterns are *axisymmetric*. This assumption was not justified mathematically however, and it would be worthwhile to investigate more general buckling patterns which do not assume axisymmetry.

The main difficulty in implementing these two ideas is that the energy functional was greatly simplified by the use of the van der Neut substitution (3.149). For a spherical shell pressurised by a hydrostatic load, Koiter used the substitution to decouple the surface invariant χ from the radial displacement w and the remaining surface invariant ψ in the energy functional. This greatly simplified the analysis. For our configuration, which has a non-uniform pre-buckling stress distribution in the shell and a complicated term due to the energy in the matrix, this substitution will not have the same effect (apart from the axisymmetric case, in which χ is arbitrary and can be set to zero without loss of generality). This will also be the case if we consider additional terms in the shell energy functional due to the use of a different shell theory.

We also note that *imperfections* in the shell cause it to buckle at a lower critical stress than a pristine shell would. Koiter analysed this effect for a shell undergoing hydrostatic pressure by including an additional term in the energy functional, but to

follow the reasoning for the embedded shell would be more difficult for the reasons outlined above.

7.2.2 The asymptotic analysis

The analysis of Chapter 4 can be extended by considering the limits $h/\widehat{R} \to 0$ and $G_{\mathrm{s}}/G_{\mathrm{m}} \to 0$ separately. In this case we would be unable to assume that the circumferential displacement v_θ was zero, and the term in the functional that whose coefficient was D given by (4.258) would no longer be neglected.

7.2.3 The buckled shell

In Chapter 5, the overriding concern was the validity of the convergence acceleration method. These concerns would be allayed if the exact form of the convergence was known: for example, if the convergence was of the form (5.203) with σ known (and possibly different for each Love stress function coefficient). Alternatively, if the convergence was of a different form we could construct convergence acceleration methods which were tailor-made for such sequences. Any further research into the work of this chapter should thus attempt to uncover the convergence properties.

An alternative approach is to consider the solution as the sum of a regular part and a singular part, to try and obtain a problem which has no singularity and thus is more likely to be numerically tractable. Likewise, we may be able to formulate an asymptotic or asymptotic-numerical approach, as indicated in Section 5.6.

Another option is to consider a more accurate post-buckling behaviour than the simplistic model of the split shell. Koiter used higher-order terms in the energy functional of the shell in order to determine special cases of the post-buckling behaviour for a shell experiencing hydrostatic pressure. However, as explained above in Section 7.2.1, the non-uniform stress distribution in the shell, and especially the influence of the attached matrix, cause the analysis to become much more difficult. Other effects such as delamination between the shell and matrix may also become important.

7.2.4 Homogenisation methods

The obvious extension to the work of Chapter 6 is to extend the analysis from dilute composites to the case where the inclusions are reasonably close to one another. For elastic inclusions this was analysed by Chen and Acrivos [19]. Their analysis required the effect on a reference inclusion of a second inclusion situated nearby. This means that axisymmetry is no longer applicable, and if we were to extend the results to shell inclusions, we would need the buckling criterion for a pair of embedded shells. This is, needless to say, a challenging task.

Appendix A

Elasticity Theory

This appendix provides a basis for Chapter 3 by reviewing the theory of linear elasticity, and in particular the application of that theory to thin shells. We will derive the stress–strain relations in general curvilinear coordinates, before specialising to spherical polar coordinates, as the geometry of the problem under consideration (the spherical shell) is clearly based on these coordinates. The notation is largely a combination of that of Green and Zerna [37] and of Koiter [51]. Indices of lower-case Latin letters vary over 1 to 3 while lower-case Greek letters vary over 1 to 2. The summation convention applies unless the symbol $\not\Sigma_i$ is used, which implies no summation on i.

A.1 General curvilinear coordinates

Any curvilinear coordinate system has at its heart a set of three coordinates,

$$(\theta_1, \theta_2, \theta_3) \ , \tag{A.1}$$

and a definition of the position vector in terms of these coordinates,

$$\boldsymbol{r} \ = \ \boldsymbol{r}(\theta_1, \theta_2, \theta_3) \ . \tag{A.2}$$

The *covariant base vectors* $\boldsymbol{g}_i$ of the coordinate system are given by

$$\boldsymbol{g}_i \ = \ \boldsymbol{r}_{,i} \ , \tag{A.3}$$

where a comma followed by the index i denotes partial differentiation with respect to θ_i, from where we can define the *covariant metric tensors* by

$$g_{ij} \ = \ \boldsymbol{g}_i \cdot \boldsymbol{g}_j \ , \tag{A.4}$$

where the dot represents the scalar product. The *contravariant base vectors* are defined by the relation

$$\boldsymbol{g}_i \cdot \boldsymbol{g}^j \ = \ \delta_i^j \tag{A.5}$$

(which is the Kronecker delta), and the *contravariant metric tensors* by

$$g^{ij} = \boldsymbol{g}^i \cdot \boldsymbol{g}^j \ . \tag{A.6}$$

The following identities hold:

$$\boldsymbol{g}^i = g^{ij}\boldsymbol{g}_j \ , \tag{A.7}$$

$$\boldsymbol{g}_i = g_{ij}\boldsymbol{g}^j \ . \tag{A.8}$$

If the base vectors are orthogonal, we have that

$$g^{ij} = 0 \qquad \text{if } i \neq j \ , \tag{A.9}$$

$$g^{ii} = \frac{1}{g_{ii}} \qquad \not{\Sigma}_i \ . \tag{A.10}$$

A.1.1 Vectors

A vector $\boldsymbol{v}$ can be described in the coordinate system (θ_i) in two ways. The vector is said to have *covariant components*,

$$v_i = \boldsymbol{v} \cdot \boldsymbol{g}_i \ , \tag{A.11}$$

and *contravariant components*,

$$v^i = \boldsymbol{v} \cdot \boldsymbol{g}^i \ . \tag{A.12}$$

By equation (A.5), the vector can be represented as

$$\boldsymbol{v} = v_i\boldsymbol{g}^i \ , \tag{A.13}$$

$$\text{or} \qquad \boldsymbol{v} = v^i\boldsymbol{g}_i \ . \tag{A.14}$$

In other words, the two sets of vectors $\boldsymbol{g}_i$ and $\boldsymbol{g}^i$ form bases for vectors in $\mathbb{R}^3$. From equations (A.4), (A.6), (A.13) and (A.14), the rules for raising and lowering the index of a vector hold:

$$v^i = g^{ij}v_j \ , \tag{A.15}$$

$$v_i = g_{ij}v^j \ . \tag{A.16}$$

When differentiating a vector $\boldsymbol{v}$ with respect to one of the coordinates, we must remember that the base vectors are not necessarily independent of the coordinate. We have

$$\boldsymbol{v}_{,j} = (v_i\boldsymbol{g}^i)_{,j} \tag{A.17}$$

$$\neq v_{i,j}\boldsymbol{g}^i \ . \tag{A.18}$$

In fact

$$\boldsymbol{v}_{,j} \;=\; v_i|_j \boldsymbol{g}^i \;, \tag{A.19}$$

where $v_i|_j$ is the *covariant derivative* of v_i, given by

$$v_i|_j \;=\; v_{i,j} - \Gamma^r_{ij} v_r \;, \tag{A.20}$$

where

$$\Gamma^r_{ij} \;=\; -\boldsymbol{g}_i \cdot \boldsymbol{g}^r_{,j} \tag{A.21}$$

are the *Christoffel symbols*. We can also find the covariant derivative of v^i, given by

$$v^i|_j \;=\; v^i{}_{,j} + \Gamma^i_{rj} v^r \;. \tag{A.22}$$

A.1.2 Tensors

A *second-order tensor* $\boldsymbol{A}$ can be thought of as a linear operator that acts on a vector, generating a second vector,

$$\boldsymbol{w} \;=\; \boldsymbol{A}\boldsymbol{v} \;. \tag{A.23}$$

In the same way as for vectors, we can define components of a tensor, referred to the base vectors $\boldsymbol{g}^i$ and $\boldsymbol{g}_i$. For a second-order tensor, the four types of component are

$$A_{ij} \;=\; \boldsymbol{g}_i \cdot \boldsymbol{A}\boldsymbol{g}_j \;, \tag{A.24}$$

$$A^i_{\cdot j} \;=\; \boldsymbol{g}^i \cdot \boldsymbol{A}\boldsymbol{g}_j \;, \tag{A.25}$$

$$A^{\cdot j}_i \;=\; \boldsymbol{g}_i \cdot \boldsymbol{A}\boldsymbol{g}^j \;, \tag{A.26}$$

$$A^{ij} \;=\; \boldsymbol{g}^i \cdot \boldsymbol{A}\boldsymbol{g}^j \;, \tag{A.27}$$

which are known as the coviariant components, the mixed components (twice) and the contravariant components, respectively. The notation for the mixed tensor components assumes that the order of the indices is important; often this is not the case and the dot is omitted (*e.g.* for the Kronecker delta δ^j_i).

One important type of second-order tensor is the *dyad* or *tensor product*, which forms a tensor $\boldsymbol{u} \otimes \boldsymbol{v}$ from two vectors $\boldsymbol{u}$ and $\boldsymbol{v}$.[1] The linear transformation described by this tensor is defined as

$$(\boldsymbol{u} \otimes \boldsymbol{v})\boldsymbol{w} \;=\; \boldsymbol{u}(\boldsymbol{v} \cdot \boldsymbol{w}) \tag{A.28}$$

$$\;=\; (\boldsymbol{v} \cdot \boldsymbol{w})\boldsymbol{u} \;. \tag{A.29}$$

[1] This is equivalent to the outer product in linear algebra, which takes two vectors $\boldsymbol{a}$ and $\boldsymbol{b}$ and forms the matrix $\boldsymbol{a}\boldsymbol{b}^{\mathrm{T}}$.

While not every tensor can be described by a tensor product of two vectors, it can be shown from equations (A.24)–(A.27) and (A.29) that all tensors can be decomposed according to

$$\begin{aligned} \boldsymbol{A} &= A_{kl}\,\boldsymbol{g}^k \otimes \boldsymbol{g}^l && \text{(A.30)} \\ &= A^k_{\cdot l}\,\boldsymbol{g}_k \otimes \boldsymbol{g}^l && \text{(A.31)} \\ &= A^{\cdot l}_k\,\boldsymbol{g}^k \otimes \boldsymbol{g}_l && \text{(A.32)} \\ &= A^{kl}\,\boldsymbol{g}_k \otimes \boldsymbol{g}_l\ . && \text{(A.33)} \end{aligned}$$

We often refer to the components of a tensor simply as a tensor, for simplicity (as long as the coordinates that the components are referred to are known).

The rules for raising and lowering indices also hold for tensors, *e.g.*

$$\begin{aligned} A^{ij} &= g^{ir} A_r^{\cdot j} && \text{(A.34)} \\ &= g^{ir} g^{js} A_{rs}\ . && \text{(A.35)} \end{aligned}$$

We can also define covariant derivatives for tensors, for example

$$\begin{aligned} A_{ij}|_r &= A_{ij,r} - \Gamma^m_{ir} A_{mj} - \Gamma^m_{jr} A_{im}\ , && \text{(A.36)} \\ A^{ij}|_r &= A^{ij}{}_{,r} + \Gamma^i_{rm} A^{mj} + \Gamma^j_{rm} A^{im}\ . && \text{(A.37)} \end{aligned}$$

We can also consider tensors of higher order, most notably fourth-order tensors. These can be expressed by

$$\mathbb{A} = A_{ijkl}\,\boldsymbol{g}^i \otimes \boldsymbol{g}^j \otimes \boldsymbol{g}^k \otimes \boldsymbol{g}^l\ , \qquad \text{(A.38)}$$

with similar relations to define the mixed and contravariant components.

A.2 Linear elasticity

Elasticity is part of the study of the relationship between displacement and stress in a deformable material. A material is said to be perfectly elastic if, on applying external forces to a material and then removing them, the material returns to the pre-stressed state.

The displacement in an elastic material is defined as a vector $\boldsymbol{u}$. If the material is *linearly* elastic, the strain tensor is given by

$$e_{ij} = \frac{1}{2}\left(u_i|_j + u_j|_i\right)\ . \qquad \text{(A.39)}$$

The state of stress in the material is described by the stress tensor, $\boldsymbol{\tau}$. If the material experiences a body force $\boldsymbol{f}$, then the equilibrium equation, derived from conservation of momentum, gives us

$$\tau^{ij}|_j + \rho f^i = \rho \ddot{u}^i\ , \qquad \text{(A.40)}$$

where a dot represents differentiation with respect to time. For static deformations without body forces,

$$\tau^{ij}|_j \;=\; 0\,. \tag{A.41}$$

Conservation of angular momentum tells us that the stress tensor is symmetric, or

$$\tau^{ij} \;=\; \tau^{ji}\,. \tag{A.42}$$

Finally we need to find a relationship between stress and strain. For linearly elastic materials this is *Hooke's law*, which supposes that the stress is linearly dependent on the strain. Mathematically,

$$\tau^{ij} \;=\; A^{ijkl}e_{kl}\,, \tag{A.43}$$

where A^{ijkl} is the fourth-order *elasticity tensor*. We will assume that the material is isotropic, whereby the elasticity tensor simplifies to

$$A^{ijkl} \;=\; \lambda g^{ij}g^{kl} + G(g^{ik}g^{jl} + g^{il}g^{jk})\,, \tag{A.44}$$

where g^{ij} are the contravariant metric tensors, and λ and G are the Lamé moduli of the material (G is also known as the shear modulus, or the rigidity modulus). We will often use other material parameters [86], such as the bulk modulus

$$K \;=\; \lambda + \frac{2}{3}G\,, \tag{A.45}$$

the Poisson ratio

$$\nu \;=\; \frac{\lambda}{2(\lambda+G)}\,, \tag{A.46}$$

and Young's modulus

$$E \;=\; 2G(1+\nu)\,. \tag{A.47}$$

The potential energy density of the linearly elastic material is given by

$$V \;=\; \frac{1}{2}\tau^{ij}e_{ij} \tag{A.48}$$

$$\;=\; \frac{1}{2}A^{ijkl}e_{ij}e_{kl}\,. \tag{A.49}$$

Thus the stored energy in a three-dimensional body Ω made of the elastic material is given by

$$W \;=\; \iiint_\Omega \frac{1}{2}A^{ijkl}e_{ij}e_{kl}\,\mathrm{d}V\,. \tag{A.50}$$

A.3 Spherical polar coordinates

We now proceed to find the spherical polar formulation of a number of the previous geometrical and elasticity relations, for future reference.

The Cartesian coordinate system (x, y, z) is written in terms of the spherical polar coordinates (R, θ, ϕ) by

$$x = R\sin\theta\cos\phi \,, \tag{A.51}$$
$$y = R\sin\theta\sin\phi \,, \tag{A.52}$$
$$z = R\cos\theta \,, \tag{A.53}$$

for $R \in [0, \infty)$, $\theta \in [0, \pi]$ and $\phi \in [0, 2\pi)$. We can thus find the position vector in spherical polar coordinates in terms of the Cartesian base vectors $(\boldsymbol{e}_x, \boldsymbol{e}_y, \boldsymbol{e}_z)$,

$$\boldsymbol{r} = R\sin\theta\cos\phi\,\boldsymbol{e}_x + R\sin\theta\sin\phi\,\boldsymbol{e}_y + R\cos\theta\,\boldsymbol{e}_z \,. \tag{A.54}$$

From this we can find the covariant base vectors,

$$\boldsymbol{g}_1 = \sin\theta\cos\phi\,\boldsymbol{e}_x + \sin\theta\sin\phi\,\boldsymbol{e}_y + \cos\theta\,\boldsymbol{e}_z \,, \tag{A.55}$$
$$\boldsymbol{g}_2 = R\cos\theta\cos\phi\,\boldsymbol{e}_x + R\cos\theta\sin\phi\,\boldsymbol{e}_y - R\sin\theta\,\boldsymbol{e}_z \,, \tag{A.56}$$
$$\boldsymbol{g}_3 = -R\sin\theta\sin\phi\,\boldsymbol{e}_x + R\sin\theta\cos\phi\,\boldsymbol{e}_y \,. \tag{A.57}$$

Now, we find that the covariant metric tensors become

$$g_{11} = 1 \,, \tag{A.58}$$
$$g_{22} = R^2 \,, \tag{A.59}$$
$$g_{33} = R^2\sin^2\theta \,, \tag{A.60}$$
$$g_{ij} = 0 \qquad \text{if } i \neq j \,, \tag{A.61}$$

implying that the coordinates are orthogonal, which means that the contravariant metric tensors become

$$g^{11} = 1 \,, \tag{A.62}$$
$$g^{22} = \frac{1}{R^2} \,, \tag{A.63}$$
$$g^{33} = \frac{1}{R^2\sin^2\theta} \,, \tag{A.64}$$
$$g^{ij} = 0 \qquad \text{if } i \neq j \,. \tag{A.65}$$

Additionally, the contravariant base vectors in spherical coordinates become

$$\boldsymbol{g}^1 = \boldsymbol{g}_1 \,, \tag{A.66}$$
$$\boldsymbol{g}^2 = \frac{1}{R^2}\,\boldsymbol{g}_2 \,, \tag{A.67}$$
$$\boldsymbol{g}^3 = \frac{1}{R^2\sin^2\theta}\,\boldsymbol{g}_3 \,. \tag{A.68}$$

In the spherical coordinate system, the only non-zero Christoffel symbols are

$$\Gamma^1_{22} = -R \,, \tag{A.69}$$
$$\Gamma^1_{33} = -R\sin^2\theta \,, \tag{A.70}$$
$$\Gamma^2_{12} = \frac{1}{R} \,, \tag{A.71}$$
$$\Gamma^2_{33} = -\sin\theta\cos\theta \,, \tag{A.72}$$
$$\Gamma^3_{13} = \frac{1}{R} \,, \tag{A.73}$$
$$\Gamma^3_{23} = \cot\theta \,. \tag{A.74}$$

Thus, we note that the covariant derivatives of a general vector v_i are given by

$$v_1|_1 = v_{1,1} \,, \tag{A.75}$$
$$v_1|_2 = v_{1,2} - \frac{1}{R}v_2 \,, \tag{A.76}$$
$$v_1|_3 = v_{1,3} - \frac{1}{R}v_3 \,, \tag{A.77}$$
$$v_2|_1 = v_{2,1} - \frac{1}{R}v_2 \,, \tag{A.78}$$
$$v_2|_2 = v_{2,2} + Rv_1 \,, \tag{A.79}$$
$$v_2|_3 = v_{2,3} - \cot\theta v_3 \,, \tag{A.80}$$
$$v_3|_1 = v_{3,1} - \frac{1}{R}v_3 \,, \tag{A.81}$$
$$v_3|_2 = v_{3,2} - \cot\theta v_3 \,, \tag{A.82}$$
$$v_3|_3 = v_{3,3} + R\sin^2\theta v_1 + \sin\theta\cos\theta v_2 \,. \tag{A.83}$$

A.3.1 Elasticity in spherical coordinates

In this section we will find the relationship between the displacement, strain and stress using the information about spherical polar coordinates given in the previous section.

Using equations (A.39) and (A.75)–(A.83), we find that the components of strain referred to spherical polar coordinates become

$$e_{11} = u_{1,1} \,, \tag{A.84}$$
$$e_{12} = \frac{1}{2}(u_{1,2} + u_{2,1}) - \frac{1}{R}u_2 \,, \tag{A.85}$$
$$e_{13} = \frac{1}{2}(u_{1,3} + u_{3,1}) - \frac{1}{R}u_3 \,, \tag{A.86}$$
$$e_{22} = u_{2,2} + Ru_1 \,, \tag{A.87}$$
$$e_{23} = \frac{1}{2}(u_{2,3} + u_{3,2}) - \cot\theta u_3 \,, \tag{A.88}$$
$$e_{33} = u_{3,3} + R\sin^2\theta u_1 + \sin\theta\cos\theta u_2 \,. \tag{A.89}$$

Next, we use equations (A.43), (A.44) and (A.62)–(A.65) to determine the stress–strain relations in spherical polar coordinates. Defining the *dilatation* Δ by

$$\begin{aligned} \Delta &= g^{kl}e_{kl} && \text{(A.90)} \\ &= e_{11} + \frac{1}{R^2}e_{22} + \frac{1}{R^2\sin^2\theta}e_{33}\ , && \text{(A.91)} \end{aligned}$$

we find that

$$\begin{aligned} \tau^{11} &= \lambda\Delta + 2Ge_{11}\ , && \text{(A.92)} \\ \tau^{12} &= \frac{2G}{R^2}e_{12}\ , && \text{(A.93)} \\ \tau^{13} &= \frac{2G}{R^2\sin^2\theta}e_{13}\ , && \text{(A.94)} \\ \tau^{22} &= \frac{\lambda}{R^2}\Delta + \frac{2G}{R^4}e_{22}\ , && \text{(A.95)} \\ \tau^{23} &= \frac{2G}{R^4\sin^2\theta}e_{23}\ , && \text{(A.96)} \\ \tau^{33} &= \frac{\lambda}{R^2\sin^2\theta}\Delta + \frac{2G}{R^4\sin^4\theta}e_{33}\ . && \text{(A.97)} \end{aligned}$$

A.3.2 Physical components

The base vectors $\boldsymbol{g}_i$ and $\boldsymbol{g}^i$ are not, in general, unit vectors. In other words, covariant and contravariant components of tensors and vectors referred to these base vectors are not the *physical* components. In particular, different components of the same tensor may have different units. Occasionally we will find it easier to manipulate physical components rather than covariant or contravariant components. To facilitate this, we first find the unit vectors associated with the base vectors. In spherical polar coordinates,

$$\begin{aligned} \boldsymbol{e}_R &= \frac{1}{|\boldsymbol{g}_1|}\boldsymbol{g}_1\ , && \text{(A.98)} \\ \boldsymbol{e}_\theta &= \frac{1}{|\boldsymbol{g}_2|}\boldsymbol{g}_2\ , && \text{(A.99)} \\ \boldsymbol{e}_\phi &= \frac{1}{|\boldsymbol{g}_3|}\boldsymbol{g}_3\ , && \text{(A.100)} \end{aligned}$$

so that the unit vectors are related to the Cartesian base vectors by

$$\begin{pmatrix} \boldsymbol{e}_R \\ \boldsymbol{e}_\theta \\ \boldsymbol{e}_\phi \end{pmatrix} = \begin{pmatrix} \sin\theta\cos\phi & \sin\theta\sin\phi & \cos\theta \\ \cos\theta\cos\phi & \cos\theta\sin\phi & -\sin\theta \\ -\sin\phi & \cos\phi & 0 \end{pmatrix} \begin{pmatrix} \boldsymbol{e}_x \\ \boldsymbol{e}_y \\ \boldsymbol{e}_z \end{pmatrix}\ . \qquad \text{(A.101)}$$

Inverting the matrix, we obtain the Cartesian vectors in terms of the spherical polar unit vectors,

$$\begin{pmatrix} \boldsymbol{e}_x \\ \boldsymbol{e}_y \\ \boldsymbol{e}_z \end{pmatrix} = \begin{pmatrix} \sin\theta\cos\phi & \cos\theta\cos\phi & -\sin\phi \\ \sin\theta\sin\phi & \cos\theta\sin\phi & \cos\phi \\ \cos\theta & -\sin\theta & 0 \end{pmatrix} \begin{pmatrix} \boldsymbol{e}_R \\ \boldsymbol{e}_\theta \\ \boldsymbol{e}_\phi \end{pmatrix}\ . \qquad \text{(A.102)}$$

In terms of the base vectors,

$$\boldsymbol{e}_R = \boldsymbol{g}_1 = \boldsymbol{g}^1 \,, \tag{A.103}$$

$$\boldsymbol{e}_\theta = \frac{1}{R}\boldsymbol{g}_2 = R\boldsymbol{g}^2 \,, \tag{A.104}$$

$$\boldsymbol{e}_\phi = \frac{1}{R\sin\theta}\boldsymbol{g}_3 = R\sin\theta\boldsymbol{g}^3 \,. \tag{A.105}$$

Now, to find the physical components of a vector $\boldsymbol{v}$, we take equations (A.13) and (A.14), replacing the base vectors by the unit vectors from equations (A.103)–(A.105). Then, we compare with

$$\boldsymbol{v} = v_R\boldsymbol{e}_R + v_\theta\boldsymbol{e}_\theta + v_\phi\boldsymbol{e}_\phi \,, \tag{A.106}$$

to find the physical components (v_R, v_θ, v_ϕ) in terms of v_i or v^i. In particular,

$$v_R = v_1 = v^1 \,, \tag{A.107}$$

$$v_\theta = \frac{v_2}{R} = Rv^2 \,, \tag{A.108}$$

$$v_\phi = \frac{v_3}{R\sin\theta} = R\sin\theta v^3 \,. \tag{A.109}$$

We can perform the same operation to find the physical components of a tensor $\boldsymbol{A}$. From equations (A.30)–(A.33), we replace the base vectors by the unit vectors according to equations (A.103)–(A.105). The physical components are found by comparing to

$$\begin{aligned}\boldsymbol{A} = {} & A_{RR}(\boldsymbol{e}_R\otimes\boldsymbol{e}_R) + A_{R\theta}(\boldsymbol{e}_R\otimes\boldsymbol{e}_\theta) + A_{R\phi}(\boldsymbol{e}_R\otimes\boldsymbol{e}_\phi) \\ & + A_{\theta R}(\boldsymbol{e}_\theta\otimes\boldsymbol{e}_R) + A_{\theta\theta}(\boldsymbol{e}_\theta\otimes\boldsymbol{e}_\theta) + A_{\theta\phi}(\boldsymbol{e}_\theta\otimes\boldsymbol{e}_\phi) \\ & + A_{\phi R}(\boldsymbol{e}_\phi\otimes\boldsymbol{e}_R) + A_{\phi\theta}(\boldsymbol{e}_\phi\otimes\boldsymbol{e}_\theta) + A_{\phi\phi}(\boldsymbol{e}_\phi\otimes\boldsymbol{e}_\phi) \,.\end{aligned} \tag{A.110}$$

In particular,

$$A_{RR} = A^{11} \,, \tag{A.111}$$

$$A_{R\theta} = RA^{12} \,, \tag{A.112}$$

$$A_{R\phi} = R\sin\theta\, A^{13} \,, \tag{A.113}$$

$$A_{\theta R} = RA^{21} \,, \tag{A.114}$$

$$A_{\theta\theta} = R^2A^{22} \,, \tag{A.115}$$

$$A_{\theta\phi} = R^2\sin\theta\, A^{23} \,, \tag{A.116}$$

$$A_{\phi R} = R\sin\theta\, A^{31} \,, \tag{A.117}$$

$$A_{\phi\theta} = R^2\sin\theta\, A^{32} \,, \tag{A.118}$$

$$A_{\phi\phi} = R^2\sin^2\theta\, A^{33} \,. \tag{A.119}$$

As an example, the stress components τ_{RR} and $\tau_{R\theta}$, using equations (A.92)–(A.93) are given by

$$\begin{aligned} \tau_{RR} &= \tau^{11} && \text{(A.120)} \\ &= \lambda\Delta + 2Ge_{11} \ , && \text{(A.121)} \\ \text{and} \qquad \tau_{R\theta} &= R\tau^{12} && \text{(A.122)} \\ &= \frac{2G}{R}e_{12} \ . && \text{(A.123)} \end{aligned}$$

Using equations (A.84)–(A.85), these become

$$\begin{aligned} \tau_{RR} &= \lambda\Delta + 2Gu_{1,1} \ , && \text{(A.124)} \\ \tau_{R\theta} &= \frac{2G}{R}\left[\frac{1}{2}(u_{1,2} + u_{2,1}) - \frac{u_2}{R}\right] \ . && \text{(A.125)} \end{aligned}$$

But, from equations (A.107)–(A.108), $u_1 = u_R$ and $u_2 = Ru_\theta$, so

$$\begin{aligned} \tau_{RR} &= \lambda\Delta + 2G\frac{\partial u_R}{\partial R} \ , && \text{(A.126)} \\ \tau_{R\theta} &= G\left[\frac{1}{R}\frac{\partial u_R}{\partial \theta} + \frac{1}{R}\frac{\partial}{\partial R}(Ru_\theta) - \frac{2u_\theta}{R}\right] && \text{(A.127)} \\ &= G\left[\frac{1}{R}\frac{\partial u_R}{\partial \theta} + R\frac{\partial}{\partial R}\left(\frac{u_\theta}{R}\right)\right] \ . && \text{(A.128)} \end{aligned}$$

The pattern followed here is repeated throughout the thesis — in other words, if the indices are numerical then the quantities will be referred to the base vectors, while subscript R, θ and ϕ refer to the physical components.

A.4 Shell theory

Having found the relations between stress, strain and displacement in three dimensional elasticity, we will now simplify them in the case where the deformable body is a thin shell. Before this, however, we will need to examine the tensor description of surfaces.

A.4.1 Surface geometry

We will consider the case where the position vector of a point in space is given by

$$\boldsymbol{r} = \bar{\boldsymbol{r}}(\theta_1, \theta_2) + \theta_3\boldsymbol{a}_3 \ . \qquad \text{(A.129)}$$

The position vector is described in this way so that a surface is defined on setting $\theta_3 = 0$, the surface being given by

$$\bar{\boldsymbol{r}}(\theta_1, \theta_2) = 0 \ . \qquad \text{(A.130)}$$

The vector $\boldsymbol{a}_3$, which depends only on θ_1 and θ_2, is kept perpendicular to the surface and is known as the normal vector. By convention we make it a unit vector.

Substituting the position vector (A.129) into equation (A.3) to find the covariant base vectors, we obtain

$$\boldsymbol{g}_\alpha = \boldsymbol{a}_\alpha + \theta_3 \boldsymbol{a}_{3,\alpha} \,, \tag{A.131}$$

$$\boldsymbol{g}_3 = \boldsymbol{a}_3 \,, \tag{A.132}$$

where

$$\boldsymbol{a}_\alpha = \bar{\boldsymbol{r}}_{,\alpha} \,. \tag{A.133}$$

We can therefore use $\boldsymbol{a}_\alpha$ as covariant base vectors for the surface defined by equation (A.130). The sign of $\boldsymbol{a}_3$ is thus chosen so that $(\boldsymbol{a}_1, \boldsymbol{a}_2, \boldsymbol{a}_3)$ form a right-handed basis.

We can now form metric tensors for the surface,

$$a_{\alpha\beta} = \boldsymbol{a}_\alpha \cdot \boldsymbol{a}_\beta \,, \tag{A.134}$$

contravariant base vectors $\boldsymbol{a}^\alpha$, satisfying

$$\boldsymbol{a}_\alpha \cdot \boldsymbol{a}^\beta = \delta_\alpha^\beta \,, \tag{A.135}$$

and contravariant metric tensors

$$a^{\alpha\beta} = \boldsymbol{a}^\alpha \cdot \boldsymbol{a}^\beta \,. \tag{A.136}$$

The contravariant metric tensors can also be found from

$$a^{11} = \frac{a_{22}}{a} \,, \tag{A.137}$$

$$a^{12} = a^{21} = -\frac{a_{12}}{a} \,, \tag{A.138}$$

$$a^{22} = \frac{a_{11}}{a} \,, \tag{A.139}$$

where

$$a = a_{11}a_{22} - a_{12}a_{21} \tag{A.140}$$

is the determinant of the tensor $a_{\alpha\beta}$.

Raising or lowering of an index of a tensor or vector is acheived through the tensors $a^{\alpha\beta}$ and $a_{\alpha\beta}$, for example

$$v^\alpha = a^{\alpha\gamma} v_\gamma \,, \tag{A.141}$$

$$v_\alpha = a_{\alpha\gamma} v^\gamma \,, \tag{A.142}$$

$$A^\alpha_{.\beta} = a^{\alpha\gamma} A_{\gamma\beta} \,. \tag{A.143}$$

The tensor $a_{\alpha\beta}$ is also known as the first fundamental tensor of the surface. Another concept which is important in the theory of surfaces is the second fundamental tensor of the surface, given by

$$b_{\alpha\beta} \;=\; -\boldsymbol{a}_\alpha \cdot \boldsymbol{a}_{3,\beta} \;=\; -\boldsymbol{a}_\beta \cdot \boldsymbol{a}_{3,\alpha} \;=\; \boldsymbol{a}_3 \cdot \boldsymbol{a}_{\alpha,\beta} \;=\; \boldsymbol{a}_3 \cdot \boldsymbol{a}_{\beta,\alpha} \,. \tag{A.144}$$

Using this, equation (A.131) becomes

$$\boldsymbol{g}_\alpha \;=\; \mu_\alpha^\beta \boldsymbol{a}_\beta \,, \tag{A.145}$$

where

$$\mu_\alpha^\beta \;=\; \delta_\alpha^\beta - \theta_3 b_\alpha^\beta \,. \tag{A.146}$$

The tensor $b_{\alpha\beta}$ allows us to describe the curvature of the surface, especially the *mean curvature*,

$$H \;=\; \frac{1}{2} b_\alpha^\alpha \;=\; \frac{1}{2} a^{\alpha\beta} b_{\alpha\beta} \,, \tag{A.147}$$

and the *Gaussian curvature*,

$$K \;=\; \frac{b}{a} \;=\; b_1^1 b_2^2 - b_2^1 b_1^2 \,, \tag{A.148}$$

where b is the determinant of the tensor $b_{\alpha\beta}$.

Finally, we need to consider covariant differentiation. For vectors, we find that

$$v_\lambda|_\alpha \;=\; v_{\lambda,\alpha} - \bar{\Gamma}_{\lambda\alpha}^\mu v_\mu \,, \tag{A.149}$$

$$v^\lambda|_\alpha \;=\; v^\lambda{}_{,\alpha} + \bar{\Gamma}_{\mu\alpha}^\lambda v^\mu \,, \tag{A.150}$$

where the Christoffel symbols are given by

$$\bar{\Gamma}_{\beta\gamma}^\alpha \;=\; \boldsymbol{a}^\alpha \cdot \boldsymbol{a}_{\beta,\gamma} \,. \tag{A.151}$$

The same pattern of covariant differentiation holds for tensors, following equations (A.36)–(A.37). It is useful to note that covariant derivatives of the metric tensors are zero, *i.e.*

$$a^{\alpha\beta}|_\lambda \;=\; a_{\alpha\beta}|_\lambda \;=\; 0 \,. \tag{A.152}$$

A.4.2 Strain and stress measures

There are a multitude of different shell theories in the literature. The most comprehensive exposition is by Koiter [51], who derived the full nonlinear theory of shells from first principles. In the context of shell theory, the nonlinear theory assumes that the strain measures in the shell are nonlinear functions of displacement. We will be interested in shell buckling, for which it is essential that we use the nonlinear theory rather than the linear theory.

Now, the position vector of any point in the shell is given by equation (A.129) for θ_3 in the range

$$-\frac{h}{2} \leqslant \theta_3 \leqslant \frac{h}{2} \,, \tag{A.153}$$

where h is the thickness of the shell, which is assumed to be constant. Therefore $\bar{\boldsymbol{r}}(\theta_1, \theta_2)$ is defined as the position vector of points on the middle-surface of the shell.

To find the strain measures in the shell, Koiter [51] considers two states of the shell: a position vector $\boldsymbol{r}$ before deformation, and a position vector $\widehat{\boldsymbol{r}}$ following deformation. From these, the fundamental tensors $a_{\alpha\beta}$, $b_{\alpha\beta}$, $\widehat{a}_{\alpha\beta}$ and $\widehat{b}_{\alpha\beta}$ are formed. Then, the *middle-surface strain tensor* $\gamma_{\alpha\beta}$, and the *tensor of changes of curvature* $\rho_{\alpha\beta}$ are defined by

$$\gamma_{\alpha\beta} = \frac{1}{2}(\widehat{a}_{\alpha\beta} - a_{\alpha\beta}) \,, \tag{A.154}$$

$$\rho_{\alpha\beta} = \widehat{b}_{\alpha\beta} - b_{\alpha\beta} \,, \tag{A.155}$$

respectively. Next, the displacement vector of the shell is denoted by

$$\boldsymbol{v} = \widehat{\boldsymbol{r}} - \boldsymbol{r} \,. \tag{A.156}$$

Expressing this in terms of components referred to the base vectors $\boldsymbol{a}^\alpha$, $\boldsymbol{a}^3$, we define the in-surface displacement components v_α and the normal displacement w by

$$\boldsymbol{v} = v_\alpha \boldsymbol{a}^\alpha + w\boldsymbol{a}^3 \,. \tag{A.157}$$

Now, while we need to consider nonlinear measures of strain, these can be simplified based on assumptions on the form of the resulting displacement. If we assume that the characteristic wavelength of the deformation pattern is much less than the radius of curvature of the shell, we are justified in using the *shallow shell approximation*, for which

$$\gamma_{\alpha\beta} = \theta_{\alpha\beta} + \frac{1}{2} w_{,\alpha} w_{,\beta} \,, \tag{A.158}$$

$$\rho_{\alpha\beta} = w|_{\alpha\beta} \,, \tag{A.159}$$

where $\theta_{\alpha\beta}$, the *linearised* middle-surface strain tensor, is given by

$$\theta_{\alpha\beta} \;=\; \frac{1}{2}(v_\alpha|_\beta + v_\beta|_\alpha) - b_{\alpha\beta}w \;. \tag{A.160}$$

The shallow shell approximation is the simplest nonlinear theory, given that it only contains one nonlinear term.

Now, the measures of stress in the shell are the stress resultants $n^{\alpha\beta}$ and the stress couples $m^{\alpha\beta}$. We can determine these from the stress tensor τ^{ij} in the shell [37]. First, define

$$\eta \;=\; 1 - 2\theta_3 H + \theta_3^2 K \;, \tag{A.161}$$

where H and K are the mean and Gaussian curvatures, from equations (A.147) and (A.148) respectively. Then, where μ^α_λ is given in equation (A.146), define the tensor

$$\sigma^{\alpha\beta} \;=\; \eta\mu^\alpha_\lambda \tau^{\beta\lambda} \;, \tag{A.162}$$

whence we define the stress resultants and stress couples by

$$n^{\alpha\beta} \;=\; \int_{-h/2}^{h/2} \sigma^{\alpha\beta}\,\mathrm{d}\theta_3 \;, \tag{A.163}$$

$$m^{\alpha\beta} \;=\; \int_{-h/2}^{h/2} \sigma^{\alpha\beta}\theta_3\,\mathrm{d}\theta_3 \;. \tag{A.164}$$

If we are considering the *linear* theory of shells, for which $\rho_{\alpha\beta}$ is as given previously and $\gamma_{\alpha\beta} = \theta_{\alpha\beta}$, it can be shown [37] that

$$n^{\alpha\beta} \;=\; hE^{\alpha\beta\lambda\mu}\gamma_{\lambda\mu} \;, \tag{A.165}$$

$$m^{\alpha\beta} \;=\; \frac{h^3}{12}E^{\alpha\beta\lambda\mu}\rho_{\lambda\mu} \;, \tag{A.166}$$

where

$$E^{\alpha\beta\lambda\mu} \;=\; G\left(a^{\alpha\lambda}a^{\beta\mu} + a^{\alpha\mu}a^{\beta\lambda} + \frac{2\nu}{1-\nu}a^{\alpha\beta}a^{\lambda\mu}\right) \tag{A.167}$$

is the elasticity tensor for shells. Here G is the shear modulus and ν is the Poisson ratio. Using this tensor we can define the potential energy density of a shell,

$$V \;=\; \frac{1}{2}hE^{\alpha\beta\lambda\mu}\gamma_{\alpha\beta}\gamma_{\lambda\mu} + \frac{1}{24}h^3E^{\alpha\beta\lambda\mu}\rho_{\alpha\beta}\rho_{\lambda\mu} \;, \tag{A.168}$$

so that the stored energy of the shell is

$$W \;=\; \iint_{\substack{\text{mid-shell}\\ \text{surface}}} V\,\mathrm{d}S \;. \tag{A.169}$$

A.4.3 Surface geometry in spherical polar coordinates

The shell that we will be considering is spherical, with a middle surface of radius $\widehat{R}$ and a given thickness h. We will now write the shell tensors assuming that the coordinates are

$$\theta_1 = \theta \,, \tag{A.170}$$
$$\theta_2 = \phi \,, \tag{A.171}$$
$$\theta_3 = R - \widehat{R} \,, \tag{A.172}$$

where θ, ϕ and R are given in equations (A.51)–(A.53). It is important to note that the choices of the coordinates are different here than in Section A.3. The reason for our choice here is that θ_1 and θ_2 are defined to be the in-surface coordinates of the middle-surface of the shell, while θ_3 is a coordinate perpendicular to the other two with a value of zero on the surface itself.

Now, $\bar{\boldsymbol{r}}(\theta_1, \theta_2)$ is the position vector of the middle-surface of the shell. In our coordinates this is given by

$$\bar{\boldsymbol{r}}(\theta_1, \theta_2) = \widehat{R}\sin\theta\cos\phi\,\boldsymbol{e}_x + \widehat{R}\sin\theta\sin\phi\,\boldsymbol{e}_y + \widehat{R}\cos\theta\,\boldsymbol{e}_z \,. \tag{A.173}$$

This implies that

$$\boldsymbol{a}_1 = \widehat{R}\cos\theta\cos\phi\,\boldsymbol{e}_x + \widehat{R}\cos\theta\sin\phi\,\boldsymbol{e}_y - \widehat{R}\sin\theta\,\boldsymbol{e}_z \,, \tag{A.174}$$
$$\boldsymbol{a}_2 = -\widehat{R}\sin\theta\sin\phi\,\boldsymbol{e}_x + \widehat{R}\sin\theta\cos\phi\,\boldsymbol{e}_y \,. \tag{A.175}$$

The remaining base vector $\boldsymbol{a}_3$ happens to be the unit vector in the R direction, namely

$$\boldsymbol{a}_3 = \sin\theta\cos\phi\,\boldsymbol{e}_x + \sin\theta\sin\phi\,\boldsymbol{e}_y + \cos\theta\,\boldsymbol{e}_z \,. \tag{A.176}$$

The covariant metric tensors $a_{\alpha\beta}$ become

$$a_{11} = \widehat{R}^2 \,, \tag{A.177}$$
$$a_{12} = a_{21} = 0 \,, \tag{A.178}$$
$$a_{22} = \widehat{R}^2\sin^2\theta \,, \tag{A.179}$$

so that $a = \widehat{R}^4\sin^2\theta$ and thus the contravariant metric tensors are given by

$$a^{11} = \frac{1}{\widehat{R}^2} \,, \tag{A.180}$$
$$a^{12} = a^{21} = 0 \,, \tag{A.181}$$
$$a^{22} = \frac{1}{\widehat{R}^2\sin^2\theta} \,. \tag{A.182}$$

The tensor $b_{\alpha\beta}$, from equation (A.144), is found to be

$$b_{11} = -\widehat{R}\,, \tag{A.183}$$

$$b_{12} = b_{21} = 0\,, \tag{A.184}$$

$$b_{22} = -\widehat{R}\sin^2\theta\,, \tag{A.185}$$

giving us the mean and Gaussian curvature,

$$H = -\frac{1}{\widehat{R}}\,, \tag{A.186}$$

$$K = \frac{1}{\widehat{R}^2}\,, \tag{A.187}$$

respectively. Finally, the only non-zero components of the Christoffel symbols are

$$\bar{\Gamma}^1_{22} = -\sin\theta\cos\theta\,, \tag{A.188}$$

$$\bar{\Gamma}^2_{12} = \cot\theta\,. \tag{A.189}$$

A.4.4 Physical components of shell displacements

In terms of the spherical polar unit vectors given in equation (A.101), the base vectors $\boldsymbol{a}^i$ and $\boldsymbol{a}_i$ become

$$\boldsymbol{a}_1 = \widehat{R}\,\boldsymbol{e}_\theta\,, \tag{A.190}$$

$$\boldsymbol{a}^1 = \frac{1}{\widehat{R}}\,\boldsymbol{e}_\theta\,, \tag{A.191}$$

$$\boldsymbol{a}_2 = \widehat{R}\sin\theta\,\boldsymbol{e}_\phi\,, \tag{A.192}$$

$$\boldsymbol{a}^2 = \frac{1}{\widehat{R}\sin\theta}\,\boldsymbol{e}_\phi\,, \tag{A.193}$$

$$\boldsymbol{a}_3 = \boldsymbol{e}_R\,, \tag{A.194}$$

$$\boldsymbol{a}^3 = \boldsymbol{e}_R\,. \tag{A.195}$$

Thus, if we compare the displacement vector $\boldsymbol{v}$ in terms of base vectors and unit vectors,

$$\boldsymbol{v} = v_\alpha\boldsymbol{a}^\alpha + w\boldsymbol{a}^3 \tag{A.196}$$

$$= v^\alpha\boldsymbol{a}_\alpha + w\boldsymbol{a}_3 \tag{A.197}$$

$$= v_R\boldsymbol{e}_R + v_\theta\boldsymbol{e}_\theta + v_\phi\boldsymbol{e}_\phi\,, \tag{A.198}$$

we find that

$$v_R = w\,, \tag{A.199}$$

$$v_\theta = \frac{v_1}{\widehat{R}} = \widehat{R}v^1\,, \tag{A.200}$$

$$v_\phi = \frac{v_2}{\widehat{R}\sin\theta} = \widehat{R}\sin\theta\,v^2\,. \tag{A.201}$$

Appendix B

Associated Legendre Functions

The associated Legendre functions $P_n^{(m)}(\mu)$ satisfy the associated Legendre equation,

$$(1-\mu^2)\frac{\mathrm{d}^2 P_n^{(m)}}{\mathrm{d}\mu^2} - 2\mu\frac{\mathrm{d}P_n^{(m)}}{\mathrm{d}\mu} + \left[n(n+1) - \frac{m^2}{1-\mu^2}\right] P_n^{(m)}(\mu) \;=\; 0\,, \qquad \text{(B.1)}$$

where the degree n is a non-negative integer, and the order m takes the values $0, 1, \ldots, n$. We can also define Legendre functions for negative n by setting

$$P_n^{(m)}(\mu) \;=\; P_{-n-1}^{(m)}(\mu) \qquad \text{(B.2)}$$

for $n = -1, -2, -3, \ldots$. Legendre functions of order zero are polynomials for integer n and are thus known as Legendre polynomials. Some useful relations between Legendre functions given by Lebedev [57] are shown below.

$$(1-\mu^2)\frac{\mathrm{d}P_n^{(m)}}{\mathrm{d}\mu} \;=\; (n+m)P_{n-1}^{(m)}(\mu) - n\mu P_n^{(m)}(\mu)\,, \qquad \text{(B.3)}$$

$$P_n^{(m)}(\mu) \;=\; (-1)^m(1-\mu^2)^{m/2}\frac{\mathrm{d}^m P_n^{(0)}}{\mathrm{d}\mu^m}\,, \qquad \text{(B.4)}$$

$$\mu P_n^{(0)\prime}(\mu) - P_{n-1}^{(0)\,\prime}(\mu) \;=\; nP_n^{(0)}(\mu)\,, \qquad \text{(B.5)}$$

$$P_{n+1}^{(0)\,\prime}(\mu) - P_{n-1}^{(0)\,\prime}(\mu) \;=\; (2n+1)P_n^{(0)}(\mu)\,, \qquad \text{(B.6)}$$

$$\mu P_n^{(m)}(\mu) \;=\; \frac{n-m+1}{2n+1}P_{n+1}^{(m)}(\mu) + \frac{n+m}{2n+1}P_{n-1}^{(m)}(\mu)\,. \qquad \text{(B.7)}$$

From equations (B.3) and (B.4) we find that

$$(1-\mu^2)P_n^{(0)\prime}(\mu) \;=\; nP_{n-1}^{(0)}(\mu) - n\mu P_n^{(0)}(\mu) \qquad \text{(B.8)}$$

$$\;=\; \frac{n(n+1)}{2n+1}\left[P_{n-1}^{(0)}(\mu) - P_{n+1}^{(0)}(\mu)\right]\,, \qquad \text{(B.9)}$$

and

$$P_n^{(1)}(\mu) \;=\; -\sqrt{1-\mu^2}P_n^{(0)\prime}(\mu) \qquad \text{(B.10)}$$

$$\Rightarrow \quad P_n^{(1)\prime}(\mu) \;=\; \frac{\mu}{\sqrt{1-\mu^2}}P_n^{(0)\prime}(\mu) - \sqrt{1-\mu^2}P_n^{(0)\prime\prime}(\mu)\,. \qquad \text{(B.11)}$$

The orthogonality condition is

$$\int_{-1}^{1} P_k^{(m)}(\mu) P_l^{(m)}(\mu)\,\mathrm{d}\mu \;=\; \frac{2}{2k+1}\frac{(k+m)!}{(k-m)!}\delta_{kl}\;. \tag{B.12}$$

Some useful specific examples are

$$P_0^{(0)}(\mu) \;=\; 1\;, \tag{B.13}$$

$$P_1^{(0)}(\mu) \;=\; \mu\;, \tag{B.14}$$

$$P_2^{(0)}(\mu) \;=\; \frac{1}{2}(3\mu^2-1)\;, \tag{B.15}$$

$$P_0^{(1)}(\mu) \;=\; 0\;, \tag{B.16}$$

$$P_1^{(1)}(\mu) \;=\; -\sqrt{1-\mu^2}\;, \tag{B.17}$$

$$P_2^{(1)}(\mu) \;=\; -3\mu\sqrt{1-\mu^2}\;. \tag{B.18}$$

Appendix C

Some Identities Involving Lattice Sums

In this appendix we prove two results involving the Coulombic lattice sums S_n, which were defined in equation (2.169).

C.1 Restrictions on the value of a lattice sum to ensure periodicity

Here we show that, with reference to equations (2.185)–(2.190), the functions $\chi_i^{(\mathrm{m})}$ would not be periodic unless $S_2 = \pm\pi$ for $i = 1, 2$ respectively. We consider the function $\chi_1^{(\mathrm{m})}$ only; the result for $\chi_2^{(\mathrm{m})}$ follows by using the identity (2.191).

Substituting for $\left(\frac{1+\alpha}{1-\alpha}\right)\phi_n$ from (2.154) into (2.151), we obtain

$$\chi_1^{(\mathrm{m})} = \Re\left\{\sum_{n=1}^{\infty}\left[\left(\frac{\gamma}{2}\right)^{2n}\phi_n Z^{-n} + Z^n\sum_{m=1}^{\infty}(-1)^m\left(\frac{\gamma}{2}\right)^{2m}\phi_m\binom{m+n-1}{n}S_{m+n}\right]\right\} . \quad \text{(C.1)}$$

We set $\eta_n = \phi_n(\gamma/2)^{2n}$ for brevity, and evaluate the above expression at the points $(X, Y) = (\pm 1/2, 0)$. Then

$$\chi_1^{(\mathrm{m})}(\pm\tfrac{1}{2}, 0) = \sum_{n=1}^{\infty}\left[\eta_n(\pm 1)^n 2^n + (\pm 1)^n 2^{-n}\sum_{m=1}^{\infty}(-1)^m\eta_m\binom{m+n-1}{n}S_{m+n}\right] . \quad \text{(C.2)}$$

Now, for periodicity we must have

$$\chi_1^{(\mathrm{m})}(+\tfrac{1}{2}, 0) - \chi_1^{(\mathrm{m})}(-\tfrac{1}{2}, 0) = 0 . \quad \text{(C.3)}$$

Thus

$$\sum_{\substack{n=1\\ n \text{ odd}}}^{\infty} \left[\eta_n 2^n + 2^{-n} \sum_{m=1}^{\infty} (-1)^m \eta_m \binom{m+n-1}{n} S_{m+n} \right] \;=\; 0 \quad \text{(C.4)}$$

$$\Rightarrow \qquad \sum_{k=1}^{\infty} \left[\eta_{2k-1} 2^{2k-1} + 2^{-2k+1} \sum_{m=1}^{\infty} (-1)^m \eta_m \binom{m+2k-2}{2k-1} S_{m+2k-1} \right] \;=\; 0\,. \quad \text{(C.5)}$$

Now, $S_{m+2k-1} = 0$ unless m is odd. Thus

$$\sum_{k=1}^{\infty} \left[\eta_{2k-1} 2^{2k-1} - 2^{-2k+1} \sum_{j=1}^{\infty} \eta_{2j-1} \binom{2j+2k-3}{2k-1} S_{2j+2k-2} \right] \;=\; 0\,, \qquad \text{(C.6)}$$

which can be rewritten, on changing the order of summation, as

$$\sum_{j=1}^{\infty} \Gamma_j \eta_{2j-1} \;=\; 0\,, \qquad \text{(C.7)}$$

where

$$\Gamma_j \;=\; \sum_{k=1}^{\infty} \left[2^{2k-1} \delta_{jk} - 2^{-(2k-1)} \binom{2j+2k-3}{2k-1} S_{2j+2k-2} \right]\,. \qquad \text{(C.8)}$$

In general, therefore, to satisfy (C.7), we must have $\Gamma_j = 0$ for each $j = 1, 2, \ldots$. In particular, we need $\Gamma_1 = 0$, or

$$\sum_{k=1}^{\infty} \frac{S_{2k}}{2^{2k}} \;=\; 1\,. \qquad \text{(C.9)}$$

Of the quantities in this sum, each is known definitively except for S_2. We find that

$$S_2 \;=\; 4 \left[1 - \sum_{j=1}^{\infty} \frac{S_{4j}}{2^{4j}} \right]\,, \qquad \text{(C.10)}$$

since (apart from S_2) we know that $S_k = 0$ unless k is an integer multiple of 4.

Now, consider the lattice Λ defined in equation (2.165), which we rewrite for convenience:

$$\Lambda \;=\; \left\{ (k,l) \in \mathbb{Z}^2 \;:\; (k,l) \neq (0,0) \right\}\,. \qquad \text{(C.11)}$$

Define the lattice

$$\Lambda^* \;=\; \Lambda \cup (0,0)\,, \qquad \text{(C.12)}$$

then the *Weierstrass zeta function* for Λ^* is defined [25] by

$$\zeta(z) \;=\; \frac{1}{z} + \sum_{\substack{\lambda \in \Lambda^* \setminus (0,0)\\ =\Lambda}} \left[\frac{1}{z-\lambda} + \frac{1}{\lambda} + \frac{z}{\lambda^2} \right]\,. \qquad \text{(C.13)}$$

This can be expanded in a series

$$\zeta(z) = \frac{1}{z} - \sum_{\lambda\in\Lambda}\sum_{m=2}^{\infty}\frac{z^m}{\lambda^{m+1}} \tag{C.14}$$

$$= \frac{1}{z} - \sum_{m=2}^{\infty} z^m S_{m+1} \tag{C.15}$$

$$= \frac{1}{z} - \sum_{j=1}^{\infty} z^{4j-1} S_{4j} \ . \tag{C.16}$$

Evaluating this function at $z = 1/2$ gives

$$\zeta(1/2) = 2 - \sum_{j=1}^{\infty}\frac{S_{4j}}{2^{4j-1}} \tag{C.17}$$

$$= 2\left(1 - \sum_{j=1}^{\infty}\frac{S_{4j}}{2^{4j}}\right) \tag{C.18}$$

$$= \frac{S_2}{2} \tag{C.19}$$

from (C.10). However, it can be shown [60] that $\zeta(1/2) = \pi/2$. Thus

$$S_2 = \pi \ , \tag{C.20}$$

as required.

C.2 The proof of equation (2.268)

In this section we will show that

$$\sum_{j=1}^{\infty}\frac{(-1)^{n+j}}{2^{2n+2j-2}}\binom{4n+4j-5}{4j-2}S_{4n+4j-4} = 1 \ , \tag{C.21}$$

which was the one step omitted from the analysis of the sum Σ on page 42. This proof was suggested to the author by David Allwright.

Let $\wp$ be the Weierstrass elliptic function for the lattice Λ^* given in (C.12). This is defined [25] by

$$\wp(z) = \frac{1}{z^2} + \sum_{\lambda\in\Lambda}\left(\frac{1}{(z-\lambda)^2} - \frac{1}{\lambda^2}\right) \tag{C.22}$$

$$= \frac{1}{z^2} + \sum_{\lambda\in\Lambda}\sum_{m=1}^{\infty}(m+1)\lambda^{-(m+2)}z^m \qquad \text{for } |z| < \min|\lambda| \tag{C.23}$$

$$= \frac{1}{z^2} + \sum_{m=1}^{\infty}(m+1)S_{m+2}z^m \ . \tag{C.24}$$

However, $S_m = 0$ unless m is a multiple of 4. Set $m + 2 = 4k$ in the sum, then

$$\wp(z) \;=\; \frac{1}{z^2} + \sum_{k=1}^{\infty} (4k-1) S_{4k} z^{4k-2} \,. \tag{C.25}$$

On differentiating this expression $4n-4$ times, we obtain

$$\wp^{(4n-4)}(z) \;=\; (4n-3)!\, z^{-(4n-2)} + \sum_{k=n}^{\infty} \frac{(4k-1)!}{(4k-4n+2)!} S_{4k} z^{4k-4n+2} \,. \tag{C.26}$$

Evaluating this expression at $z = z_0 := (1+\mathrm{i})/2$, we obtain

$$\begin{aligned}
\wp^{(4n-4)}(z_0) \;&=\; (4n-3)!\, 2^{2n-1} \exp\left(-\frac{\mathrm{i}\pi}{2}(2n-1)\right) \\
&\qquad + \sum_{k=n}^{\infty} \frac{(4k-1)!}{(4k-4n+2)!} S_{4k} 2^{2n-2k-1} \exp\left(\frac{\mathrm{i}\pi}{2}(2k-2n+1)\right) && \text{(C.27)} \\
&=\; (4n-3)!\, 2^{2n-1} \mathrm{e}^{-\frac{\mathrm{i}\pi}{2}(2n-1)} \left\{ 1 + \sum_{k=n}^{\infty} \binom{4k-1}{4k-4n+2} \frac{(-1)^k}{2^{2k}} S_{4k} \right\} && \text{(C.28)} \\
&=\; (4n-3)!\, 2^{2n-1} \mathrm{e}^{-\frac{\mathrm{i}\pi}{2}(2n-1)} \\
&\qquad \times \left\{ 1 - \sum_{j=1}^{\infty} \binom{4n+4j-5}{4j-2} \frac{(-1)^{n+j} S_{4n+4n-4}}{2^{2n+2j-2}} \right\} \,. && \text{(C.29)}
\end{aligned}$$

Thus (C.21) is equivalent to the statement that $\wp^{(4n-4)}(z_0) = 0$. However, $\wp(z) = \wp(z-1)$ by the definition (C.22) above. Thus

$$\begin{aligned}
\wp(z_0 + \mathrm{i}z) \;&=\; \wp(z_0 + \mathrm{i}z - 1) && \text{(C.30)} \\
&=\; \wp(z_0 + \mathrm{i}z - z_0 + \mathrm{i}z_0) && \text{(C.31)} \\
&=\; \wp(\mathrm{i}(z_0 + z)) && \text{(C.32)} \\
&=\; -\wp(z_0 + z) \,, && \text{(C.33)}
\end{aligned}$$

by equation (C.25). Differentiating $4n-4$ times, we have

$$\mathrm{i}^{4n-4} \wp^{(4n-4)}(z_0 + \mathrm{i}z) \;=\; -\wp^{(4n-4)}(z_0 + z) \,, \tag{C.34}$$

which we evaluate at $z = 0$ to obtain

$$\begin{aligned}
\wp^{(4n-4)}(z_0) \;&=\; -\wp^{(4n-4)}(z_0) && \text{(C.35)} \\
&=\; 0 \,, && \text{(C.36)}
\end{aligned}$$

which establishes the identity.

Appendix D

Coefficients for the Split Shell

In this appendix we note down the exact forms for the coefficients of equations (5.112)–(5.117). The term $\delta_{n,0}$ that occasionally appears is Kronecker's delta.

$$A_n^1 = \left[-(n+1)n(n-1)\lambda_{n-1} + \frac{[4(1-\nu_\mathrm{s})(2n+1)-2n]\,n(n-1)}{2n-1} \right] R_0^{n-2} , \quad \text{(D.1)}$$

$$A_n^2 = \frac{(n+1)(2n+5)\,[2\nu_\mathrm{s}-(n-2)(n+1)]}{2n+3} R_0^n , \quad \text{(D.2)}$$

$$A_n^3 = \frac{n(2n-3)\,[n(n+3)-2\nu_\mathrm{s}]}{2n-1} R_0^{-n-1} , \quad \text{(D.3)}$$

$$A_n^4 = -\frac{2(1-2\nu_\mathrm{s})}{R_0^3}\delta_{n,0} + \left[n(n+1)(n+2)\lambda_{-(n+2)} + \frac{2(n+2)(n+1)\,[2(1-\nu_\mathrm{s})(2n+1)-(n+1)]}{2n+3} \right] R_0^{-n-3} , \quad \text{(D.4)}$$

$$B_n^1 = \left[-(n+1)(n-1)\lambda_{n-1} + \frac{2(n-1)\,[2(1-\nu_\mathrm{s})(2n+1)-n]}{2n-1} \right] R_0^{n-2} , \quad \text{(D.5)}$$

$$B_n^2 = \frac{(2n+5)\,[2(1-\nu_\mathrm{s})-(n+1)^2]}{2n+3} R_0^n , \quad \text{(D.6)}$$

$$B_n^3 = \frac{(2n-3)\,[2(1-\nu_\mathrm{s})-n^2]}{2n-1} R_0^{-n-1} , \quad \text{(D.7)}$$

$$B_n^4 = \left[-n(n+2)\lambda_{-(n+2)} - \frac{2(n+2)\,[2(1-\nu_\mathrm{s})(2n+1)-(n+1)]}{2n+3} \right] R_0^{-n-3} , \quad \text{(D.8)}$$

$$C_n^1 = \left[-(n+1)n(n-1)\lambda_{n-1} + \frac{[4(1-\nu_\mathrm{s})(2n+1)-2n]\,n(n-1)}{2n-1} \right] R_1^{n-2} , \quad \text{(D.9)}$$

$$C_n^2 = \frac{(n+1)(2n+5)\,[2\nu_\mathrm{s}-(n-2)(n+1)]}{2n+3} R_1^n , \quad \text{(D.10)}$$

$$C_n^3 = \frac{n(2n-3)\,[n(n+3)-2\nu_\mathrm{s}]}{2n-1} R_1^{-n-1} , \quad \text{(D.11)}$$

$$C_n^4 = -\frac{2(1-2\nu_\mathrm{s})}{R_1^3}\delta_{n,0} + \left[n(n+1)(n+2)\lambda_{-(n+2)} + \frac{2(n+2)(n+1)\,[2(1-\nu_\mathrm{s})(2n+1)-(n+1)]}{2n+3} \right] R_1^{-n-3} , \quad \text{(D.12)}$$

$$C_n^5 = -\frac{n(2n-3)\left[n(n+3)-2\nu_{\rm m}\right]}{2n-1}R_1^{-n-1}\,,$$
(n even) (D.13)

$$C_n^6 = -n(n+1)(n+2)R_1^{-n-3}\,,$$
(n even) (D.14)

$$C_n^7 = -\frac{2(n+2)(n+1)\left[2(1-\nu_{\rm m})(2n+1)-(n+1)\right]}{2n+3}R_1^{-n-3}\,,$$
(n even) (D.15)

$$C^8 = -\frac{2q_z}{3}\,, \quad (D.16)$$

$$C^9 = -\left(q_R+\frac{q_z}{3}\right)\,, \quad (D.17)$$

$$D_n^1 = \left[-(n+1)(n-1)\lambda_{n-1}+\frac{2(n-1)\left[2(1-\nu_{\rm s})(2n+1)-n\right]}{2n-1}\right]R_1^{n-2}\,, \quad (D.18)$$

$$D_n^2 = \frac{(2n+5)\left[2(1-\nu_{\rm s})-(n+1)^2\right]}{2n+3}R_1^{n}\,, \quad (D.19)$$

$$D_n^3 = \frac{(2n-3)\left[2(1-\nu_{\rm s})-n^2\right]}{2n-1}R_1^{-n-1}\,, \quad (D.20)$$

$$D_n^4 = \left[-n(n+2)\lambda_{-(n+2)}-\frac{2(n+2)\left[2(1-\nu_{\rm s})(2n+1)-(n+1)\right]}{2n+3}\right]R_1^{-n-3}; \quad (D.21)$$

$$D_n^5 = -\frac{(2n-3)\left[2(1-\nu_{\rm m})-n^2\right]}{2n-1}R_1^{-n-1}\,,$$
(n even) (D.22)

$$D_n^6 = n(n+2)R_1^{-n-3}\,,$$
(n even) (D.23)

$$D_n^7 = \frac{2(n+2)\left[2(1-\nu_{\rm m})(2n+1)-(n+1)\right]}{2n+3}R_1^{-n-3}\,,$$
(n even) (D.24)

$$D^8 = -\frac{q_z}{3}\,, \quad (D.25)$$

$$E_n^1 = \frac{1}{2G_{\rm s}}\left[-n(n+1)\lambda_{n-1}+\frac{2n\left[2(1-\nu_{\rm s})(2n+1)-n\right]}{2n-1}\right]R_1^{n-1}\,, \quad (D.26)$$

$$E_n^2 = \frac{1}{2G_{\rm s}}\frac{(n+1)(2n+5)\left[4(1-\nu_{\rm s})-(n+2)\right]}{2n+3}R_1^{n+1}\,, \quad (D.27)$$

$$E_n^3 = -\frac{1}{2G_{\rm s}}\frac{n(2n-3)\left[4(1-\nu_{\rm s})+(n-1)\right]}{2n-1}R_1^{-n}\,, \quad (D.28)$$

$$E_n^4 = \frac{(1-2\nu_{\rm s})}{2G_{\rm s}R_1^2}\delta_{n,0}+\frac{1}{2G_{\rm s}}\left[-n(n+1)\lambda_{-(n+2)}+\frac{2(n+1)\left[(n+1)-2(1-\nu_{\rm s})(2n+1)\right]}{2n+3}\right]R_1^{-n-2}\,, \quad (D.29)$$

$$E_n^5 = \frac{1}{2G_{\rm m}}\frac{n(2n-3)\left[4(1-\nu_{\rm m})+(n-1)\right]}{2n-1}R_1^{-n}\,,$$
(n even) (D.30)

$$E_n^6 = \frac{1}{2G_{\rm m}} n(n+1) R_1^{-n-2} \,, \quad (n \text{ even}) \tag{D.31}$$

$$E_n^7 = -\frac{1}{2G_{\rm m}} \frac{2(n+1)\left[-2(1-\nu_{\rm m})(2n+1)+(n+1)\right]}{2n+3} R_1^{-n-2} \,, \quad (n \text{ even}) \tag{D.32}$$

$$E^8 = -\frac{R_1 q_z}{3G_{\rm m}} \,, \tag{D.33}$$

$$E^9 = -\frac{(1-2\nu_{\rm m}) R_1 (3q_R + q_z)}{6G_{\rm m}(1+\nu_{\rm m})} \,, \tag{D.34}$$

$$F_n^1 = \frac{1}{2G_{\rm s}} \left[-(n+1)\lambda_{n-1} + \frac{4(1-\nu_{\rm s})(2n+1)-2n}{2n-1} \right] R_1^{n-1} \,, \tag{D.35}$$

$$F_n^2 = -\frac{1}{2G_{\rm s}} \frac{(2n+5)\left[4(1-\nu_{\rm s})+(n+1)\right]}{2n+3} R_1^{n+1} \,, \tag{D.36}$$

$$F_n^3 = -\frac{1}{2G_{\rm s}} \frac{(2n-3)\left[4(1-\nu_{\rm s})-n\right]}{2n-1} R_1^{-n} \,, \tag{D.37}$$

$$F_n^4 = \frac{1}{2G_{\rm s}} \left[n\lambda_{-(n+2)} + \frac{4(1-\nu_{\rm s})(2n+1)-2(n+1)}{2n+3} \right] R_1^{-n-2} \,, \tag{D.38}$$

$$F_n^5 = \frac{1}{2G_{\rm m}} \frac{(2n-3)\left[4(1-\nu_{\rm m})-n\right]}{2n-1} R_1^{-n} \,, \quad (n \text{ even}) \tag{D.39}$$

$$F_n^6 = -\frac{1}{2G_{\rm m}} n R_1^{-n-2} \,, \quad (n \text{ even}) \tag{D.40}$$

$$F_n^7 = -\frac{1}{2G_{\rm m}} \frac{4(1-\nu_{\rm m})(2n+1)-2(n+1)}{2n+3} R_1^{-n-2} \,, \quad (n \text{ even}) \tag{D.41}$$

$$F^8 = -\frac{R_1 q_z}{6G_{\rm m}} \,. \tag{D.42}$$

References

[1] D.J. Allwright, G.W. Jones, and W. Parnell. Acoustic scattering from a strained region. In *Proceedings of the 53rd European Study Group with Industry, Manchester, 2005*, pages E1–E14, 2006.
http://www.maths-in-industry.org/67/

[2] N.S. Bakhvalov and G.P. Panasenko. *Homogenization: Averaging Processes in Periodic Media*. Nauka, 1984 (in Russian). English translation published by Kluwer Academic Publishers, 1989.

[3] G.K. Batchelor. Transport properties of two-phase materials with random structure. *Annual Review of Fluid Mechanics*, **6**:227–255, 1974.
doi:10.1146/annurev.fl.06.010174.001303

[4] M.F. Beatty. The Mullins effect in a pure shear. *Journal of Elasticity*, **59**(1–3):369–392, 2000.
doi:10.1023/A:1011007522361

[5] M.F. Beatty and S. Krishnaswamy. A theory of stress-softening in incompressible isotropic materials. *Journal of the Mechanics and Physics of Solids*, **48**(9):1931–1965, 2000.
doi:10.1016/S0022-5096(99)00085-X

[6] C.M. Bender and S.A. Orszag. *Advanced Mathematical Methods for Scientists and Engineers*. McGraw–Hill, 1978.

[7] A. Bensoussan, J.-L. Lions, and G.C. Papanicolaou. *Asymptotic Analysis for Periodic Structures*. North Holland, 1978.

[8] M. Bilgen and M.F. Insana. Elastostatics of a spherical inclusion in homogeneous biological media. *Physics in Medicine and Biology*, **43**(1):1–20, 1998.
doi:10.1088/0031-9155/43/1/001

[9] P. Bjørstad, G. Dahlquist, and E. Grosse. Extrapolation of asymptotic expansions by a modified Aitken δ^2-formula. *BIT Numerical Mathematics*,

21(1):56–65, 1981.
doi:10.1007/BF01934071

[10] A.F. Blanchard and D. Parkinson. Breakage of carbon–rubber networks by applied stress. *Industrial and Engineering Chemistry*, **44**(4):799–812, 1952. doi:10.1021/ie50508a034

[11] H. Bouasse and Z. Carrière. Sur les courbes de traction du caoutchouc vulcanisé. *Annales de la Faculté des Sciences de l'Université de Toulouse, 2^e série*, **5**(3):257–283, 1903.

[12] D.O. Brush and B.O. Almroth. *Buckling of Bars, Plates and Shells*. McGraw–Hill, 1975.

[13] K.G. Budden. *The propagation of radio waves: The theory of radio waves of low power in the ionosphere and magnetosphere*. Cambridge University Press, 1985.

[14] F. Bueche. Molecular basis for the Mullins effect. *Journal of Applied Polymer Science*, **4**(10):107–114, 1960. doi:10.1002/app.1960.070041017

[15] F. Bueche. Mullins effect and rubber–filler interaction. *Journal of Applied Polymer Science*, **5**(15):271–281, 1961. doi:10.1002/app.1961.070051504

[16] J. Bussert and P. Beaver. Soviet submarine hull coatings. *Jane's Defence Weekly*, **8**(13):763–765, 1987.

[17] W.E. Byerly. *An Elementary Treatise on Fourier's Series and Spherical, Cylindrical, and Ellipsoidal Harmonics, with Applications to Problems in Mathematical Physics*. Ginn, 1893.

[18] S.J. Chapman. A mean-field model of superconducting vortices in three dimensions. *SIAM Journal on Applied Mathematics*, **55**(5):1259–1274, 1995. doi:10.1137/S0036139994263665

[19] H.-S. Chen and A. Acrivos. The effective elastic moduli of composite materials containing spherical inclusions at non-dilute concentrations. *International Journal of Solids and Structures*, **14**(5):349–364, 1978. doi:10.1016/0020-7683(78)90017-3

[20] R.M. Christensen. *Mechanics of Composite Materials*. Wiley, 1979.

[21] D. Cioranescu and P. Donato. *An Introduction to Homogenization*. Oxford University Press, 1999.

[22] D. Cioranescu, J. Saint Jean Paulin, and H. Lanchon. Elastic-plastic torsion of heterogeneous cylindrical bars. *Journal of the Institute of Mathematics and its Applications*, **24**(4):353–378, 1979.
doi:10.1093/imamat/24.4.353

[23] C.D. Coman. Inhomogeneities and localised buckling patterns. *IMA Journal of Applied Mathematics*, **71**(1):133–152, 2006.
doi:10.1093/imamat/hxh088

[24] T.S. Cook and F. Erdogan. Stresses in bonded materials with a crack perpendicular to the interface. *International Journal of Engineering Science*, **10**(8):677–697, 1972.
doi:10.1016/0020-7225(72)90063-8

[25] E.T. Copson. *An Introduction to the Theory of Functions of a Complex Variable*. Oxford University Press, 1935.

[26] J.P. Delahaye and B. Germain-Bonne. The set of logarithmically convergent sequences cannot be accelerated. *SIAM Journal on Numerical Analysis*, **19**(4):840–844, 1982.
doi:10.1137/0719059

[27] A. DeSimone, J.-J. Marigo, and L. Teresi. A damage mechanics approach to stress softening and its application to rubber. *European Journal of Mechanics — A/Solids*, **20**(6):873–892, 2001.
doi:10.1016/S0997-7538(01)01171-8

[28] A. Dorfmann and R.W. Ogden. A constitutive model for the Mullins effect with permanent set in particle-reinforced rubber. *International Journal of Solids and Structures*, **41**(7):1855–1878, 2004.
doi:10.1016/j.ijsolstr.2003.11.014

[29] A.H. England. *Complex Variable Methods in Elasticity*. Wiley, 1971.

[30] J.D. Eshelby. The determination of the elastic field of an ellipsoidal inclusion, and related problems. *Proceedings of the Royal Society of London, Ser. A*, **241**(1226):376–396, 1957.
doi:10.1098/rspa.1957.0133

[31] S.-L. Fok. *Buckling of a Spherical Shell embedded in an Elastic Medium loaded by a Far-field Hydrostatic Pressure*. M.Sc. thesis, University of Oxford, 1999.

[32] S.-L. Fok and D.J. Allwright. Buckling of a spherical shell embedded in an elastic medium loaded by a far-field hydrostatic pressure. *The Journal of Strain Analysis for Engineering Design*, **36**(6):535–544, 2001. doi:10.1243/0309324011514692

[33] J.N. Goodier. Concentration of stress around spherical and cylindrical inclusions and flaws. *Transactions of the ASME*, **55**(APM-55-7):39–44, 1933.

[34] S. Govindjee and J. Simo. A micro-mechanically based continuum damage model for carbon black-filled rubbers incorporating Mullins' effect. *Journal of the Mechanics and Physics of Solids*, **39**(1):87–112, 1991. doi:10.1016/0022-5096(91)90032-J

[35] S. Govindjee and J.C. Simo. Mullins' effect and the strain amplitude dependence of the storage modulus. *International Journal of Solids and Structures*, **29**(14–15):1737–1751, 1992. doi:10.1016/0020-7683(92)90167-R

[36] S. Govindjee and J.C. Simo. Transition from micro-mechanics to computationally efficient phenomenology: carbon black filled rubbers incorporating Mullins' effect. *Journal of the Mechanics and Physics of Solids*, **40**(1):213–233, 1992. doi:10.1016/0022-5096(92)90324-U

[37] A.E. Green and W. Zerna. *Theoretical Elasticity*. Oxford University Press, 1954.

[38] G. Grimmett and D. Welsh. *Probability: An Introduction*. Oxford University Press, 1986.

[39] M.E. Gurtin. *The Linear Theory of Elasticity*, **VIa/2** of *Encyclopedia of Physics*, pages 1–295. Springer-Verlag, 1972.

[40] J.A.C. Harwood, L. Mullins, and A.R. Payne. Stress softening in natural rubber vulcanizates. Part II. Stress softening effects in pure gum and filler loaded rubbers. *Journal of Applied Polymer Science*, **9**(9):3011–3021, 1965. doi:10.1002/app.1965.070090907

[41] J.A.C. Harwood, L. Mullins, and A.R. Payne. Stress-softening in rubbers — a review. *Journal of the Institution of the Rubber Industry*, **1**:17–27, 1967.

[42] Z. Hashin. The moduli of an elastic solid, containing spherical particles of another elastic material. In W. Olszak, editor, *Proceedings of the IUTAM Symposium "Non-Homogeneity in Elasticity and Plasticity", Warsaw, Poland*, 1959.

[43] W.L. Holt. Behavior of rubber under repeated stresses. *Rubber Chemistry and Technology*, **5**(1):79–89, 1932.

[44] G.A. Holzapfel. *Nonlinear Solid Mechanics — A Continuum Approach for Engineering*. Wiley, 2000.

[45] H.H.H. Homeier. Scalar Levin-type sequence transformations. *Journal of Computational and Applied Mathematics*, **122**(1–2):81–147, 2000.
doi:10.1016/S0377-0427(00)00359-9

[46] C.O. Horgan. Anti-plane shear deformations in linear and nonlinear solid mechanics. *SIAM Review*, **37**(1):53–81, 1995.
doi:10.1137/1037003

[47] J. Huang. Integral representations of harmonic lattice sums. *Journal of Mathematical Physics*, **40**(10):5240–5246, 1999.
doi:10.1063/1.533027

[48] M.A. Johnson and M.F. Beatty. A constitutive equation for the Mullins effect in stress controlled uniaxial extension experiments. *Continuum Mechanics and Thermodynamics*, **5**(4):301–318, 1993.
doi:10.1007/BF01135817

[49] M.A. Johnson and M.F. Beatty. The Mullins effect in uniaxial extension and its influence on the transverse vibration of a rubber string. *Continuum Mechanics and Thermodynamics*, **5**(2):83–115, 1993.
doi:10.1007/BF01141446

[50] M.A. Johnson and M.F. Beatty. The Mullins effect in equibiaxial extension and its influence on the inflation of a balloon. *International Journal of Engineering Science*, **33**(2):223–245, 1995.
doi:10.1016/0020-7225(94)E0052-K

[51] W.T. Koiter. On the nonlinear theory of thin elastic shells. *Proceedings of the Koninklijke Nederlandse Akademie van Wetenschappen (Royal Dutch Academy of Sciences), Ser. B*, **69**:1–54, 1966.

[52] W.T. Koiter. The nonlinear buckling problem of a complete spherical shell under uniform external pressure. *Proceedings of the Koninklijke Nederlandse Akademie van Wetenschappen (Royal Dutch Academy of Sciences), Ser. B*, **72**:40–123, 1969.

[53] S. Krishnaswamy and M.F. Beatty. The Mullins effect in compressible solids. *International Journal of Engineering Science*, **38**(13):1397–1414, 2000. doi:10.1016/S0020-7225(99)00125-1

[54] S. Krishnaswamy and M.F. Beatty. Damage induced stress-softening in the torsion, extension and inflation of a cylindrical tube. *The Quarterly Journal of Mechanics and Applied Mathematics*, **54**(2):295–327, 2001. doi:10.1093/qjmam/54.2.295

[55] H.L. Langhaar. *Energy Methods in Applied Mechanics*. Wiley, 1962.

[56] F. Laraba-Abbes, P. Ienny, and R. Piques. A new 'tailor-made' methodology for the mechanical behaviour analysis of rubber-like materials: II. Application to the hyperelastic behaviour characterization of a carbon-black filled natural rubber vulcanizate. *Polymer*, **44**(3):821–840, 2003. doi:10.1016/S0032-3861(02)00719-X

[57] N.N. Lebedev. *Special Functions and their Applications*. Dover, 1972.

[58] M.J. Lighthill. *Waves in Fluids*. Cambridge University Press, 1978.

[59] R.C. Lin and U. Schomburg. A finite elastic–viscoelastic–elastoplastic material law with damage: theoretical and numerical aspects. *Computer Methods in Applied Mechanics and Engineering*, **192**(13–14):1591–1627, 2003. doi:10.1016/S0045-7825(02)00649-7

[60] C.-B. Ling. Evaluation of Weierstrass zeta functions. *SIAM Review*, **21**(1):146–147, 1979. doi:10.1137/1021020

[61] C.-B. Ling and K.-L. Yang. On symmetrical strain in solids of revolution in spherical co-ordinates. *Journal of Applied Mechanics*, **18A**:367–370, 1951.

[62] D.E. Littlewood. *A University Algebra*. Heinemann, 1958.

[63] S.H. Liu and E.B. Nauman. On the micromechanics of composites containing spherical inclusions. *Journal of Materials Science*, **25**(4):2071–2076, 1990. doi:10.1007/BF01045766

[64] A.E.H. Love. *A Treatise on the Mathematical Theory of Elasticity*. Cambridge University Press, fourth edition, 1927. Reprinted by Dover, 1944.

[65] A.I. Lur'e. *Three-dimensional Problems of the Theory of Elasticity*. Interscience, 1964.

[66] G. Marckmann, E. Verron, L. Gornet, G. Chagnon, P. Charrier, and P. Fort. A theory of network alteration for the Mullins effect. *Journal of the Mechanics and Physics of Solids*, **50**(9):2011–2028, 2002. doi:10.1016/S0022-5096(01)00136-3

[67] S. Mazzullo. Stress field around an N-layered spherical inclusion. In W.A. Green and M. Mićunović, editors, *Proceedings of the European Mechanics Colloquium 214, 'Mechanical Behaviour of Composites and Laminates', Kupari, Yugoslavia, 1986*, pages 245–253, 1987.

[68] C. Miehe. Discontinuous and continuous damage evolution in Ogden-type large-strain elastic materials. *European Journal of Mechanics — A/Solids*, **14**(5):697–720, 1995.

[69] G.W. Milton. *The Theory of Composites*. Cambridge University Press, 2002.

[70] A.B. Movchan and S.K. Serkov. The Pólya–Szegő matrices in asymptotic models of dilute composites. *European Journal of Applied Mathematics*, **8**(6):595–621, 1997. doi:10.1017/S095679259700315X

[71] L. Mullins. Effect of stretching on the properties of rubber. *Journal of Rubber Research*, **16**:275–289, 1947.

[72] L. Mullins. Effect of stretching on the properties of rubber. *Rubber Chemistry and Technology*, **21**(2):281–300, 1948.

[73] L. Mullins. Thixotropic behavior of carbon black in rubber. *Journal of Physical and Colloid Chemistry*, **54**(2):239–251, 1950. doi:10.1021/j150476a006

[74] L. Mullins and N.R. Tobin. Theoretical model for the elastic behavior of filler-reinforced vulcanized rubbers. *Rubber Chemistry and Technology*, **30**:555–571, 1957.

[75] A. Neumaier. Solving ill-conditioned and singular linear systems: a tutorial on regularization. *SIAM Review*, **40**(3):636–666, 1998.
doi:10.1137/S0036144597321909

[76] N.A. Nicorovici and R.C. McPhedran. Transport properties of arrays of elliptical cylinders. *Physical Review E*, **54**(2):1945–1957, 1996.
doi:10.1103/PhysRevE.54.1945

[77] R.W. Ogden and D.G. Roxburgh. A pseudo-elastic model for the Mullins effect in filled rubber. *Proceedings of the Royal Society of London, Ser. A*, **455**(1988):2861–2877, 1999.
doi:10.1098/rspa.1999.0431

[78] N. Osada. A convergence acceleration method for some logarithmically convergent sequences. *SIAM Journal on Numerical Analysis*, **27**(1):178–189, 1990.
doi:10.1137/0727012

[79] W. Parnell. *Elastic Wave Scattering From a Strained Region*. M.Sc. thesis, University of Oxford, 2000.
http://eprints.maths.ox.ac.uk/14/

[80] W.T. Perrins, D.R. McKenzie, and R.C. McPhedran. Transport properties of regular arrays of cylinders. *Proceedings of the Royal Society of London, Ser. A*, **369**(1737):207–225, 1979.
doi:10.1098/rspa.1979.0160

[81] W.T. Perrins, R.C. McPhedran, and D.R. McKenzie. Optical properties of dense regular cermets with relevance to selective solar absorbers. *Thin Solid Films*, **57**(2):321–326, 1979.
doi:10.1016/0040-6090(79)90171-8

[82] I. Runge. Zur elektrischer leitfähigkeit metallischer aggregate. *Zeitschrift für Technische Physik*, **6**:61–68, 1925.

[83] M. Sahimi. *Heterogeneous Materials I. Linear Transport and Optical Properties*. Springer-Verlag, 2003.

[84] E. Sanchez-Palencia. *Non-homogeneous Media and Vibration Theory*, **127** of *Lecture Notes in Physics*. Springer-Verlag, 1980.

[85] D.A. Smith and W.F. Ford. Acceleration of linear and logarithmic convergence. *SIAM Journal on Numerical Analysis*, **16**(2):223–240, 1979.
doi:10.1137/0716017

[86] I.N. Sneddon and D.S. Berry. *The Classical Theory of Elasticity*, **VI** of *Encyclopedia of Physics*, pages 1–126. Springer-Verlag, 1958.

[87] I.N. Sneddon and M. Lowengrub. *Crack Problems in the Classical Theory of Elasticity*. Wiley, 1969.

[88] I.S. Sokolnikoff. *Mathematical Theory of Elasticity*. McGraw–Hill, 1956.

[89] J.W. Strutt (Lord Rayleigh). On the influence of obstacles arranged in rectangular order upon the properties of a medium. *Philosophical Magazine*, **34**:481–502, 1892.

[90] A.S.J. Suiker and C.S. Chang. Application of higher-order tensor theory for formulating enhanced continuum models. *Acta Mechanica*, **142**(1–4):223–234, 2000.
doi:10.1007/BF01190020

[91] O. Tamate and T. Yamada. Stresses in an infinite body with a partially bonded circular cylindrical inclusion under longitudinal shear. *The Technology Reports of the Tôhoku University*, **34**(1):161–171, 1969.

[92] L.N. Trefethen and D. Bau. *Numerical Linear Algebra*. SIAM, 1997.

[93] L.R.G. Treloar. *The Physics of Rubber Elasticity*. Oxford, 1958.

[94] M.K. Wadee and A.P. Bassom. Effects of exponentially small terms in the perturbation approach to buckling. *Proceedings of the Royal Society of London, Ser. A*, **455**(1986):2351–2370, 1999.
doi:10.1098/rspa.1999.0407

[95] J.A.C. Weideman and S.C. Reddy. A MATLAB differentiation matrix suite. *ACM Transactions on Mathematical Software*, **26**(4):465–519, 2000.
doi:10.1145/365723.365727

[96] E.J. Weniger. Nonlinear sequence transformations for the acceleration of convergence and the summation of divergent series. *Computer Physics Reports*, **10**(5–6):189–371, 1989.
doi:10.1016/0167-7977(89)90011-7

[97] J.R. Willis. A comparison of the fracture criteria of Griffith and Barenblatt. *Journal of the Mechanics and Physics of Solids*, **15**(3):151–162, 1967.
doi:10.1016/0022-5096(67)90029-4

[98] P.A. Yakubenko. Global capillary instability of an inclined jet. *Journal of Fluid Mechanics*, **346**:181–200, 1997.

[99] F. Zhaohua and R.D. Cook. Beam elements on two-parameter elastic foundations. *Journal of Engineering Mechanics*, **109**(6):1390–1402, 1983.

[100] S. Zimmerman. *Submarine Technology for the 21st Century*. Trafford, 2000.